UNIVERSITY
OF OSLO

Master's thesis

Quadratic Coupled Cluster Theory

A Study of Static and Dynamic Properties

Håkon Kvernmoen

60 ECTS study points

Department of Physics
Faculty of Mathematics and Natural Sciences

June 6, 2024

Håkon Kvernmoen

Quadratic Coupled Cluster Theory

A Study of Static and Dynamic Properties

Supervisor:
Morten Hjorth-Jensen and Håkon Emil Kristiansen

Abstract

Coupled cluster methods are one the cornerstones for *ab initio* treatments of interactive many-body quantum systems, being the preferred choice for calculations on small to intermediate-sized molecules. However, considering systems with large correlations, the standard coupled cluster formulation can yield both qualitatively and quantitatively wrong results.

With a computational complexity comparable to the standard coupled cluster methods, a modified ansatz referred to as quadratic coupled cluster has been shown to improve upon the standard methods for certain systems containing large correlations. By including more contributions in the parameterization of the many-body wavefunction, multielectron bond breaking has been studied with promising results.

We have implemented the quadratic theory at the doubles level and extended the method to include both singles and doubles. The energy, electric dipole, and quadrupole moment have been compared between the quadratic and standard methods, aided by the introduction of novel configurational weights. Furthermore, we have derived and implemented the equations of motion for the quadratic coupled cluster methods, leading to a study of real-time evolution for the theory.

By defining a measure for non-hermiticity, we find that both the reduced one- and two-body density matrices are one order of magnitude more hermitian for the quadratic methods when compared to the standard ansatz, even when considering systems where the latter performs well. Moreover, the density matrices are closer to full configuration interaction results, however, this is not manifested in dipole and quadrupole moments due to a beneficial error cancelation in the standard methods. The absorption spectrum of CH^+ extracted from the time-dependent induced dipole moment, using the quadratic methods, indicates no difference in excitation energies relative to the standard methods. However, the results suffer from a low-resolution in the frequency domain.

Acknowledgements

First and foremost, this work did not happen in a vacuum. I want to express my gratitude to my supervisors, Morten Hjorth-Jensen and Håkon Emil Kristiansen, who have helped me make this thesis a reality.

Morten, you are an excellent teacher, and I enjoyed our prolonged discussions, particularly when they moved toward the topic of Tolkien's mythos. Your open door policy, "*speak, friend, and enter*", followed by kind words and optimism has been invaluable.

Håkon, thank you for introducing me to such an interesting topic. I have enjoyed my Monday trips down to the Hylleraas Center, where the constructive feedback you have given me has been vital. Your enthusiasm for this work is very much appreciated. I could not have done this without you.

Through my bachelor's degree, I have had the pleasure of being a part of Fysikkforeningen and Lillefy. Please, never change. I would also like to show my gratitude to the people at the computational science program and CCSE, an excellent place to write a master's thesis. Daily ping-pong matches have been key during the last two years.

To my family, mamma og pappa, thank you for being so supportive in my endeavor to study physics. Your comforting words have been crucial when things look so bleak. Last but not least, my dear Veslemøy. Thank you for all your support, and for putting up with me in these final days of stress. You are truly a wonderful person, I owe you more than words can express.

Contents

Chapter 1

Introduction

Quantum mechanics is one of the pillars of modern physics. The theory aims to describe the microscopic world, most often applied to the length scales of a single molecule and below. Solving problems with multiple interactive particles, even in classical mechanics, rarely results in analytical solutions. This is also true for quantum mechanical treatments, where analytical solutions of one- and two-particle systems are priced possessions, published in both books and articles [1–6]. With an increasing system size, approximate treatments are required. This field of study, known as many-body quantum theory, often relies on numerical approximations to describe multiple interactive particles.

To serve this end, a range of *ab initio* (from first principles) approximate methods have been developed. Each method has its area of application, dependent on the characteristics of the system at hand. The Hartree-Fock (HF) method [7–9] is one of the earliest endeavors in quantum many-body theory, developed in the early 1930s. Today, the largest systems are treated with density functional theory (DFT) [10], with some approximations reaching as far as one million particles [11–13]. However, small to intermediate-sized molecules are most accurately described by post-HF methods, sometimes referred to as wavefunction methods, with configuration interaction (CI) theory [14], many-body perturbation theory (MBPT) [15] and coupled cluster (CC) theory [16, 17] being the most popular choices. It is the latter realm of post-HF methods, particularly CC theory, with which this work is concerned.

Even in the domain of post-HF methods, no single method exhibits every desirable property. In this regard, we present a list of desired characteristics that a generally applicable post-HF method should respect, based on the work of J. A. Pople and R. J. Bartlett [18, 19]. The list is non-comprehensive and does not imply any specific order of relevance:

I. The method in question should have a tractable time and memory complexity. Without this, the method will become computationally infeasible when increasing the number of interactive particles in the system.

II. A method-specific truncation scheme, where higher-order contributions can be added to systematically improve the accuracy of the results. In the untruncated limit, the results from full diagonalization should be recovered.

III. Energy calculations with a truncation scheme should yield an upper bound to the results from full diagonalization, such that the energy is variational.

IV. Energy calculations should be size-consistent. Considering two non-interactive subsystems A and B, the energy from a calculation of the composite system AB should yield the same results as that of two separate calculations of A and B, $E(AB) = E(A) + E(B)$.

1.1 Coupled Cluster

Today, CC theory is often referred to as the gold standard electronic structure method applied to small and medium-sized atoms and molecules [20, 21]. The method delivers accurate results for various properties at equilibrium geometries, where the particles in the system are most often weakly correlated. However, realms with strong correlations are more challenging. In particular,

the breaking of multielectron bonds can result in quantitative and qualitative wrong behavior, a consequence of CC not being a variational method [22]. The bond breaking, or dissociation, of the nitrogen molecule (N_2) is the most commonly studied example, with various modifications to CC suggested to alleviate the non-physical behavior [22, 23].

We will consider quadratic coupled cluster (QCC) theories, introduced by Van Voorhis and Head-Gordon within a doubles truncated scheme (QCCD) [24], which is an approximation to the extended coupled-cluster (ECC) theory of Arponen et al. [25]. They found that QCCD produced a better approximation to a variational treatment of CC, resulting in qualitatively correct multielectron bond breaking. Even though the QCCD equations at face value scales in time as $\mathcal{O}(n^{12})$ with n representing the system size, a shrewd rewrite reduces this to $\mathcal{O}(n^6)$, equalling that of standard CC [26]. This was later expanded to a singles and doubles scheme (QCCSD) in Ref. [27].

The currently reported properties of QCC only include energy calculations, particularly for multielectron bond breaking. However, due to the QCC theories' more accurate approximation of a variational CC functional, other properties such as the reduced density matrices are also of interest. To this aim, we introduce configurational weights that aid in probing the composition of the CC ansatz.

Furthermore, to the best of our knowledge, the application of QCC as a solution to the time-dependent Schrödinger equation has not been attempted. By deriving the equations of motion (EOMs) for different QCC truncations, we study the time evolution of atoms and molecules within the dipole approximation. An application of this is estimating absorption spectra from the induced dipole moment after subjecting the system to a short external perturbation [28, 29]. This is known to agree with excitation energies from equation-of-motion CC (EOM-CC) [30] and CC response theory (CCRT) [31].

The standard CC theories are known to accurately describe states dominated by single excitations using this approach; however, the accuracy decreases for excited states with large double excitation components. Due to QCC giving a more balanced doubles description in strongly correlated systems, such as for N_2 dissociation, we aim to investigate whether QCC can give improved excitation energies in comparison to standard CC.

1.2 Goals

Much mathematical and numerical work has been performed to reach the goal of calculating absorption spectra from real-time quadratic CC theory. We present an initial outline of the necessary milestones:

I. Implement a structure to handle basis functions, including calculating matrix elements and other necessary components, in addition to an HF solver.

II. Implement the CC doubles (CCD) method and extend to the CC singles and doubles (CCSD) truncation, benchmarking with well-known scientific software. Since strongly correlated stretched geometry systems will be explored, a proper fixed-point convergence scheme with adjustable options is necessary.

III. Recreate the QCCD scheme of Van Voorhis and Head-Gordon, extending to the QCCSD truncation. Because there are few results available for quadratic theories, it is important to thoroughly validate the implementation against existing literature.

IV. Perform time evolution with the standard CC methods, using different external potentials. Derive and implement the QCCD and QCCSD EOMs, allowing for time propagation of the quadratic theory. Since QCC time propagation has not yet been performed, methods to ensure that the implementation is self-consistent must be applied.

1.3 Structure

This thesis is structured in seven chapters. Chapter Two contains an introduction to the second quantization formalism, presenting the necessary mathematical tools for what follows. Some additional topics, such as how absorption spectra are estimated are also included, complemented by a short presentation of the HF and CI methods. Chapter Three gives a thorough introduction to

CC theory, beginning with the traditional presentation concerning energy calculations and ending with the derivation of the quadratic EOMs and the introduction of CC configurational weights.

Chapter Four presents selected topics regarding the numerical implementation and optimization techniques, followed by Chapter Five showing the validity of the work. Results are presented in Chapter Six, with Chapter Seven containing concluding remarks. Lastly, additional details and results are included in Appendix A, with Appendices B to D containing some longer algebraic expressions.

Chapter 2

Preliminaries

Before we begin discussing coupled cluster theory, some preliminary information is in order. We start by introducing the fundamental equation that governs non-relativistic quantum mechanics, namely the Schrödinger equation, followed by some conventional approximations for solving molecular problems. Thereafter, the second quantization formalism will be introduced, providing a mathematical basis for representing multiparticle states, operators, and inner products. Some selected topics such as time-dependent perturbations, absorption spectra, and spin-restriction are also discussed. We end this chapter with a brief introduction to the Hartree-Fock (HF) theory and the configuration interaction (CI) theory.

Much of the following is material present in many-body and quantum chemistry textbooks. The purpose of this chapter is not to give a pedagogical and comprehensive introduction to the underlying formalism, but rather serve as a synopsis providing the necessary tools to discuss standard and quadratic CC theory. For a more in-depth introduction, we recommend in particular the excellent book by Shavitt and Bartlett [21] in addition to the incredibly extensive book by Helgaker et al. [32].

2.1 Units

In this thesis we always work with *atomic units* [33], meaning we set the four following quantities to unity:

$$\hbar = e = m_e = 4\pi\epsilon_0 = 1.$$

Here $\hbar$ is the reduced Planck constant, e the elementary charge, m_e the electron mass, and ϵ_0 the vacuum permittivity. Two physical quantities are named in this set of units, namely the unit of length being a Bohr radius $a_0 = 4\pi\epsilon_0\hbar^2/m_e e^2$ and the unit of energy being a Hartree $E_h = \hbar^2/m_e a_0^2$. For quantities other than energy and length, the abbreviation a.u. will be used.

Quantity	Expression	Also used
Energy	E_h	eV[†]
Length	a_0	Å[‡]
Time	$\hbar/E_h$	
Freqency	$E_h/\hbar$	
Electric Field	E_h/ea_0	
Electric Dipole Moment	ea_0	D[§]
Electric Quadrupole Moment	ea_0^2	DÅ

[†] Electronvolt
[‡] Ångström
[§] Debye

Table 2.1: The relevant atomic units we will apply in this thesis. Some equivalents are also given, which are used in the literature we compare with.

2.2 The Schrödinger Equation

Properties of atoms and molecules, both static and dynamic, are governed by an N particle quantum state $|\Psi(t)\rangle$. The time evolution of the state is governed by the *time-dependent Schrödinger equation* (TDSE),

$$i\frac{\mathrm{d}}{\mathrm{d}t}\Psi(\boldsymbol{x}_1 \dots \boldsymbol{x}_N, t) = \hat{H}\Psi(\boldsymbol{x}_1 \dots \boldsymbol{x}_N, t), \tag{2.1}$$

where $\boldsymbol{x}_i$ is the coordinate for a single particle, i the imaginary unit and t time. Equation 2.1 applies the coordinate representation of $|\Psi(t)\rangle$, $\Psi(\boldsymbol{x}_1, \dots, \boldsymbol{x}_N, t) = \langle \boldsymbol{x}_1 \dots \boldsymbol{x}_N | \Psi(t)\rangle$, where $\boldsymbol{x}$ is a compound notation including both the spatial coordinates $\boldsymbol{r}$ and possible eigenspin projections σ, $\boldsymbol{x} \equiv (\boldsymbol{r}, \sigma)$. Lastly, $\hat{H}$ is a linear and hermitian operator referred to as the Hamiltonian, the energy operator of the system. Equation 2.1 is a partial differential equation (PDE) and to solve it we must specify an initial state $\Psi(t_0)$. Assuming that the Hamiltonian is independent of time, the spatial part of Eq. 2.1 can be reduced to the *time-independent Schrödinger equation* (TISE),

$$\hat{H}\Psi(\boldsymbol{x}_1 \dots \boldsymbol{x}_N) = E\Psi(\boldsymbol{x}_1 \dots \boldsymbol{x}_N), \tag{2.2}$$

where E is the energy of Ψ. In contrast to the TDSE, the time-independent SE is an ordinary differential equation (ODE) formulated as an eigenvalue problem. Solving Eq. 2.2 yields a set of solutions Ψ_n referred to as the eigenstates of $\hat{H}$ with associated energies E_n. The eigenpair (E_0, Ψ_0) with the smallest eigenvalue is the ground state of the system, with all other being excited states. Dynamics of the initial state $\Psi(t_0)$ can then be found through the solution of Eq. 2.1,

$$\Psi(\boldsymbol{x}_1 \dots \boldsymbol{x}_N, t) = \hat{U}(t, t_0)\Psi(\boldsymbol{x}_1 \dots \boldsymbol{x}_N, t_0) = e^{-i\hat{H}(t-t_0)}\Psi(\boldsymbol{x}_1 \dots \boldsymbol{x}_N, t_0), \tag{2.3}$$

with $U(t, t_0)$ as the unitary time evolution operator, propagating the initial state from time t_0 to time t. The states $\Psi(t_0)$ need not be one of the eigenstates from the TISE, but it can always be expanded using a linear combination of the eigenstates. In this thesis we will always apply $\Psi(t_0) = \Psi_0$, meaning that only the ground state will be propagated in time.

The Hamiltonian operator is commonly partitioned into terms acting on a different number of coordinates. Terms reducing to sums acting on n coordinates at a time are referred to as n-body terms. We will only consider one- and two-body contributions, generally expressed as

$$\hat{H} = \sum_{i=1}^{N} \hat{h}(\boldsymbol{x}_i) + \sum_{i>j}^{N} \hat{v}(\boldsymbol{x}_i, \boldsymbol{x}_j), \tag{2.4}$$

where $\hat{h}(\boldsymbol{x}_i)$ is the one-body term acting on a single-particle coordinate, while $\hat{v}(\boldsymbol{x}_i, \boldsymbol{x}_j)$ furnishes the two-body interaction, acting on two particle coordinates at a time. The particular expressions for $\hat{h}$ and $\hat{v}$ are system-dependent. For atoms and molecules, the general form of $\hat{H}$ is the *molecular Hamiltonian* [34],

$$\hat{H} = -\sum_{i=1}^{N} \frac{1}{2}\nabla_i^2 - \sum_{A=1}^{N} \frac{1}{2M_A}\nabla_A^2 - \sum_{i=1}^{N}\sum_{A=1}^{M} \frac{Z_A}{r_{iA}} + \sum_{i>j} \frac{1}{r_{ij}} + \sum_{A>B}^{M} \frac{Z_A Z_B}{r_{AB}}. \tag{2.5}$$

In Eq. 2.5, the indices i and A refer to the N electrons and M atomic nuclei in the system, respectively, with ∇_i^2 and ∇_A^2 as the corresponding Laplacian operators. Furthermore, we define $r_{iA} \equiv \|\boldsymbol{r}_i - \boldsymbol{r}_A\|$ as the relative electron-nucleus, $r_{ij} \equiv \|\boldsymbol{r}_i - \boldsymbol{r}_j\|$ electron-electron and $r_{AB} = \|\boldsymbol{r}_A - \boldsymbol{r}_B\|$ nucleus-nucleus distances. Lastly, Z_A is a (positive) integer, representing the charge of nucleus A, while M_A is the ratio of the nucleus and electron mass.

From left to right, the five terms of Eq. 2.5 account for the electron and nucleus kinetic energy, the electron-nucleus attraction, in addition to the electron-electron and the nucleus-nucleus repulsion. Here we have assumed the atomic nuclei to be point charges, neglecting any nucleon-nucleon interaction in addition to spin-orbit and relativistic effects. We will further only consider the electronic degrees of freedom, applying the Born-Oppenheimer approximation and thus fixing the positions of the nuclei. The nucleus only enters the problem as a static electric field, creating bound states of electrons. This reduces the two-body electron-nucleus attraction to a one-body external potential for the electrons. Additionally, for molecules containing multiple nuclei, the nucleus-nucleus repulsion can be integrated out, resulting in a constant nuclear repulsion energy contribution [34]. The result is the *electronic Hamiltonian*,

$$\hat{h}(\boldsymbol{x}_i) = -\frac{1}{2}\nabla_i^2 - \sum_{A=1}^{M} \frac{Z_A}{r_{iA}}, \quad \hat{v}(\boldsymbol{x}_i, \boldsymbol{x}_j) = \frac{1}{r_{ij}}, \tag{2.6}$$

here explicitly separated into one- and two-body terms, following Eq. 2.4. The electronic Hamiltonian of Eq. 2.6 accounts for the majority of electron properties in atoms and molecules.

Despite the various approximations leading to Eq. 2.6, finding solutions to the TISE presents a significant challenge. The only analytically solved atomic system with a full specter in the Bohr-Oppenheimer approximation is the hydrogen atom, where no electron-electron interaction is present. Solving the TISE as the ODE presented in Eq. 2.2 requires solving for a function of $3N$ variables. Discretizing space uniformly in each dimension using P points requires a total of P^{3N} points, quickly becoming infeasible even for small P. Furthermore, time propagation through Eq. 2.3 is also difficult, especially if the Hamiltonian is time-dependent. Common for many approximate methods is the introduction of a single-particle picture, applying a single function $\phi(\boldsymbol{x})$ to each of the individual particles. Assuming a separable solution, Ψ can be approximated as

$$\Phi_0^{\mathrm{H}}(\boldsymbol{x}_1, \ldots, \boldsymbol{x}_N) = \prod_{i=1}^{N} \phi_i(\boldsymbol{x}_i), \tag{2.7}$$

referred to as a *Hartree product*. However, for fermionic systems, this form is not satisfactory due to the lack of antisymmetry when exchanging particle coordinates. The simplest way to incorporate this is by ordering the states in a determinant, referred to as a Slater determinant (or simply a determinant),

$$\Phi_0(\boldsymbol{x}_1, \ldots, \boldsymbol{x}_N) = \frac{1}{\sqrt{N!}} \begin{vmatrix} \phi_1(\boldsymbol{x}_1) & \phi_2(\boldsymbol{x}_1) & \ldots & \phi_N(\boldsymbol{x}_1) \\ \phi_1(\boldsymbol{x}_2) & \phi_2(\boldsymbol{x}_2) & \ldots & \phi_N(\boldsymbol{x}_2) \\ \vdots & \vdots & \ddots & \vdots \\ \phi_1(\boldsymbol{x}_N) & \phi_2(\boldsymbol{x}_N) & \ldots & \phi_N(\boldsymbol{x}_N) \end{vmatrix}. \tag{2.8}$$

Due to the antisymmetric property of the determinant under an interchange of columns or rows, antisymmetry under particle exchange is naturally incorporated in Eq. 2.8. The methods presented later are all based on determinants similar to Eq. 2.8, which plays an integral part in approximative methods for fermionic systems. Additionally, linear combinations of different determinants will be important, which makes the form of Eq. 2.8 troublesome to work with. This motivates the introduction of a more compact formalism.

2.3 Second Quantization Representation

We will in the following give a brief overview of the *second quantization* formalism for spin-1/2 fermions [1]. Thereafter, the introduction of a finite basis will give us the tools to represent multiple determinants, in addition to the evaluation of inner products. The material presented here will follow closely Refs. [32, 34, 35], in particular Ref. [21].

2.3.1 Canonical Anticommutation Relations

The second quantization formalism introduces the creation operators $a_p^\dagger$ and annihilation operators a_p which, as the name entails, *create* and *annihilate* a particle in state p respectively. With $|0\rangle$ as the vacuum state, containing zero particles, and $|p\rangle$ as a single-particle state, the action of the creation and annihilation operators gives

$$a_p^\dagger |0\rangle = |\phi_p\rangle\,, \quad a_p |\phi_p\rangle = |0\rangle\,, \quad a_p^\dagger |p\rangle = 0, \quad a_p |0\rangle = 0. \tag{2.9}$$

Additionally, creation and annihilation operators enable us to work with states containing different amounts of particles, with a single $a_p^\dagger$ and a_p raising and lowering the particle number by one respectively. Furthermore, $a_p^\dagger$ and a_q follow the *canonical anticommutation relations* (CAR)

$$\{\, a_p^\dagger, a_q \,\} = a_p^\dagger a_q + a_q a_p^\dagger = \delta_{pq}, \quad \{\, a_p^\dagger, a_q^\dagger \,\} = \{\, a_p, a_q \,\} = 0. \tag{2.10}$$

Using Eq. 2.10, we can build multi-particle states with subsequent applications of creation operators,

$$|\phi_p \phi_q\rangle = a_p^\dagger a_q^\dagger |0\rangle = -a_q^\dagger a_p^\dagger |0\rangle = -|\phi_q \phi_p\rangle\,, \tag{2.11}$$

with the CAR assuring antisymmetry with particle exchange. This also implies that two particles can not occupy the same state,

$$\{\, a_p^\dagger, a_p^\dagger \,\} = a_p^\dagger a_p^\dagger + a_p^\dagger a_p^\dagger = 0 \implies a_p^\dagger a_p^\dagger = 0. \tag{2.12}$$

It is important to note that the state $|\phi_p \phi_q\rangle$ from Eq. 2.11 is *not* the tensor product of two states as the shorthand is commonly interpreted in quantum mechanics, that is

$$|\phi_p \phi_q\rangle \neq |\phi_p\rangle \otimes |\phi_q\rangle\,.$$

Rather it behaves like a determinant

$$|\phi_p \phi_q\rangle = \frac{1}{\sqrt{2}}(|\phi_p\rangle \otimes |\phi_q\rangle - |\phi_q\rangle \otimes |\phi_p\rangle),$$

which often leads to confusion. In fact, $|\phi_p \phi_q\rangle$ will be referred to as a determinant despite the coordinate representation $\langle \boldsymbol{x}_1 \boldsymbol{x}_2 | \phi_p \phi_q \rangle$ being the object commonly perceived as a determinant. This distinction is often interpreted from context, but for clarity when the state $|\phi_p\rangle \otimes |\phi_q\rangle$ is meant we will write $|pq\rangle$. Unfortunately, this jumble is inherited from the field, but in practice

[1] The proclamation of quantization being performed a second time might seem curious, implying some sort of first quantization. First quantization, in this context, refers to the fact that operators such as those in Eq. 2.6 often imply the discretization of observables, for instance, energy and momentum. This is of course not always the case, such as the free particle, but nevertheless, the name stuck. Alternative names such as occupation number representation might be more descriptive.

does not cause any major confusion. The coordinate space determinant given by Eq. 2.8 will therefore be exchanged in favor of

$$|\Phi_0\rangle = \prod_{i=1}^{N} a_i^\dagger |0\rangle \,, \tag{2.13}$$

which is usually referred to as the reference determinant, or the reference for short.

For practical calculations, a finite set of L basis functions is chosen

$$\mathcal{B} \equiv \{\, \phi_p(\boldsymbol{x}) \,\}_{p=1}^{L} \,,$$

referred to as the *basis set*. We partition $\mathcal{B}$ into two non-overlapping subsets:

$$\mathcal{B}_o \equiv \{\, \phi_i(\boldsymbol{x}) \,\}_{i=1}^{N} \,,$$

being the *occupied states* with N as the number of particles and

$$\mathcal{B}_v \equiv \{\, \phi_a(\boldsymbol{x}) \,\}_{a=N+1}^{L} \,,$$

being the *virtual states*, containing the $M \equiv L - N$ other functions not included in $\mathcal{B}_o$. For a clearer notation, the lexicographical indices $i, j, \ldots$ will be used for $\mathcal{B}_o$, $a, b, \ldots$ for $\mathcal{B}_v$ and $p, q, \ldots$ for $\mathcal{B}$. This alleviates the need for explicit ranges in sums since the specific symbol decides which functions we are referring to. The indices correspond to specific combinations of the relevant quantum numbers for the chosen basis set. For instance, choosing the solutions to the non-interacting one-dimensional harmonic oscillator gives a single principle quantum number n [36]. In the electronic case, we have to account for the two possible spin projections $m_s \in \{-\frac{1}{2}, +\frac{1}{2}\}$, despite not changing the functional form of the basis function at a specific n. Thus, to enumerate a basis function in $\mathcal{B}$, we map every n, m_s pair to a single number p.

2.3.2 Multiple Determinants

New determinants with the same number of particles as $|\Phi_0\rangle$ can be created by changing the single-particle states occupied in the reference. The annihilation operator a_i removes one particle from the occupied set and creates an $N-1$ particle state, called a *hole* state [2]. To move back to an N-particle state, we must act with a creation operator $a_a^\dagger$, adding back a virtual state (a particle). This determinant is called a *one-particle one-hole* (1p1h) excitation, related to the reference by

$$|\Phi_i^a\rangle = a_a^\dagger a_i \, |\Phi_0\rangle \,. \tag{2.14}$$

This combination of operators is so common that we define

$$\hat{X}_i^a \equiv a_a^\dagger a_i, \tag{2.15}$$

as a 1p1h excitation operator. By subsequent application of different particle and hole creation operators, we can create higher-order excited determinants, such as 2p2p states, 3p3p states, and so on. Alternatively, we refer to 1p1h excitations as "singles excitations", 2p2h as "doubles", and so on. If a large enough basis set is used, such that $L \geq 2N$, we can move as far as NpNh excited determinants. With n particle creation operators $ab\ldots$ and n hole creation operators $ij\ldots$ we can in general create an npnp excitation,

$$|\Phi_{ij\ldots}^{ab\ldots}\rangle = a_a^\dagger a_i a_b^\dagger a_j \ldots |\Phi_0\rangle = \hat{X}_i^a \hat{X}_j^b \ldots |\Phi_0\rangle = \hat{X}_{ij\ldots}^{ab\ldots} |\Phi_0\rangle \,. \tag{2.16}$$

In Eq. 2.16 we have defined

$$\hat{X}_{ij\ldots}^{ab\ldots} \equiv \hat{X}_i^a \hat{X}_i^b \ldots = a_a^\dagger a_i a_b^\dagger a_j \ldots, \tag{2.17}$$

as the n-fold excitation operator by the chained application of Eq. 2.15. All creation operators in Eq. 2.17 refer to states from the virtual sets, and all annihilation operators refer to states from the

[2] a_i can be interpreted as a hole creation operator.

occupied set. Therefore, the indices in Eq. 2.10 can never be equal and therefore their anticommutator will evaluate to zero [3]. Thus the excitation operators are antisymmetric with respect to an interchange of upper or lower indices,

$$\hat{X}^{ab\ldots}_{ij\ldots} = -\hat{X}^{ba\ldots}_{ij\ldots} = -\hat{X}^{ab\ldots}_{ji\ldots} = \hat{X}^{ba\ldots}_{ji\ldots} = \ldots. \tag{2.18}$$

Additionally, moving $\hat{X}^{ab\ldots}_{ij\ldots}$ past $\hat{X}^{cd\ldots}_{kl\ldots}$ requires an even number of second quantization operator permutations, meaning that they commute with each other independent of excitation order

$$\left[\hat{X}^{ab\ldots}_{ij\ldots}, \hat{X}^{cd\ldots}_{kl\ldots}\right] = 0. \tag{2.19}$$

By taking the hermitian conjugate of the excitation operators, we define de-excitation operators

$$(\hat{X}^{ab\ldots}_{ij\ldots})^\dagger = (a_a^\dagger a_i a_b^\dagger a_j \ldots)^\dagger = a_i^\dagger a_a a_j^\dagger a_b \ldots \equiv \hat{Y}^{ij\ldots}_{ab\ldots}, \tag{2.20}$$

which contains particle and hole annihilation operators. Therefore, applying Eq. 2.20 to an excited determinant will reduce the excitation level, if there is a correspondence between the indices in the state and the de-excitation operator. The antisymmetric and commutation properties of the excitation operators from Eqs. 2.18 and 2.19 are equally valid for the de-excitation operators. Importantly, however, excitation and de-excitation operators do not commute with each other

$$\left[\hat{X}^{ab\ldots}_{ij\ldots}, \hat{Y}^{ij\ldots}_{ab\ldots}\right] \neq 0. \tag{2.21}$$

Sums and products of multiple higher-order excitations become cumbersome due to the large number of indices. The notation used thus far will often be necessary, however, when we want to refer to a general excitation or de-excitation, we can apply an abstract notation common in quantum chemistry. Greek letters refer to excitation order (or excitation rank), meaning μ refers to a μpμp excitation. When we have a sum over one of these indices, it is understood that each order is also summed over internally. For instance, a linear combination of determinants with terms up to and including double determinants can be expressed as

$$C_0 \left|\Phi_0\right\rangle + \sum_{ai} C_i^a \hat{X}_i^a \left|\Phi_0\right\rangle + \sum_{\substack{a>b \\ i>j}} C_{ij}^{ab} \hat{X}_{ij}^{ab} \left|\Phi_0\right\rangle = \sum_{\mu=0}^{2} C_\mu \left|\Phi_\mu\right\rangle = \sum_{\mu=0}^{2} C_\mu \hat{X}_\mu \left|\Phi_0\right\rangle. \tag{2.22}$$

Considering the sum over doubly excited states in Eq. 2.22, we note the restriction on the particle and hole indices. This is due to the index permutation antisymmetry of Eq. 2.18, where removing the restrictions on one of the sums would introduce the same term appearing twice, with an opposite sign. Working with restricted sums can quickly become untidy. Thus, the same antisymmetry can be enforced on the coefficients $C_{ij}^{ab} = -C_{ij}^{ba} = \ldots$, mirroring the symmetry of the excitation operators. This gives us the ability to intentionally include symmetry redundant terms, which we can account for by a simple constant,

$$\sum_{\substack{a>b \\ i>j}} C_{ij}^{ab} \hat{X}_{ij}^{ab} \left|\Phi_0\right\rangle = \frac{1}{4} \sum_{abij} C_{ij}^{ab} \hat{X}_{ij}^{ab} \left|\Phi_0\right\rangle. \tag{2.23}$$

In general, for an n-fold excited determinant, there are $n!$ ways to permute the upper indices and $n!$ ways to permute the lower indices, giving a necessary factor of $(n!)^{-2}$ to account for the over counting. This can pose some confusion, for instance when considering derivatives with respect to C_{ij}^{ab}, as they are now *not* independent. However, the unrestricted sums of Eq. 2.23 are both easier to work with and more amendable for computer implementation, therefore being preferred in the final expressions.

[3] In the case that some of the virtual or occupied indices are equal, we whole chain will evaluate to zero since $a_a^\dagger a_a^\dagger = a_i a_i = 0$

2.3.3 Wick's Theorem

The introduction of what is now called *Wick's theorem* (WT) gives a structured method for the evaluation of inner products of second quantization operators [37]. Here we only present the results needed in practice. For a complete proof see for instance Ref. [38], while a more comprehensive exposition can be found in Ref. [21]. In particular, we will need the time-independent WT, ordered with respect to the reference determinant. This requires the introduction of two concepts, *normal ordering* and *contractions*. To aid the following discussion, we refer to a general composition of creation and annihilation operators as operator string

Normal ordering is a bookkeeping tool that we apply to an operator string, denoted as $\{\ldots\}$. When applied, the operators within are ordered such that all particle-hole creation operators are to the left of all particle-hole annihilation operators, such that the resulting operator string will yield zero when evaluated as a reference expectation value. With $\hat{Q}$ as a general operator string, while $\hat{R}$ is the normal ordered result, we have

$$\{\hat{Q}\} \equiv (-1)^{\sigma}\hat{R}, \quad \langle\Phi_0|\hat{R}|\Phi_0\rangle = 0. \tag{2.24}$$

In Eq. 2.24, a phase factor of $(-1)^{\sigma}$ needs to be included, where σ is the number of permutations required to achieve the normal ordering. Normal ordering differs from commutation, where commuting $a_a^\dagger$ and a_b yields a factor of δ_{ab} in addition to the sign change. The normal ordered product is in general not unique.

The contraction between two operators relates them with the corresponding normal ordered product. With $\hat{A}$ and $\hat{B}$ as either creation or annihilation operators, we define the contraction of $\hat{A}$ and $\hat{B}$ as

$$\overbrace{\hat{A}\hat{B}} \equiv \hat{A}\hat{B} - \{\hat{A}\hat{B}\}. \tag{2.25}$$

Applying the definition of Eq. 2.25 to every particle-hole contraction pair, we find that the only two non-zero contractions are

$$\overbrace{a_i^\dagger a_j} = \delta_{ij}, \qquad \overbrace{a_a a_b^\dagger} = \delta_{ab}. \tag{2.26}$$

From Eq. 2.26 the rules for general indices follow. Contracting a general creation or annihilation operator with particle-hole creation or annihilation operators gives

$$\begin{aligned} \overbrace{a_i^\dagger a_q} &= \delta_{iq}, & \overbrace{a_p^\dagger a_j} &= \delta_{pj}, \\ \overbrace{a_a a_p^\dagger} &= \delta_{ap}, & \overbrace{a_q a_b^\dagger} &= \delta_{qb}. \end{aligned} \tag{2.27}$$

Considering Eq. 2.27 we must exercise additional caution since the index p has a larger range that includes both a and i. In practice, this means that a sum over a and p containing a δ_{ap}, collapses the p sum to only be a sum over a (and not the other way around).

Lastly, the contractions between two general states p and q follow from Eqs. 2.26 and 2.27, where we must enforce the range when considering the specific contraction,

$$\overbrace{a_p^\dagger a_q} = \delta_{pq\in\mathcal{B}_o}, \qquad \overbrace{a_p a_q^\dagger} = \delta_{pq\in\mathcal{B}_v}. \tag{2.28}$$

With all possible contractions covered in Eqs. 2.26 to 2.28, we can consider general operator stings. A general operator string can be written as the sum over every possible contraction between operators

$$\hat{A}\hat{B}\hat{C}\hat{D}\ldots = \sum_{\substack{\text{all}\\ \text{ctr.}}} \left\{ \overbrace{\hat{A}\hat{B}\hat{C}\hat{D}}\ldots \right\}. \tag{2.29}$$

In Eq. 2.29 every possible contraction is considered (including zero contractions, one contraction, two contractions, and so on). Despite many contractions being trivially zero due to Eqs. 2.26 to 2.28, this still yields numerous terms. However, since the single contractions always yield a scalar (the Kronecker delta), terms without fully contracted operators can be written as a chain of Kronecker deltas multiplied by a normal ordered string. Hence, when this is evaluated in an

inner product between the reference states, every partially contracted term will be zero, leaving only the fully contracted terms

$$\langle\Phi_0|\hat{A}\hat{B}\hat{C}\hat{D}\ldots|\Phi_0\rangle = \sum_{\substack{\text{all full}\\ \text{ctr.}}} \left\{ \hat{A}\hat{B}\hat{C}\hat{D}\ldots \right\}. \tag{2.30}$$

The simplification from Eq. 2.29 to Eq. 2.30 is very useful for direct calculations. However, we will almost always deal with products of different normal ordered strings. This allows for the application of the *generalized Wick's theorem* (GWT) [39]. Here the only possible non-zero contractions are those between different normal ordered strings. In particular, when considering inner products between different excited determinants, the usefulness of the GWT is paramount since both the excitation and de-excitation operators are in normal order, giving

$$\langle\Phi_\mu|\Phi_\nu\rangle = \langle\Phi_0|\hat{Y}_\mu\hat{X}_\nu|\Phi_0\rangle = \delta_{\mu\nu}, \tag{2.31}$$

displaying that unique determinants are orthonormal. If both of the operator strings $\hat{A}$ and $\hat{B}$ are individually normal ordered, we define the sum of every non-zero contraction where at least one of the operators from $\hat{A}$ is connected to $\hat{B}$ as $\{\hat{A}\hat{B}\}_\text{c}$. Using Eq. 2.25, we can then write the product of $\hat{A}$ and $\hat{B}$ as

$$\hat{A}\hat{B} = \{\hat{A}\hat{B}\} + \{\hat{A}\hat{B}\}_\text{c}. \tag{2.32}$$

Calculations using WT and GWT are not explicitly presented in what follows but serve as the cornerstone for all evaluations of inner products in this thesis.

2.4 Operators

Following the discussion on multiparticle states and inner products, we continue with discussing how operators are resented in the second quantization formalism. We begin by rewriting the one- and two-body components of the Hamiltonian using creation and annihilation operators. Thereafter, the introduction of reduced density matrices will allow us to compute general operator expectation values. Lastly, following the introduction of time-dependent Hamiltonians, we will discuss how the absorption spectrum of different systems can be estimated from real-time calculations.

2.4.1 Hamiltonians

To complete our discussion on the second quantization formalism, we will express the many-body Hamiltonian from Eq. 2.4 using creating and annihilation operators. Given a choice of a single-particle basis, we need the corresponding matrix representations of the one- and two-body operators

$$\langle p|\hat{h}|q\rangle \equiv h_{pq} = \int \mathrm{d}\boldsymbol{x}\, \phi_p^*(\boldsymbol{x})\hat{h}(\boldsymbol{x})\phi_q(\boldsymbol{x}), \tag{2.33}$$

$$\langle pq|\hat{v}|rs\rangle \equiv v_{rs}^{pq} = \int \mathrm{d}\boldsymbol{x}\,\mathrm{d}\boldsymbol{x}'\, \phi_p^*(\boldsymbol{x})\phi_q^*(\boldsymbol{x}')\hat{v}(\boldsymbol{x},\boldsymbol{x}')\phi_r(\boldsymbol{x})\phi_s(\boldsymbol{x}'), \tag{2.34}$$

which we collectively call the matrix elements. The one-body matrix elements of Eq. 2.33 are hermitian $h_{pq}^* = h_{qp}$, while the two-body matrix elements of Eq. 2.34 are symmetric concerning simultaneous interchange of upper and lower indices, $v_{rs}^{pq} = v_{sr}^{qp}$, in addition to being hermitian in the sense that $(v_{rs}^{pq})^* = v_{pq}^{rs}$. Additionally, by defining the *antisymmetric matrix element* $u_{rs}^{pq} \equiv v_{rs}^{pq} - v_{sr}^{pq}$, we gain antisymmetry when interchanging upper or lower indices, $u_{rs}^{pq} = -u_{sr}^{pq} = -u_{rs}^{qp} = u_{sr}^{qp}$. The Hamiltonian from Eq. 2.4 can then by expressed as

$$\hat{H} = \hat{H}_0 + \hat{W} = \sum_{pq} h_{pq} a_p^\dagger a_q + \frac{1}{4}\sum_{pqrs} u_{rs}^{pq} a_p^\dagger a_q^\dagger a_s a_r, \tag{2.35}$$

with $\hat{H}_0$ and $\hat{W}$ containing the one- and two-body terms respectively. Since the indices p, q, r, and s refer to both virtual and occupied states, Eq. 2.35 is not normal ordered with respect to the reference state. By the application of WT we rewrite $\hat{H}$ as

$$\hat{H} = E_{\text{ref}} + \sum_{pq} h_{pq} \{ a_p^\dagger a_q \} + \sum_{pqi} u_{qi}^{pi} \{ a_p^\dagger a_q \} + \frac{1}{4} \sum_{pqrs} u_{rs}^{pq} \{ a_p^\dagger a_q^\dagger a_s a_r \}, \tag{2.36}$$

where we have defined E_{ref} as the *reference energy*, appearing as a new effective "zero-body" operator, being the reference state expectation value of $\hat{H}$

$$E_{\text{ref}} = \langle \Phi_0 | \hat{H} | \Phi_0 \rangle = \sum_i h_{ii} + \frac{1}{2} \sum_{ij} u_{ij}^{ij}. \tag{2.37}$$

All other terms of Eq. 2.36 are explicitly normal ordered with respect to the reference. We now have two one-body terms, which we collect in the definition of a new one-body operator referred to as the *Fock operator* $\hat{F}_N$

$$f_{pq} \equiv h_{pq} + \sum_i u_{qi}^{pi}, \quad \hat{F}_N \equiv f_{pq} \{ a_p^\dagger a_q \}. \tag{2.38}$$

Similarly, defining the normal ordered two-body term as $\hat{W}_{\text{N}}$, we express the Hamiltonian as the reference energy and a fully normal ordered Hamiltonian $\hat{H}_{\text{N}}$

$$\hat{H} = E_{\text{ref}} + \hat{F}_{\text{N}} + \hat{W}_{\text{N}} = E_{\text{ref}} + \hat{H}_{\text{N}}. \tag{2.39}$$

We will separate energy expectation values of Eq. 2.39 into two main contributions, namely the introduced reference energy contribution and the $\hat{H}_{\text{N}}$ contribution, referred to as the *correlation energy*. The separation into reference and correlation energy is not only practical but also illustrates the two different regimes we will be working with. Improving the reference energy is done by methods considering only a single determinant, where the mean-field Hartree-Fock method is most prevalent. We will focus on the correlation energy contribution, where electron correlations are included through the excited determinants.

2.4.2 General Operators and Densities

The matrix representation of Eqs. 2.33 and 2.34 are not exclusive to energy operators. Exchanging the operators with an arbitrary one-body operator $\hat{A}(\boldsymbol{x})$ and two-body operator $\hat{B}(\boldsymbol{x}, \boldsymbol{x}')$, we can compute additional observables using the single-particle basis. Defining the *reduced one-body density* of a state $|\Psi\rangle$ as

$$\gamma_{qp} \equiv \langle \Psi | a_p^\dagger a_q | \Psi \rangle, \tag{2.40}$$

and considering the one-body operators $\hat{A}$:

$$\hat{A} = \sum_{pq} A_{pq} a_p^\dagger a_q, \tag{2.41}$$

we can calculate the expectation value of $\hat{A}$ using Eq. 2.40,

$$\langle A \rangle = \langle \Psi | \hat{A} | \Psi \rangle = \sum_{pq} A_{pq} \langle \Psi | a_p^\dagger a_q | \Psi \rangle = \sum_{pq} A_{pq} \gamma_{qp} = \text{tr}\,(\gamma A). \tag{2.42}$$

Here $\text{tr}\,(\dots)$ in Eq. 2.42 denotes the matrix trace. The one-body density is hermitian, $\gamma_{pq} = \gamma_{qp}^*$, with a trace equal to the number of particles, $\text{tr}\,(\gamma) = N$. Similarly, the *reduced two-body density* is defined as

$$\Gamma_{pq}^{rs} \equiv \langle \Psi | a_p^\dagger a_q^\dagger a_s a_r | \Psi \rangle. \tag{2.43}$$

Considering the two-body operator $\hat{B}$:

$$\hat{B} = \frac{1}{4} \sum_{pqrs} B_{rs}^{pq} a_p^\dagger a_q^\dagger a_s a_r, \tag{2.44}$$

where the matrix elements are made to be antisymmetric in exchange of upper and lower index, $B^{pq}_{rs} = -B^{pq}_{sr} = -B^{qp}_{rs} = B^{qp}_{sr}$, the expectation value of $\hat{B}$ can be calculated using Eq. 2.43

$$\langle B \rangle = \langle \Psi | \hat{B} | \Psi \rangle = \frac{1}{2} \sum_{pqrs} B^{pq}_{rs} \langle \Psi | a^\dagger_p a^\dagger_q a_s a_r | \Psi \rangle = \frac{1}{2} \sum_{pqrs} B^{pq}_{rs} \Gamma^{rs}_{pq}. \tag{2.45}$$

From the CAR we also find the two-body density to be antisymmetric in upper and lower indices $\Gamma^{pq}_{rs} = -\Gamma^{qp}_{rs} = -\Gamma^{pq}_{sr} = \Gamma^{qp}_{sr}$ in addition to the hermitian-like property $(\Gamma^{pq}_{rs})^* = \Gamma^{rs}_{pq}$. Considering the complete sum of Γ^{pq}_{pq}, we can by commuting a_p to $a^\dagger_p$ see that

$$\sum_{pq} \langle \Psi | a^\dagger_p a^\dagger_q a_q a_p | \Psi \rangle = \sum_{pq} \langle \Psi | a^\dagger_p a_p a^\dagger_q a_q | \Psi \rangle - \sum_{p} \langle \Psi | a^\dagger_p a_p | \Psi \rangle = N(N-1), \tag{2.46}$$

where Eq. 2.46 will be referred to as the trace of the reduced two-body density. The reduced one-body density is related to the particle density,

$$\rho(\boldsymbol{r}) = \sum_{pq} \phi^*_p(\boldsymbol{r}) \gamma_{qp} \phi_q(\boldsymbol{r}), \tag{2.47}$$

being the spatial electron density which when integrated over $\boldsymbol{r}$ gives N.

Other than the energy expectation value, we will consider the electric dipole and quadrupole moments with the convention of Ref. [40]. We partition the total dipole moment of a molecule into two contributions $\boldsymbol{\mu}^{\text{nuc}}$ and $\boldsymbol{\mu}^{\text{e}}$ which accounts for the positively charged nuclei and negatively charged electrons respectively, with $\boldsymbol{\mu} = \boldsymbol{\mu}^{\text{nuc}} + \boldsymbol{\mu}^{\text{e}}$ giving the total dipole moment. In the Born-Oppenheimer approximation, the nuclei are treated as point charges, giving the contribution

$$\mu^{\text{nuc}}_\alpha = \sum_A Z_A r_{A\alpha}, \tag{2.48}$$

with α representing one of the three cartesian coordinates x, y and z, while Z_A and $\boldsymbol{r}_A$ represents the nuclei charges and positions respectively. On the other hand, the electrons are treated quantum mechanically, which when accounting for the negative charge can be expressed using the particle density of Eq. 2.47 giving

$$\mu^{\text{e}}_\alpha = -\int \mathrm{d}\boldsymbol{r} \rho(\boldsymbol{r}) r_\alpha = -\sum_{pq} \gamma_{qp} \langle p | r_\alpha | q \rangle . \tag{2.49}$$

Thus to compute the electron dipole moment from Eq. 2.49, the matrix elements of the position operator must be calculated in the single-particle basis.

Moving on to the quadrupole moment, we consider a 3×3 matrix index by the cartesian coordinates $\alpha, \beta = x, y, z$

$$Q_{\alpha\beta} = Q^{\text{nuc}}_{\alpha\beta} + Q^{\text{e}}_{\alpha\beta}, \tag{2.50}$$

where we again have a contribution from the classically treated nuclei $Q^{\text{nuc}}_{\alpha\beta}$ and quantum mechanically treated electrons $Q^{\text{e}}_{\alpha\beta}$. The nuclear quadrupole moment is a sum of point charges, given in traceless form as

$$Q^{\text{nuc}}_{\alpha\beta} = \frac{1}{2} \sum_I Z_I \left(r_{I\alpha} r_{I\beta} - \boldsymbol{r}^2_I \delta_{\alpha\beta} \right). \tag{2.51}$$

The electronic quadrupole moment is an integral over Eq. 2.47

$$Q^{\text{e}}_{\alpha\beta} = -\frac{1}{2} \int \mathrm{d}\boldsymbol{r} \rho(\boldsymbol{r}) \left(3 r_\alpha r_\beta - \boldsymbol{r}^2 \delta_{\alpha\beta} \right) = \sum_{pq} \gamma_{qp} Q^{\alpha\beta}_{pq}, \tag{2.52}$$

where we have defined

$$Q^{\alpha\beta}_{pq} \equiv \frac{1}{2} \left(\langle p | r_\alpha r_\beta | q \rangle - \delta_{\alpha\beta} \langle p | \boldsymbol{r}^2 | q \rangle \right), \tag{2.53}$$

being the matrix representation of the electron quadrupole operator. Equation 2.53 requires computing the quadratic and cross terms of two position operators ($x^2, xy, \ldots$) using the single-particle basis functions.

We will always consider our system in the nuclear charge center, placing the origin at

$$\boldsymbol{r}_c \equiv \sum_A \frac{Z_A}{Z_{\text{tot}}} \boldsymbol{r}_A, \quad Z_{\text{tot}} = \sum_A Z_A. \tag{2.54}$$

Translating the coordinate system following Eq. 2.54 has the convenient property of reducing the nuclear dipole moment of Eq. 2.48 to zero, such that $\mu_\alpha = \mu_\alpha^{\text{e}}$. This does however not remove the nuclear quadrupole moment of Eq. 2.51.

For a complete ab initio treatment, different methods would yield slightly different values for $Q_{\alpha\beta}^{\text{nuc}}$. This is because the energy of a molecule can be optimized with respect to the positions of the different nuclei, known as geometry optimization [41–43].

However, we will only compare the dipole and quadrupole moments between methods at a constant equilibrium geometry, such that $Q_{\alpha\beta}^{\text{nuc}}$ will be method-independent. Therefore, Eqs. 2.49 and 2.52 will be referred to as the dipole and quadrupole moment henceforth.

2.4.3 Time-Dependent Hamiltonians

The time-dependent potentials we have applied in this work all consider the system interacting with an external monochromatic electromagnetic field $\boldsymbol{E}(r,t)$. We will assume that the wavelength of $\boldsymbol{E}$ is large when compared to the system size, such that the field can be treated within the dipole approximation. This reduces the field to be spatially homogeneous, only being dependent on time $\boldsymbol{E}(\boldsymbol{r},t) \approx \boldsymbol{E}(t)$. The electromagnetic field can then be expressed in the dipole approximation as [44],

$$\boldsymbol{E}_\alpha(t) = \sin(\omega t) G(t) \boldsymbol{\epsilon}, \tag{2.55}$$

where ω is the field frequency, $G(t)$ the time-dependent electric field amplitude and $\boldsymbol{\epsilon}$ the unit polarization vector. Coupling the electric field to the time-dependent Hamiltonian, we consider the interaction operator

$$\hat{V}(t) = -\hat{\boldsymbol{\mu}} \cdot \boldsymbol{E}(t), \tag{2.56}$$

here expressed in length gauge, where $\hat{\boldsymbol{\mu}}$ is the dipole operator. The interaction operator of Eq. 2.56 can be expressed as a one-body operator in the second quantization formalism as

$$\hat{V}(t) = \sum_{pq} v_{pq}(t) a_p^\dagger a_q, \tag{2.57}$$

where $v_{pq}(t)$ are the time-dependent matrix elements

$$v_{pq}(t) = \sum_\alpha \langle p | r_\alpha | q \rangle \, E_\alpha(t). \tag{2.58}$$

Equation 2.58 shows that the time dependence of the interaction potential only resides in the field, where the single-particle basis functions are fixed during propagation. The density matrices from Eqs. 2.40 and 2.43 however will evolve in time, meaning that expectation values such as the energy will change when the system moves away from the ground state. Due to the field being treated in a semi-classical way, the total energy will not be constant when Eq. 2.56 is non-zero.

A particular application of the time propagation presented here is the ability to estimate excitation energies through the time-dependent dipole moment. With the ground state as the initial state at $t_0 = 0$, we apply an external potential until some time t'. The interaction potential will add energy to the system, where the propagated state can be expressed as a linear combination of excited states, with coefficients $c_A(t')$ determined at time t'. Through Eq. 2.3, the evolution after t' is determined by the excited state energies. Thus, after the interaction has been turned off, the system follows

$$|\Psi(t)\rangle = \sum_A c_A(t') e^{-iE_A t} |\Psi_A\rangle, \tag{2.59}$$

with $t > t'$. Each dipole moment component of the state can then be calculated as a function of time,

$$\mu_\alpha(t) = \langle\Psi(t)|\hat{\mu}_\alpha|\Psi(t)\rangle = \sum_{AB} c_A^*(t')c_B(t')e^{i(E_A-E_B)t}\langle\Psi_A|\hat{\mu}_\alpha|\Psi_B\rangle\,. \tag{2.60}$$

Defining the energy difference between two excited states as $\Delta E_{AB} \equiv E_A - E_B$, the Fourier transform of Eq. 2.60 yields

$$\tilde{\mu}_\alpha(\omega) = \frac{1}{2\pi}\int \mathrm{d}t\mu_\alpha(t)e^{-i\omega t} = \sum_{AB} c_A^*(t')c_B(t')\delta(\Delta E_{AB}-\omega)\langle\Psi_A|\hat{\mu}_\alpha|\Psi_B\rangle\,. \tag{2.61}$$

The right-hand side of Eq. 2.61 illuminates how the Fourier transformed dipole moment relates to excitation energies. Firstly, the presence of the delta function means that $\tilde{\mu}_\alpha(\omega)$ gives non-zero values only when the frequency is equal to one of the possible eigenstate transitions. However, $\langle\Psi_A|\hat{\mu}_\alpha|\Psi_B\rangle$ has to be non-zero for this particular transition, meaning it must be dipole allowed. Additionally, the effect of the interaction potential must result in a state which is populated by both $|\Psi_A\rangle$ and $|\Psi_B\rangle$, such that $c_A(t') \neq 0$ and $c_B(t') \neq 0$ for $\tilde{\mu}_\alpha(\omega)$ to be non-zero for this particular transition.

The properties of Eq. 2.61 can be used to estimate an absorption spectrum for different systems. We define the induced dipole moment [45]

$$\mu^I_{\alpha\beta}(t) \equiv \mu_{\alpha\beta}(t) - \mu_\alpha(0), \tag{2.62}$$

with $\mu^I_{\alpha\beta}(t)$ being the α component of the induced dipole moment when the field is polarized in the β direction, while $\mu_\alpha(0)$ is the α component of the permanent dipole moment in the ground state without an external field. The Fourier transform of the induced dipole moment is then used to calculate the dipole polarization tensor [45],

$$A_{\alpha\beta}(\omega) = \frac{1}{2\pi}\int \mathrm{d}t\,\mu^I_{\alpha\beta}(t)e^{-\gamma t}e^{-i\omega t}, \tag{2.63}$$

where the induced dipole signal is modulated by an exponentially decaying damping factor $\exp(-\gamma t)$. We apply a constant $\gamma > 0$ value to ensure that the induced dipole moment vanishes at large times, artificially making the time-dependent state move towards the time-independent ground state. The imaginary part of the dipole polarization tensor is related to the dipole-allowed absorption spectrum through [45, 46]

$$S(\omega) = \frac{4\pi\omega}{3c}\,\mathrm{Im}\{A_{xx}(\omega) + A_{yy}(\omega) + A_{zz}(\omega)\}, \tag{2.64}$$

where c is the speed of light in vacuum. Equation 2.64 is a function that peaks around energy transition frequencies, similar to that of Eq. 2.61. In obtaining $S(\omega)$, we calculate the three field polarizations independently, such that the ground state is propagated for $\boldsymbol{\epsilon} = \hat{\boldsymbol{e}}_x, \hat{\boldsymbol{e}}_y$, and $\hat{\boldsymbol{e}}_z$. For atoms, the diagonal terms of Eq. 2.63 are independent of polarization direction such that $A_{xx}(\omega) = A_{yy}(\omega) = A_{zz}(\omega)$. Linear molecules are invariant under continuous rotations around the symmetry axis, meaning that two dipole polarization tensor components are required. Therefore, we need to compute $A_{\alpha\alpha}$ with the field polarized parallel and orthogonal to the symmetry axis. For general molecules, all three diagonal components of the dipole polarization tensor are independent. Thus, dependent on system symmetries, one to three calculations are required to obtain the absorption spectrum [47].

Which states we manage to populate in Eq. 2.60 depends on the Fourier transform of the external potential from Eq. 2.55. If a single frequency is used, the choice must lay in the neighborhood of an excited state energy, referred to as a resonance frequency [44]. A particularly useful choice is a weak δ-kick perturbation [46],

$$\boldsymbol{E}_{\text{kick}} \equiv \kappa\delta(t)\boldsymbol{\epsilon}, \tag{2.65}$$

where κ is the field strength. Equation 2.65 is physically unrealizable, but serves as a good theoretical tool due to the Fourier transform being a constant. Thus, every dipole-allowed transition to excited states could occur and if κ is weak enough, only transitions from the ground state will be present.

2.5 Spin Restriction

Thus far, the basis functions we have discussed include the spin degree of freedom, $\phi_p(\boldsymbol{x}) = \phi_p(\boldsymbol{r}, \sigma)$. We separate the spin projection from the index p, such that $p = (P, \sigma)$, with σ being the spin projection and P being the other relevant quantum numbers. For each P, there are two different spin projections $\sigma = \uparrow, \downarrow$ corresponding to the orthonormal spinors

$$\chi(\uparrow) = \begin{pmatrix} 1 \\ 0 \end{pmatrix}, \quad \chi(\downarrow) = \begin{pmatrix} 0 \\ 1 \end{pmatrix}. \tag{2.66}$$

Thereafter, we express a single-particle state as $\phi_p(\boldsymbol{x}) = \phi_{P\sigma}(\boldsymbol{x}) = \phi_P(\boldsymbol{r})\chi(\sigma)$, where $\phi_P(\boldsymbol{r})$ is a spatial basis function. We will only deal with closed-shell systems with a spin-independent Hamiltonian. The usefulness of this space-spin separation is apparent by considering the evaluation of the one-body matrix element from Eq. 2.33, with $\hat{h}(\boldsymbol{x}) = \hat{h}(\boldsymbol{r})$,

$$h_{pq} = \langle p|\hat{h}|q\rangle = \langle P\sigma_p|\hat{h}|Q\sigma_q\rangle = \langle \sigma_p|\sigma_q\rangle \int \mathrm{d}\boldsymbol{r}\, \phi_P^*(\boldsymbol{r})\hat{h}(\boldsymbol{r})\phi_Q(\boldsymbol{r}) \equiv \delta_{\sigma_p\sigma_q} h_{PQ} \tag{2.67}$$

with σ_p and σ_q being the spin projections of state p and q respectively, while the spinor inner product reduces to $\delta_{\sigma_p\sigma_q}$ using Eq. 2.66. Working with h_{PQ} instead of h_{pq} reduces the number of matrix elements by a factor of four. Performing the same operations on Eq. 2.34 gives v_{RS}^{PQ}, reducing the number of elements by a factor of 16. This is known as a spin-restriction, where the basis set is effectively halved, such that $\{\phi_p\}_{p=1}^{L} \to \{\phi_P\}_{P=1}^{L/2}$ where L is even.

The restricted scheme can be formulated by introducing the singlet excitation operator [32]

$$\hat{E}_{PQ} = a_{P\uparrow}^\dagger a_{Q\uparrow} + a_{P\downarrow}^\dagger a_{Q\downarrow}, \tag{2.68}$$

with $a_{P\sigma}^\dagger$ and $a_{P\sigma}$ creating an annihilating $|P\sigma\rangle$, respectively. We define restricted versions of the singles and doubles excitation operators as [48],

$$\hat{X}_I^A \equiv \hat{E}_{AI}, \quad \hat{X}_{IJ}^{AB} \equiv \hat{E}_{AI}\hat{E}_{BJ}, \tag{2.69}$$

in addition to the singles and doubles de-excitation operators,

$$\hat{Y}_A^I \equiv \hat{E}_{IA}, \quad \hat{Y}_{AB}^{IJ} \equiv \frac{1}{3}\hat{E}_{JB}\hat{E}_{IA} + \frac{1}{6}\hat{E}_{IB}\hat{E}_{JA}. \tag{2.70}$$

Equations 2.69 and 2.70 are defined such that

$$\langle \Phi_\mu|\Phi_\nu\rangle = \langle \Phi_0|\hat{Y}_\mu\hat{X}_\nu|\Phi_0\rangle = \delta_{\mu\nu}. \tag{2.71}$$

Lastly, a general Hamiltonian with a one- and two-body term can be expressed as [32]

$$\hat{H} = \sum_{PQ} h_{PQ}\hat{E}_{PQ} + \frac{1}{2}\sum_{PQRS} v_{RS}^{PQ}\left(\hat{E}_{PQ}\hat{E}_{RS} - \delta_{QR}\hat{E}_{PS}\right), \tag{2.72}$$

where the two-body matrix elements are no longer antisymmetric, but still symmetric wrt. simultaneous exchange of upper and lower indices $v_{RS}^{PQ} = v_{SR}^{QP}$.

The definition of restricted excitation and de-excitation operators allows us to develop a general theory applicable to both general and restricted schemes. However, when explicit expressions are required, the relevant operator must be applied.

2.6 Hartree-Fock Theory

The Hartree-Fock (HF) method optimizes the reference energy by considering a single-particle change of basis, constrained to give orthonormal basis functions. Originally Hartree [7] devised a scheme applying the Hartree product (Eq. 2.7) as the many-body state, but due to the lack of antisymmetry from particle exchange the method was unsuitable for fermionic systems. Fock and

Slater [8, 9] independently expanded the framework, applying the Slater Determinant (Eq. 2.8). We will consider HF in a fixed single-particle basis, resulting in the *Roothaan-Hall* equations [34].

Let $\phi(\boldsymbol{x})$ represent the chosen single-particle basis, while $\tilde{\phi}_p(\boldsymbol{x})$ represents the HF basis. The two bases are related through the transformation

$$\tilde{\phi}_p(\boldsymbol{x}) = \sum_q C_{qp}\phi_q(\boldsymbol{x}), \tag{2.73}$$

where C_{qp} are in general complex coefficients, determining the change of basis. The HF method minimizes the reference energy with respect to the coefficients C,

$$\begin{aligned}\mathcal{E}[\{\phi_p\}] &= \sum_i \tilde{h}_{ii} + \frac{1}{2}\sum_{ij}\tilde{u}_{ij}^{ij} \\ &= \sum_i\sum_{pq} C_{pi}^* C_{qi} h_{pq} + \frac{1}{2}\sum_{ij}\sum_{pqrs} C_{pi}^* C_{qj}^* C_{ri} C_{sj} u_{rs}^{pq},\end{aligned} \tag{2.74}$$

where the tilde denotes that the matrix elements are expressed in the HF basis. Additionally, we constrain the minimization to only produce orthonormal basis functions. This allows the chosen basis functions to not necessarily be orthonormal, but the transformation to the HF basis will always yield orthonormal basis functions. Basis function overlaps are calculated through

$$\langle p|q\rangle \equiv s_{pq} = \int \mathrm{d}x \phi_p(\boldsymbol{x})^* \phi_q(\boldsymbol{x}),$$

which we use to formulate the orthonormality constraint, with ϵ_{ij} as Lagrange multipliers

$$\begin{aligned}\mathcal{C}[\{\phi_p\}] &= \sum_{ij}\epsilon_{ji}\left(\delta_{ij} - \tilde{s}_{ij}\right) \\ &= \sum_{ij}\sum_{pq}\epsilon_{ji}\left(\delta_{ij} - C_{pi}^* C_{qj} s_{pq}\right) = 0.\end{aligned} \tag{2.75}$$

Combining the energy functional of Eq. 2.74 with the orthonormality constraint, we find the Lagrangian to be

$$\mathcal{L}[\{C_{pq}\}] = \mathcal{E}[\{\phi_p\}] + \mathcal{C}[\{\phi_p\}]. \tag{2.76}$$

Thereafter, we minimize $\mathcal{L}$ with respect to the coefficients C_{pq}^* [4]. The derivative of the constraint is

$$\frac{\partial \mathcal{C}}{\partial C_{pq}^*} = -\sum_r s_{pr} C_{rj}\epsilon_{jq}., \tag{2.77}$$

while the derivative of the energy functional

$$\frac{\partial \mathcal{E}}{\partial C_{pq}^*} = \sum_r h_{pr} C_{rq} + \sum_{rst}\rho_{ts} u_{rs}^{pt} C_{rq} = \sum_r F_{pr} C_{rq}, \quad \rho_{ts} \equiv \sum_i C_{ti}^* C_{si}. \tag{2.78}$$

In Eq. 2.78, we have defined ρ as the HF density matrix, while F_{pq} are the matrix elements of the Fock operator (similar to Eq. 2.38), where the occupied states are transformed to the HF basis,

$$F_{pq} = \langle p|\hat{h}|q\rangle + \sum_i \langle p\tilde{i}|\hat{u}|q\tilde{i}\rangle\,.$$

The derivative of $\mathcal{L}$ then follows from Eqs. 2.77 and 2.78, giving the *non-canonical HF equations*

$$\frac{\partial \mathcal{L}}{\partial C_{pq}^*} = 0 \implies F_{pr} C_{rq} = s_{pr} C_{rj}\epsilon_{jq}. \tag{2.79}$$

Further simplifications are possible following Eq. 2.79. Firstly, consider the Lagrangian multipliers in Eq. 2.76. Since the Lagrangian is a real quantity, ϵ_{ij} must be hermitian when considering

[4] $\mathcal{L}$ is real, optimizing wrt. C_{pq} only gives the conjugated equation.

$s_{ij}^* = s_{ji}$ and can thus be diagonalized by a unitary transformation. By enforcing ϵ_{ji} to be diagonal through the C_{pq} transformation, Eq. 2.79 reduces to a generalized eigenvalue problem

$$F(C)C = sC\epsilon, \tag{2.80}$$

which is known as the *canonical HF equations*, or in particular the Roothaan-Hall equations since we have applied a finite basis. It is important to note that F in Eq. 2.80 depend on the coefficients C. Therefore, this eigenvalue problem must be solved iteratively by guessing the initial C matrix.

Furthermore, the presence of the overlap matrix in Eq. 2.80 is unproblematic, and there are various methods to deal with this [49]. However, changing s_{ij} changes the inner product between the basis functions, and thus C will not be a unitary transformation. If the fixed basis applied is orthonormal, no special consideration is needed and the resulting transformation will be unitary.

When later methods are presented, we will always discuss methods and perform calculations applying an optimized HF basis. This relies on finding a solution to Eq. 2.80, and thereafter transforming the matrix elements through Eq. 2.73. Not only will the reference energy improve, but other properties such as having orthonormal basis functions will be crucial for what follows. Importantly, Brillouin's theorem states that in an HF basis, the matrix element of the many-body Hamiltonian between the reference and a singly excited determinant must be zero [50]

$$\langle \Phi_0 | \hat{H} | \Phi_i^a \rangle = 0, \tag{2.81}$$

which corresponds to a diagonal Fock matrix. The assurance of Eq. 2.81 reduces the importance of singly excited determinants in a multi-determinant approximation since $\hat{H}$ can not connect the reference directly with singles determinants. However, single excitations can and will contribute through higher-order excitations such as $|\Phi_{ij}^{ab}\rangle$ [34].

2.7 Configuration Interaction

The full configuration interaction (FCI) method is one of the most important post-HF methods. Given a single-particle basis, an FCI calculation will give the exact result (within the specific basis). Unfortunately, for large basis sets and a large number of particles, such calculations are unfeasible. However, it serves as a great benchmarking tool when applied to small basis sets.

We begin by expanding a state as a linear combination of every possible excited determinant available for the system in question,

$$|\Psi\rangle = \sum_{\mu=0}^{N} \hat{C}_\mu |\Phi_0\rangle, \qquad \hat{C}_\mu = C_\mu \hat{X}_\mu, \tag{2.82}$$

where the coefficients $C_\mu = C_0, C_i^a, C_{ij}^{ab}, \ldots$ are the parameters we need to determine. Applying a variational treatment, the coefficients can be determined by optimizing the energy gradient with respect to the complex conjugate of the coefficients as we did in the HF case

$$E = \frac{\langle \Psi | \hat{H} | \Psi \rangle}{\langle \Psi | \Psi \rangle}, \qquad \frac{\partial E}{\partial C_\mu^*} = 0. \tag{2.83}$$

Rearranging Eq. 2.83 and expanding through Eq. 2.82 we get,

$$\begin{aligned} E \langle \Psi | \Psi \rangle &= \langle \Psi | \hat{H} | \Psi \rangle, \\ E \sum_\nu C_\nu^* C_\nu &= \sum_{\nu\sigma} C_\sigma^* C_\nu \langle \Phi_\sigma | \hat{H} | \Phi_\nu \rangle, \end{aligned} \tag{2.84}$$

$$\frac{\partial E}{\partial C_\mu^*} \sum_\nu C_\nu^* C_\nu + E C_\mu = \sum_\nu C_\nu \langle \Phi_\mu | \hat{H} | \Phi_\nu \rangle, \tag{2.85}$$

where we have used the orthonormallity properties of the excited determinants and the derivative with respect to C_μ^* has been applied in Eq. 2.85. Lastly, inserting the stationary condition of Eq. 2.83 into Eq. 2.85 we recognize the solution as an eigenvalue problem,

$$\sum_\nu H_{\mu\nu} C_\nu = E C_\mu, \tag{2.86}$$

where we have defined the block matrix $H_{\mu\nu} = \langle \Phi_\mu | \hat{H} | \Phi_\nu \rangle$. In the process of diagonalizing $H_{\mu\nu}$, the sets of eigenvalues and eigenvectors are of special importance. By considering the double derivative of Eq. 2.83, one can show that the solution to Eq. 2.86 with the smallest eigenvalue corresponds to the minima of Eq. 2.83. Furthermore, the second largest is a first-order saddle point, the third a second-order saddle point, and so on [32]. We associate these solutions with the ground state and excited states respectively, all of which are available to us when performing an FCI calculation.

Unfortunately, an FCI calculation requires the consideration of the number of determinants N_D growing as

$$N_\mathrm{D} = \binom{L}{N},, \tag{2.87}$$

giving a factorial time and space complexity. This motivates the truncation of Eq. 2.82 to include fewer determinants. A natural approach is starting with the inclusion of smaller excitation orders, such as only including 1p1h determinants (named "S" for singles), only 2p2h ("D" for doubles), and so on. This creates a hierarchy of truncated FCI methods, following the naming convention CIX where X are the excited determinants included. The most popular truncations for intermediate-sized systems are those of CID and CISD accounting for most of the correlation energy when considering atoms and molecules at equilibrium geometries [51]. Due to the determinant combinatorics, the complexity of such a method is dominated by the highest excitation order m, which scales as $\mathcal{O}(N^m M^{m+2})$ [52]. This places CID and CISD in the $\mathcal{O}(n^6)$ range, with n being the system size.

An important property of truncated CI methods comes from the Hylleraas-Undheim theorem [53, 54]. This guarantees that energies calculated in a reduced determinant space $\mathcal{S}'$ increase with respect to the larger space $\mathcal{S}$ if $\mathcal{S}'$ is a subspace of $\mathcal{S}$ [5]. As a consequence of the Hylleraas-Undheim theorem, these truncations will all be variational, getting closer and closer to the FCI solution when larger determinant spaces are considered.

[5] And of course calculated in the same basis set

Chapter 3

Coupled Cluster Theory

Coupled cluster (CC) theory originated in the late 1950s, developed by Coester and Kümmel to tackle problems in the field of nuclear physics [16, 17]. In 1966, Čížek reformulated the method to atomic and molecular problems [55], popularizing the method in the field of quantum chemistry.

We begin by introducing the exponential ansatz, the most characteristic attribute of CC theories, and discuss some consequences of this choice. Thereafter, how the CC equations are solved is discussed, focusing on why the perturbative approach is the natural choice. However, this leads to some challenges, in particular regarding how expectation values should be evaluated. By taking a brief interlude, and introducing the bivariational principle, a resolution to these problems is presented.

With the tools from the bivariational formalism, quadratic CC can be defined. Subsequently, the time evolution of both standard and quadratic CC is discussed, and finalized by the derivation of the EOMs for QCCSD. Lastly, a novel introduction of configurational weights is introduced to investigate the determinant composition of the CC parametrizations.

3.1 Cluster Operators

Common for all CC calculations is the introduction of excitation *cluster operators* $\hat{T}_n$. These operators create a linear combination of every possible rank-n excitation, defined by

$$\hat{T}_n \equiv \frac{1}{(n!)^2} \sum_{\substack{ab\ldots \\ ij\ldots}} \tau_{ij\ldots}^{ab\ldots} \hat{X}_{ij\ldots}^{ab\ldots} \equiv \frac{1}{(n!)^2} \sum_{\substack{ab\ldots \\ ij\ldots}} \tau_{ij\ldots}^{ab\ldots} a_a^\dagger a_i a_b^\dagger a_j \ldots, \tag{3.1}$$

where $\tau_{ij\ldots}^{ab\ldots}$ are coefficients deciding the importance from each excited determinant, referred to as the amplitudes. If a real single-particle basis is chosen, the amplitudes will in the time-independent case remain real. However, they are in general complex quantities, being especially apparent when considering propagation in time. The lack of sum restrictions gives antisymmetry in upper and lower index permutations such as Eq. 2.23. For most use cases, the relevant operators are $\hat{T}_1$ and $\hat{T}_2$, given explicitly as

$$\hat{T}_1 = \sum_{ai} \tau_i^a \hat{X}_i^a = \sum_{ai} \tau_i^a a_a^\dagger a_i, \tag{3.2}$$

$$\hat{T}_2 = \frac{1}{4} \sum_{abij} \tau_{ij}^{ab} \hat{X}_{ij}^{ab} = \frac{1}{4} \sum_{abij} \tau_{ij}^{ab} a_a^\dagger a_i a_b^\dagger a_j. \tag{3.3}$$

From the CAR, we know that particle excitation operators commute according to Eq. 2.19, which implies that cluster operators must commute as well

$$\left[\hat{T}_n, \hat{T}_m\right] = 0.$$

Closely related to the $\hat{T}_n$ operators are the de-excitation cluster operators $\hat{\Lambda}_n$. Instead of creating an excited determinant that increases the excitation rank, we now de-excite and lower the excitation rank. Resembling Eq. 3.1, the rank-n de-excitation cluster operator is defined by

$$\hat{\Lambda}_n \equiv \frac{1}{(n!)^2} \sum_{\substack{ab\ldots \\ ij\ldots}} \lambda_{ab\ldots}^{ij\ldots} \hat{Y}_{ab\ldots}^{ij\ldots} = \frac{1}{(n!)^2} \sum_{\substack{ab\ldots \\ ij\ldots}} \lambda_{ab\ldots}^{ij\ldots} a_i^\dagger a_a a_j^\dagger a_b. \tag{3.4}$$

The structure of the $\hat{\Lambda}_n$ operators give many of the same properties as $\hat{T}_n$, that is antisymmetric rank-2 amplitudes (λ_{ab}^{ij}) and commutation between $\hat{\Lambda}_n$ and $\hat{\Lambda}_m$. It is important to note however that excitation and de-excitation cluster operators do not commute, that is

$$\left[\hat{T}_n, \hat{\Lambda}_m\right] \neq 0. \tag{3.5}$$

Lastly, we collect cluster excitation operators and de-excitation operators of different ranks

$$\hat{T} = \sum_{\mu \geq 1} \tau_\mu \hat{X}_\mu = \hat{T}_1 + \hat{T}_2 + \ldots, \tag{3.6}$$

$$\hat{\Lambda} = \sum_{\mu \geq 1} \lambda_\mu \hat{Y}_\mu = \hat{\Lambda}_1 + \hat{\Lambda}_2 + \ldots, \tag{3.7}$$

where $\hat{T}$ and $\hat{\Lambda}$ create and annihilate every excited determinant respectively.

3.2 Projected Coupled Cluster Theory

The following section presents some general features of CC theory, in addition to how and why solving for the amplitudes is performed in a projected manner when only energy calculations are considered.

3.2.1 The Ansatz

In coupled-cluster theory, an exponential ansatz is used to represent the many-body state[1]

$$|\Psi\rangle = e^{\hat{T}} |\Phi_0\rangle, \tag{3.8}$$

[1]To minimize the number of sub- and superscripts, Ψ will be presented with a subscript only when compared to states from a different method. If no subscript is present, the exponential ansatz is assumed.

with $|\Phi_0\rangle$ as the reference determinant, defined in Eq. 2.13. In contrast to the linear parametrization of FCI from Eq. 2.82, the CC ansatz from Eq. 3.8 is nonlinear. Expanding the exponential and collecting terms corresponding to the same excitation orders we get

$$\begin{aligned} |\Psi_{\text{CC}}\rangle &= \left(1 + \hat{T} + \frac{1}{2!}\hat{T}^2 + \frac{1}{3!}\hat{T}^3 + \dots\right)|\Phi_0\rangle\,, \\ &= \left(1 + \hat{T}_1 + \left[\hat{T}_2 + \frac{1}{2}\hat{T}_1^2\right] + \left[\hat{T}_3 + \hat{T}_1\hat{T}_2 + \frac{1}{6}\hat{T}_1^3\right] + \dots\right)|\Phi_0\rangle\,. \end{aligned} \tag{3.9}$$

Similarly, the linear FCI ansatz is expanded as

$$|\Psi_{\text{FCI}}\rangle = \left(1 + \hat{C}_1 + \hat{C}_2 + \hat{C}_3 + \dots\right)|\Phi_0\rangle\,, \tag{3.10}$$

where we have used intermediate normalization $\langle\Phi_0|\Psi_{\text{FCI}}\rangle = C_0 = 1$. Comparing order by order, we find a direct map between the $\hat{C}_n$ operators of FCI and $\hat{T}_n$ cluster operators

$$\hat{C}_1 = \hat{T}_1, \tag{3.11}$$

$$\hat{C}_2 = \hat{T}_2 + \frac{1}{2}\hat{T}_1^2, \tag{3.12}$$

$$\hat{C}_3 = \hat{T}_3 + \hat{T}_1\hat{T}_2 + \frac{1}{6}\hat{T}_1^3. \tag{3.13}$$

Expressions for general $\hat{C}_n$ and $\hat{T}_n$ relations are found in the literature, for instance in Ref. [56]. Importantly, each $\hat{C}_n$ order has contributions from $\hat{T}_n$ and terms of lower excitation rank. This means that both $\hat{C}$ and $\hat{T}$ contains the same number of parameters and by recursion we can invert the relation expressing every $\hat{T}_n$ using parts from $\hat{C}$ such as in Eqs. 3.14 to 3.16

$$\hat{T}_1 = \hat{C}_1, \tag{3.14}$$

$$\hat{T}_2 = \hat{C}_2 - \frac{1}{2}\hat{C}_1^2, \tag{3.15}$$

$$\hat{T}_3 = \hat{C}_3 - \hat{C}_1\hat{C}_2 + \frac{1}{3}\hat{C}_1^3. \tag{3.16}$$

Again this can be generalized to $n > 3$. Consequently, FCI and CC are equal when all cluster operators are included, being two different parametrizations of the same state. However, as discussed in Sec. 2.7, the inclusion of every excitation operator, be it $\hat{C}$ or $\hat{T}$, yields exponentially scaling calculations that are intractable for larger systems. Therefore, just as in CI, the cluster operator has to be truncated in practice. The naming convention follows that of truncated CI, where the inclusion of just $\hat{T} \approx \hat{T}_2$ is label CCD (doubles), $\hat{T} \approx \hat{T}_1 + \hat{T}_2$ CCSD (singles and doubles) and so on.

Considering the singles and doubles truncation, we repeat the comparison of Eqs. 3.9 and 3.10 giving the expanded CISD and CCSD states

$$|\Psi_{\text{CISD}}\rangle = \left(1 + \hat{C}_1 + \hat{C}_2\right)|\Phi_0\rangle\,, \tag{3.17}$$

$$\begin{aligned} |\Psi_{\text{CCSD}}\rangle &= \left(1 + \hat{T} + \frac{1}{2}\hat{T}^2 + \frac{1}{6}\hat{T}^3 + \dots\right)|\Phi_0\rangle\,, \\ &= \left(1 + \hat{T}_1 + \left[\hat{T}_2 + \frac{1}{2}\hat{T}_1^2\right] + \left[\hat{T}_1\hat{T}_2 + \frac{1}{6}\hat{T}_1^3\right] + \dots\right)|\Phi_0\rangle\,. \end{aligned} \tag{3.18}$$

The linear ansatz of Eq. 3.17 only includes singles and doubles excitations. This is in contrast to the exponential ansatz of Eq. 3.18, where higher-order excitations are created through repeated applications of $\hat{T}_1$ and $\hat{T}_2$ cluster operators. However, there is a nuance to this, since these higher excitations are given in terms of the τ_a^i and τ_{ij}^{ab} amplitudes. Therefore, the higher-order excitation coefficients are decided by the single and double excitations.

Another benefit of CC over CI is that, when the expansions of Eqs. 3.9 and 3.10 are truncated, the former is size-consistent while the latter is not [20, 35]. As mentioned in the introduction, size-consistency is a property of an approximative method. Considering two non-interacting subsystems A and B, an energy calculation of the composite system $E(AB)$ should be equal to the sum of two energy calculations where each subsystem is considered separately [57]. That is

$$E(AB) = E(A) + E(B),$$

with $E(A)$ and $E(B)$ representing the energy from two separate calculation on subsystem A and B respectively. The exponential ansatz from Eq. 3.8 encompasses the key property that the wave function of two non-interactive systems are multiplicatively separable, ensuring additively of energy [21]. This property will be especially important for us when performing calculations in bond breaking regions.

It should be mentioned that the very similar concept of size-extensivity is often discussed in tandem with size-consistency, with the two terms being notoriously used interchangeably [58]. This property is not consistently defined in the literature and is almost exclusively discussed for perturbative methods. Size-extensivity generally describes the property of $NE(A) = E(NA)$ when considering N non-interacting subsystems A, with similar relations for other quantities. Concerning the version of size-extensivity presented here regarding energies, it is an implication of size-consistency.

3.2.2 Solving for the Amplitudes

Starting with the exponential ansatz from Eq. 3.8, the time-independent Schrödinger equation takes the form

$$\hat{H}e^{\hat{T}}\left|\Phi_0\right\rangle = Ee^{\hat{T}}\left|\Phi_0\right\rangle. \tag{3.19}$$

The most natural approach for solving Eq. 3.19 would be to consider Hamiltonian expectation value

$$E = \frac{\langle\Phi_0|e^{\hat{T}^\dagger}\hat{H}e^{\hat{T}}|\Phi_0\rangle}{\langle\Phi_0|e^{\hat{T}^\dagger}e^{\hat{T}}|\Phi_0\rangle}, \tag{3.20}$$

and perform a variational optimization with respect to the amplitudes τ. This method however is not feasible. Inverting the operator exponential requires a sign change in the argument, thus a consequence of $\exp(\hat{T}^\dagger) \neq \exp(-\hat{T})$ is an explicit calculation of the normalization in Eq. 3.20. Thus, expanding the denominator we find

$$\langle\Phi_0|e^{\hat{T}^\dagger}e^{\hat{T}}|\Phi_0\rangle = \langle\Phi_0|\left[1+\hat{T}^\dagger+\frac{1}{2}(\hat{T}^\dagger)^2+\ldots\right]\left[1+\hat{T}+\frac{1}{2}\hat{T}^2+\ldots\right]|\Phi_0\rangle \neq 1. \tag{3.21}$$

Evaluating the normalization of Eq. 3.21 involves computing numerous inner products that feature lengthy second quantization operator strings. Additionally, expanding the numerator of Eq. 3.20 in the same manner, poses the same problem. For a variational treatment, the number of inner products to evaluate scales with the number of particles N, giving the same complexity as that of FCI [35]. If additionally $\hat{T}$ is truncated, the FCI complexity remains while the quality of the result will not reproduce FCI due to higher-order excitations being approximated by the amplitudes corresponding to the truncation level.

This approach was performed at the doubles level in Ref. [24] under the name variational coupled cluster doubles (VCCD). The reasoning behind this was not to construct a post-HF method to approximate FCI, but rather measure the inherent error of the CCD parametrization. Attempts at variational treatment of Eq. 3.20 applied to more realistic systems are collectively referred to as variational coupled cluster (VCC) [59], which all rely on truncating the expansion at some order. Higher-order excitations are in general less important, legitimizing the removal of higher-order terms. However, where to perform the truncation is not an easy task, and there is not a general good choice when considering arbitrary systems.

Efforts in constructing a unitary exponential ansatz have also been made, collectively referred to as unitary coupled cluster (UCC) [60, 61]. These methods often define $\hat{\sigma} \equiv \hat{T} - \hat{T}^\dagger$, using $\hat{\sigma}$ in the exponential ansatz instead. This fulfills $\exp(\sigma^\dagger) = \exp(-\sigma)$, making the state normalized. The expansion required to calculate the $\hat{H}$ expectation value however still does not terminate at any fixed order, such that an arbitrary truncation is necessary.

The traditional way of resolving the problem of Eq. 3.20, considers projecting the reference onto Eq. 3.19, resulting in

$$\langle\Phi_0|\hat{H}e^{\hat{T}}|\Phi_0\rangle = E, \tag{3.22}$$

where intermediate normalization $\langle\Phi_0|\Psi\rangle = 1$ ensures that there is no inner product to evaluate on the right-hand side. The left-hand side, however, contains an inner product that truncates

exactly at double excitations in the exponential expansion. Similarly, we can project excited determinants onto Eq. 3.19, giving a set of non-linear equations for the amplitudes

$$\langle \Phi_\mu | \hat{H} e^{\hat{T}} | \Phi_0 \rangle = E \langle \Phi_\mu | e^{\hat{T}} | \Phi_0 \rangle . \tag{3.23}$$

Eqs. 3.22 and 3.23 can be solved through fix-point iterations, and are collectively called the unlinked coupled cluster equations [35]. The presence of the energy in Eq. 3.23 gives a coupling between the amplitude and energy equations, such that they can not be solved independently. In practice, the unlinked form is cumbersome to work with.

Commonly we rather use another set of equations, referred to as the linked coupled cluster equations [20, 21, 35]. Instead of directly projecting with the reference, we rather preemptively multiply Eq. 3.19 by $\exp\left(-\hat{T}\right)$ giving

$$e^{-\hat{T}} \hat{H} e^{\hat{T}} |\Phi_0\rangle = \overline{H} |\Phi_0\rangle = E |\Phi_0\rangle , \tag{3.24}$$

where we have defined $\overline{H} = \exp(-\hat{T})\hat{H}\exp(\hat{T})$ which constitutes a similarity transform of the Hamiltonian, aptly referred to as the similarity transformed Hamiltonian. Since $\hat{H}$ and $\overline{H}$ are related through a similarity transformation, they share the same spectrum and thus will have the same energy. If we now perform the reference and excited determinant projections, we arrive at the linked CC equations

$$\langle \Phi_0 | \overline{H} | \Phi_0 \rangle = E_{\text{ref}} + \langle \Phi_0 | \overline{H}_{\text{N}} | \Phi_0 \rangle = E, \tag{3.25}$$

$$\langle \Phi_\mu | \overline{H} | \Phi_0 \rangle = \langle \Phi_\mu | \overline{H}_{\text{N}} | \Phi_0 \rangle = 0, \quad \mu \geq 1. \tag{3.26}$$

Note that reference energy in Eqs. 3.25 and 3.26 separates naturally in the similarity transformation, where $\overline{H}_{\text{N}}$ is the contributions containing second quantization operators. Now the amplitude equations of Eq. 3.25 do not depend on the energy, meaning that they are not coupled anymore. Secondly, the similarity transformed $\overline{H}$ remarkably truncates at a finite order of $\hat{T}$, independent of both the number of particles and excitation orders included. Using the Hausdorff expansion [35], $\overline{H}$ can be expanded as a sum of chained commutators

$$\overline{H} = e^{-\hat{T}} \hat{H} e^{\hat{T}} = \hat{H} + \left[\hat{H}, \hat{T}\right] + \frac{1}{2!}\left[\left[\hat{H}, \hat{T}\right], \hat{T}\right] + \frac{1}{3!}\left[\left[\left[\hat{H}, \hat{T}\right], \hat{T}\right], \hat{T}\right] + \ldots . \tag{3.27}$$

In the case where $\hat{T}$ appears on the left-hand side of $\hat{H}$, this product can be expanded using Eq. 2.32 since both $\hat{T}$ and $\hat{H}$ are normal ordered, giving

$$\hat{H}\hat{T} = \{\hat{H}\hat{T}\} + \{\hat{H}\hat{T}\}_{\text{c}}. \tag{3.28}$$

If we consider Hamiltonians containing one- and two-body operators, we can at most have a product of four creation and annihilation operators. The connected terms of $\{\hat{H}\hat{T}\}_{\text{c}}$, by definition, need one Wick contraction with at least one operator from $\hat{H}$. Thus, $\{\hat{H}\hat{T}\}_{\text{c}}$ can at most contain products of three second quantization operators.

If we rather consider the case where $\hat{T}$ appears on the right-hand side of $\hat{H}$, we know that *any* contraction between $\hat{T}$ and $\hat{H}$ will yield zero since $\hat{T}$ contains only $a_a^\dagger$ and a_i operators which gives $\{\hat{T}\hat{H}\}_{\text{c}} = 0$. Furthermore, since both $\hat{T}$ and $\hat{H}$ contain an even number of operators, no sign change can occur when interchanging them inside the normal order product. Therefore the product can be expressed as

$$\hat{T}\hat{H} = \{\hat{T}\hat{H}\} + \{\hat{T}\hat{H}\}_{\text{c}} = \left\{\hat{H}\hat{T}\right\} . \tag{3.29}$$

Using Eqs. 3.28 and 3.29 we have the necessary tools to simplify the first commutator in the Hausdorff expansion of Eq. 3.27. This gives

$$\left[\hat{H}, \hat{T}\right] = \{\hat{H}\hat{T}\}_{\text{c}}. \tag{3.30}$$

The connected term $\{\hat{H}\hat{T}\}_{\text{c}}$ is again a new operator with an even number of second quantization operators, but now $\hat{H}$ has at most three second quantization operators available for further contractions. Repeating the argument gives the second commutator

$$\left[\left[\hat{H}, \hat{T}\right], \hat{T}\right] = \{\{\hat{H}\hat{T}\}_{\text{c}}\hat{T}\}_{\text{c}}, \tag{3.31}$$

which is a new normal ordered operator with at most two available connections to $\hat{H}$. Considering then the third and fourth commutator of Eq. 3.27, we get similar chains of connected terms. However, the fifth commutator will give zero, since every second quantization operator in $\hat{H}$ is connected to one of the $\hat{T}$ operators. Consequently, the Hausdorff expansion from Eq. 3.27 truncates at the fourth order of nested commutators, drastically reducing the complexity of the necessary terms.

The Hausdorff expansion of the similarity-transformed Hamiltonian is often written as

$$\overline{H} = \{\hat{H}e^{\hat{T}}\}_{\mathrm{c}}, \tag{3.32}$$

where we now only get contributions from connected terms where $\hat{T}$ appears on the right-hand side of $\hat{H}$ with at most four $\hat{T}$ operators.

3.2.3 Expectation Values

The perturbative nature of the CC theory presented thus far is mostly concerned with finding a manageable solution for ground state energy calculations. However, there exists a multitude of other quantities and expectation values to calculate for a given system, which might be difficult to properly represent using the CC ansatz of Eq. 3.8. If a CC calculation gives a ground state energy close to that of an exact FCI calculation, the quality of the approximate state is not guaranteed to be satisfactory as $|\Psi_{\mathrm{CC}}\rangle$ might not be a good representation of $|\Psi_{\mathrm{FCI}}\rangle$.

We will illustrate this by considering how an expectation value $\langle A\rangle$ of a general operator $\hat{A}$ might be calculated. The variational expectation value,

$$\langle A\rangle = \frac{\langle\Psi|\hat{A}|\Psi\rangle}{\langle\Psi|\Psi\rangle} = \frac{\langle\Phi_0|e^{\hat{T}^\dagger}\hat{A}e^{\hat{T}}|\Phi_0\rangle}{\langle\Phi_0|e^{\hat{T}^\dagger}e^{\hat{T}}|\Phi_0\rangle}, \tag{3.33}$$

would seem like a reasonable starting point. However, as discussed in Sec. 3.2.2, the presence of the exp $(\hat{T}^\dagger)$ operator to the left of $\hat{A}$ results in an expansion that only truncates at the N-particle limit. Expansion truncation at various orders of $\hat{T}$ has been applied, see for example Refs. [55, 62]. However, such an expansion is problematic for the same reasons as Eq. 3.20. Additionally, the amplitudes τ are not determined variationally which is an issue. Inserting $\hat{A} = \hat{H}$ gives a different energy from what is obtained by solving Eq. 3.25.

Following the similarity transformation approach of Eq. 3.24, another possibility is to define the expectation value of an operator $\hat{A}$ as

$$\langle A\rangle = \langle\Phi_0|e^{-\hat{T}}\hat{A}e^{\hat{T}}|\Phi_0\rangle\,, \tag{3.34}$$

which we know from Sec. 3.2.2 truncates at second or fourth order in $\hat{T}$ if $\hat{A}$ is a one or two-body operator respectively. If $\hat{A} = \hat{H}$, we instantly recover the CC energy given by Eq. 3.25. In the case where $\hat{T}$ includes every excitation order, Eq. 3.34 is identical to Eq. 3.33 since

$$\begin{aligned}
\langle\Phi_0|e^{\hat{T}^\dagger}\hat{A}e^{\hat{T}}|\Phi_0\rangle &= \langle\Phi_0|e^{\hat{T}^\dagger}e^{\hat{T}}(e^{-\hat{T}}\hat{A}e^{\hat{T}})|\Phi_0\rangle\,, \\
&= \sum_{\mu=0}^{N}\langle\Phi_0|e^{\hat{T}^\dagger}e^{\hat{T}}\,|\Phi_\mu\rangle\langle\Phi_\mu|\,e^{-\hat{T}}\hat{A}e^{\hat{T}}|\Phi_0\rangle\,, \\
&= \langle\Phi_0|e^{\hat{T}^\dagger}e^{\hat{T}}|\Phi_0\rangle\langle\Phi_0|e^{-\hat{T}}\hat{A}e^{\hat{T}}|\Phi_0\rangle\,.
\end{aligned} \tag{3.35}$$

In Eq. 3.35 we have applied the many-body resolution of the identity, where only the reference projection of the similarity transformed $\hat{A}$ is non-zero from Eq. 3.26. This approach has been discussed in Ref. [56], but has not been widely applied.

There is however a major drawback with both the suggested approaches of Eqs. 3.33 and 3.34. The Hellmann-Feynmann theorem [63] states that a first-order perturbation of the energy by an operator $\hat{A}$ can be used to calculate the expectation value of $\hat{A}$ by considering a derivative with respect to its (small) perturbation $\epsilon \in \mathbb{R}$,

$$\frac{\partial}{\partial\epsilon}E(\hat{H}+\epsilon\hat{A})\Big|_{\epsilon=0} = \langle A\rangle\,. \tag{3.36}$$

Neither approach obeys the Hellmann-Feynmann theorem [32, 64].

3.3 Bivariational Formulation

The most common approach to deal with the theoretical problems described in Sec. 3.2.3 reformulates the CC theory presented previously as a functional minimization problem. From the discussion in Sec. 3.2.2, invoking the variational principle directly results in a computationally impractical problem.

Originally introduced by Arponen [65], the CC ansatz can be parameterized by two independent states, where we aim for a stationary functional with respect to variations of both states. In practice, this is done by introducing a new set of amplitudes, associated with the new parameterization. Helgaker and Jørgensen independently introduced the same formalism [66, 67], interpreting the new amplitudes as Lagrange multipliers for a constrained optimization problem.

In the context of standard CC calculations for static properties, regarding the new amplitudes as Lagrange multipliers or novel wave function parameters does not significantly impact the work described in this study. However, in the discussion of extended theories and dynamical processes, interpreting the new amplitudes as wave function parameters on an equal footing with τ becomes more helpful.

3.3.1 The Bivariational Principle

The bivariational principle (BIVP) takes the energy functional [64, 65, 68, 69]

$$\mathcal{H}[\Psi', \Psi] = \frac{\langle \Psi' | \hat{H} | \Psi \rangle}{\langle \Psi' | \Psi \rangle}, \tag{3.37}$$

as the starting point, where $\langle \Psi' |$ and $| \Psi \rangle$ are two independent state parameterizations, referred to hereon as the left- and right-states. In the language of variational calculus, we consider small variations in Ψ' and Ψ such that Eq. 3.37 is stationary. Starting with the left-state, we find

$$\mathcal{H}[\Psi' + \delta\Psi', \Psi] = \frac{\langle \Psi' + \delta\Psi' | \hat{H} | \Psi \rangle}{\langle \Psi' + \delta\Psi' | \Psi \rangle} = \frac{\langle \Psi' | \hat{H} | \Psi \rangle + \langle \delta\Psi' | \hat{H} | \Psi \rangle}{\langle \Psi' | \Psi \rangle + \langle \delta\Psi' | \Psi \rangle}. \tag{3.38}$$

We expand the denominator in Eq. 3.38 using the relation

$$(1 + x)^{-1} = 1 - x + x^2 + \dots,$$

which to the first order in the variation gives

$$\begin{aligned} \left[\langle \Psi' | \Psi \rangle + \langle \delta\Psi' | \Psi \rangle \right]^{-1} &= \langle \Psi' | \Psi \rangle^{-1} \left[1 + \frac{\langle \delta\Psi' | \Psi \rangle}{\langle \Psi' | \Psi \rangle} \right]^{-1}, \\ &= \langle \Psi' | \Psi \rangle^{-1} \left[1 - \frac{\langle \delta\Psi' | \Psi \rangle}{\langle \Psi' | \Psi \rangle} \right] + \mathcal{O}(\delta\Psi'^2). \end{aligned} \tag{3.39}$$

Inserting the result from Eq. 3.39 back into Eq. 3.37 and only keeping terms up to first order in the variation yields

$$\begin{aligned} \mathcal{H}[\Psi' + \delta\Psi', \Psi] &= \frac{\langle \Psi' | \hat{H} | \Psi \rangle}{\langle \Psi' | \Psi \rangle} + \frac{\langle \delta\Psi' | \hat{H} | \Psi \rangle}{\langle \Psi' | \Psi \rangle} - \frac{\langle \Psi' | \hat{H} | \Psi \rangle}{\langle \Psi' | \Psi \rangle} \frac{\langle \delta\Psi' | \Psi \rangle}{\langle \Psi' | \Psi \rangle}, \\ &= \mathcal{H}[\Psi', \Psi] + \frac{\langle \delta\Psi' | \hat{H} - \mathcal{H}[\Psi', \Psi] | \Psi \rangle}{\langle \Psi' | \Psi \rangle}. \end{aligned} \tag{3.40}$$

Similarly, calculating the variation of Eq. 3.37 with respect to the right state we find that

$$\mathcal{H}[\Psi', \Psi + \delta\Psi] = \mathcal{H}[\Psi', \Psi] + \frac{\langle \Psi' | \hat{H} - \mathcal{H}[\Psi', \Psi] | \delta\Psi \rangle}{\langle \Psi' | \Psi \rangle}. \tag{3.41}$$

Demanding that the response in $\mathcal{H}$ from arbitrary $\delta\Psi$ and $\delta\Psi'$ variations vanishes for some particular configuration Ψ'_*, Ψ_* we find two eigenvalue equations

$$\hat{H} | \Psi_* \rangle = \mathcal{H}[\Psi'_*, \Psi_*] | \Psi_* \rangle, \tag{3.42}$$

$$\langle \Psi'_* | \hat{H} = \langle \Psi'_* | \mathcal{H}[\Psi'_*, \Psi_*], \tag{3.43}$$

under the assumption that $\langle \Psi' | \Psi \rangle \neq 0$.

From Eqs. 3.42 and 3.43 we note that the stationary functional results in a pair of left- and right-eigenvalues with the same eigenvalue, which we define as the energy of the system

$$E \equiv \mathcal{H}[\Psi'_*, \Psi_*].$$

Furthermore, the normalization of Eq. 3.37 can be resolved by redefining $\langle \widetilde{\Psi}| = \langle \Psi'| \,/\, \langle \Psi' | \Psi \rangle$ as the left-state. This simplifies the energy functional to

$$\mathcal{H}[\widetilde{\Psi}, \Psi] = \langle \widetilde{\Psi} | \hat{H} | \Psi \rangle \,, \tag{3.44}$$

which equals the energy of the system when evaluated at the stationary point. The two parameterizations now represent a normalized state in the sense that $\langle \widetilde{\Psi} | \Psi \rangle = 1$. In contrast to the variational principle, the BIVP does not in general provide an upper bound to the ground state energy [64]. However, defining the expectation value of an operator $\hat{A}$ as

$$\langle \hat{A} \rangle = \langle \widetilde{\Psi} | \hat{A} | \Psi \rangle$$

the Hellmann-Feynamnn theorem is obeyed if the left- and right-states are derived from the stationary point of Eq. 3.44 [64].

3.3.2 Coupled Cluster Functional

We will now apply the formalism from Sec. 3.3.1 with specific $\langle \widetilde{\Psi}|$ and $|\Psi\rangle$ parameterizations. The standard choices are

$$|\Psi\rangle = e^{\hat{T}} |\Phi_0\rangle \,, \quad \langle \widetilde{\Psi}| = \langle \Phi_0| \,(1 + \hat{\Lambda}) e^{-\hat{T}}, \tag{3.45}$$

where $|\Psi\rangle$ is the same parameterization as applied in Eq. 3.8, while we allow $\langle \widetilde{\Psi}|$ to contain the de-excitation cluster operators from Eq. 3.7. The left-state contains the inverse of the exponentiated excitation cluster operators, such that $\langle \widetilde{\Psi} | \Psi \rangle = 1$ is obeyed. With the energy functional of Eq. 3.44, this parameterization yields

$$\mathcal{H} = \langle \Phi_0 | (1 + \hat{\Lambda}) e^{-\hat{T}} \hat{H} e^{\hat{T}} | \Phi_0 \rangle \,. \tag{3.46}$$

In finding the stationary points of Eq. 3.46, we require the derivatives of $\mathcal{H}$ with respect to the parameters τ and λ to be zero.

$$\frac{\partial \mathcal{H}}{\partial \tau_\mu} = 0, \quad \frac{\partial \mathcal{H}}{\partial \lambda_\mu} = 0.$$

Starting with λ, we note that the only dependence resides in $\hat{\Lambda}$

$$\frac{\partial \hat{\Lambda}}{\partial \lambda_\mu} = \frac{\partial \lambda_\nu}{\partial \lambda_\mu} \hat{Y}_\nu = \hat{Y}_\mu,$$

consequently, we find

$$\frac{\partial \mathcal{H}}{\partial \lambda_\mu} = \langle \Phi_0 | \hat{Y}_\mu e^{-\hat{T}} H e^{\hat{T}} | \Phi_0 \rangle = \langle \Phi_\mu | \overline{H} | \Phi_0 \rangle = 0, \tag{3.47}$$

which we recognize as the linked τ amplitude equation of Eq. 3.26. Importantly, this equation is independent of λ. The algebraic expression for the CCSD τ equations is presented in Eqs. C.2 and C.3.

Considering the derivative with respect to τ, the only dependence is present in $\exp\left(\pm\hat{T}\right)$. Using this we find

$$\frac{\partial e^{\pm\hat{T}}}{\partial \tau_\mu} = \pm \frac{\partial \hat{T}}{\partial \tau_\mu} e^{\pm\hat{T}} = \pm \hat{X}_\mu e^{\pm\hat{T}}. \tag{3.48}$$

Furthermore, excitation operators commute with the excitation cluster operators such that the derivative of the similarity transformed Hamiltonian becomes

$$\frac{\partial \overline{H}}{\partial \tau_\mu} = e^{-\hat{T}} \hat{H} e^{\hat{T}} \hat{X}_\mu - \hat{X}_\mu e^{-\hat{T}} \hat{H} e^{\hat{T}} = \left[\overline{H}, \hat{X}_\mu\right], \tag{3.49}$$

and it follows that

$$\frac{\partial \mathcal{H}}{\partial \tau_\mu} = \langle \Phi_0 | (1 + \hat{\Lambda}) \left[\overline{H}, \hat{X}_\mu\right] | \Phi_0 \rangle = 0. \tag{3.50}$$

The stationary condition of Eq. 3.50 gives an equation for λ which can be solved by fixed point iterations. In contrast to the τ amplitude equations, this depends on both τ and λ. The algebraic expressions for the CCSD λ equations are expressed in Eqs. C.4 and C.5.

Lastly, the CC energy equation can be retrieved by evaluating the energy functional of Eq. 3.46 at the stationary point, where Eq. 3.47 is satisfied, which yields

$$\begin{aligned} \mathcal{H} &= \langle \Phi_0 | e^{-\hat{T}} \hat{H} e^{\hat{T}} | \Phi_0 \rangle + \lambda_\mu \langle \Phi_0 | \hat{Y}_\mu e^{-\hat{T}} \hat{H} e^{\hat{T}} | \Phi_0 \rangle , \\ &= E + \lambda_\mu \frac{\partial \mathcal{H}}{\partial \lambda_\mu} = E, \end{aligned} \tag{3.51}$$

where E is the CC energy as defined in Eq. 3.25. For the CCSD truncation, the energy equation is given by Eq. C.1.

The consequence of this is twofold. Firstly, the original linked energy and amplitude equations are recovered, being completely independent of λ. Solving the τ amplitudes determines the right-state parameterization, giving the CC energy. Secondly, Eq. 3.50 gives an additional set of λ amplitude equations, which can be solved for a representation of the left-state parameterization. Furthermore, due to Eqs. 3.47 and 3.51 being λ independent, we can first solve for the τ amplitudes and the energy with the same equations as in Sec. 3.2.2. If we are interested in properties derived from $\langle \widetilde{\Psi} |$, Eq. 3.50 needs to be solved where the τ amplitudes are now fixed.

3.3.3 Density Matrices

To compute the expectation value of a general operator (both one- and two-body), a representation of reduced density matrices in the bivariational framework is central. From the definitions of Eqs. 2.40 and 2.43, a problem arises since we treat the left- and right-states differently. A natural extension is the definition in Ref. [20],

$$\gamma_{pq} \equiv \langle \widetilde{\Psi} | a_q^\dagger a_p | \Psi \rangle , \qquad \Gamma_{rs}^{pq} \equiv \langle \widetilde{\Psi} | a_r^\dagger a_s^\dagger a_q a_p | \Psi \rangle , \tag{3.52}$$

which conforms with the Hellmann-Feynamnn theorem [65]. For the CCSD truncation, γ_{pq} is expressed in Eqs. C.6 to C.9, while Γ_{rs}^{pq} is expressed in Eqs. C.10 to C.18.

The usefulness of this definition can be seen by calculating the expectation value of $\hat{H}$, an operator with both one- and two-body components:

$$\begin{aligned} \langle H \rangle &= \sum_{pq} h_{pq} \gamma_{qp} + \frac{1}{2} \sum_{pqrs} u_{rs}^{pq} \Gamma_{pq}^{rs}, \\ &= \sum_{pq} h_{pq} \langle \widetilde{\Psi} | a_p^\dagger a_q | \Psi \rangle + \frac{1}{2} \sum_{pqrs} u_{rs}^{pq} \langle \widetilde{\Psi} | a_p^\dagger a_q^\dagger a_s a_r | \Psi \rangle , \\ &= \langle \widetilde{\Psi} | \hat{H} | \Psi \rangle = E. \end{aligned} \tag{3.53}$$

Equation 3.53 recovers the energy expression from Eq. 3.46. However, since $|\Psi\rangle$ and $\langle \widetilde{\Psi}|$ are not hermitian conjugate pairs, we lose some properties of γ_{pq} and Γ_{rs}^{pq}. Specifically the hermiticity properties are lost, such that $\gamma_{qp}^* \neq \gamma_{pq}$ and $(\Gamma_{rs}^{pq})^* \neq \Gamma_{pq}^{rs}$. The antisymmetry of Γ_{rs}^{pq} when exchanging either upper or lower indices, in addition to the trace properties, are unchanged.

The consequences of non-hermitian reduced density matrices are not to be overlooked. When performing a CC calculation, we aim for small values of both $\gamma_{pq} - \gamma_{qp}^*$ and $\Gamma_{rs}^{pq} - (\Gamma_{pq}^{rs})^*$. If this is not the case, we risk poor estimates for both energy and other expectation values. Consequently,

estimated expectation values of hermitian operators can not generally be considered real, which can be problematic when considering time evolution.

Following the comparison between the CISD state and the CCSD right-state from Eqs. 3.17 and 3.18, we expand the left-state parameterization of Eq. 3.45 and compare excitation with the conjugated CISD state

$$\langle \Psi_{\text{CISD}}| = \langle \Phi_0| \left(1 + \hat{C}_1^\dagger + \hat{C}_2^\dagger\right), \tag{3.54}$$

$$\langle \widetilde{\Psi}_{\text{CCSD}}| = \langle \Phi_0| \left(\left[1 - \hat{\Lambda}_1\hat{T}_1 - \hat{\Lambda}_2\hat{T}_2 - \frac{1}{2}\hat{\Lambda}_2\hat{T}_1^2\right] + \left[\hat{\Lambda}_1 - \hat{\Lambda}_2\hat{T}_1\right] - \hat{\Lambda}_2 \right). \tag{3.55}$$

In view of Eqs. 3.54 and 3.55, in contrast to right-parameterization, the same excitations orders are present in the conjugate states. This suggests an imbalance between the left- and right-state parameterizations, where cluster operator coupling only produces higher-order excitations for the latter. Note that a direct comparison of operators between Eqs. 3.54 and 3.55 is infeasible due to $\langle \Psi_{\text{CISD}}|$ being intermediately normalized, where $\langle \widetilde{\Psi}_{\text{CCSD}}|$ is rather normalized by the inner product with the right-state parameterization.

3.4 Extended Theories

The class of extended coupled cluster (ECC) theories proposed by Arponen et al. suggests a more general parameterization of the left-state [25],

$$\langle \tilde{\Psi}| = \langle \Phi_0| e^{\hat{\Lambda}} e^{-\hat{T}} = \langle \Phi_0| (1 + \hat{\Lambda} + \frac{1}{2}\hat{\Lambda}^2 + \frac{1}{6}\hat{\Lambda}^3 + \ldots) e^{-\hat{T}}. \tag{3.56}$$

The inclusion of the exponential of the de-excitation operators in Eq. 3.56 allows for higher-excitation orders to contribute. This is done to mimic the full variational approach of Eq. 3.33, which suffers from exponential scaling. In contrast, Eq. 3.56 allows for a polynomial time scaling of the amplitude equations, with a polynomial order independent of the number of particles [70]. In the CCD approximation, the left-state of Eq. 3.45 will at most allow for contributions from doubles excitations (through $\hat{\Lambda}_2$), while the expansion of Eq. 3.56 (ECCD) allows for additional de-excitations accounting for all terms generated through the finite BCH expansion of $\overline{H}$, giving energy contributions proportional to $\hat{\Lambda}_2^2$ and $\hat{\Lambda}_2^3$.

Though polynomial scaling is far more reasonable than exponential, applications to real systems still have to be comparable to standard CC and CI. By truncating $\exp(\hat{\Lambda})$ in Eq. 3.56 to second order in $\hat{\Lambda}$

$$e^{\hat{\Lambda}} \approx 1 + \hat{\Lambda} + \frac{1}{2}\hat{\Lambda}^2,$$

we arrive at the method referred to as the quadratic coupled cluster (QCC). This particular truncation level allows for the same scaling as CC at the doubles level [24, 26]. In Ref [26], the ECCD approximation is considered, where the most efficient factorized solution can be solved in $\mathcal{O}(n^{10})$ time, if one allows for storage of $\mathcal{O}(n^6)$ intermediately calculated tensors, with n representing the system size. This is far more costly than the CCD scaling of $\mathcal{O}(n^6)$ in time at the cost of $\mathcal{O}(n^4)$ memory storage. By disregarding terms beyond second order in $\hat{\Lambda}$, it is shown that through specific intermediate calculations, a $\mathcal{O}(n^6)$ solution is possible [26]. In the same way as QCC is a second order ECC approximation in $\hat{\Lambda}$, the standard CC theory derived in Sec. 3.3.2 can be viewed as an approximation of ECC to first order in $\hat{\Lambda}$.

3.4.1 Adding the Quadratic Term

Following the approach in Ref. [26], we expand the exponentiated de-excitation operators from the ECC ansatz given by Eq. 3.56 and truncate at the second order in $\hat{\Lambda}$, i.e.,

$$\langle \widetilde{\Psi}| = \langle \Phi_0| e^{\hat{\Lambda}} e^{-\hat{T}} \approx \langle \Phi_0| (1 + \hat{\Lambda} + \frac{1}{2}\hat{\Lambda}^2) e^{-\hat{T}}. \tag{3.57}$$

The right-state parameterization of Eq. 3.45 is unchanged from standard CC. Consequently, the energy functional follows as

$$\mathcal{H}_{\text{Q}} = \langle \Phi_0|(1 + \hat{\Lambda} + \frac{1}{2}\hat{\Lambda}^2) e^{-\hat{T}} \hat{H} e^{\hat{T}} |\Phi_0\rangle = \mathcal{H} + \frac{1}{2} \langle \Phi_0|\hat{\Lambda}^2 e^{-\hat{T}} H e^{\hat{T}} |\Phi_0\rangle, \tag{3.58}$$

with $\mathcal{H}$ as the energy functional of standard CC from Eq. 3.46, while $\mathcal{H}_{\mathrm{Q}}$ is the QCC energy functional. Invoking the BIVP, the stationary conditions from Eqs. 3.47 and 3.50 must be extended. Starting with the derivative with respect to λ, the additional derivative of $\hat{\Lambda}^2$ yields

$$\frac{\partial \hat{\Lambda}^2}{\partial \lambda_\mu} = \frac{\partial \hat{\Lambda}}{\partial \lambda_\mu}\hat{\Lambda} + \hat{\Lambda}\frac{\partial \hat{\Lambda}}{\partial \lambda_\mu} = 2\hat{Y}_\mu \hat{\Lambda}, \tag{3.59}$$

where the new set of τ amplitude equations for the quadratic theory becomes

$$\frac{\partial \mathcal{H}_{\mathrm{Q}}}{\partial \lambda_\mu} = \langle \Phi_\mu | (1 + \hat{\Lambda})\overline{H}|\Phi_0\rangle = \frac{\partial \mathcal{H}}{\partial \lambda_\mu} + \langle \Phi_\mu | \hat{\Lambda}\overline{H}|\Phi_0\rangle = 0, \tag{3.60}$$

where $\partial\mathcal{H}/\partial\lambda_\mu$ is given by Eq. 3.47. In contrast to standard CC, the τ amplitudes equations are dependent on λ and thus can not be solved independently.

The inclusion of $\hat{T}$ is structurally unchanged from the standard CC theory, however, the $\hat{\Lambda}^2$ term has to be accounted for. With the result from Eq. 3.50, the quadratic λ amplitude equations becomes,

$$\frac{\partial \mathcal{H}_{\mathrm{Q}}}{\partial \tau_\mu} = \langle \Phi_0 | (1 + \hat{\Lambda} + \frac{1}{2}\hat{\Lambda}^2)[\overline{H}, \hat{X}_\mu]|\Phi_0\rangle = \frac{\partial \mathcal{H}}{\partial \tau_\mu} + \frac{1}{2}\langle \Phi_0 | \hat{\Lambda}^2[\overline{H}, \hat{X}_\mu]|\Phi_0\rangle = 0. \tag{3.61}$$

Inserting the stationary condition for the τ amplitudes from Eq. 3.60, the quadratic energy functional reduces to

$$\begin{aligned}
\mathcal{H}_{\mathrm{Q}} &= \langle \Phi_0 | (1 + \hat{\Lambda} + \frac{1}{2}\hat{\Lambda}^2)\overline{H}|\Phi_0\rangle, \\
&= E + \sum_\mu \lambda_\mu \langle \Phi_\mu | (1 + \frac{1}{2}\hat{\Lambda})\overline{H}|\Phi_0\rangle, \\
&= E + \sum_\mu \lambda_\mu \left(\frac{\partial \mathcal{H}_{\mathrm{Q}}}{\partial \lambda_\mu} - \frac{1}{2}\langle \Phi_\mu | \hat{\Lambda}\overline{H}|\Phi_0\rangle \right), \\
&= E - \sum_\mu \frac{\lambda_\mu}{2}\langle \Phi_\mu | \hat{\Lambda}\overline{H}|\Phi_0\rangle \equiv E_{\mathrm{Q}},
\end{aligned} \tag{3.62}$$

where E is the standard energy expression from Eq. 3.51, while E_{Q} is defined as the quadratic energy evaluated at stationary τ and λ. In contrast to the standard CC energy, E_{Q} gains a quadratic dependence on λ. Therefore, both τ and λ must be converged before a final energy estimate can be made.

The density matrices are defined in the same way as conventional CC. With $\tilde{\gamma}_{pq}$ and $\tilde{\Gamma}^{pq}_{rs}$ as the one- and two-body density matrices from Eq. 3.52, the quadratic density matrices are expressed as

$$\gamma_{pq} \equiv \langle \widetilde{\Psi} | a_q^\dagger a_p | \Psi \rangle = \tilde{\gamma}_{pq} + \frac{1}{2}\langle \Phi_0 | \hat{\Lambda}^2 e^{-\hat{T}} a_q^\dagger a_p e^{\hat{T}} | \Phi_0 \rangle, \tag{3.63}$$

$$\Gamma^{pq}_{rs} \equiv \langle \widetilde{\Psi} | a_r^\dagger a_s^\dagger a_q a_p | \Psi \rangle = \tilde{\Gamma}^{pq}_{rs} + \frac{1}{2}\langle \Phi_0 | \hat{\Lambda}^2 e^{-\hat{T}} a_r^\dagger a_s^\dagger a_q a_p e^{\hat{T}} | \Phi_0 \rangle. \tag{3.64}$$

For the QCCSD truncation, the additional terms to the reduced one-body density matrix are expressed in Eqs. D.13 to D.16, while the additional two-body terms are expressed in Eqs. D.17 to D.25

Equations 3.63 and 3.64 recreates the energy expectation value of the Hamiltonian for the quadratic theory,

$$\mathcal{H}_{\mathrm{Q}} = \sum_{pq} h_{pq}\gamma_{qp} + \frac{1}{2}\sum_{pqrs} u^{pq}_{rs}\Gamma^{rs}_{pq},$$

just as Eq. 3.52 for the standard theory.

Expanding the quadratic left-parameterization of Eq. 3.54, we find

$$\begin{aligned}\langle\widetilde{\Psi}_{\mathrm{QCCSD}}| = \langle\widetilde{\Psi}_{\mathrm{CCSD}}| + \langle\Phi_0|\Bigg(&\left[\frac{1}{2}\hat{\Lambda}_1^2\left(\frac{1}{2}\hat{T}_1^2 - \hat{T}_2\right) + \hat{\Lambda}_1\hat{\Lambda}_2\left(\hat{T}_1\hat{T}_2 - \frac{1}{6}\hat{T}_1^3\right) + \hat{\Lambda}_2^2\left(\frac{1}{24}\hat{T}_1^4 - \frac{1}{3}\hat{T}_1^2\hat{T}_2\right)\right] \\ &+ \left[-\frac{1}{2}\hat{\Lambda}_1^2\hat{T}_1 + \hat{\Lambda}_1\hat{\Lambda}_2\left(\frac{1}{2}\hat{T}_1^2 - \hat{T}_2\right) + \hat{\Lambda}_2^2\left(\frac{1}{3}\hat{T}_1^3 - \hat{T}_1\hat{T}_2\right)\right] \\ &+ \left[\hat{\Lambda}_2^2\left(\frac{1}{2}\hat{T}_1^2 - \hat{T}_2\right) - \hat{\Lambda}_1\hat{\Lambda}_2\hat{T}_1\right] + \left[\hat{\Lambda}_1\hat{\Lambda}_2 - \hat{\Lambda}_2^2\hat{T}_1\right] + \hat{\Lambda}_2^2\Bigg),\end{aligned} \tag{3.65}$$

where $\langle\widetilde{\Psi}_{\mathrm{CCSD}}|$ are the CCSD contributions from 3.55. In contrast to both CISD and (the left) CCSD parameterization which truncates at the doubles level, the QCCSD left-parameterization includes up to quadruply excited determinants, estimated through coupled $\hat{\Lambda}$ operators. In this sense, $\langle\widetilde{\Psi}_{\mathrm{QCCSD}}|$ is capable of estimating excitations above the methods' truncation level, similar to that of the right-state parameterization.

3.5 Time-Dependent Coupled Cluster Theory

The conventional approach for real-time evolution of coupled cluster theories is the minimization of Arponen's bivariational action [65], being a generalization of the Dirac-Frenkel principle [71]. We define the time-dependent CC Lagrangian as

$$\mathcal{L} = \mathcal{L}[\widetilde{\Psi}, \Psi, t] = \langle\widetilde{\Psi}(t)|i\partial_t - \hat{H}(t)|\Psi(t)\rangle = \langle\widetilde{\Psi}(t)|i\partial_t|\Psi(t)\rangle - \mathcal{H}(t), \tag{3.66}$$

where we now allow both the left- and right-state parameterizations, in addition to the Hamiltonian, to be time-dependent. The single-particle basis is kept static during the time propagation, thus all time dependence of the state is placed in the amplitudes

$$\hat{T}(t) = \sum_{\mu\geq 1}\tau_\mu(t)\hat{X}_\mu, \quad \hat{\Lambda}(t) = \sum_{\mu\geq 1}\lambda_\mu(t)\hat{Y}_\mu.$$

The CC bivariational action between two times t_0 and t_1 is defined as,

$$S[\tilde{\Psi}, \Psi] = \int_{t_0}^{t_1} \mathrm{d}t\, \mathcal{L}(\tilde{\Psi}, \Psi, t), \tag{3.67}$$

where we aim to find a stationary point such that,

$$\delta S = 0, \tag{3.68}$$

when varying the CC amplitudes. For Eq. 3.68 to hold true, the amplitudes $\tau_\mu \equiv \tau_\mu(t)$ and $\lambda_\mu \equiv \lambda_\mu(t)$ must simultaneously obey the Euler-Lagrange equations [72]

$$\frac{\mathrm{d}}{\mathrm{d}t}\left(\frac{\partial\mathcal{L}}{\partial\dot{\tau}_\mu}\right) = \frac{\partial\mathcal{L}}{\partial\tau_\mu}, \tag{3.69}$$

$$\frac{\mathrm{d}}{\mathrm{d}t}\left(\frac{\partial\mathcal{L}}{\partial\dot{\lambda}_\mu}\right) = \frac{\partial\mathcal{L}}{\partial\lambda_\mu}, \tag{3.70}$$

where the dot indicates a time derivative. Equations 3.69 and 3.70 define the equations of motion (EOM) for the CC amplitudes.

3.5.1 Standard Coupled Cluster

With the standard CC left- and right-states from Eq. 3.45, the Lagrangian becomes

$$\mathcal{L} = \langle\Phi_0|(1+\hat{\Lambda})e^{-\hat{T}}\partial_t e^{\hat{T}}|\Phi_0\rangle - \mathcal{H}(t). \tag{3.71}$$

First, we consider the term containing the time-derivative, which acts on the right-state parameterization

$$\frac{\partial}{\partial t} e^{\hat{T}} |\Phi_0\rangle = \frac{\partial \hat{T}}{\partial t} e^{\hat{T}} |\Phi_0\rangle = \sum_{\mu \geq 1} \dot{\tau}_\mu \hat{X}_\mu e^{\hat{T}} |\Phi_0\rangle .$$

Considering the inner product with $\langle \widetilde{\Psi}|$ and noting that excitation and excitation cluster operators commute, the time derivative term of Eq. 3.71 yields

$$\sum_{\mu \geq 1} i\dot{\tau}_\mu \langle \Phi_0 | (1 + \hat{\Lambda}) \hat{X}_\mu | \Phi_0 \rangle = \sum_{\mu,\nu \geq 1} i\dot{\tau}_\mu \lambda_\nu \langle \Phi_0 | \hat{Y}_\nu \hat{X}_\mu | \Phi_0 \rangle = \sum_{\mu \geq 1} i\dot{\tau}_\mu \lambda_\mu, \tag{3.72}$$

where we have expanded $\hat{\Lambda}$ and collapsed the sum using the orthonormality of determinants. Thus, Eq. 3.71 then reduces to

$$\mathcal{L} = i \sum_\mu \dot{\tau}_\mu \lambda_\mu - \mathcal{H}(t). \tag{3.73}$$

To find the EOMs, we have to evaluate the derivatives in Eqs. 3.69 and 3.70. There is no dependence of $\dot{\lambda}_\mu$ in $\mathcal{H}(t)$ and therefore $\mathcal{L}$ is independent of $\dot{\lambda}$. This means that the left-hand side of Eq. 3.70 is zero, such that

$$\begin{aligned} \frac{\partial \mathcal{L}}{\partial \lambda_\mu} &= i\dot{\tau}_\mu - \frac{\partial \mathcal{H}}{\partial \lambda_\mu} = 0, \\ \dot{\tau}_\mu &= -i \frac{\partial \mathcal{H}}{\partial \lambda_\mu}, \end{aligned} \tag{3.74}$$

which is a set of non-linear first-order ODEs in time, determining the evolution of τ. Furthermore, the algebraic expression for $\partial \mathcal{H} / \partial \lambda_\mu$ is unchanged from Eq. 3.47, except for the time-dependence in $\hat{H}$.

Next, considering the derivative of the Lagrangian with respect to τ we obtain

$$\begin{aligned} \frac{\partial \mathcal{L}}{\partial \tau_\mu} &= -\frac{\partial \mathcal{H}}{\partial \tau_\mu}, \\ \frac{\partial \mathcal{L}}{\partial \dot{\tau}_\mu} &= i\lambda_\mu. \end{aligned}$$

Insertion of the above result into the Euler-Lagrange equation from Eq. 3.69 yields the EOMs for the λ amplitudes

$$\dot{\lambda}_\mu = i \frac{\partial \mathcal{H}}{\partial \tau_\mu}. \tag{3.75}$$

In particular, the CCSD equations of motion are given explicitly as

$$\dot{\tau}_i^a = -i \frac{\partial \mathcal{H}}{\partial \lambda_a^i} = -i \langle \Phi_0 | \hat{Y}_a^i e^{-\hat{T}(t)} \hat{H}(t) e^{\hat{T}(t)} | \Phi_0 \rangle , \tag{3.76}$$

$$\dot{\tau}_{ij}^{ab} = -i \frac{\partial \mathcal{H}}{\partial \lambda_{ab}^{ij}} = -i \langle \Phi_0 | \hat{Y}_{ab}^{ij} e^{-\hat{T}(t)} \hat{H}(t) e^{\hat{T}(t)} | \Phi_0 \rangle , \tag{3.77}$$

$$\dot{\lambda}_a^i = i \frac{\partial \mathcal{H}}{\partial \tau_i^a} = i \langle \Phi_0 | \big(1 + \hat{\Lambda}(t)\big) e^{-\hat{T}(t)} [\hat{H}(t), \hat{X}_i^a] e^{\hat{T}(t)} | \Phi_0 \rangle , \tag{3.78}$$

$$\dot{\lambda}_{ab}^{ij} = i \frac{\partial \mathcal{H}}{\partial \tau_{ij}^{ab}} = i \langle \Phi_0 | \big(1 + \hat{\Lambda}(t)\big) e^{-\hat{T}(t)} [\hat{H}(t), \hat{X}_{ij}^{ab}] e^{\hat{T}(t)} | \Phi_0 \rangle . \tag{3.79}$$

Moreover, for the CCD truncation, only Eq. 3.77 and Eq. 3.79 are needed.

3.5.2 Quadratic Coupled Cluster

The addition of the $\hat{\Lambda}^2$ term in the CC Lagrangian yields a similar structure as the standard case discussed in Sec. 3.5.1. With the left-state parameterization from Eq. 3.57, the time-dependent QCC Lagrangian becomes

$$\mathcal{L}_Q = \langle\Phi_0|(1+\hat{\Lambda}+\frac{1}{2}\hat{\Lambda}^2)e^{-\hat{T}}\partial_t e^{\hat{T}}|\Phi_0\rangle - \mathcal{H}_Q(t), \tag{3.80}$$

with $\mathcal{H}_Q(t)$ as the time-dependent quadratic energy functional. The dependence on $\hat{T}(t)$ is unchanged when compared to standard CC, thus the only structural difference is the need to account for $\hat{\Lambda}^2$ in the time derivative term of Eq. 3.72, giving

$$\sum_{\mu\geq 1} i\dot{\tau}_\mu \langle\Phi_0|(1+\hat{\Lambda}+\frac{1}{2}\hat{\Lambda}^2)\hat{X}_\mu|\Phi_0\rangle = \sum_{\mu\geq 1} i\dot{\tau}_\mu\lambda_\mu + \sum_{\mu\geq 1}\frac{i\dot{\tau}_\mu}{2}\langle\Phi_0|\hat{\Lambda}^2\hat{X}_\mu|\Phi_0\rangle\,. \tag{3.81}$$

Finding the τ equations, we note that both $\mathcal{H}_Q$ and Eq. 3.81 are independent of $\dot{\lambda}$. Therefore, the left-hand side of Eq. 3.70 is zero. The EOMs for τ follow from the Euler-Lagrange equations

$$\begin{aligned}\frac{\partial\mathcal{L}_Q}{\partial\lambda_\mu} &= i\dot{\tau}_\mu + \sum_{\nu\geq 1} i\dot{\tau}_\nu\langle\Phi_0|\hat{Y}_\mu\hat{\Lambda}\hat{X}_\nu|\Phi_0\rangle - \frac{\partial\mathcal{H}_Q}{\partial\lambda_\mu} = 0,\\ \dot{\tau}_\mu &= -i\frac{\partial\mathcal{H}_Q}{\partial\lambda_\mu} - \sum_{\nu\geq 1}\dot{\tau}_\nu\langle\Phi_0|\hat{Y}_\mu\hat{\Lambda}\hat{X}_\nu|\Phi_0\rangle\,.\end{aligned} \tag{3.82}$$

Moving on to the λ equations, we make use of the fact that $\mathcal{H}_Q$ is independent of $\dot{\tau}$. This means that only terms which stem from Eq. 3.81 needs to be considered for the $\dot{\tau}$ derivative. Thus,

$$\begin{aligned}\frac{\partial\mathcal{L}_Q}{\partial\dot{\tau}_\mu} &= i\lambda_\mu + \frac{i}{2}\langle\Phi_0|\hat{\Lambda}^2\hat{X}_\mu|\Phi_0\rangle\,,\\ \frac{\mathrm{d}}{\mathrm{d}t}\left(\frac{\partial\mathcal{L}_Q}{\partial\dot{\tau}_\mu}\right) &= i\dot{\lambda}_\mu + i\langle\Phi_0|\dot{\hat{\Lambda}}\hat{\Lambda}|\Phi_0\rangle\,,\\ &= i\dot{\lambda}_\mu + \sum_{\nu\geq 1} i\dot{\lambda}_\nu\langle\Phi_0|\hat{Y}_\nu\hat{\Lambda}\hat{X}_\mu|\Phi_0\rangle\,.\end{aligned} \tag{3.83}$$

Eq. 3.81 is independent of τ, such that only the energy functional contributes to the right-hand side of Eq. 3.69. Then, the EOMs for the λ-amplitudes are obtained from the Euler-Lagrange equations

$$\begin{aligned}i\dot{\lambda}_\mu + \sum_{\nu\geq 1} i\dot{\lambda}_\nu\langle\Phi_0|\hat{Y}_\nu\hat{\Lambda}\hat{X}_\mu|\Phi_0\rangle &= -\frac{\partial\mathcal{H}_Q}{\partial\tau_\mu},\\ \dot{\lambda}_\mu = i\frac{\partial\mathcal{H}_Q}{\partial\tau_\mu} - \sum_{\nu\geq 1}\dot{\lambda}_\nu\langle\Phi_0|\hat{Y}_\nu\hat{\Lambda}\hat{X}_\mu|\Phi_0\rangle\,.\end{aligned} \tag{3.84}$$

Comparing the EOMs for QCC (Eqs. 3.82 and 3.84) with those from standard CC (Eqs. 3.74 and 3.75), there is a key difference in that the amplitude equations are dependent on their own time derivative. How this manifests itself for different truncation schemes will be discussed in the following subsection.

3.5.3 Truncations of Quadratic Coupled Cluster

Considering the terms of Eqs. 3.82 and 3.84 which are not amplitude derivatives of $\mathcal{H}_Q$, we find

$$\sum_{\nu\geq 1}\dot{\tau}_\nu\langle\Phi_0|\hat{Y}_\mu\hat{\Lambda}\hat{X}_\nu|\Phi_0\rangle = \sum_{\nu,\sigma\geq 1}\dot{\tau}_\nu\lambda_\sigma\langle\Phi_0|\hat{Y}_\mu\hat{Y}_\sigma\hat{X}_\nu|\Phi_0\rangle = \sum_{\nu,\sigma\geq 1}\dot{\tau}_\nu\lambda_\sigma\delta_{\mu+\sigma,\nu}, \tag{3.85}$$

$$\sum_{\nu\geq 1}\dot{\lambda}_\nu\langle\Phi_0|\hat{Y}_\nu\hat{\Lambda}\hat{X}_\mu|\Phi_0\rangle = \sum_{\nu,\sigma\geq 1}\dot{\lambda}_\nu\lambda_\sigma\langle\Phi_0|\hat{Y}_\nu\hat{Y}_\sigma\hat{X}_\mu|\Phi_0\rangle = \sum_{\nu,\sigma\geq 1}\dot{\lambda}_\nu\lambda_\sigma\delta_{\nu+\sigma,\mu}. \tag{3.86}$$

We will refer to Eqs. 3.85 and 3.86 as the coupling terms. The excitations induced by the $\hat{X}$ must be de-excited by the product of the two $\hat{Y}$ operators. For QCCD, the only excitations included in

the sums are $\sigma = \nu = 2$ with $\mu = 2$. Since we have two $\hat{Y}$ operators, but only one $\hat{X}$, these will not give any contributions. The QCCD EOMs can then be expressed as

$$\dot{\tau}_{ij}^{ab} = -i\frac{\partial \mathcal{H}_{\mathrm{Q}}}{\partial \lambda_{ab}^{ij}}, \tag{3.87}$$

$$\dot{\lambda}_{ab}^{ij} = i\frac{\partial \mathcal{H}_{\mathrm{Q}}}{\partial \tau_{ij}^{ab}}. \tag{3.88}$$

For QCCSD however, the sums over ν and σ, in addition to μ, include both singles and doubles excitations. From Eq. 3.85 we need $\mu + \sigma = \nu$ for a non-zero contribution, which is fulfilled in the τ singles equation where $\mu = 1$, if $\sigma = 1$ and $\nu = 2$. This contribution is

$$\begin{aligned}
&\sum_{\substack{b>c\\ j>k}} \sum_{dl} \dot{\tau}_{jk}^{bc} \lambda_d^l \left\langle \Phi_0 | \hat{Y}_a^i \hat{Y}_d^l \hat{X}_{jk}^{bc} | \Phi_0 \right\rangle, \\
=&\frac{1}{4} \sum_{bj} \lambda_b^j \dot{\tau}_{ij}^{ab} - \lambda_b^j \dot{\tau}_{ij}^{ba} - \lambda_b^j \dot{\tau}_{ji}^{ab} + \lambda_b^j \dot{\tau}_{ji}^{ba}, \\
=&\sum_{bj} \lambda_b^j \dot{\tau}_{ij}^{ab}.
\end{aligned} \tag{3.89}$$

Similarly, Eq. 3.86 requires $\nu + \sigma = \mu$, which gives a contribution in the doubles equation with $\mu = 2$ when $\nu = \sigma = 1$. Explicitly, this contribution yields,

$$\begin{aligned}
&\sum_{cdkl} \dot{\lambda}_c^k \lambda_d^l \left\langle \Phi_0 | \hat{Y}_c^k \hat{Y}_d^l \hat{X}_{ij}^{ab} | \Phi_0 \right\rangle, \\
=&\dot{\lambda}_a^i \lambda_b^j - \dot{\lambda}_a^j \lambda_b^i - \dot{\lambda}_b^i \lambda_a^j + \dot{\lambda}_b^j \lambda_a^i, \\
=&\hat{P}(ab)\hat{P}(ij) \dot{\lambda}_a^i \lambda_b^j,
\end{aligned} \tag{3.90}$$

where we have used the permutation operator $\hat{P}(pq)$ which permutes two indices of an arbitrary tensor $A_{\ldots p \ldots q \ldots}$ defined by

$$\hat{P}(pq) A_{\ldots p \ldots q \ldots} \equiv A_{\ldots p \ldots q \ldots} - A_{\ldots q \ldots p \ldots}. \tag{3.91}$$

From Eqs. 3.89 and 3.90 we have found that $\dot{\tau}_1$ depends on $\dot{\tau}_2$ and similarly $\dot{\lambda}_2$ depends on $\dot{\lambda}_1$. By substitution, we can then express the QCCSD EOMs as

$$\dot{\tau}_i^a = -i\left(\frac{\partial \mathcal{H}_{\mathrm{Q}}}{\partial \lambda_a^i} - \sum_{bj} \lambda_b^j \frac{\partial \mathcal{H}_{\mathrm{Q}}}{\partial \lambda_{ab}^{ij}} \right), \tag{3.92}$$

$$\dot{\tau}_{ij}^{ab} = -i\frac{\partial \mathcal{H}_{\mathrm{Q}}}{\partial \lambda_{ab}^{ij}}, \tag{3.93}$$

$$\dot{\lambda}_a^i = i\frac{\partial \mathcal{H}_{\mathrm{Q}}}{\partial \tau_i^a}, \tag{3.94}$$

$$\dot{\lambda}_{ab}^{ij} = i\left(\frac{\partial \mathcal{H}_{\mathrm{Q}}}{\partial \tau_{ij}^{ab}} - \hat{P}(ab)\hat{P}(ij) \frac{\partial \mathcal{H}_{\mathrm{Q}}}{\partial \tau_i^a} \lambda_b^j \right). \tag{3.95}$$

In contrast to the QCCD (Eqs. 3.87 and 3.88) and standard CC (for any truncation), the QCCSD EOMs are structurally different due to coupling of the amplitude time derivatives.

3.6 Configuration Weights

In the bivariational formulation of CC theory, the left- and right-parameterization together define the many-electron quantum state [73, 74]. Thus, determining which excited determinants contribute to the CC state is non-trivial, as the contributions to $|\Psi\rangle$ and $\langle\widetilde{\Psi}|$ are in general not identical.

To aid in determining the composition of the CC parameterization, we propose a set of configurational coefficients

$$c_\mu \equiv \langle \Phi_\mu | \Psi \rangle \,, \tag{3.96}$$

$$\tilde{c}_\mu \equiv \langle \widetilde{\Psi} | \Phi_\mu \rangle \,, \tag{3.97}$$

being coefficients for the determinant expansion of $|\Psi\rangle$ and $\langle \widetilde{\Psi}|$

$$|\Psi\rangle = \sum_\mu |\Phi_\mu\rangle\langle\Phi_\mu|\Psi\rangle = \sum_\mu c_\mu \, |\Phi_\mu\rangle \,,$$

$$\langle\widetilde{\Psi}| = \sum_\mu \langle\widetilde{\Psi}|\Phi_\mu\rangle\langle\Phi_\mu| = \sum_\mu \tilde{c}_\mu \, \langle\Phi_\mu| \,.$$

The coefficients c_μ defined by Eq. 3.96, truncates only in the N particle limit, while in a truncated CC scheme, the $\tilde{c}_\mu$ coefficients of Eq. 3.97 spans a constant number of ranks.

This allows us to define configurational weights as

$$W_\mu^{\mathrm{CC}} \equiv \tilde{c}_\mu c_\mu, \tag{3.98}$$

encompassing information from both the left- and right-state. Similarly, the normalized FCI state from Eq. 2.82 can be used to define FCI configurational weights

$$1 = \langle \Psi_{\mathrm{FCI}} | \Psi_{\mathrm{FCI}} \rangle = \sum_{\mu\nu} \langle \Phi_\mu | \Phi_\nu \rangle \, C_\mu^* C_\nu = \sum_\mu |C_\mu|^2 = \sum_\mu W_\mu^{\mathrm{FCI}}, \tag{3.99}$$

where W_μ^{FCI} describes the percentage occupancy of a specific excited determinant. From Eq. 3.99 we observe that $W_\mu^{\mathrm{FCI}} \geq 0$ where a summation over all orders gives unity.

In contrast to the FCI coefficients, $c_\mu^* \neq \tilde{c}_\mu$ in general since $|\Psi\rangle^\dagger \neq \langle\widetilde{\Psi}|$. Consequently, there is no guarantee that $W_\mu^{\mathrm{CC}} \in [0, 1]$, thus the CC weights might not be completely analogous to the FCI weights. However, since the bivariational principle requires $\langle\widetilde{\Psi}|\Psi\rangle = 1$, the weights must sum to one

$$1 = \langle\widetilde{\Psi}|\Psi\rangle = \sum_\mu \langle\widetilde{\Psi}|\Phi_\mu\rangle\langle\Phi_\mu|\Psi\rangle = \sum_\mu W_\mu.$$

In this sense we can compare W_μ^{CC} to W_μ^{FCI}, possibly giving insight into how the CC states approximate the FCI state. For further discussion, we will discard the superscript where $W_\mu = W_\mu^{\mathrm{CC}}$ if not specified otherwise.

For both the CCD and CCSD truncations, $\tilde{c}_\mu$ exactly truncates at the doubles level due to the presence of $\hat{\Lambda}_2$ in the left-state parameterization. In the quadratic scheme, this is increased to the quadruple level due to $\hat{\Lambda}_2^2$. The reference weight,

$$W_0 = \tilde{c}_0 c_0 = \langle\widetilde{\Psi}|\Phi_0\rangle \, \langle\Phi_0|\Psi\rangle \,, \tag{3.100}$$

is a scalar, while for the excited determinants, we will be most interested in the sum of each order. Explicitly, the quantities of interest (in addition to W_0) are

$$W_{\mathrm{S}} = \sum_{ai} W_i^a, \quad W_{\mathrm{D}} = \frac{1}{(2!)^2} \sum_{abij} W_{ij}^{ab}, \quad W_{\mathrm{T}} = \frac{1}{(3!)^2} \sum_{\substack{abc \\ ijk}} W_{ijk}^{abc}, \quad W_{\mathrm{Q}} = \frac{1}{(4!)^2} \sum_{\substack{abcd \\ ijkl}} W_{ijkl}^{abcd}. \tag{3.101}$$

For CCD and CCSD we have the constraint $W_0 + W_{\mathrm{D}} = 1$ and $W_0 + W_{\mathrm{S}} + W_{\mathrm{D}} = 1$ respectively, while for QCCD $W_0 + W_{\mathrm{D}} + W_{\mathrm{Q}} = 1$ and finally QCCSD $W_0 + W_{\mathrm{S}} + W_{\mathrm{D}} + W_{\mathrm{T}} + W_{\mathrm{Q}} = 1$.

3.6.1 CCSD Weights

We start with the right-state coefficients c_μ. Reference to doubles overlaps for the right-state parameterization are expressed as

$$c_0 = \langle\Phi_0|\Psi\rangle = \langle\Phi_0|\Phi_0\rangle = 1, \tag{3.102}$$

$$c_i^a = \langle\Phi_i^a|\Psi\rangle = \langle\Phi_i^a|\hat{T}_1|\Phi_0\rangle = \tau_i^a, \tag{3.103}$$

$$c_{ij}^{ab} = \langle\Phi_{ij}^{ab}|\Psi\rangle = \langle\Phi_{ij}^{ab}|\hat{T}_2 + \frac{1}{2}\hat{T}_1^2|\Phi_0\rangle = \hat{P}(ab)\tau_i^a\tau_j^b + \tau_{ij}^{ab}, \tag{3.104}$$

with the permutation operators defined by Eq. 3.91. The CCD c_μ equations are obtained by inserting $\tau_i^a = 0$.

For the left-state coefficients $\tilde{c}_\mu$, the truncation follows the truncation in $\hat{T}$ and $\hat{\Lambda}$. Therefore, for both CCSD and CCD, calculating overlaps with triple excited determinants and above will give zero. The reference, singles, and doubles coefficients are explicitly given by

$$\begin{aligned}\tilde{c}_0 = \langle\widetilde{\Psi}|\Phi_0\rangle &= \langle\Phi_0|\left(1+\hat{\Lambda}\right)e^{-\hat{T}}|\Phi_0\rangle = \langle\Phi_0|1-\hat{\Lambda}_1\hat{T}_1-\hat{\Lambda}_2\left(\hat{T}_2-\frac{1}{2}\hat{T}_1^2\right)|\Phi_0\rangle \\ &= 1-\sum_{ai}\lambda_a^i\tau_i^a-\frac{1}{4}\sum_{abij}\lambda_{ab}^{ij}\left(\tau_{ij}^{ab}-\hat{P}(ij)\tau_i^a\tau_j^b\right), \end{aligned} \tag{3.105}$$

$$\begin{aligned}\tilde{c}_i^a = \langle\widetilde{\Psi}|\Phi_i^a\rangle &= \langle\Phi_0|\left(1+\hat{\Lambda}\right)e^{-\hat{T}}|\Phi_i^a\rangle = \langle\Phi_0|\hat{\Lambda}_1-\hat{\Lambda}_2\hat{T}_1|\Phi_i^a\rangle \\ &= \lambda_a^i-\sum_{jb}\lambda_{ab}^{ij}\tau_j^b, \end{aligned} \tag{3.106}$$

$$\begin{aligned}\tilde{c}_{ij}^{ab} = \langle\widetilde{\Psi}|\Phi_{ij}^{ab}\rangle &= \langle\Phi_0|\left(1+\hat{\Lambda}\right)e^{-\hat{T}}|\Phi_{ij}^{ab}\rangle = \langle\Phi_0|\hat{\Lambda}_2|\Phi_{ij}^{ab}\rangle \\ &= \lambda_{ab}^{ij}. \end{aligned} \tag{3.107}$$

With Eqs. 3.102 and 3.104 for c_μ and Eqs. 3.105 and 3.107 for $\tilde{c}_\mu$, we can compute weights for the CCD and CCSD truncations.

3.6.2 QCCSD Weights

Quadratic CC applies the same right-state parameterization to that of normal CC, thus the expressions for the c_μ coefficients (Eqs. 3.102 and 3.104) are unchanged. However, the $\tilde{c}_\mu$ coefficients will get additional terms due to the inclusion of $\hat{\Lambda}^2$. With $\langle\widetilde{\Psi}_\mathrm{Q}|$ as the QCC left-state of Eq. 3.57 and $\langle\widetilde{\Psi}|$ as the standard CC left-state of Eq. 3.45, the new contribution can be separated

$$\langle\widetilde{\Psi}_\mathrm{Q}|\Phi_\mu\rangle = \langle\widetilde{\Psi}|\Phi_\mu\rangle + \frac{1}{2}\left\langle\Phi_0\middle|\hat{\Lambda}^2 e^{-\hat{T}}\middle|\Phi_\mu\right\rangle,$$

giving an additional term to consider for the reference, singles and doubles weights.

Starting with the reference overlap, we note that the action of $\hat{\Lambda}^2$ can de-excite double to quadruple determinants. In orders of $\hat{T}$, the lowest contribution comes from the first order ($\hat{T}_2$) and the highest contribution from the fourth order ($\hat{T}_1^4$). Expanding we find

$$\begin{aligned}&\langle\Phi_0|\left(\hat{\Lambda}_1+\hat{\Lambda}_2\right)^2 e^{-\hat{T}}|\Phi_0\rangle \\ &= \langle\Phi_0|\left(\hat{\Lambda}_1^2+2\hat{\Lambda}_1\hat{\Lambda}_2+\hat{\Lambda}_2^2\right)\left(-\hat{T}+\frac{1}{2}\hat{T}^2-\frac{1}{3!}\hat{T}^3+\frac{1}{4!}\hat{T}^4\right)|\Phi_0\rangle \\ &= \langle\Phi_0|\hat{\Lambda}_1^2\left(-\hat{T}_2+\frac{1}{2}\hat{T}_1^2\right)+2\hat{\Lambda}_1\hat{\Lambda}_2\left(\hat{T}_1\hat{T}_2-\frac{1}{6}\hat{T}_1^3\right)+\hat{\Lambda}_2^2\left(\frac{1}{2}\hat{T}_2^2-\frac{1}{2}\hat{T}_1^2\hat{T}_2+\frac{1}{24}\hat{T}_1^4\right)|\Phi_0\rangle. \end{aligned} \tag{3.108}$$

For an explicit expression of Eq. 3.108 see Eq. B.1.

Considering the singles contribution, we still have the double to quadruple de-excitations from the $\hat{\Lambda}^2$ terms. However, since we consider the overlap with a singly excited state, the exp $\left(-\hat{T}\right)$ expansion can now only include singles to triples excitations. This gives

$$\begin{aligned}&\langle\Phi_0|\left(\hat{\Lambda}_1+\hat{\Lambda}_2\right)^2 e^{-\hat{T}}|\Phi_i^a\rangle \\ &= \langle\Phi_0|\left(\hat{\Lambda}_1^2+2\hat{\Lambda}_1\hat{\Lambda}_2+\hat{\Lambda}_2^2\right)\left(-\hat{T}+\frac{1}{2}\hat{T}^2-\frac{1}{3!}\hat{T}^3\right)|\Phi_i^a\rangle \\ &= \langle\Phi_0|-\hat{\Lambda}_1^2\hat{T}_1+2\hat{\Lambda}_1\hat{\Lambda}_2\left(-\hat{T}_2+\frac{1}{2}\hat{T}_1^2\right)+\hat{\Lambda}_2^2\left(\hat{T}_1\hat{T}_2-\frac{1}{6}\hat{T}_1^3\right)|\Phi_i^a\rangle. \end{aligned} \tag{3.109}$$

The explicit expression for Eq. 3.109 is given by Eq. B.2.

Contributions to the doubles' coefficients requires expanding exp $\left(-\hat{T}\right)$ to the second order in

$\hat{T}$, thus

$$\begin{aligned}
&\langle\Phi_0|\left(\hat{\Lambda}_1+\hat{\Lambda}_2\right)^2 e^{-\hat{T}}|\Phi_{ij}^{ab}\rangle \\
&=\langle\Phi_0|\left(\hat{\Lambda}_1^2+2\hat{\Lambda}_1\hat{\Lambda}_2+\hat{\Lambda}_2^2\right)\left(1-\hat{T}+\frac{1}{2}\hat{T}^2\right)|\Phi_{ij}^{ab}\rangle \\
&=\langle\Phi_0|\hat{\Lambda}_1^2-2\hat{\Lambda}_1\hat{\Lambda}_2\hat{T}_1+\hat{\Lambda}_2^2\left(-\hat{T}_2+\frac{1}{2}\hat{T}_1^2\right)|\Phi_{ij}^{ab}\rangle\,, \qquad (3.110)
\end{aligned}$$

with the explicit algebraic expression given in Eq. B.3.

The additional non-zero coefficients not present in standard CCSD theory are from determinants with triple and quadruple excitations. In the triples case, we can only include excitations from $\hat{T}_1$ appearing in the first order of $\hat{T}$. For the quadruples coefficients, there is only one contribution from the quadruples de-excitation $\hat{\Lambda}_2^2$ connected with the identity from the exponential expansion. Thus the left-state triples and quadruples coefficients are

$$\tilde{c}_{ijk}^{abc} = \frac{1}{2}\langle\Phi_0|2\hat{\Lambda}_1\hat{\Lambda}_2-\hat{\Lambda}_2^2\hat{T}_1|\Phi_{ijk}^{abc}\rangle\,, \qquad (3.111)$$

$$\tilde{c}_{ijkl}^{abcd} = \frac{1}{2}\langle\Phi_0|\hat{\Lambda}_2^2|\Phi_{ijkl}^{abcd}\rangle\,, \qquad (3.112)$$

complemented with algebraic expressions given in Eqs. B.4 and B.5 respectively.

Lastly, for calculations of W_T and W_Q, the triple and quadruple right-state coefficients are necessary. For the triples case, we need to include contributions from $\hat{T}^2$ and $\hat{T}^3$ in the exponential expansion, while the additional $\hat{T}^4$ contributions must be included in the quadruples case. Therefore,

$$c_{ijk}^{abc} = \langle\Phi_{ijk}^{abc}|\hat{T}_1\hat{T}_2+\frac{1}{6}\hat{T}_1^3|\Phi_0\rangle\,, \qquad (3.113)$$

$$c_{ijkl}^{abcd} = \langle\Phi_{ijkl}^{abcd}|\frac{1}{2}\hat{T}_2^2+\frac{1}{2}\hat{T}_1^2\hat{T}_2+\frac{1}{24}\hat{T}_1^4|\Phi_0\rangle\,. \qquad (3.114)$$

with algebraic expressions in Eqs. B.6 and B.7 respectively.

Chapter 4

Implementation

This chapter contains some selected topics regarding the numerical implementation of the methods introduced thus far. Due to the verbosity of the quadratic CC equations, the current project contains over 30,000 lines of code, thus in-depth coverage of every moving part was not found constructive to include in this thesis.

However, some key elements are explained, such as how matrix elements and contractions are treated. We elaborate on how the CC equations are solved, with some discussion on convergence improvement techniques. Additionally, optimization in regard to rewriting the amplitude equations both with intermediates and $\hat{T}_1$-transformations is discussed.

For the time propagation methods, we consider different numerical integration techniques based on the work available in the literature. Additionally, imaginary-time propagation is introduced [75].

4.1 Program Elements

The code developed in this thesis is implemented in the `Python` programming language, structured as a package referred to as `quadratictheory`[1]. The drawback of using `Python` instead of compiled programming languages like `C++` and `Fortran` is generally a reduction in computational efficiency. Despite this, `Python` accelerates the development process, such that adding or changing features can be implemented in a shorter amount of time. Additionally, the functionality from the array programming library `NumPy` [76] allows for interfacing with the low-level languages such as `C` and `Fortran` applying the low-level routines of the Basic Linear Algebra Subprograms (BLAS)

The one- and two-body matrix elements of the Hamiltonian are stored in two- and four-dimensional `NumPy` arrays respectively and can be indexed similarly: h_{pq} = `h[p,q]`, u^{pq}_{rs} = `u[p,q,r,s]`. This is done for easier manipulations but comes at the cost of requiring the storage of L^4 two-body elements in memory, where L is the basis set size. The memory requirements for u^{pq}_{rs} become a bottleneck, constraining the size of basis sets that we can employ. Storage of the τ and λ amplitudes is also performed using individual arrays for each order, having a maximum size of M^2N^2 for τ^{ab}_{ij} and λ^{ij}_{ab}, where N is the number of particles and $M = L - N$ the number of virtual states.

Tensor contractions are performed using the `einsum` function from the `NumPy` library. This allows for easy formulation of general tensor contractions without the need to manually map every contraction to a matrix-matrix or matrix-vector multiplication.

4.1.1 Solving the Roothan-Hall Equations

The Roothan-Hall equations (Eq. 2.80) can be solved iteratively. Given a reasonable initial guess for $C^{(0)}$, we can construct the density $\rho^{(0)}$ and Fock matrix $F^{(0)}$. Diagonalizing the Fock matrix then gives a new set of coefficients $C^{(1)}$, which we use to repeat the process until self-consistency is reached. The general procedure is then

$$F(C^{(n)})C^{(n+1)} = sC^{(n+1)}\epsilon^{(n+1)}. \tag{4.1}$$

The choice of initial conditions $C^{(0)}$ influences convergence. For the iterative procedure to reach self-consistency, the initial guess must be "in the basin of attraction" of the HF minimum [77]. The simplest approach is guessing the identity $C^{(0)}_{pq} = \delta_{pq}$, giving the density $\rho^{(0)}_{ij} = \delta_{ij}$. Applying the identity guess, the converged HF basis is assumed to not be widely different from the computational basis, which is not guaranteed. Another approach is using the coefficient matrix that diagonalizes the one-body Hamiltonian, referred to as the core-guess. Even though more of the systems' properties are present in this guess, properties from electron interactions such as nuclear core screening of electrons are not captured. There exists a plethora of different initial guesses that can improve the rate of convergence, but only the identity and core guesses have been implemented here. For a more in-depth discussion see, for example, Ref. [78].

We also need to define a convergence criterion for the iterative procedure. Again there are multiple possibilities to define this. In this work, the Frobenius norm of the difference of density matrices between iterations has been used, $\|D^{(n+1)} - D^{(n)}\|_{\mathrm{F}}$. The iterative procedure continues until the norm is smaller than a predetermined threshold.

In general, the HF minimum is not unique [79], and convergence, particularly at stretched geometries, can be hard to achieve [77]. Therefore, an interface with the RHF solver from `PySCF` [80, 81] has been implemented and used where the simpler implementation presented here yielded major convergence problems.

4.1.2 Solving the Coupled Cluster Amplitude Equations

The CC amplitude equations for any truncation are computationally expensive to solve, and an efficient scheme is crucial for practical applications. Similarly to the method applied to solve the HF equation, an iterative scheme is applied. We define the parameter p_μ, representing either τ_μ

[1] Openly available at: https://github.com/hkve/quadratictheory

or λ_μ. Newtons method for p_μ can then be formulated as

$$p_\mu^{(n+1)} = p_\mu^{(n)} - \sum_\nu (J_{\mu\nu}^{(n)})^{-1} A_\nu^{(n)}, \tag{4.2}$$

where A_μ and $J_{\mu\nu} = \partial A_\mu / \partial p_\nu$ are the derivative and Jacobian of the energy functional with respect to p_μ. The superscript n denotes the n-th iteration, indicating that both the derivative and Jacobian are evaluated at $p_\mu^{(n)}$. Defining $\Delta p_\mu^{(n)} \equiv p_\mu^{(n+1)} - p_\mu^{(n)}$ and multiplying Eq. 4.2 by the Jacobian we have that

$$\sum_\nu J_{\mu\nu}^{(n)} \Delta p_\nu^{(n)} = -A_\nu^{(n)}. \tag{4.3}$$

The energy functional derivative has the same algebraic expressions as the amplitude equations. At every order, we can extract contributions from A_μ containing amplitudes which have a single contraction with the Fock operator.

With $f_\mu p_\mu$ as the result of these contractions and B_μ as every other term, we separate the derivative as

$$A_\mu = f_\mu p_\mu + B_\mu. \tag{4.4}$$

The Fock contracted term $f_\mu p_\mu$ of Eq. 4.4 can, for $\mu = 1$, be written as,

$$\sum_c f_{ac} p_i^c - \sum_k f_{ki} p_k^a = (\epsilon_a - \epsilon_i) p_i^a, \tag{4.5}$$

where we have assumed that a canonical HF basis is used giving a diagonal Fock matrix, $f_{pq} = \delta_{pq}\epsilon_p$. Similarly, for $\mu = 2$, we find

$$\sum_c \left(f_{bc} p_{ij}^{ac} - f_{ac} p_{ij}^{bc} \right) - \sum_k \left(f_{kj} p_{jk}^{ab} - f_{ki} p_{jk}^{ab} \right) = (\epsilon_a + \epsilon_b - \epsilon_i - \epsilon_j) p_{ij}^{ab}. \tag{4.6}$$

This approach can be generalized to any excitation order. Defining ϵ_μ as the difference between the virtual and occupied single-particle energies from Eqs. 4.5 and 4.6, the energy functional derivative of Eq. 4.4 can be written as,

$$A_\mu = \epsilon_\mu p_\mu + B_\mu, \tag{4.7}$$

where ϵ_μ refers to

$$\epsilon_i^a \equiv \epsilon_a - \epsilon_b, \quad \epsilon_{ij}^{ab} \equiv \epsilon_a + \epsilon_b - \epsilon_i - \epsilon_j,$$

for $\mu = 1$ and $\mu = 2$.

Moreover, the Jacobian can then be written as

$$J_{\mu\nu} = \frac{\partial A_\mu}{\partial p_\nu} = \epsilon_\mu \delta_{\mu\nu} + \frac{\partial B_\mu}{\partial p_\nu}. \tag{4.8}$$

We want to solve Eq. 4.3 for p_μ. This requires solving the system of linear equations for Δp_μ, in addition to calculating $J_{\mu\nu}$. When dealing with a large number of amplitudes, this quickly becomes computationally expensive. Therefore, the Jacobian is approximated as

$$J_{\mu\nu} \approx \epsilon_\mu \delta_{\mu\nu}, \tag{4.9}$$

which is diagonal. The justification for this is rooted in Møller-Plesset perturbation theory, where the contribution from the diagonal Fock matrix appears at the zeroth order in the perturbation, while terms stemming from B_μ (such as $\hat{W}$ contributions) only appears at the first order in the perturbation, giving a diagonally dominant Jacobian [32]. With a diagonal Jacobian, the inversion is just element-wise division such that the solution of Eq. 4.3 can be expressed as

$$\Delta p^{(n)} = -\epsilon_\mu^{-1} A_\mu^{(n)}, \tag{4.10}$$

which requires the evaluation of A_μ at every iteration. The amplitudes can then be updated according to

$$p_\mu^{(n+1)} = p_\mu^{(n)} + \Delta p_\mu^{(n)}, \tag{4.11}$$

giving a new set of amplitudes which we again can use to evaluate the energy functional derivative, defining our iterative procedure. We define convergence using the Frobenius norms of the amplitude equations, stopping the iterative procedure when every $\|A_\mu^{(n)}\|_{\mathrm{F}}$ is smaller than a predetermined threshold.

4.1.3 Linear Mixing and DIIS

When iterative procedures are difficult to converge, modifying the update rule of Eq. 4.11 can limit rapid changes between iterations. One way to combat oscillating solutions is linear mixing [82]

$$p_\mu^{(n+1)} = p_\mu^{(n)} + \alpha \Delta p_\mu^{(n)}, \tag{4.12}$$

with $\alpha \in [0, 1]$ being the relaxation parameter. Increasing α decreases how much the amplitudes are allowed to change between iterations. Despite improving convergence in certain situations, relaxed mixing requires a larger number of iterations due to the constraint on iteration-wise amplitude change.

The most popular convergence scheme in quantum chemistry is the Direct Inversion of the Iterative Subspace (DIIS) method [32, 83, 84]. Collecting every amplitude in a vector $\boldsymbol{p}^{(n)}$, DIIS constructs the next set of amplitudes as a linear combination of the previous amplitudes

$$\boldsymbol{p}^{(n+1)} = \sum_{i=0}^{n} c_i \boldsymbol{p}^{(i)}, \tag{4.13}$$

where the coefficients c_i are optimized based on minimizing $\Delta \boldsymbol{p}^{(n)} \equiv \boldsymbol{p}^{(n+1)} - \boldsymbol{p}^{(n)}$, constrained with summing to unity. This requires storing the amplitudes of every iteration, but only the $n' < n$ last amplitudes are used in practice. For a more comprehensive description of how the coefficients are determined, refer to App. A.1.

For particularly challenging problems, a combination of Eqs. 4.12 and 4.13 can be applied. If the initial iterations contain amplitudes far from the converged solution, adding these to the DIIS linear combination can reduce the quality of the next guess. Therefore, relaxed mixing can be performed for the initial iterations, while switching to DIIS when $\|A_\mu^{(n)}\|_{\mathrm{F}}$ becomes sufficiently small or after a fixed number of iterations. We will call this method the soft-start DIIS mixing.

Even though the mixing techniques presented focused on CC fixed-point iterations, they are equally applicable to the self-consistency iterations of HF discussed in Sec. 4.1.1. Here we have chosen to perform the mixing to the Fock matrix as suggested in [32]. By defining

$$\Delta F(C^{(n)}) \equiv F(C^{(n+1)}) - F(C^{(n)}), \tag{4.14}$$

as the change in the Fock matrix between two successive iterations, an update rule on the form of Eq. 4.11 can be formulated as

$$F(C^{(n+1)}) = F(C^{(n)}) + \Delta F(C^{(n)}). \tag{4.15}$$

Thus, both relaxed and DIIS mixing can be applied to achieve self-consistency of the HF equations.

4.2 Gaussian Basis Sets

When applying different post-HF methods, the accuracy of all methods is limited by the choice of basis set. Pushing results closer and closer to an FCI solution does not necessarily yield properties closer to reality, but serves as a better approximation under the limit of the basis set applied. In the following, we summarize how these are created in the field of quantum chemistry.

The analytical solution of the hydrogen atom in the Born-Oppenheimer approximation yields position space wave functions [36],

$$\psi_{nlm}(r,\theta,\phi) = \sqrt{\left(\frac{2}{n}\right)^3 \frac{(n-l-1)!}{2n(n+l)!}} e^{-r/n} \left(\frac{2r}{n}\right)^l \left[L_{n-l-1}^{2l+1}(2r/n)\right] Y_l^m(\theta,\phi), \tag{4.16}$$

where (r,θ,ϕ) express the spherical coordinates, centered around the proton. L and Y are respectively the associated Laguerre polynomials and spherical harmonics, whilst n is the principle, l orbital angular moment, and m orbital angular moment projection quantum numbers. Due to Eq. 4.16 being the solutions of an analytically solvable atomic system, it could be considered natural to apply them to larger atoms as well. However, the $E > 0$ continuum states must be included to form a complete single-particle basis, thus they are no fit for general quantum chemistry computations [85–87].

Slater Type Orbitals (STOs) [88]

$$\phi_{nlm}^{\text{STO}} = N Y_l^m(\theta,\phi) r^{n-1} e^{-\eta r}, \tag{4.17}$$

with n, l and m as the same quantum numbers as Eq. 4.16 with η determining how fast the function goes to zero, have a functional form similar to the Hydrogen solutions, but contain no radial nodes. However, when considering more than two nuclear centers, the two-electron integrals of Eq. 4.17 can not be solved analytically [89].

The usage of Gaussian-type orbitals (GTOs) are the most commonly applied functions in quantum chemistry [90, 91]. In Cartesian form, these are expressed as

$$\phi_{l_x l_y l_z}^{\text{GTO}}(\boldsymbol{r}) = N x_{\text{A}}^{l_x} y_{\text{A}}^{l_y} z_{\text{A}}^{l_z} e^{-\zeta r_{\text{A}}^2}, \tag{4.18}$$

where the subscript A indicates $\boldsymbol{r}_A \equiv \boldsymbol{r} - \boldsymbol{A}$ with $\boldsymbol{A}$ being the position of a nucleus, ζ parameterizing the width of the Gaussian and N the normalization constant. The l_x, l_y, and l_z exponents determine the number of nodes in the x, y, and z direction respectively, related to the orbital angular momentum through $l_x + l_y + l_z = l$ [89]. There are multiple properties of the GTOs making them easier to work with, and a detailed review will not be given here. However, it is worth mentioning the Gaussian Product Theorem, stating that the product of two Gaussians will be a new Gaussian [91]. For an in-depth review of how to calculate kinetic, nuclear attraction, and electron repulsion integrals, see for example, Ref. [92].

There exists a plethora of different basis sets built from GTOs. Many of these are collected in databases such as the `Basis Set Exchange` [93]. We make use of the integration functionality of `PySCF` to calculate the Gaussian integrals [80, 81], serving as an interface to Gaussian integration framework `libcint` [94].

When discussing different basis sets, we note two particularities. Basis functions with l larger than the highest occupied electron state of a particular atom are often added, referred to as polarization functions. Furthermore, basis functions with a large spatial extent (small ζ_A in Eq. 4.18) are also included for some basis sets. These functions are referred to as diffuse or augmented basis functions [95]. The named basis sets applied in this work are listed below

- **sto-ng**. Each basis function is a linear combination of n different GTOs. The n Gaussian widths and n coefficients from the linear combination are optimized by performing a least square fit to functions like Eq. 4.17 [96]. For H and He atoms one spatial function is used, while atoms Li-Ne have five spatial functions. Concretely, we will apply sto-3g.

- **DZ**, **DZP**. Commonly named double zeta basis set, twice the amount of STOs are used for each electron when compared to sto-ng [97]. Thus H and He atoms will each have two spatial functions, while Li-Ne contains ten spatial functions. Polarized functions (recognized by a trailing P) can be added, increasing the number of functions for each atom [98].

- **X-YZg**. Split-valence double zeta basis sets developed by Ditchfield et al. [99]. In this notation, X represents the number of Gaussians used for each core electron, while valence electrons are treated with two spatial functions, constructed using Y and Z Gaussians each. The addition of a "*" indicates that a polarization function is added for every atom except H and He, while the addition of "**" gives every atom polarization functions. Additionally, a "+" indicates that diffuse functions are added for atoms heavier than He, while "++" adds diffuse functions for every atom. In particular, we will use 6-31g, 6-31g*.

- **X-YZWg** Split-valence double triple basis sets. Similar to the split-valence of Pople, but three spatial functions are used for valence electrons instead of two, as specified by W. We will apply the 6-311++G(d,p) basis set [100, 101], where (d,p) indicates what type of polarization functions are included (corresponding the "**" of the split-valence double zeta basis sets).
- **cc-pVnZ**. This class of basis sets have been introduced by Dunning Jr [102, 103]. Here "cc-p" and "V" are abbreviations for correlation-consistent polarized valence, with $n = \mathrm{D}, \mathrm{T}, \ldots$ determining the number of spatial functions for each atom. These basis sets have become quite popular for ground state energy calculation, as they are designed to converge energy estimates when increasing the basis set complexity for post-HF methods [104]. We will apply cc-pVDZ and cc-pVTZ containing 5 and 14 spatial functions for H and He, whilst 14 and 30 spatial functions for Li-Ne respectively.

4.3 Intermediates

Solving the amplitude equations for both CC and QCC requires many tensor contractions. Using CCD as an example, a naive implementation would directly use the expression from Eq. C.3 with $\tau_i^a = 0$. For accurate calculation of most interacting systems, the virtual set $\mathcal{B}_v$ needs to contain a larger amount of basis functions than the number of particles. Therefore, we assume that $M > N$ in the following analysis. From the $\hat{T}_2$ equations for the CCD approximation, we consider a term contracting over two particles and two hole indices

$$\frac{\partial \mathcal{H}}{\partial \lambda_{ij}^{ab}} \supset \frac{1}{4} \sum_{klcd} u_{cd}^{kl} \tau_{ij}^{cd} \tau_{kl}^{ab}. \tag{4.19}$$

Each element resulting from this sum would require $\mathcal{O}(N^2M^2)$ operations, which must be done for every a, b and i, j giving a total cost of $\mathcal{O}(N^4M^4)$. However, if we first calculate the *intermediate* tensors

$$\chi_{cd}^{ab} = \frac{1}{4} \sum_{kl} \tau_{kl}^{ab} u_{cd}^{kl},$$

we can then evaluate the expression from Eq. 4.19 by considering the sum

$$\sum_{cd} \tau_{ij}^{cd} \chi_{cd}^{ab} = \frac{1}{4} \sum_{klcd} u_{cd}^{kl} \tau_{ij}^{cd} \tau_{kl}^{ab}.$$

The construction of χ_{cd}^{ab} requires $\mathcal{O}(N^2M^4)$ operations, with the final sum also requiring $\mathcal{O}(N^2M^4)$. This means that we have reduced the expression from Eq. 4.19 from $\mathcal{O}(N^4M^4)$ operations to two parts requiring $\mathcal{O}(N^2M^4)$ operations. This speedup is not free however, since to store χ_{cd}^{ab} we need to allow for an additional memory usage of $\mathcal{O}(M^4)$ for our intermediate calculation. Further reductions can be performed by adding more terms to the intermediate tensor, allowing for multiple terms to be calculated at once. Adding the u_{cd}^{ab} term from the CCD $\hat{T}_2$ equations we can absorb this into χ_{ij}^{ab} giving,

$$\begin{aligned}
\frac{\partial \mathcal{H}}{\partial \lambda_{ij}^{ab}} &\supset \frac{1}{2} \sum_{cd} u_{cd}^{ab} \tau_{ij}^{cd} + \frac{1}{4} \sum_{klcd} u_{cd}^{kl} \tau_{ij}^{cd} \tau_{kl}^{ab}, \\
&= \sum_{cd} \tau_{ij}^{cd} \left[\frac{1}{2} u_{cd}^{ab} + \frac{1}{4} \sum_{kl} \tau_{kl}^{ab} u_{cd}^{kl} \right], \\
&= \sum_{cd} \tau_{ij}^{cd} \chi_{cd}^{ab}.
\end{aligned}$$

This does not reduce time or memory scaling but allows calculating multiple terms simultaneously and therefore speeding up calculations. Lastly when dealing with more complex contraction structures such as the CCSD $\hat{T}_1$ and $\hat{T}_2$ amplitude equations, reusing intermediates is possi-

ble. Considering first two terms from the $\hat{T}_1$ equation (Eq. C.2) we define χ_{kc} as

$$\begin{aligned}\frac{\partial \mathcal{H}}{\partial \lambda_i^a} &\supset \sum_{kc} f_{kc}\tau_{ik}^{ac} + \sum_{klcd} u_{cd}^{kl}\tau_k^c\tau_{li}^{da}, \\ &= \sum_{kc}\tau_{ik}^{ac}\left[f_{kc} + \sum_{ld}\tau_l^d u_{cd}^{kl}\right], \\ &= \sum_{kc}\tau_{ik}^{ac}\chi_{kc}.\end{aligned}$$

From the $\hat{T}_2$ equation (Eq. C.3), we can recognize the same intermediate in two of the permutation terms

$$\begin{aligned}\frac{\partial \mathcal{H}}{\partial \lambda_{ij}^{ab}} &\supset -\hat{P}(ab)\sum_{kc}\tau_k^a\tau_{ij}^{cb}f_{kc} - \hat{P}(ab)\sum_{klcd}\tau_k^c\tau_l^a\tau_{ij}^{db}u_{cd}^{kl}, \\ &= -\hat{P}(ab)\sum_{kc}\tau_k^a\tau_{ij}^{cb}\left[f_{kc} + \sum_{ld}\tau_l^d u_{cd}^{kl}\right], \\ &= -\hat{P}(ab)\sum_{kc}\tau_k^a\tau_{ij}^{cb}\chi_{kc}.\end{aligned}$$

These three techniques are important factors when aiming to solve larger systems since reducing time scaling from an 8th-order polynomial to a 6th-order polynomial allows to push for significantly larger system sizes. For truncations such as CCD and CCSD, different choices of intermediates have been studied in detail [105]. Even for the more complex QCCD equations, a workable set has been formulated [24, 26], reducing the plain $\mathcal{O}(M^6N^6)$ equations to the more reasonable $\mathcal{O}(M^6)$ through the use of intermediates.

In this work, the tensor computer algebra system `Drudge` [106] is applied. `Drudge` allows for the evaluation of expectation values of long-second quantization operator strings, in addition to the basic calculus. With the associated framework `Gristmill` [107], tensor contraction structures can automatically be factorized, generating sets of intermediates. Both `Drudge` and `Gristmill` are based on the `SymPy` [108] package, allowing for the application of more complex operations.

4.4 $\hat{T}_1$-transformation

For CC approximations including both singles and doubles, the explicit dependence of τ_1 amplitudes can be removed by introducing a change of basis. This reduces the number of terms required for the τ_2, λ_1 and λ_2 equations, at the cost of transforming the one- and two-body matrix elements of the Hamiltonian.

Considering the similarity transformed Hamiltonian from Eq. 3.24, we only perform the transformation using the $\hat{T}_1$ cluster operators,

$$\overline{H} = e^{-\hat{T}_1-\hat{T}_2}\hat{H}e^{\hat{T}_1+\hat{T}_2} = e^{-\hat{T}_2}\widetilde{H}e^{\hat{T}_2}, \tag{4.20}$$

where $\widetilde{H} \equiv e^{-\hat{T}_1}\hat{H}e^{\hat{T}_1}$ is referred to as the $\hat{T}_1$-transformed Hamiltonian [109]. Applying Eq. 2.32, following the same argument as in Sec. 3.2.2, we find that the Hausdorff expansion of a transformation of a creation operator truncates after a single commutator,

$$\tilde{a}_p^\dagger = e^{-\hat{T}_1}a_p^\dagger e^{\hat{T}_1} = \{a_p^\dagger e^{\hat{T}_1}\}_{\mathrm{C}} = a_p^\dagger + [a_p^\dagger, \hat{T}_1]\,. \tag{4.21}$$

Using the anticommutation relations of Eq. 2.11, we find that the commutator reduces to,

$$[a_p^\dagger, \hat{T}_1] = \sum_{ai}\tau_i^a\left(a_p^\dagger a_a^\dagger a_i - a_a^\dagger a_i a_p^\dagger\right) = -\sum_{ai}\delta_{pi}\tau_i^a a_a^\dagger,$$

and the $\hat{T}_1$-transformed creation operator can be written as

$$\tilde{a}_p^\dagger = a_p^\dagger - \sum_{ai}\delta_{pi}\tau_i^a a_a^\dagger. \tag{4.22}$$

Likewise, the $\hat{T}_1$-transformed annihilation operator is given by

$$\tilde{a}_p = a_p + \sum_{ai} \delta_{pa} \tau_i^a a_i. \tag{4.23}$$

Defining an expanded matrix form of τ_1 of size $L \times L$ as

$$\mathcal{T}_{qp} = \delta_{qp} - \sum_i \delta_{qa} \delta_{pi} \tau_i^a,$$

we can express the transformation of Eq. 4.22 with a single matrix $\mathcal{S} \equiv I - \mathcal{T}$,

$$a_p^\dagger - \sum_{ai} \delta_{pi} \tau_i^a a_a^\dagger = \sum_q \delta_{qp} a_q^\dagger - \sum_{qi} \delta_{qa} \delta_{pi} \tau_i^a a_q^\dagger = \sum_q (\delta_{qp} - \mathcal{T}_{qp}) a_q^\dagger \equiv \sum_q \mathcal{S}_{qp} a_q^\dagger. \tag{4.24}$$

Similarly, Eq. 4.23 can be expressed using the transformation matrix $\widetilde{\mathcal{S}} \equiv I + \mathcal{T}^T$,

$$\tilde{a}_p = \sum_q \widetilde{\mathcal{S}}_{qp} a_q. \tag{4.25}$$

Using Eqs. 4.24 and 4.25 the T_1-transformed matrix elements of the Hamiltonian are given by [32]

$$\widetilde{h}_{pq} \equiv \sum_{rs} \mathcal{S}_{pr} \widetilde{\mathcal{S}}_{qs} h_{rs}, \tag{4.26}$$

$$\widetilde{u}_{rs}^{pq} \equiv \sum_{tuvw} \mathcal{S}_{pt} \mathcal{S}_{qu} \widetilde{\mathcal{S}}_{rv} \widetilde{\mathcal{S}}_{sw} u_{vw}^{tu}, \tag{4.27}$$

giving the $\hat{T}_1$ transformed Hamiltonian

$$\widetilde{H} = e^{-\hat{T}} \hat{H} e^{\hat{T}_1} = \widetilde{H}_0 + \widetilde{W} = \sum_{pq} \widetilde{h}_{pq} a_p^\dagger a_q + \frac{1}{4} \sum_{pqrs} \widetilde{u}_{rs}^{pq} a_p^\dagger a_q^\dagger a_s a_r. \tag{4.28}$$

When using Eq. 4.28 in favor of Eq. 2.35, the one- and two-body matrix elements are no longer hermitian, that is $\widetilde{h}_{pq} \neq \widetilde{h}_{qp}^*$ and $(u_{rs}^{pq})^* \neq u_{pq}^{rs}$. Since the present implementation applies raw storage of both one- and two-body matrix elements, this loss of symmetry is unproblematic.

The strategy to solve singles and doubles schemes with a $\hat{T}_1$-transformed Hamiltonian involves constructing $\widetilde{H}$, which is dependent on the CC solution through τ_1. Therefore, the transformations of Eqs. 4.26 and 4.27 must be evaluated at every iteration. Given some initial guess for the amplitudes, we perform the transformation, constructing $\widetilde{H}$ for the current iteration. Thereafter, the other amplitude equations can be evaluated without any contribution from the τ_1 amplitudes. We update the amplitudes in the same way as Eq. 4.11, where we again construct $\widetilde{H}$ and evaluate all other amplitude equations. This process is repeated, ending when the same convergence criteria as in Sec. 4.1.2 is met.

For standard CC, the CCSD τ_2 amplitude equation reduce to that of CCD. Iterating a time-independent calculation for λ then requires no change of basis, since τ is already converged. However, these equations differ from the CCD λ equations due to the presence of Λ_1. However, for the quadratic theory, the τ and λ amplitudes must be solved simultaneously. In contrast to CCSD, the QCCSD τ_2 equations do not reduce to QCCD due to the λ dependence, but all τ_1 dependence is removed for all τ_2, λ_1 and λ_2 equations. Time propagation requires calculating Eqs. 4.26 and 4.27 at every time step, for both standard and quadratic schemes, since τ_1 evolves in time. Additionally, if density matrices are calculated in the $\hat{T}_1$ transformed basis, the matrix representation of all other operators must be transformed as well.

Formally, the scaling for both standard and quadratic schemes does not change when performing the $\hat{T}_1$ transformation. However, the number of terms that we need to calculate reduces, since τ_1 is not present in the τ_2, λ_1, and λ_2 equations. The penalty of this optimization is the need to perform the $\mathcal{O}(L^5)$ transformation of Eq. 4.27, which is expensive for large L.

4.5 Imaginary Time Evolution

An excellent test to validate the self-consistency between the ground state solutions and the EOMs is performing imaginary time evolution [75]. Consider a general state at $t_0 = 0$, $|\psi(0)\rangle$. Expanding

$|\psi(0)\rangle$ in the eigenstates of a time-independent Hamiltonian $\{|\psi_i\rangle\}$, the time evolution operator $e^{-i\hat{H}t}$ gives an energy-dependent phase factor for each eigenstate

$$|\psi(t)\rangle = e^{-i\hat{H}t}\,|\psi(0)\rangle = \sum_i c_i e^{-iE_i t}\,|\psi_i\rangle\,. \tag{4.29}$$

If we make a change of variables to imaginary time $\pi \equiv it$, the evolution of Eq. 4.29 changes from rotations in the complex plane to exponential decay,

$$|\psi(\pi)\rangle = e^{-\hat{H}\pi}\,|\psi(0)\rangle = e^{-E_0\pi}\sum_i c_i e^{-(E_i-E_0)\pi}\,|\psi_i\rangle\,. \tag{4.30}$$

Here $E_i - E_0 > 0$ is the excitation energy with E_0 defined as the ground state energy. If the ground state is non-degenerate and present in the linear combination ($c_0 \neq 0$), $|\psi(\pi)\rangle$ goes towards $c_0 e^{-E_0\pi}\,|\psi_0\rangle$ for large π.

For propagation of CC, where the left- and right-states are parameterized independently, more care must be taken. As discussed in detail by Kvaal [69], the adjoint SE does not yield the same exponential decaying form as the non-adjoint SE,

$$-i\frac{\partial}{\partial t}\,\langle\Psi| = \langle\Psi|\,\hat{H} \rightarrow \frac{\partial}{\partial \pi}\,\langle\Psi| = \langle\Psi|\,\hat{H},$$

which is unproblematic for a variational treatment where $|\Psi\rangle$ and $\langle\Psi|$ are hermitian conjugate pairs. However, this is not the case for the CC states $|\Psi\rangle$ and $\langle\tilde{\Psi}|$. A solution to this is to differentiate between *forward imaginary time* π_+ and *backwards imaginary time* π_-, defined as

$$\pi_\pm \equiv \pm it, \tag{4.31}$$

which gives a sign difference in the relation with the (real) time derivative

$$\frac{\partial}{\partial t} = \frac{\partial \pi_\pm}{\partial t}\frac{\partial}{\partial \pi_\pm} = \pm i\frac{\partial}{\partial \pi_\pm},$$

which gives the correct form for both equations. Thus, we find that

$$i\frac{\partial}{\partial t}\,|\Psi\rangle = \hat{H}\,|\Psi\rangle \rightarrow \frac{\partial}{\partial \pi_+}\,|\Psi\rangle = -\hat{H}\,|\Psi\rangle\,, \tag{4.32}$$

$$-i\frac{\partial}{\partial t}\,\langle\Psi| = \langle\Psi|\,\hat{H} \rightarrow \frac{\partial}{\partial \pi_-}\,\langle\Psi| = -\,\langle\Psi|\,\hat{H}. \tag{4.33}$$

Hence, we propagate the τ equations through π_+ and the λ equations through π_- [110]. This corresponds to changing the overall factor of $\pm i$ on the right-hand side of for instance the CCSD amplitude equations (Eqs. 3.76 to 3.79) or QCCSD amplitude equations (Eqs. 3.92 to 3.95) to a factor of -1. The initial state we will use is the HF solution, such that all amplitudes are initialized to zero.

4.6 Numerical integration

For all the truncated CC methods presented here, the time evolution of a particular state requires solving a coupled set of non-linear first-order differential equations. This is expressed compactly as

$$\dot{\boldsymbol{y}} = \boldsymbol{f}(\boldsymbol{y}(t), t), \quad \boldsymbol{y} \in \mathbb{C}^{N_A}, \quad \boldsymbol{f} : \mathbb{C}^{N_A} \times \mathbb{R} \mapsto \mathbb{C}^{N_A}, \tag{4.34}$$

with N_A being the total number of τ and λ amplitudes. The exact form of $\boldsymbol{y}$ and $\boldsymbol{f}$ depends on the truncation in question, the external Hamilton which is applied, in addition to the system.

In general, Eq. 4.34 can not be solved analytically, and therefore numerical integration methods must be used to find an approximate solution. Discretizing time into m equally spaced values $t_n = n\Delta t$, $n = 0, 1, \ldots, m$, the goal is to approximate $\boldsymbol{y}(t_n)$ through some iterative process given the initial condition $\boldsymbol{y}_0 = \boldsymbol{y}(t_0)$. Importantly, the quality of the results relies on a suitable choice of the time step Δt.

The simplest practical method available to us is the explicit 4th order Runge-Kutta method (RK4), requiring four evaluations of $\boldsymbol{f}$ between two times t_n and t_{n+1}. This introduces a local error in each step of $\mathcal{O}(\Delta t^5)$, giving a total accumulated error $\mathcal{O}(\Delta t^4)$ [111].

For certain calculations, where the external potential is strong, applications of the RK4 method result in low-quality or unstable dynamics [47, 48, 74]. A study by Pedersen and Kvaal [74] suggested applying a symplectic integrator [112], giving more stable results for properties like energy conservation and reducing oscillations of the imaginary components of expectation values. The integrator termed by the authors as a *Gauss integrator* (GI) is implicit, and integrates a time step by interpolating the numerical solution by a polynomial of order s. This requires solving a set of nonlinear equations for each time step, achieved using a fixed point procedure converged to a tolerance ϵ. If not stated otherwise, $s = 3$ with $\epsilon = 10^{-5}$ has been applied in this work, such as in Ref. [48].

Other numerical integration methods have been applied in the literature. For instance, the standard RK4 has been shown to produce more stable results when an adaptive time step has been applied [113]. Exponential RK4 methods have also been used in [114], implementing a scheme from [115].

Therefore, some care has to be taken when considering time propagation, considering reasonable time steps for specific systems and external potentials. This is especially relevant when considering propagation of the quadratic methods since this introduces λ dependence into the τ equations (QCCD Eqs. 3.87 and 3.88, QCCSD Eqs. 3.92 to 3.95). Additionally, the extra terms stemming from the time derivative dependence of the QCCSD equations could potentially result in more difficult integration.

We employ the integration facilities of `SciPy` [116], which contains functionality for mapping the complex ODE problem of N_A variables from Eq. 4.34 to a real problem of $2N_A$ variables. Additionally, the same interface allows for the integration of purely real versions of Eq. 4.34 which is beneficial for imaginary time evolution.

Chapter 5

Validation

When developing larger scientific programs, proper tests and validation schemes are imperative. This is particularly important when considering new or extending already existent methods, as no quantitative benchmark can be performed by comparing to previous work.

To this aim, we found it constructive to have performed a thorough validation procedure. This includes checking results against `PySCF` for the standard methods, in addition to a quantitative comparison between the present quadratic CC implementation to the results reported in the literature. Furthermore, imaginary time evolution is performed for all implemented CC schemes. In particular, for QCCD and QCCSD, this procedure gives strong merit to the correctness of the derived EOMs. Lastly, we compare the CC and QCC real-time dynamics to time-dependent FCI results from the literature.

5.1 Two Particles

For two-electron systems, CC methods that include both singles and doubles excitations are formally equivalent to FCI. This means that both CCSD and QCCSD should produce the same energies, despite having differences in both the amplitude and energy equations. Furthermore, considering only double excitations, the quadratic de-excitations from $\hat{\Lambda}_2^2$ present in the QCCD theory will not contribute and thus QCCD reduces to CCD for $N = 2$.

We have performed ground state energy calculations of He and H_2 in Tables 5.1 and 5.2 respectively. Across the three basis sets applied here CCSD, QCCSD, and FCI are in excellent agreement. Additionally, QCCD correctly reduces to CCD for both systems.

Basis set	CCD	QCCD	CCSD	QCCSD	FCI
6-31g	-2.870145	-2.870145	-2.870162	-2.870162	-2.870162
cc-pVDZ	-2.887592	-2.887592	-2.887595	-2.887595	-2.887595
cc-pVTZ	-2.900209	-2.900209	-2.900232	-2.900232	-2.900232

Table 5.1: Ground state energy calculations of the $N = 2$ electron He atom, applying progressively larger basis sets. The calculations have been performed for CCD, QCCD, CCSD, QCCSD, and FCI, with all CC methods converged to 10^{-8} in the τ and/or λ amplitudes. Energies are in Hartree atomic units E_h

Basis set	CCD	QCCD	CCSD	QCCSD	FCI
6-31g	-1.151621	-1.151621	-1.151691	-1.151691	-1.151691
cc-pVDZ	-1.163327	-1.163327	-1.163455	-1.163455	-1.163455
cc-pVTZ	-1.172199	-1.172199	-1.172337	-1.172337	-1.172337

Table 5.2: Computed ground state energies of H_2, applying progressively larger basis sets. The calculations have been performed for CCD, QCCD, CCSD, QCCSD, and FCI, with all CC methods converged to 10^{-8} in the τ and/or λ amplitudes. Equilibrium geometry optimized by a CCSD calculation in the cc-pVTZ basis has been applied [117], with the bond distance between the two H atoms being $R_\mathrm{e} = 1.4040\ a_0$. Energies are are in E_h.

5.2 Standard Coupled Cluster

For systems with more than two particles, CC theories truncated at (singles) doubles level will in general differ from FCI. Due to the popularity of the standard CC methods, implementations of both CCD and CCSD are present in most quantum chemistry software. By applying the functionality from `PySCF`, ground state energy calculations can be compared to the present implementation.

The initial test cases consist of systems of atoms, where the nucleus creates a single confining potential. In particular, CC calculations for the Be, O, Ne, and Ar systems have been performed using progressively larger basis sets, see Table 5.3. Additionally, the calculations have been performed in both general and restricted schemes. For both the doubles and the singles and doubles truncation, the two different implementations agree to the numerical precision expected from the convergence threshold.

Similarly, test cases including multiple atoms have been performed for the LiH, CH^+, and HF molecules with the results being summarized in Table 5.4. Again we reproduce the results from `PySCF` to numerical precision, both at equilibrium and stretched geometries.

Based on the compliance with `PySCF`, all four of the standard CCD, CCSD, RCCD, and RCCSD implementations converge to the correct τ amplitudes. These components are essential for the development of quadratic methods, which are implemented by directly extending the standard methods.

System	Basis set	CCD §	RCCD §	CCD ‡	CCSD §	RCCSD §	CCSD ‡
Be	6-31g	-14.613234	-14.613234	-14.613234	-14.613518	-14.613518	-14.613518
	cc-pVDZ	-14.616943	-14.616943	-14.616943	-14.617369	-14.617369	-14.617369
	cc-pVTZ	-14.623033	-14.623033	-14.623033	-14.623559	-14.623559	-14.623559
O	6-31g	-74.748687	-74.748687	-74.748687	-74.748801	-74.748801	-74.748801
	cc-pVDZ	-74.820496	-74.820496	-74.820496	-74.820742	-74.820742	-74.820742
	cc-pVTZ	-74.892297	-74.892297	-74.892296	-74.892937	-74.892937	-74.892937
Ne	6-31g	-128.588658	-128.588658	-128.588658	-128.588995	-128.588995	-128.588995
	cc-pVDZ	-128.679515	-128.679515	-128.679515	-128.679637	-128.679637	-128.679637
	cc-pVTZ	-128.810060	-128.810060	-128.810060	-128.810814	-128.810814	-128.810814
Ar	6-31g	-526.812583	-526.812583	-526.812583	-526.812880	-526.812880	-526.812880
	cc-pVDZ	-526.956194	-526.956194	-526.956194	-526.956227	-526.956227	-526.956227
	cc-pVTZ	-527.066046	-527.066046	-527.066046	-527.066360	-527.066360	-527.066360

‡ Results from `PySCF`
§ This work

Table 5.3: Computed CCD and CCSD ground state energies in E_h using both general and restricted schemes for the Be, O (singlet), Ne and Ar atoms. Various sized basis sets have been applied, with convergence set to 10^{-8} in the τ amplitudes.

System	Geometry	CCD §	CCD ‡	CCSD §	CCSD ‡
LiH	R_e	-8.036371	-8.036371	-8.036576	-8.036576
	$2R_e$	-7.960254	-7.960254	-7.965803	-7.965803
CH^+	R_e	-38.030926	-38.030926	-38.031726	-38.031726
	$2R_e$	-37.894425	-37.894425	-37.904358	-37.904358
HF	R_e	-100.343726	-100.343726	-100.344893	-100.344893
	$2R_e$	-100.150297	-100.150297	-100.160053	-100.160053

‡ Results from `PySCF`
§ This work

Table 5.4: Computed CCD and CCSD ground state energies for the LiH, CH^+, and HF molecules, calculated in a cc-pVDZ basis. For each molecule, results from two geometries are presented with $R_e = 3.0519, 2.1373, 1.7291\ a_0$ being the equilibrium geometries optimized by CCSD in the cc-pVDZ basis set [117] for LiH, CH^+ and HF respectively. All calculations have been converged to 10^{-8} in the τ amplitudes.

Other tests have been performed, which are not listed here. This includes making sure that the trace of the one- and two-body density matrices are N and $N(N-1)$ respectively. Additionally, we have checked that computing $\langle \hat{H} \rangle$ from Eq. 3.53 yields the CC energy, which serves as a validity check for the density matrices. Explicit validation of the Hellmann-Feynmann theorem has also been performed, applying the central finite difference for numerical derivation. This was tested for both dipole and quadrupole moments, with excellent agreement. Deviations between Eqs. 2.41 and 3.36 followed $\mathcal{O}(\epsilon^2)$ as a function of ϵ, in agreement with the error scaling of the central finite-difference approximation of the first derivative.

5.3 Quadratic Coupled Cluster

Compared to the standard CC methods, reported results for quadratic CC are less prevalent in the literature, making validation more challenging. The original article of Van Voorhis and Head-Gordon [24] does report FCI and QCCD results for N_2 and H_2O dissociation. However, these energies were calculated using a Brueckner basis [21], where the basis was chosen to maximize the overlap with the FCI state. This is done by applying Thouless' theorem, which states that acting on the reference determinant with the exponentiated singles cluster operator can transform

it to any other non-orthogonal determinant [118],

$$|\widetilde{\Phi}_0\rangle = e^{\hat{T}_1} |\Phi_0\rangle \,. \tag{5.1}$$

Maximizing the overlap between the determinant and the FCI state then requires solving

$$\frac{\partial}{\partial \tau_i^a} \langle \Psi_{\mathrm{FCI}} | \widetilde{\Phi}_0 \rangle = \langle \Psi_{\mathrm{FCI}} | \widetilde{\Phi}_i^a \rangle = 0. \tag{5.2}$$

If Eq. 5.2 is fulfilled, $|\widetilde{\Phi}_0\rangle$ will be the Brueckner determinant. Performing the transformation of Eq. 5.1, the Brueckner determinant can be used as the reference determinant. From Eq. 5.2, this should decrease the importance of single excitations, increasing the accuracy of the CC calculation when only considering the doubles truncation.

Despite Eq. 5.1 producing a good reference state, the procedure proposed requires the FCI solution. This approach can be applied to small problems but is in general not possible for larger systems and basis sets. Therefore, we rather compare to the N_2 QCCSD energy results from Fan et al. [27], where a restricted HF reference has been applied. Deviations here are attributed to [27] applying a "1s" frozen-core approximation, meaning that the two single-particle states with the lowest energy are removed from the CC calculation (but included in the HF calculation).

Table 5.5 compares the frozen-core results with this work (without a frozen-core approximation), where the inclusion of the two 1s single-particle functions systematically decreases the FCI energy. This difference however is very small, indicating that the contribution from particle-hole excitations of the 1s states is small. The QCCSD energy deviations from the respective FCI calculations are also very similar, deviating by the same order of magnitude as the FCI calculations.

R [a_0]	FCI ‡ [E_h]	QCCSD ‡ [mE_h]	FCI § [E_h]	QCCSD § [mE_h]
1.5	-106.72012	0.886	-106.72049	0.888
2.0	-107.62324	1.988	-107.62355	1.899
2.5	-107.65188	3.443	-107.65209	3.446
3.0	-107.54661	3.909	-107.54674	3.915
3.5	-107.47344	5.294	-107.47351	5.295
4.0	-107.44782	15.815	-107.44785	15.792
4.5	-107.44150	27.792	-107.44152	27.470
5.0	-107.43955	35.335	-107.43955	35.332
5.5	-107.43867	39.983	-107.43867	39.981
6.0	-107.43827	42.609	-107.43827	42.609
7.0	-107.43805	44.839	-107.43805	44.838
8.0	-107.43803	45.508	-107.43803	45.506

‡ Results from [27], with a 1s frozen-core approximation.
§ This work, without frozen-core approximation.

Table 5.5: Comparison of N_2 ground state energies calculated at different geometries in the sto-3g basis. FCI results are in E_h, while the QCCSD results are presented as the deviation from FCI in mE_h. Note that the results from [27] have frozen the two lowest-lying single-particle states in the correlated calculation. Results from this work have been converged to 10^{-4} in the τ and λ amplitudes.

Comparing with the dissociation results from [24], we find that the present implementation qualitatively reproduces the dissociation curves of H_2O and N_2, shown in Figure 5.3. For H_2O (see Figure 5.1a), we stretch the molecule by separating each hydrogen atom by a distance R from the oxygen atom. Distances larger than 4.5 a_0 resulted in a non-convergent HF calculation and thus no CC calculations could be performed. Both CCD and QCCD yield errors of a few mE_h around the equilibrium geometry. When increasing the hydrogen-oxygen distance, electron correlation becomes more important and the accuracy of both CCD and QCCD decreases. However, at approximately 3.5 a_0, the CCD correlation energy decreases substantially, giving a nonphysical local maximum resulting in severe errors at maximum separation. However, QCCD does not suffer from the local maximum and therefore retains errors on the order of mE_h.

The N_2 results presented in Figure 5.1b show similar behavior, where the collapse of the CCD dissociation curve is more pronounced than for H_2O. Qualitatively QCCD dissociates correctly

with errors only slightly larger than those given for QCCSD in Table 5.5. CCD on the other hand deviates with more than 200 mE_h at maximum separation, in addition to a qualitatively wrong curve.

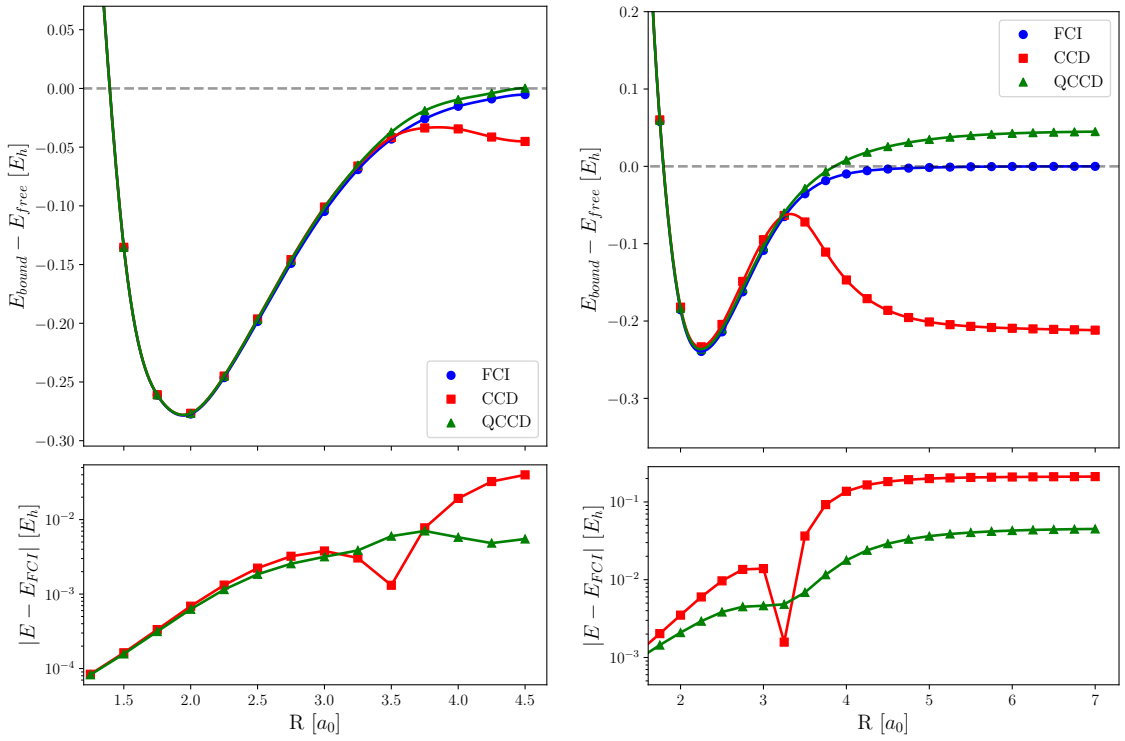

(a) H_2O **(b)** N_2

Figure 5.1: Upper: Ground state energy as a function of atomic separation for H_2O and N_2, subtracted by the FCI energy at infinite separation. Lower: The difference between CC energy estimates and FCI. Calculations are done using CCD and QCCD in the sto-3g basis set, all converged to 10^{-4} in the τ and λ amplitudes. The points have been fitted with a cubic spline to more easily see the shape of the dissociation curve.

Tests for the reduced one- and two-body density matrices, in addition to explicitly testing the Hellmann-Feynmann theorem, have been performed for both QCCD and QCCSD. This concerns the same techniques as was applied to standard CC.

5.4 Imaginary Time Propagation

In order to validate the implementation of the CC EOMs, we have performed imaginary time propagation as outlined in Sec. 4.5 for the He and Be atoms, in addition to the LiH and CH^+ molecules. Furthermore, we can solve for the ground state through fixed point iterations giving amplitudes τ_μ^{gs} and λ_μ^{gs}, which should be equal to the results from the imaginary time propagation. As such, we do not only investigate the correctness of the EOMs but also assert that the amplitude equations and EOMs are consistent with each other.

With the ground state amplitudes from fixed point iterations at hand, we can calculate the norm of the deviations $\delta\tau_\mu = \|\tau_\mu(\pi_+) - \tau_\mu^{\text{gs}}\|_{\text{F}}$ and $\delta\lambda_\mu = \|\lambda_\mu(\pi_-) - \lambda_\mu^{\text{gs}}\|_{\text{F}}$ as a function of $\pi_\pm$. Additionally, the energy deviation from the ground state $\delta E = |E(\tau_\pm) - E^{\text{gs}}|$ and energy change at each iteration $\delta E^{(n)} = |E^{(n+1)} - E^{(n)}|$ has been calculated. Since both $\dot{\tau}$ and $\dot{\lambda}$ go towards zero when the ground state is approached, convergence was determined by all $\|\dot{\tau}_\mu\|_{\text{F}}$ and $\|\dot{\lambda}_\mu\|_{\text{F}}$ amplitudes falling below a predetermined threshold ϵ.

Figure 5.2 shows convergence towards the ground state for LiH for QCCSD in the cc-pVDZ basis set. In Figure 5.2a, $E(\pi_\pm)$ goes towards E_{gs} exponentially, stabilizing with a difference of approximately 10^{-12} E_h at $\pi_\pm = 80$. This difference is two orders of magnitude smaller than the converged amplitude difference of $\epsilon = 10^{-10}$ and therefore attributed to numerical precision. The energy difference between two successive iterations displays similar behavior, reaching machine

precision at $\pi_\pm = 80$. Figure 5.2b shows that the amplitudes go towards the ground state, also exponentially.

Further results are presented for QCCD and QCCSD in Table 5.6 and Table 5.7 respectively. For all systems tested, the convergence behavior was similar to Figure 5.2. It is not guaranteed that $\delta\tau_\mu, \delta\lambda_\mu < \epsilon$ since the EOMs norms $\left\|\dot{\tau}_\mu\right\|_\mathrm{F}$ and $\left\|\dot{\lambda}_\mu\right\|_\mathrm{F}$ were used to determine convergence, however we expect and find them to be in the same order of magnitude as the amplitude convergence threshold ϵ. For the CCD and CCSD results for imaginary time propagation, see App. A.2.

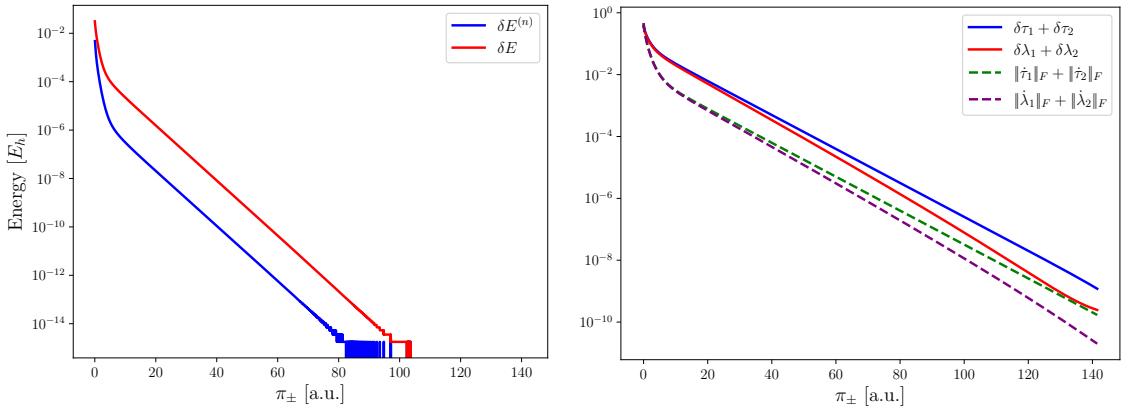

(a) Absolute energy difference from the ground state energy δE, and energy difference between each iteration $\delta E^{(n)}$ as a function of imaginary time

(b) Frobenius norm of the difference from the ground state amplitudes $\delta\tau_i$ and $\delta\lambda_i$, in addition to the norms of the EOMs $\left\|\dot{\tau}_\mu\right\|_\mathrm{F}$ and $\left\|\dot{\lambda}_\mu\right\|_\mathrm{F}$ as a function of imaginary time

Figure 5.2: Convergence of QCCSD imaginary time propagation for LiH in the cc-pVDZ basis. The integration was done using the Gaussian integrator with a time step $\Delta t = 0.05$, with the procedure stopping when the Frobenius norm of the time derivative of all amplitudes were less than $\epsilon = 10^{-10}$.

System	Basis	π'_+	$\log_{10}\epsilon$	$\delta\tau_2(\pi'_+)$	$\delta\lambda_2(\pi'_-)$
He	cc-pVDZ	7.70	−12	$2.804 \cdot 10^{-13}$	$2.179 \cdot 10^{-13}$
Be	sto-3g	57.25	−12	$4.898 \cdot 10^{-13}$	$2.097 \cdot 10^{-12}$
Be	cc-pVDZ	74.10	−12	$1.084 \cdot 10^{-12}$	$2.819 \cdot 10^{-12}$
LiH	sto-3g	36.70	−10	$1.840 \cdot 10^{-10}$	$1.526 \cdot 10^{-10}$
LiH	cc-pVDZ	39.30	−10	$1.772 \cdot 10^{-10}$	$1.434 \cdot 10^{-10}$
CH^+	sto-3g	59.00	−10	$2.772 \cdot 10^{-10}$	$2.153 \cdot 10^{-11}$
CH^+	cc-pVDZ	62.65	−10	$3.210 \cdot 10^{-10}$	$4.310 \cdot 10^{-11}$

Table 5.6: Results from imaginary time evolution calculated for different systems in different basis sets using QCCD. The propagation was run until all amplitude time-derivatives reached a lower value than ϵ, corresponding to the imaginary time $\pi'_\pm$. $\delta\tau_2$ and $\delta\lambda_2$ are the norms of the differences between the imaginary time evolved solution and fixed point solution converged to ϵ, both evaluated at $\pi'_\pm$. All energy differences were smaller than 10^{-12} and therefore not listed.

System	Basis	π'_+	$\log_{10}\epsilon$	$\delta\tau_1(\pi'_+)$	$\delta\lambda_1(\pi'_-)$	$\delta\tau_2(\pi'_+)$	$\delta\lambda_2(\pi'_-)$
He	cc-pVDZ	12.05	-12	$2.800 \cdot 10^{-13}$	$5.135 \cdot 10^{-13}$	$3.380 \cdot 10^{-14}$	$5.494 \cdot 10^{-14}$
Be	sto-3g	57.25	-12	0.000	0.000	$5.391 \cdot 10^{-13}$	$2.096 \cdot 10^{-12}$
Be	cc-pVDZ	74.30	-12	$1.081 \cdot 10^{-13}$	$1.033 \cdot 10^{-13}$	$6.011 \cdot 10^{-13}$	$2.938 \cdot 10^{-12}$
LiH	sto-3g	139.70	-10	$7.798 \cdot 10^{-10}$	$1.853 \cdot 10^{-10}$	$5.779 \cdot 10^{-10}$	$1.277 \cdot 10^{-10}$
LiH	cc-pVDZ	141.50	-10	$7.179 \cdot 10^{-10}$	$1.310 \cdot 10^{-10}$	$4.779 \cdot 10^{-10}$	$1.153 \cdot 10^{-10}$
CH^+	sto-3g	58.75	-10	$6.363 \cdot 10^{-12}$	$8.778 \cdot 10^{-13}$	$2.915 \cdot 10^{-10}$	$1.572 \cdot 10^{-11}$
CH^+	cc-pVDZ	62.90	-10	$9.806 \cdot 10^{-12}$	$9.633 \cdot 10^{-12}$	$3.478 \cdot 10^{-10}$	$3.446 \cdot 10^{-11}$

Table 5.7: Results from imaginary time evolution calculated for different systems in different basis sets using QCCSD. The propagation was run until all norms of the time-derivative of the amplitude equations reached a lower value than ϵ, corresponding to the imaginary time $\pi'_\pm$. $\delta\tau_1, \delta\tau_2, \delta\lambda_1$ and $\delta\lambda_2$ is the norm of the difference between the imaginary time evolved solution and fixed point solution converged to ϵ, both evaluated at $\pi'_\pm$. All energy differences were smaller than 10^{-12} and therefore not listed.

5.5 Real Time Propagation

The time-independent two particle systems from Sec. 5.1 are also excellent candidates for benchmarking the real-time evolution of the different CC methods. A study by Li et al. [119] performed time-dependent HF and FCI to the H_2 molecule undergoing a time-dependent interaction potential in the dipole approximation. Both CCSD and QCCSD reduce to FCI for two particle systems, thus giving grounds for comparisons with their work. This entails applying the envelope function

$$G(t) = \begin{cases} (\omega t/2\pi)E_{\max} & 0 \leq \omega t \leq 2\pi \\ E_{\max} & 2\pi \leq \omega t \leq 4\pi \\ (3 - \omega t/2\pi)E_{\max} & 4\pi \leq \omega t \leq 6\pi \\ 0 & 6\pi < \omega t \end{cases}, \tag{5.3}$$

with $E_{\max} = 0.07$ a.u. being the maximum field strength and $\omega = 0.1$ a.u. the field frequency. The two H atoms are displaced along the z-axis, with a relative distance $R_{\text{eq}} = 1.3897\ a_0$ as the equilibrium distance reported by Li et. al. With the dipole interaction from Eq. 2.56, we polarize the field along the z-axis such that $\boldsymbol{\epsilon} = \hat{\boldsymbol{e}}_z$. The 6-311++G(d,p) basis set has been applied, and propagated for 225 a.u. with 0.01 a.u. as the time step.

Figure 5.3a shows the z-component of the dipole moment calculated using CCSD and QCCSD, where the Gaussian integrator has been applied. Both methods qualitatively agree with the FCI results from Fig.4 in Ref. [119] by visual inspection. Additionally, Figure 5.3b displays the absolute difference of $\mu_z(t)$ between CCSD and QCCSD. The deviations are on the order of 10^{-9} a.u., attributed to the accuracy of the numerical integration.

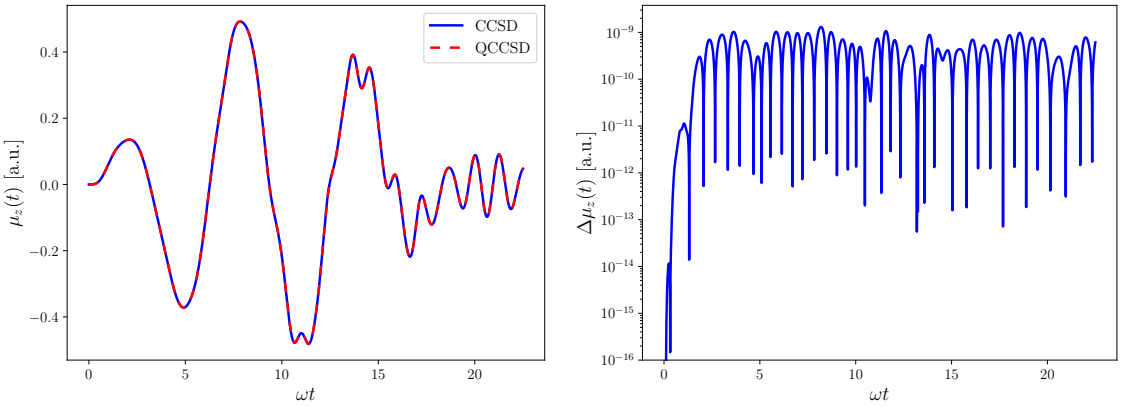

(a) z-component of the CCSD and QCCSD dipole expectation value

(b) Absolute difference between the CCSD and QCCSD z-component dipole expectation value

Figure 5.3: Time evolutions of the H_2 ground state irradiated by the dipole laser from Eq. 5.3, calculated with CCSD and QCCSD. The calculation has been run for $\omega t \in [0, 22.5]$ with a time step of $\Delta t = 0.01$ a.u., using the Gauss integrator.

Chapter 6

Results

We begin by comparing the CC configurational weights to FCI calculations of different systems at equilibrium and stretched geometries. This aids us in the following discussion, which considers multielectron bond breaking and the H_4 rectangle model system [120]. By defining a measure to quantify the non-hermiticity of the CC reduced density matrices, we study how this influences electric dipole and quadrupole moments. Thereafter, we investigate the stability of the quadratic CC methods and compare them to the standard methods, subject to a strong electric field. Lastly, we calculate the CH^+ absorption spectrum and compare CCSD and QCCSD results.

6.1 Configurational Weights

We begin by determining if the configurational weights from Sec. 3.6 are comparable to FCI. Table 6.1 shows CCSD, QCCSD and FCI results calculated for the He, Be and Ar atoms, in addition to the LiH, HF, CH^+ and BeH_2 molecules. The major contribution is from the reference, a good indication that the perturbative approach is valid in these regimes. For all of these systems, $W_D > W_S$, which can be understood from Brillouin's theorem since $\langle \Phi_0 | \hat{H} | \Phi_i^a \rangle = 0$ for the HF reference.

System	W_0			W_S			W_D		
	CCSD	QCCSD	FCI	CCSD	QCCSD	FCI	CCSD	QCCSD	FCI
He	0.9927	0.9927	0.9927	$< 10^{-4}$	$< 10^{-4}$	$< 10^{-4}$	0.0073	0.0073	0.0073
Be	0.9072	0.9072	0.9070	0.0010	0.0010	0.0010	0.0918	0.0919	0.0920
Ne	0.9726	0.9728	0.9723	$< 10^{-4}$	$< 10^{-4}$	$< 10^{-4}$	0.0274	0.0268	0.0271
LiH	0.9723	0.9723	0.9722	0.0045	0.0045	0.0045	0.0233	0.0233	0.0233
HF	0.9654	0.9658	0.9651	0.0005	0.0004	0.0004	0.0341	0.0333	0.0337
CH^+	0.9301	0.9302	0.9280	0.0010	0.0011	0.0011	0.0689	0.0680	0.0697
BeH_2	0.9706	0.9707	0.9692	0.0006	0.0006	0.0006	0.0289	0.0286	0.0296

Table 6.1: Configurational weights calculated for FCI, CCSD and QCCSD for different atomic and molecular systems. Calculations have been carried out in the cc-pVDZ and 6-31g basis set for atoms and molecules respectively. All molecular geometries are at equilibrium, listed in Table A.3.

Next, we consider stretched geometries where standard CC is known to give good energy estimates. Figure 6.1 shows LiH stretched for $R \in [2.5, 10]\ a_0$, calculated in the cc-pVDZ basis set. In the lower panel of Figure 6.1a, the energy deviation from FCI is below one mE_h for all bond distances. Similarly, the CC configurational weights of Figure 6.1b show good agreement with FCI, even when the reference contribution decreases.

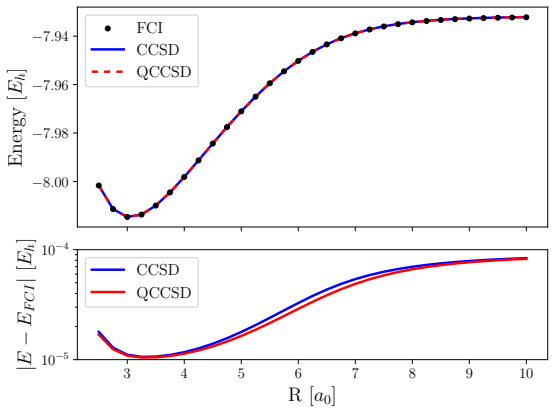

(a) LiH ground state energy.

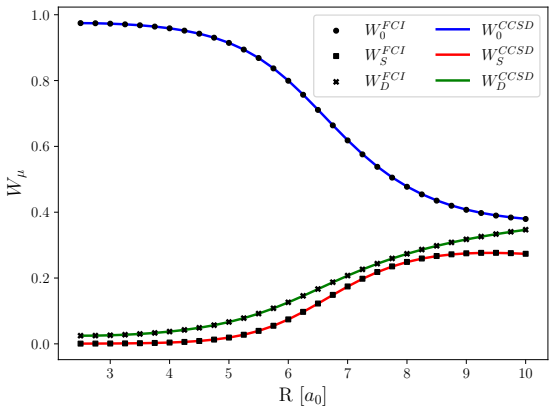

(b) LiH configurational weigths.

Figure 6.1: Configurational weights and energy for LiH in the cc-pVDZ basis set, calculated for different nuclei separations using FCI, CCSD, and QCCSD. Right (a): Ground state energy from the FCI, CCSD, and QCCSD calculation, in addition to deviation from FCI. All CC calculations were converged to 10^{-6} in the amplitudes. Left (b): Configurational weights calculated using FCI and CCSD. The QCCSD results are not shown, as the mean deviation from CCSD was of the order 10^{-5}.

Despite the excellent agreement between W_μ^{CC} and W_μ^{FCI} shown thus far, systems can be constructed where the CC energy estimates are good, whilst the weight composition is a poor approximation to FCI. Figure 6.2 shows a sketch of two different H_2 dissociation examples. In Figure 6.2a, the two nuclei are separated by a variable distance R, referred to as single H_2 dissociation. This system contains two electrons, such that both CCSD and QCCSD formally reduce to FCI. Figure 6.2b shows two identical copies of the single H_2 dissociation, which we will refer to as double $(H_2)_2$ dissociation. The two subsystems are separated by a distance D, such that if D is large enough the two subsystems will not interact with each other. Therefore, due to the CC

energy retaining size-consistency, the energy of both H_2 and $(H_2)_2$ is exact when compared to FCI, assuming that D is large. For the present work, $D = 1000\ a_0$ has been used.

Table 6.2 shows the CCSD results for both dissociations. For single H_2 dissociation, the CC configurational weights correctly reproduce those of FCI. Increasing R decreases the reference weight, while both the singles and doubles weight increases. At $R = 4R_e$, almost half of the weight contribution resides in the double weights, corresponding to single excitations in each atom.

Considering $(H_2)_2$ double dissociation, there are some deviations in the weights even at equilibrium geometry. Stretching both subsystems results in CCSD overestimating the singles and doubles weight by almost a factor of two, while the reference weight is underestimated. This is attributed to excitations of rank larger than two being present in the system. In particular, the case where all four electrons are excited is manifested as a quadruple excitation. This contribution can not be represented in the CCSD left-state, where at most double excitations contribute.

Table 6.3 shows the QCCSD weights calculated for $(H_2)_2$ double dissociation. In contrast to CCSD, triple and quadruple excitations are present in the left-state, giving a non-zero W_T and W_Q contribution. This mends the W_0, W_S and W_D estimates as well, agreeing with FCI to the fourth decimal at $3R_e$ and $4R_e$.

By adding a third H_2 molecule, giving $(H_2)_3$ triple dissociation, quintuple (5p5h) and sextuple (6p6h) contributions would become important. From size-consistency, both CCSD and QCCSD should have exact energies when compared to FCI. However, in this case, both weight estimates would suffer from the lack of higher excitation contributions in the left-state. Therefore, some care should be taken when considering the CC weight estimates, particularly for dissociated systems, due to the configurational weights not retaining size-consistency.

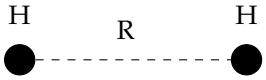

(a) Single H_2 dissociation.

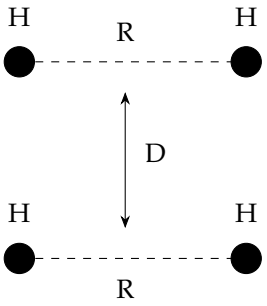

(b) Double $(H_2)_2$ dissociation.

Figure 6.2: Sketches of two different hydrogen dissociations. Left (a): Single H_2 dissociation, where the two hydrogen atoms are separated by a distance R. Right (b): Double $(H_2)_2$ dissociation, where two identical non-interactive H_2 systems are separated by a large distance D. The nuclei in each of the H_2 subsystems are separated by the distance R.

System	R	W_0		W_S		W_D	
		CCSD	FCI	CCSD	FCI	CCSD	FCI
H_2	R_e	0.9825	0.9825	$1.21 \cdot 10^{-4}$	$1.21 \cdot 10^{-4}$	0.0174	0.0174
	$2R_e$	0.9048	0.9048	$2.99 \cdot 10^{-3}$	$2.99 \cdot 10^{-3}$	0.0922	0.0922
	$3R_e$	0.6933	0.6933	0.0113	0.0113	0.2955	0.2955
	$4R_e$	0.5546	0.5546	0.0157	0.0157	0.4298	0.4298
$(H_2)_2$	R_e	0.9650	0.9653	$2.42 \cdot 10^{-4}$	$2.38 \cdot 10^{-4}$	0.0348	0.0342
	$2R_e$	0.8095	0.8186	$5.98 \cdot 10^{-3}$	$5.41 \cdot 10^{-3}$	0.1845	0.1669
	$3R_e$	0.3865	0.4806	0.0226	0.0157	0.5909	0.4098
	$4R_e$	0.1091	0.3075	0.0314	0.0174	0.8595	0.4769

Table 6.2: Configurational weights for the H_2 single dissociation and $(H_2)_2$ double dissociation, calculated for CCSD and FCI in the cc-pVDZ basis set. The equilibrium geometry of $R_e = 1.4379\ a_0$ has been used for both systems.

R	W_0		W_S		W_D		QCCSD	
	QCCSD	FCI	QCCSD	FCI	QCCSD	FCI	W_T	W_Q
R_e	0.9653	0.9653	$2.38 \cdot 10^{-4}$	$2.38 \cdot 10^{-4}$	0.0342	0.0342	$4.21 \cdot 10^{-6}$	$3.02 \cdot 10^{-4}$
$2R_e$	0.8186	0.8186	$5.41 \cdot 10^{-3}$	$5.41 \cdot 10^{-3}$	0.1669	0.1669	$5.52 \cdot 10^{-4}$	$8.51 \cdot 10^{-3}$
$3R_e$	0.4806	0.4806	0.0156	0.0157	0.4098	0.4098	$6.70 \cdot 10^{-3}$	0.0873
$4R_e$	0.3076	0.3075	0.0173	0.0174	0.4769	0.4769	0.0136	0.1847

Table 6.3: Configurational weights for the $(H_2)_2$ double dissociation, calculated for QCCSD and FCI in the cc-pVDZ basis set. Results for H_2 single dissociation are not shown, due to the weights having a mean deviation of 10^{-8} when compared to the CCSD results of Table 6.2. The equilibrium geometry of $R_e = 1.4379\ a_0$ has been used.

6.2 Stretched Geometries

Revisiting the dissociation calculations from Sec. 5.3, we repeated the N_2 ground state energy calculation in the cc-pVTZ basis set. Due to the size of the basis set, performing an FCI calculation with all 14 electrons active is unfeasible. Therefore, we can only rely on approximate methods.

In Figure 6.3a, we again find a local maximum for CCSD as was the case for the CCD sto-3g results from Figure 5.1b, that is, the nonphysical "collapse" does not disappear in the larger basis set. However, QCCSD can describe the multielectron bond-breaking. Additionally, we have included results from a CISD calculation, displaying a behavior for large R reminiscent of the lack of size-consistency. Figure 6.3b shows the correlation energy of the three post-HF methods. At $R = 4\ a_0$, CCSD has a drastic correlation energy decrease, giving rise to the local minimum in the dissociation curve. Contrastingly, CISD displays more unchanging correlation energy, attributed to the lack of particle-hole excitations higher than rank two.

The CCSD, QCCSD, and FCI reference and doubles configurational weights calculated in the sto-3g basis for N_2 are shown in Figure 6.4a. From the FCI curve, we observe that the reference contribution starts at almost one, decreasing with the increasing nuclear separation and going close to zero at large distances. The CCD weights reproduce this around the equilibrium geometry, however, the reference weight quickly plummets while the doubles weight drastically increases around the bond-breaking region. Weights from QCCD reproduce the FCI results at further nuclear separations, but deviations appear at longer distances. This is due to the increasing quadruple weights (not shown in the figure), which presumably overestimate the FCI quadruple weights. Similar to how CCSD overestimated the doubles weights for the $(H_2)_2$ double dissociation example of Table 6.2, triples or higher excitations could be important in the ground state calculation of a single nitrogen atom, resulting in non-zero contributions from quintuple excitations and higher.

In Figure 6.4b we perform the same analysis in the large cc-pVTZ basis set, with qualitatively the same results. Here the CCSD reference and double weights are even further apart, while for QCCSD they are closer.

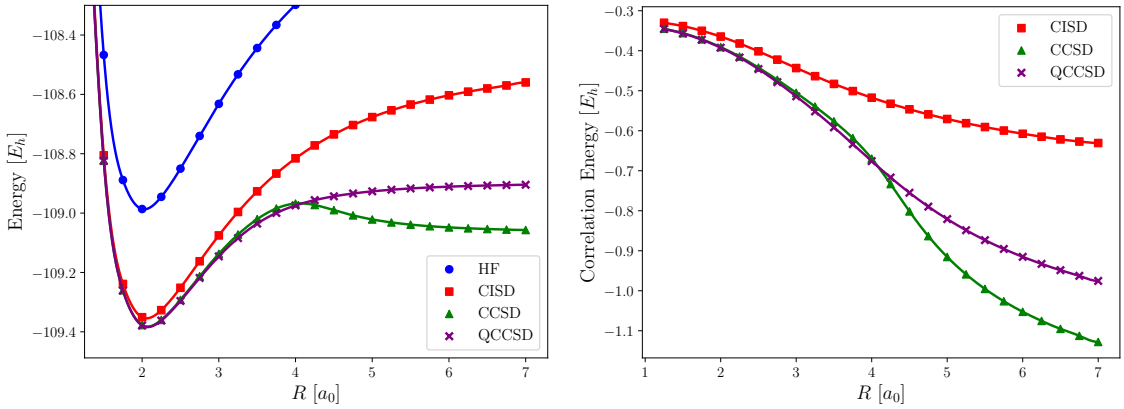

(a) Total energy of HF and post-HF methods

(b) Correlation energy of post-HF methods

Figure 6.3: Dissociation curve of N_2 using HF, CISD, CCSD, and QCCSD in the cc-pVTZ basis set. Left (a): The total energy of the system. Right (b): The correlation energy of the system.

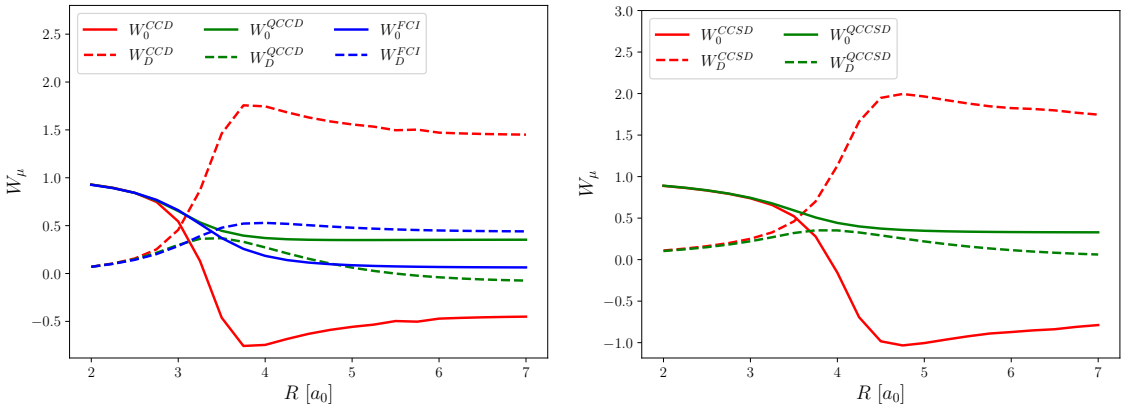

(a) CCD, QCCD and FCI configurational weights in the sto-3g basis set.

(b) CCSD and QCCSD configurational weights in the cc-pVTZ basis set.

Figure 6.4: Configurational weights for the N_2 molecule, calculated for different nuclei separation geometries. Left (a): shows the CCD, QCCD, and FCI results in the sto-3g basis. Right (a): the CCSD and QCCSD results for the cc-pVTZ basis. The single weights are not shown in the figures, due to both being very close to zero.

Next we will consider the H_4 rectangle model system [120]. Fig. 6.5 displays the geometry, where four hydrogen atoms are placed on the circumference of a circle of radius R, with the angle θ determining the distances to the nearest neighbors. We will consider the system at a fixed $R = 3.284$ a_0, while varying the angle θ. At $\theta = 90°$, the hydrogen atoms form a square, while decreasing the angle produces a rectangle where small θ forms two H_2 molecules.

In Figure 6.6a, we see the FCI, CCSD, and QCCSD energies as a function of θ. Not only is CCSD below the FCI curve, but also predicts a sharp local minimum at $\theta = 90°$, contrary to the FCI results. On the other hand, QCCSD resides above the FCI curve for all θ. However, the sharp peak is not resolved in the quadratic scheme, such that QCCSD does not exhibit the correct qualitative behavior around $\theta = 90°$.

Figure 6.6b shows the largest configurational weight for each order compared between the three methods. The QCCSD weights do produce better FCI estimates than CCSD, as expected from the energy results. However, the FCI results show a vanishing singles contribution at $\theta = 90°$, which neither CCSD nor QCCSD reproduces.

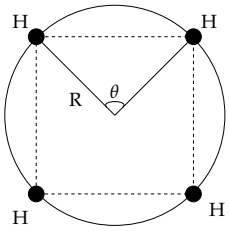

Figure 6.5: Sketch of the H_4 rectangle. The four hydrogen atoms are placed on a circle with radius R in the xy-plane. We vary the system by changing the angle θ, with $\theta = 90°$ producing a square.

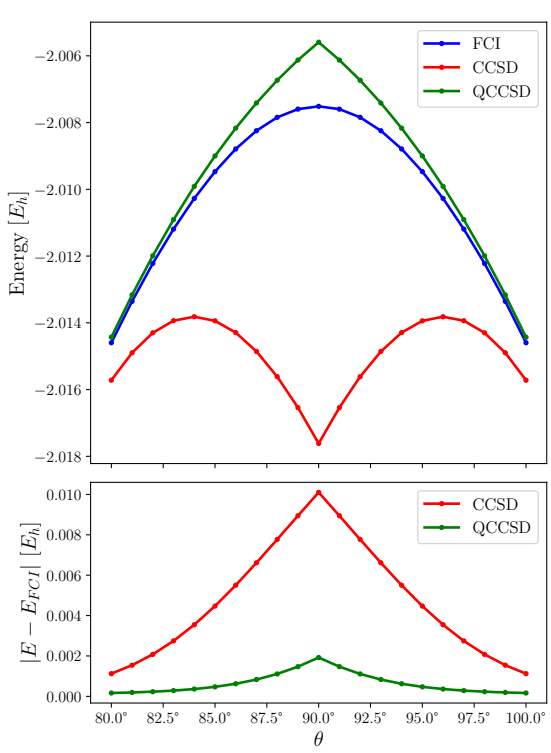

(a) Total energy and difference from FCI

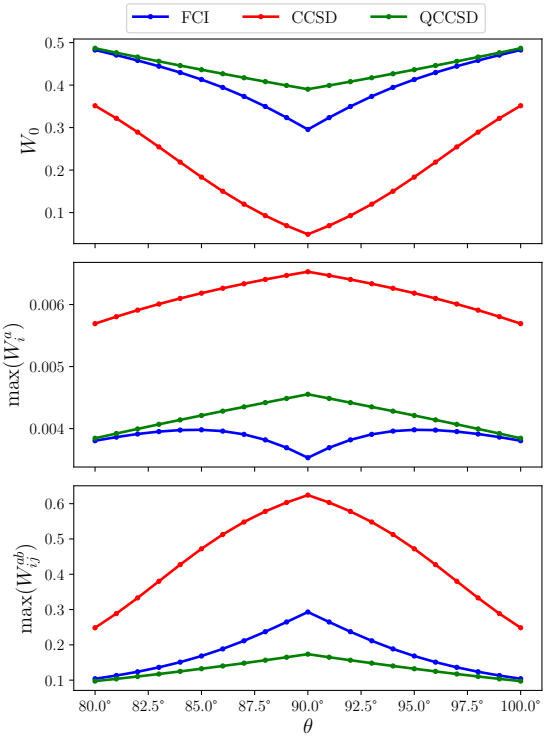

(b) Reference weight and the maximum of the singles and doubles weights.

Figure 6.6: CCSD, QCCSD, and FCI calculated ground state energies as a function of θ for the H_4 rectangle in the DZP basis set. Left (a): shows the ground state energy and deviations from FCI. Right (b): displays the reference and maximum singles and doubles weight.

6.3 Reduced Density Matrices and Electrostatics

Following the discussion of Sec. 3.3.3, the potential of non-hermitian (or non-symmetric if all wavefunction parameters are real) reduced density matrices is present in the bivariational CC formulation. Calculations constructing $\gamma^*_{qp} = \gamma_{pq}$ and $(\Gamma^{pq}_{rs})^* = \Gamma^{rs}_{pq}$ are important properties to qualitatively represent the FCI state, though not essential to achieve satisfactory expectation value estimates. To gauge this property for the standard and quadratic CC methods, we define a metric to measure the non-hermiticity,

$$N_1 \equiv \sqrt{\sum_{pq} |\gamma_{pq} - \gamma_{qp}|^2}, \quad N_2 \equiv \sqrt{\sum_{pqrs} |\Gamma^{pq}_{rs} - (\Gamma^{rs}_{pq})^*|^2}, \tag{6.1}$$

where N_1 and N_2 measure the non-hermiticity of the reduced one- and two-body density matrices respectively. For variational theories and thus FCI, $N_1 = N_2 = 0$ is guaranteed. Importantly, N_1 and N_2 are not fit for comparison between different system sizes, as the magnitudes of density

matrices are dependent on the number of particles. However, for a particular system, N_1 and N_2 can be compared between different methods.

Table 6.4 shows the non-hermiticity of various molecules, compared between the CCSD and QCCSD truncations. For the QCCSD method, we consistently find more hermitian density matrices, with both N_1 and N_2 being an order of magnitude smaller than that of CCSD. The results of Table 6.4 have been calculated in the cc-pVDZ basis set, however, the decrease in N_1 and N_2 compared to CCSD has been found to be an order of magnitude independent of the basis set.

Basis set	N_1		N_2		Ratio	
	CCSD	QCCSD	CCSD	QCCSD	γ	Γ
HF	$1.020 \cdot 10^{-2}$	$7.784 \cdot 10^{-4}$	$5.897 \cdot 10^{-2}$	$4.591 \cdot 10^{-3}$	13.11	12.84
LiH	$2.548 \cdot 10^{-4}$	$1.524 \cdot 10^{-5}$	$8.664 \cdot 10^{-4}$	$5.583 \cdot 10^{-5}$	16.72	15.52
CH^+	$6.924 \cdot 10^{-3}$	$2.967 \cdot 10^{-4}$	$3.141 \cdot 10^{-2}$	$1.353 \cdot 10^{-3}$	23.33	23.21
BeO	$1.582 \cdot 10^{-1}$	$1.304 \cdot 10^{-2}$	1.013	$8.459 \cdot 10^{-2}$	12.13	11.97
N_2	$2.081 \cdot 10^{-2}$	$7.741 \cdot 10^{-4}$	$1.451 \cdot 10^{-1}$	$5.611 \cdot 10^{-3}$	26.88	25.87
H_2O	$7.006 \cdot 10^{-3}$	$2.262 \cdot 10^{-4}$	$4.041 \cdot 10^{-2}$	$1.358 \cdot 10^{-3}$	30.97	29.75
BeH_2	$2.488 \cdot 10^{-3}$	$1.460 \cdot 10^{-4}$	$1.083 \cdot 10^{-2}$	$6.572 \cdot 10^{-4}$	17.03	16.48

Table 6.4: Frobenius norm of the non-hermitian terms of reduced one- and two-body density matrices, calculated using CCSD and QCCSD for different molecules in the cc-pVDZ basis set. The equilibrium geometries in charge center coordinates are presented in Table A.3, taken from [117]. In the ratio column, the CCSD results divided by the QCCSD results $N_i^{\text{CCSD}} / N_i^{\text{QCCSD}}$ for the one-body γ and two-body Γ reduced density matrices are displayed.

Despite the more hermitian reduced density matrices of the quadratic CC theory, deviations from the FCI densities are more relevant when considering accurate expectation values. Thus, we define

$$\delta A \equiv \langle A \rangle - \langle A \rangle^{\text{FCI}} = \text{tr}\Big\{ (\gamma - \gamma^{\text{FCI}}) A \Big\} \equiv \text{tr}\{\delta\gamma A\}, \tag{6.2}$$

where δA and $\delta\gamma$ are the differences between the CC and FCI calculated expectation values and density matrices respectively. From Eq. 6.2 we note that smaller deviations from the FCI one-body density will reduce the expectation value error, where in the limit $\gamma \to \gamma^{\text{FCI}}$ the error reduces to zero. Additionally, since the different parts of the CC density matrices are calculated through different expressions, it is constructive to partition the error into contributions from the different blocks. Considering the FCI difference in the one-body density from Eq. 6.2, the error can be separated as contributions from four different traces,

$$\begin{aligned} \delta A = \sum_{pq} \delta\gamma_{pq} A_{qp} &= \sum_{ij} \delta\gamma_{ij} A_{ji} + \sum_{ab} \delta\gamma_{ab} A_{ba} + \sum_{ai} \delta\gamma_{ia} A_{ai} + \sum_{ai} \delta\gamma_{ai} A_{ia} \\ &\equiv \delta A^{\text{oo}} + \delta A^{\text{vv}} + \delta A^{\text{ov}} + \delta A^{\text{vo}}, \end{aligned} \tag{6.3}$$

where $\delta A^{\text{oo}}, \delta A^{\text{vv}}, \delta A^{\text{ov}}$ and δA^{vo} are the error contributions from the occupied-occupied, virtual-virtual, occupied-virtual and virtual-occupied blocks of γ respectively. Due to the non-hermiticity of γ, in general $\delta A^{\text{ov}} \neq \delta A^{\text{vo}}$. For larger molecules and basis sets, performing the FCI calculation becomes too expensive such that γ^{FCI} is not available. Therefore, in the following, we will consider LiH and HF with cc-pVDZ as the largest basis set.

In Figure 6.7 the $\gamma - \gamma^{\text{FCI}}$ difference for the HF molecule in the cc-pVDZ basis set is compared between CCSD and QCCSD. Both the occupied-occupied and virtual-virtual blocks are similar between the two methods. For the off-diagonal blocks, however, the more non-hermitian nature of CCSD is apparent. Table 6.5 displays the norm of the reduced density differences, in addition to the dipole moment and quadrupole moment absolute errors for LiH and HF. The LiH results of Table 6.5a show the QCCSD density matrix error to be slightly smaller than that of CCSD, however, the differences are only of the order 10^{-4}. This is in contrast to the dipole and quadrupole errors, where the CCSD error is slightly less than half of the QCCSD error for 6-31g and 6-31g* basis sets. The HF results from Table 6.5b show similar behavior, with the gap between the reduced density matrix errors increasing, being a factor of $1/2$ to $3/4$ times smaller for QCCSD when

compared to CCSD. This is again accompanied by the QCCSD dipole and quadrupole expectation value errors being larger than that of CCSD.

The combination of the one-body density matrices of QCCSD being closer to FCI than that of CCSD, while yielding less accurate expectation value estimates, is counterintuitive in view of Eq. 6.2. Table 6.6 shows the dipole moment error partitioned into the four γ-blocks following Eq. 6.3 for LiH and HF. The error contribution from the occupied-occupied and virtual-virtual blocks are quite similar between CCSD and QCCSD. However, the occupied-virtual and virtual-occupied contributions behave differently, as suggested by Figure 6.7. Importantly, the CCSD $\delta\mu_z^{\mathrm{ov}}$ and $\delta\mu_z^{\mathrm{vo}}$ contributions underestimate and overestimate the dipole moment respectively, giving a smaller combined $\delta\mu_z$. However, QCCSD has both a smaller error in the contribution from γ^{ov} and γ^{vo}, in addition to $\delta\mu_z^{\mathrm{ov}}$ and $\delta\mu_z^{\mathrm{vo}}$ being more equal as expected from the smaller non-hermiticity. Consequently, the same cancelation from the occupied-virtual and virtual-occupied blocks is not manifested in the QCCSD theory, which in turn increases the total error in the dipole moment.

Determining if the deviations in the CCSD γ^{ov} and γ^{vo} blocks systematically result in a beneficial error cancelation would require further analysis on a wide range of systems, in addition to estimations of other expectation values. The current results from LiH and HF for the position-based dipole and quadrupole expectation values indicate that the CCSD asymmetry of Figure 6.7 is beneficial for expectation value estimates.

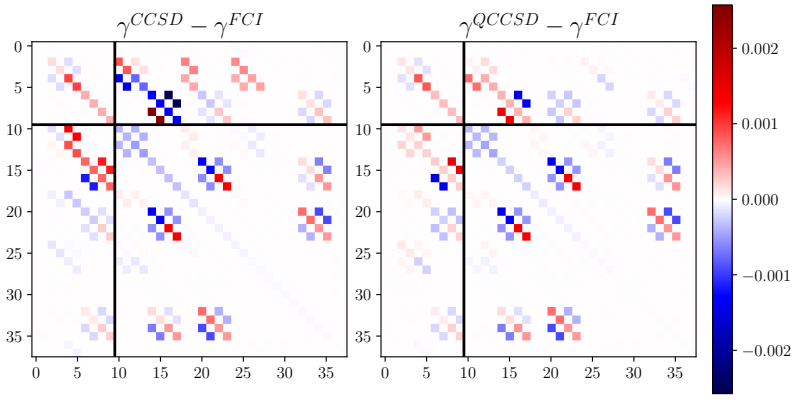

Figure 6.7: Element-wise difference of the CCSD (left) and QCCSD (right) reduced one-body density matrices with FCI for the HF molecule in the cc-pVDZ basis set. The black lines partition γ the matrix into four blocks, going clockwise from the top left as occupied-occupied $(\delta\gamma_{ij})$, occupied-virtual $(\delta\gamma_{ia})$, virtual-virtual $(\delta\gamma_{ab})$ and virtual-occupied $(\delta\gamma_{ai})$.

System	Basis set	CCSD [mea_0]				QCCSD [mea_0]			
		$\delta\mu_z^{\mathrm{oo}}$	$\delta\mu_z^{\mathrm{vv}}$	$\delta\mu_z^{\mathrm{ov}}$	$\delta\mu_z^{\mathrm{vo}}$	$\delta\mu_z^{\mathrm{oo}}$	$\delta\mu_z^{\mathrm{vv}}$	$\delta\mu_z^{\mathrm{ov}}$	$\delta\mu_z^{\mathrm{vo}}$
LiH	6-31g	0.164	0.016	-0.036	0.116	0.185	0.025	0.115	0.102
	6-31g*	0.173	4.228	-0.064	0.121	0.194	4.235	0.115	0.100
	cc-pVDZ	0.125	-14.411	-0.018	0.088	0.132	-14.409	0.084	0.079
HF	6-31g	-0.134	0.980	-3.144	2.009	-0.128	1.039	0.778	0.472
	6-31g*	-0.044	1.876	-4.629	2.243	-0.021	1.936	0.520	-0.056
	cc-pVDZ	-0.295	3.650	-3.108	2.782	-0.287	3.499	1.386	0.844

Table 6.6: Dipole moments along the z axis given as deviations from FCI in mea_0, decomposed as block contributions from $\gamma_{ij}, \gamma_{ab}, \gamma_{ia}$ and γ_{ai} calculated using CCSD and QCCSD. Results for the two molecules LiH and HF are shown in the 6-31g, 6-31g*, and cc-pVDZ basis sets.

6.4 Stability of Time-Dependent QCCSD

For two-electron systems, both CCSD and QCCSD reduce to FCI. However, as discussed in Sec. 4.6, this does not imply that time propagation will be exact or even stable, due to the necessity

Basis set	$\|\delta\gamma\|_F$		$\delta\mu_z$ [mea_0]		$\mu_z[ea_0]$	δQ_{zz} [mea_0^2]		Q_{zz} [ea_0^2]
	CCSD	QCCSD	CCSD	QCCSD	FCI	CCSD	QCCSD	FCI
6-31g	0.0056	0.0052	0.260	0.426	2.165029	0.618	0.907	7.515738
6-31g*	0.0254	0.0248	0.227	0.412	2.156752	0.565	0.929	7.341301
cc-pVDZ	0.0566	0.0562	22.714	22.816	2.226523	-18.894	-18.712	7.563480

(a) LiH

Basis set	$\|\delta\gamma\|_F$		$\delta\mu_z$ [mea_0]		$\mu_z[ea_0]$	δQ_{zz} [mea_0^2]		Q_{zz} [ea_0^2]
	CCSD	QCCSD	CCSD	QCCSD	FCI	CCSD	QCCSD	FCI
6-31g	0.0604	0.0373	-0.289	2.161	0.860226	-8.048	-10.241	1.332704
6-31g*	0.1163	0.0822	-0.784	2.474	0.750486	-1.192	-4.258	1.180081
cc-pVDZ	0.0910	0.0695	1.667	4.913	0.715342	-3.485	-7.434	1.264289

(b) HF

Table 6.5: Dipole moment along the z axis and quadrupole zz component calculated using CCSD, QCCSD, and FCI calculated in the 6-31g, 6-31g* and cc-pVDZ basis sets, for LiH (a) and HF (b). FCI results are given in ea_0 and ea_0^2 for μ_z and Q_{zz} respectively, with CCSD and QCCSD results as the deviation from FCI in mea_0 and mea_0^2.

of numerical integration. Following the discussion in Refs. [48, 74], we apply similar techniques to test the numerical stability of QCCSD compared to CCSD. We will consider the He atom subject to a laser pulse on the form of Eq. 2.55 with a sinusoidal envelope function,

$$G(t) = \begin{cases} E_{\max} \sin^2(\pi t/t_d) & t \leq t_p \\ 0 & t > t_p, \end{cases} \tag{6.4}$$

where t_p is the total duration of the pulse and $E_{\max}$ the maximum field strength. The strength of the field is set to $E_{\max} = 5.0$ a.u., with $\omega = 2.87$ a.u as the frequency of the pulse in Eq. 2.55. This field strength is quite large, where Ref. [48] found that applying an even stronger field with $E_{\max} = 100$ a.u. required a time step of 10^{-3} a.u. to be stable during a $t_d = 5$ a.u. pulse using CCSD.

We will rather consider running a calculation over a longer period of time, where the conservation of energy for $t > t_d$ is studied as a function of the time step similar to Ref. [74]. The external potential will be on for two cycles, $t_p = 4\pi/\omega$, with the total running time of $t \in [0, 10t_p]$. The time evolution will be calculated in the cc-pVDZ basis set[1].

Figure 6.8a displays the energy conservation for different time steps, compared between CCSD and QCCSD using the RK4 integrator. For the 0.1 a.u. and 0.05 a.u. time steps, RK4 inhibits poor energy conservation for both CCSD and QCCSD. When decreasing the time step to 0.01 a.u., the error at $10t_p$ reduces from approximately 10^{-3} E_h to approximately 10^{-7} E_h and 10^{-6} E_h for CCSD and QCCSD respectively. This is further reduced by two orders of magnitude when reducing the time step by half.

In Figure 6.8b we have applied the Gauss integrator, which systematically improves the energy conservation for all time steps as expected. Using the time steps of 0.1 a.u. and 0.05 a.u., the CCSD error is around two orders of magnitude smaller than QCCSD. Additionally, CCSD inhibits more oscillatory energy conservation. These oscillations are also present for QCCSD, however, the magnitude is much smaller and therefore not visible in the figure. Decreasing the time step to 0.01 a.u. and 0.005 a.u. reduces the error drastically.

For both the RK4 and Gauss integrator, the QCCSD energy conservation is worse than that of CCSD. The QCCSD EOMs contain more higher-order non-linear terms due to the inclusion of $\hat{\Lambda}^2$, making them harder to integrate. Additionally, the coupling of the time derivative of the amplitudes might also serve as a reason for the lower accuracy. Therefore, to guarantee stable results, a smaller time step is crucial for QCCSD.

[1] This field strength is exceedingly large, such that the dynamics calculated when the field is on will not be physically correct when the relatively small cc-pVDZ basis set is applied. However, since we are only interested in the energy conservation after the pulse is turned off, this is not a concern.

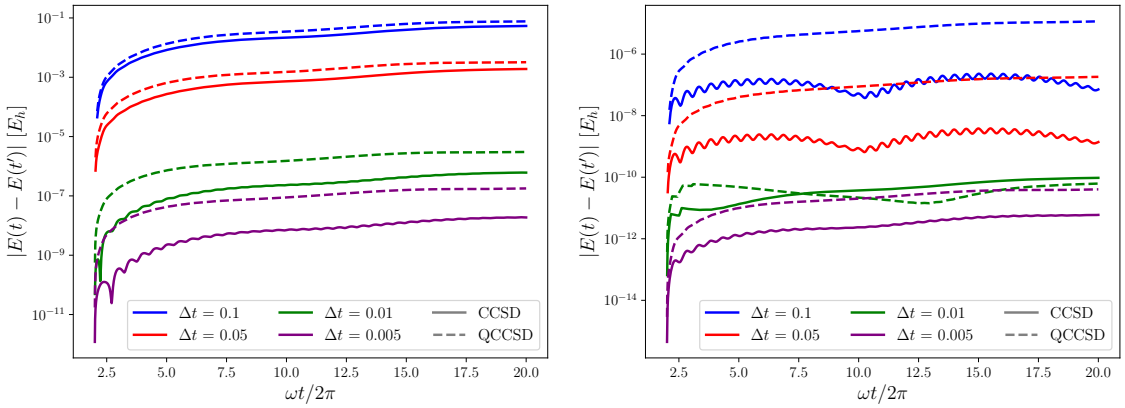

(a) 4th order Runge-Kutta

(b) Gaussian integrator

Figure 6.8: Energy conservation of CCSD and QCCSD after a single He atom has been irradiated by a strong laser pulse for different time steps Δt (in a.u.). Left (a): Results using the RK4 integrator. Left (b): results using the Gauss integrator.

6.5 Absorption Spectrum

Singlet excited states that are dominated by single excitations are generally well described by real-time CCSD spectrum analysis [47]. Doubles dominated states are however less precisely described [121]. In particular, we have looked at the CH^+ ion following the study of Koch et al. [122], which categorizes the lowest-lying singlet excited states by being either τ_1 or τ_2 dominated. They applied linear-response coupled cluster (CCLR) to estimate the energy of excited states, which is closely related to the equations of motion coupled cluster (EOM-CC) [21, 30]. From the CCSDLR calculations of Koch et al., they estimated the contributions from the τ_1 and τ_2 amplitudes, indicating if an excited state is singles or doubles dominated respectively. By performing an EOM-CCSD calculation, we compare with the absorption spectrum calculated using real-time CCSD and QCCSD, with the former expected to recreate the EOM-CCSD results.

Using the basis set from Ref. [121], we have 52 basis functions in the general scheme (without spin-restriction). We separate the C atom and H^+ ion along the z-axis, with $R_{\text{eq}} = 2.13713$ a.u. as the relative distance between them. All calculations are performed for two different polarization vectors, being parallel $\boldsymbol{\epsilon} = \hat{\boldsymbol{e}}_z$ and perpendicular $\boldsymbol{\epsilon} = \hat{\boldsymbol{e}}_y$ to the symmetry axis. The molecule is symmetric under rotations around the z-axis, such that $\mu^{\text{I}}_{xx} = \mu^{\text{I}}_{yy}$. Thus, we do not need to perform the calculation with the field polarized along the x-axis.

Table 6.7 shows the FCI and EOM-CCSD CH^+ excitation energies, in addition to the classification of which excited state is τ_1 and τ_2 dominated. The notation $\tau_1 \gg \tau_2, \tau_1 \ll \tau_2$ is used for very τ_1 and τ_2 dominated respectively, while $\tau_1 > \tau_2$ and $\tau_1 < \tau_2$ are mixed but still mostly contains τ_1 and τ_2 contributions respectively. Clearly, the τ_1 dominated excited states are closer to the FCI results than the τ_2 dominated states.

FCI† [eV]	EOM-CCSD‡ [eV]	Deviation [eV]	τ-contribution†
3.2296	3.2607	0.0311	$\tau_1 \gg \tau_2$
6.9642	7.8875	0.9233	$\tau_1 \ll \tau_2$
8.5492	9.1088	0.5596	$\tau_1 \ll \tau_2$
13.5246	13.5804	0.0558	$\tau_1 \gg \tau_2$
14.1271	14.4642	0.3271	$\tau_1 > \tau_2$
16.8331	17.3156	0.4825	$\tau_1 < \tau_2$
17.217	17.3412	0.1242	$\tau_1 \gg \tau_2$

† Koch et al. results
‡ Calculated using `PySCF`

Table 6.7: FCI and EOM-CCSD singlet excitation energies in eV. The deviation column displays the difference between the FCI and EOM-CCSD results, while the τ-contribution column describes the importance of singles and doubles τ amplitudes as reported by Koch et al. [122].

We wish to estimate the excitation energies from Table 6.7 by obtaining the absorption spectrum through real-time propagation. To maximize the population of dipole-allowed excited states, we apply the δ-kick perturbation defined by Eq. 2.65. This is realized numerically as,

$$\boldsymbol{E}_{\text{kick}}(t) = \begin{cases} \kappa/\Delta t \boldsymbol{\epsilon} & t < \Delta t \\ 0 & t > 0 \end{cases}, \tag{6.5}$$

with $\kappa = 10^{-3}$ a.u. as the perturbation strength and $\Delta t = 0.01$ a.u. the time step.

Figure 6.9a shows the zz-component of the induced dipole moment, calculated until $t_{\text{end}} = 2000$ a.u. using CCSD in the spin-restricted scheme. Using Eqs. 2.63 and 2.64, we calculate the corresponding spectrum in Figure 6.9b, with $\gamma = 0.00921$ a.u. used for the Fourier transform. The distance between neighboring points in the frequency domain is related to the total signal time through $\Delta\omega = 2\pi/t_{\text{end}}$ [123]. With $t_{\text{end}} = 2000$ a.u. for the CCSD calculation, the smallest detectable frequency difference i $\Delta\omega = 3.14\text{m}E_{\text{h}} \approx 0.085$ eV.

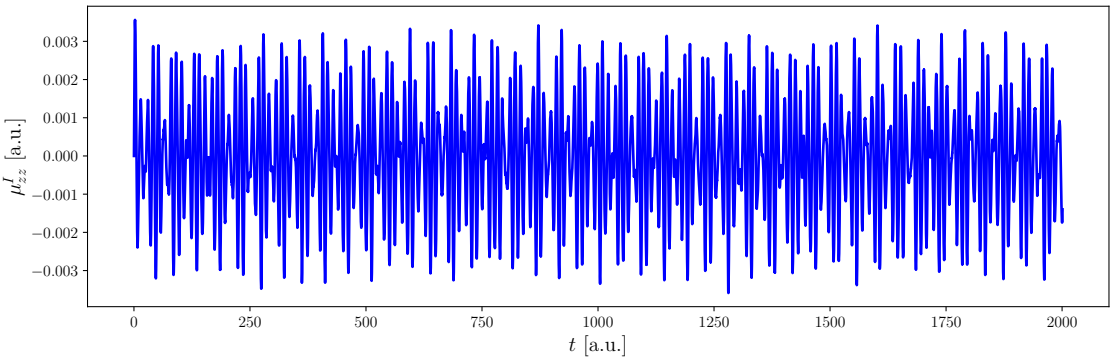

(a) The z-component of the induced dipole moment, with the field polarized along the z-axis.

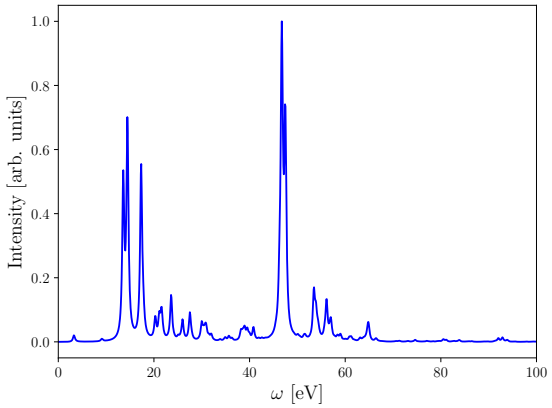

(b) Normalized $S(\omega)$ absorption spectrum, cut to the $[0, 100]$ eV range. The frequency spacing is 0.085 eV.

Figure 6.9: Excitation spectrum of CH^+ calculated from the Fourier transform of the induced dipole moment undergoing a δ-kick perturbation. Restricted CCSD has been used, propagated until $t_{\text{end}} = 2000$ a.u. using the RK4 integrator with a 0.01 a.u. time step. In (a) we have the μ^I_{zz} induced dipole moment component as a function of time, while (b) shows the corresponding absorption spectrum averaged over μ^I_{zz} and $\mu^I_{xx} = \mu^I_{yy}$.

Ideally, we would use the same setup to calculate the QCCSD spectrum for CH^+. However, the present work does not contain a spin-restricted QCCSD solver, thus the basis set is effectively doubled when compared to the RCCSD calculation. Furthermore, the $\mathcal{O}(M^6)$ scaling of QCCSD in addition to a severe increase in the number of terms made the full propagation infeasible to complete.

Despite these obstacles, we have performed $t_{\text{end}} = 200$ a.u. QCCSD time propagation with the same spacing as the CCSD calculation. Thus, by only including the first 200 a.u. of the induced dipole moment from the CCSD calculation in Figure 6.9a, we can compare a low-resolution spectrum between the two methods.

Figure 6.10a compares the diagonal terms of $\mu^{\text{I}}_{\alpha\beta}$ with the field polarized parallel and perpendicular to the molecules' symmetry axis compared between CCSD and QCCSD. Visually, the differences are very small, however they are not identical. The corresponding spectra are presented in Figure 6.10b. Some small intensity differences are present between the two methods, but the spectra are qualitatively indistinguishable. The peaks are located at the exact same energies for all excitations below 60 eV. However, the spacing between the frequency domain points is $\Delta\omega = 31.4mE_{\text{h}} \approx 0.854$ eV, which is exceedingly large.

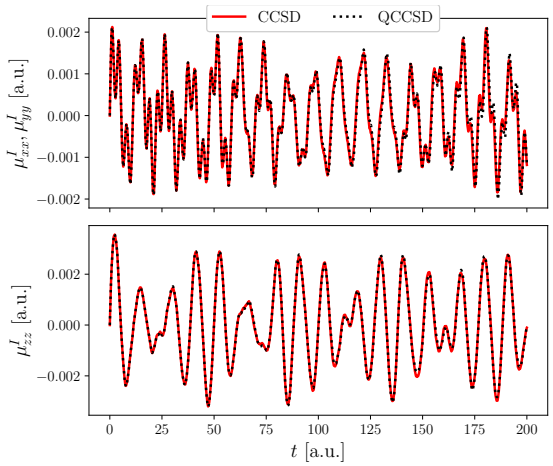

(a) The z-component of the induced dipole moment, with the field polarized along the z-axis.

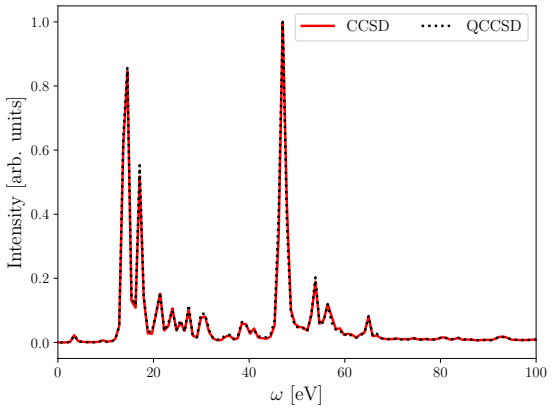

(b) Normalized $S(\omega)$ absorption spectrum, cut to the $[0, 100]$ eV range. The frequency spacing is 0.854 eV.

Figure 6.10: CH^+ excitation spectrum calculated from the Fourier transform of the induced dipole moment undergoing a δ-kick perturbation. CCSD and QCCSD are compared, both propagated until $t_{\text{end}} = 200$ a.u. using the RK4 integrator with 0.01 a.u. as the time step. In (a) we have the μ^I_{zz} induced dipole moment components as a function of time, while (b) shows the corresponding absorption spectra averaged over μ^I_{zz} and $\mu^I_{xx} = \mu^I_{yy}$.

Table 6.8 summarizes the excitation energies from Figures 6.9 and 6.10, in addition to restating the EOM-CCSD energies. Peaks are identified by using the `signal.find_peaks` functionality of `SciPy`, with a minimum height of 0.005 in the normalized spectrum. The $t_{\text{end}} = 2000$ a.u. CCSD calculation recreates all but two excitation energies, $E_{\text{EOM}} = 7.8875$ eV and $E_{\text{EOM}} = 17.3156$ eV which Koch et. al. (Table 6.7) identifies as τ_2 dominated and mostly τ_2 respectively. We assume that these are not dipole-allowed transitions.

For the shorter $t_{\text{end}} = 200$ a.u. QCCSD calculation, the excitation energies are quantitatively identical to CCSD. We attribute this to the short signal length, as the differences between QCCSD and CCSD are believed to be smaller than the present frequency domain resolution. However, the signal contains enough information to identify all the same peaks which were observed in the longer $t_{\text{end}} = 2000$ a.u. calculation. Additionally, deviations with respect to both the longer calculation and the EOM-CCSD results are smaller than the frequency domain resolution of 0.854 eV.

EOM-CCSD [eV]	CCSD [eV] $t_{\text{end}} = 2000$ a.u.	QCCSD/CCSD [eV] $t_{\text{end}} = 200$ a.u.
3.2607	3.2469	3.4191
7.8875		
9.1088	9.1425	9.4031
13.5804	13.5856	13.6766
14.4642	14.4400	14.5321
17.3156		
17.3412	17.3451	17.0957

Table 6.8: Excitation energy estimates calculated using EOM-CCSD and from the Fourier transformed induced dipole moment of CCSD and QCCSD. The second column displays results from the $t_{\text{end}} = 2000$ a.u. propagation, while the third the $t_{\text{end}} = 200$ a.u. results. Frequency resolutions are 0.085 eV and 0.854 eV for the $t_{\text{end}} = 2000$ a.u. and $t_{\text{end}} = 200$ a.u. calculations respectively.

Based on these findings, QCCSD does not improve upon the CCSD excitation energy estimates for doubles dominated states in CH^+, due to the small differences in the time-dependent induced dipole moment. However, this is not conclusive, due to the poor frequency resolution of the computed spectra. Ideally, QCCSD should be propagated until $t_{\text{end}} = 2000$ a.u. for more conclusive results.

From the results of Table 6.1, the smaller 6-31g basis set calculation of CH^+ yields a reference dominated ground state. Time-dependent fields in the dipole approximation are limited by Eq. 2.57 being a one-body operator, thus doubly excited states can not directly be created by acting on the reference. This is a possible explanation of why the first τ_2 dominated state in Figure 6.9b is so faint, as the doubly excited determinants must be created through the singly excited determinants residing in the ground state.

One possible alternative is to populate the doubles dominated excited states more aggressively. This could be achieved by applying a two-body version of the δ-kick,

$$\hat{W}(t) = \sum_{pqrs} W_{rs}^{pq}(t) a_p^\dagger a_q^\dagger a_s a_r,$$
$$W_{rs}^{pq}(t) = \kappa\delta(t)\hat{P}(ab)\hat{P}(ij)\left(\delta_{pa}\delta_{qb}\delta_{ri}\delta_{sj} + \delta_{pi}\delta_{qj}\delta_{ra}\delta_{sb}\right),$$

where κ represents the perturbation strength. The action of $\hat{W}(t)$ can by design produce both reference to doubles excitations and doubles to reference de-excitations.

Chapter 7

Conclusion

The main goal of this thesis was to derive and implement time-dependent quadratic coupled cluster theories for the doubles truncation and extend this to the singles and doubles truncation. Though the initial focus was centered around time evolution, many interesting static properties were discovered for the QCCD and QCCSD methods. In tandem with the introduction of configurational weights, our attention was shifted more towards general properties of the quadratic theory, in particular with comparison to the standard coupled cluster theory.

7.1 Summary of Results

Many different coupled cluster methods have been implemented in the present work. In total, we present functionality for CCD, RCCD, CCSD, RCCSD (both including an optional $\hat{T}_1$-transform), QCCD, and QCCSD (with an optional $\hat{T}_1$-transform), all with functionality for time evolution, in addition to an HF and RHF solver.

7.1.1 Configurational Weights and Stretched Geometries

When applied to systems at equilibrium geometries, the introduction of CC configurational weights results in quantities that are directly comparable to their FCI counterparts. For the dissociation of LiH, a system where the standard CC methods yield excellent energy estimates, the reference weight for both CCSD and QCCSD decreased while the singles and doubles weights increased as a function of nuclear separation. This showed that even in regimes where the reference does not dominate, the CC configurational weights approximated the FCI weights to a satisfactory degree.

However, by constructing the single H_2 and double $(H_2)_2$ dissociation counter-example, we found that even in a case where the energy exactly recreates that of FCI, the CCSD weights were qualitatively wrong. This is due to the lack of triple and quadruple weights, which was alleviated by performing a QCCSD calculation. Therefore, the CC weights lack size-consistency, which is important when developing a calculation quality diagnostic [124].

Additionally, we performed an N_2 dissociation calculation in the larger cc-pVTZ basis set, showing that the "variational collapse" of CCSD which QCCSD alleviates, is not an artifact of the small sto-3g basis set applied by Van Voorhis and Head-Gordon [24]. Furthermore, for the H_4 rectangle system, we found that the QCCSD energy does not collapse when compared to FCI results, but does contain a sharp maximum when the square is realized, which is not present in the FCI calculations. Thus, QCCSD produces variational results for this system, unlike a standard CCSD calculation. The behavior at the most difficult geometries is however qualitatively wrong.

7.1.2 Reduced Density Matrices

By defining a non-hermiticity measure for the reduced one- and two-body density matrices, we have compared CCSD and QCCSD calculations for different atoms and molecules at equilibrium geometries. This showed that the reduced one-body densities of QCCSD were closer to a hermitian matrix than standard CCSD, consistently by one order of magnitude using our measure.

In particular, when compared to FCI calculations of the LiH and HF systems in the 6-31g, 6-31g*, and cc-pVDZ basis sets, we found that the occupied-virtual and virtual-occupied blocks of the one-body densities are more equal for the quadratic theory.

On the other hand, the QCCSD calculated dipole and quadrupole moment were found to deviate more from FCI compared to CCSD, despite having a better estimate for the reduced one-body density. This counterintuitive result was further explored by partitioning the deviation from FCI into block contributions from the one-body density. These findings imply that the errors from the occupied-virtual and virtual-occupied blocks of the CCSD reduced one-body densities result in a beneficial error cancelation, with the former underestimating and the latter overestimating the dipole moment components. Determining if this is a systematic feature of CCSD would require studying more systems in larger basis sets.

7.1.3 Real Time Propagation

When exposing the two-electron He atom to a strong electric field, the stability of the time-dependent QCCSD EOMs was shown to be worse than those of time-dependent CCSD. This is in contrast to time-dependent CCD and QCCD, indicating that either the excessive number of τ_1 and λ_1 terms or the inherent coupling terms of the QCCSD EOMs, results in an ODE system which is significantly harder to integrate.

Estimates of the CH^+ absorption spectrum using real-time CCSD reproduced the excited energy results from EOM-CCSD, with an accuracy in agreement with the frequency resolution dictated by the total signal length. Due to the increased computational cost of performing QCCSD time propagation in a larger basis set, the CCSD and QCCSD results had to be compared with a shorter signal length. This resulted in larger errors in the frequency domain and consequently, no difference in the CCSD and QCCSD excitation energy estimates was found. However, longer signal lengths could identify the possible differences.

7.2 Future Work

The introduction of CC configurational coefficients and weights has in this thesis been applied to ground state calculations. However, the extension to time-dependent CC is straightforward. Due to the coefficients representing the left- and right-states in a determinant expansion, different properties such as the dipole moment can be expressed using $\tilde{c}_\mu$ and c_μ.

Regarding the QCCSD calculated absorption spectrum, work regarding optimization is critical. The paramount approach for closed-shell systems would be deriving and implementing spin-restriction, in particular finding an efficient set of intermediates. Undoubtedly, $\mathcal{O}(M^6)$ solutions can be found, however, the overwhelming number of terms made this inaccessible through the factorization facilities of `Gristmill`.

One possibility to simplify this is applying orbital optimization techniques [125], for instance by extending on the non-orthogonal (NO) [126, 127] or orbital adaptive (OA) [69] CC approaches. Similar to the discussed $\hat{T}_1$-transformation, both of these approaches consider transforming the single-particle basis. However, instead of eliminating only the τ_1 amplitudes, *both* τ_1 and λ_1 can be removed in the NOCC and OACC formalisms [69]. This would reduce the algebraic equations of QCCSD to that of QCCD, at the cost of a single-particle basis transformation.

If larger systems are to be considered, density fitting [128–130] or Cholesky decomposition [131] could also be applied. Density fitting and Cholesky decomposition are very useful tools to reduce the computational scaling of methods applied to chemical systems, where the Coulomb interaction integrals, v_{rs}^{pq}, are approximated by two three-index integrals. This would not only reduce the time complexity but allow us to use larger basis sets.

Appendix A

Additional Details and Results

A.1 Direct Inversion of the Iterative Subspace

The present implementation of DIIS follows the original Pulay article [83], however, some numerical instability can arise when using finite arithmetic. For more modern approaches, see [132].

Considering a set of m iterative trial steps $\boldsymbol{p}^{(1)}, \boldsymbol{p}^{(2)}, \dots \boldsymbol{p}^{(m)}$. From these, we consider constructing a new trial step $\boldsymbol{p}^{(m+1)}$ as a linear combination of the previous vectors,

$$\boldsymbol{p}^{(m+1)} = \sum_{i=1}^{m} c_i \boldsymbol{p}^{(i)}, \tag{A.1}$$

where the coefficients c_i have to be determined every iteration. With $\boldsymbol{p}^f$ as the true solution, we express every trial step as the final solution with some additional error vector $\boldsymbol{e}^{(i)}$. Inserting this in Eq. A.1 we find

$$\boldsymbol{p}^{(m+1)} = \sum_{i=1}^{m} c_i (\boldsymbol{p}^f + \boldsymbol{e}^{(i)}) = \boldsymbol{p}^f \sum_{i=1}^{m} c_i + \sum_{i=1}^{m} c_i \boldsymbol{e}^{(i)}.$$

Thus to aim for $\boldsymbol{p}^{(m+1)} \approx \boldsymbol{p}^f$ we must minimize the sum of $c_i \boldsymbol{e}^{(i)}$ with the constraint that the coefficients sum to one. Additionally, to estimate $\boldsymbol{e}^{(i)}$ we use the difference between trial vectors $\boldsymbol{e}^{(i)} \approx \Delta\boldsymbol{p}^{(i)} = \boldsymbol{p}^{(i+1)} - \boldsymbol{p}^{(i)}$. Using Eq. A.1 the error associated with $\boldsymbol{p}^{(m+1)}$ is realized as the linear combination of previous errors

$$\Delta\boldsymbol{p}^{(m)} = \boldsymbol{p}^{(m+1)} - \boldsymbol{p}^{(m)} = \sum_{i=1}^{m} c_i \Delta\boldsymbol{p}^{(i)}, \tag{A.2}$$

which we can minimize under the Euclidean norm. Defining the hermitian matrix $B_{ij} = (\Delta\boldsymbol{p}^{(i)})^\dagger (\Delta\boldsymbol{p}^{(j)})$, we formulate the Lagrangian with a single multiplier in regard to the coefficient summation constraint, [1]

$$\begin{aligned} L\left[\{c_i\}, \lambda\right] &= \left\| \Delta\boldsymbol{p}^{(m+1)} \right\|^2 - 2\lambda \left(\sum_{i=1}^{n} c_i - 1 \right) \\ &= \sum_{i,j=1}^{m} c_i^* B_{ij} c_j - 2\lambda \left(\sum_{i=1}^{n} c_i - 1 \right), \end{aligned} \tag{A.3}$$

Optimizing wrt. the coefficients and multiplier while considering the hermiticity of B, we find

$$\begin{aligned} \frac{\partial L}{\partial c_k} &= \left(\sum_{j}^{m} B_{kj} c_j \right) - \lambda = 0, \\ \frac{\partial L}{\partial \lambda} &= 1 - \sum_{i=1}^{m} c_i = 0, \end{aligned} \tag{A.4}$$

[1] The factor of two is included for a simpler form of the optimized equation.

which we can write in matrix form as a set of linear equations of dimensionality $m+1$. Additionally, by absorbing the minus sign into λ, we find a symmetric coefficient matrix

$$\begin{pmatrix} B_{11} & B_{12} & \dots & B_{1m} & 1 \\ B_{21} & B_{22} & \dots & B_{2m} & 1 \\ \vdots & \vdots & \ddots & \vdots & \vdots \\ B_{m1} & B_{m2} & \dots & B_{mm} & 1 \\ 1 & 1 & \dots & 1 & 0 \end{pmatrix} \begin{pmatrix} c_1 \\ c_2 \\ \vdots \\ c_m \\ -\lambda \end{pmatrix} = \begin{pmatrix} 0 \\ 0 \\ \vdots \\ 0 \\ 1 \end{pmatrix}. \tag{A.5}$$

In practice we do not use every previous $\boldsymbol{p}^{(i)}$ due to the large memory requirement, but rather the last $m' < m$ trial vectors.

A.2 Imaginary Time Evolution

Here we present more results from the imaginary time evolution benchmark, such as those for CCD presented in Table A.1 and CCSD presented in Table A.2.

System	Basis	π'_+	$\log_{10}\epsilon$	$\delta\tau_2(\pi'_+)$	$\delta\lambda_2(\pi'_-)$
He	cc-pVDZ	7.70	−12	$1.253 \cdot 10^{-13}$	$2.214 \cdot 10^{-13}$
Be	STO-3G	57.25	−12	$1.526 \cdot 10^{-10}$	$3.050 \cdot 10^{-11}$
Be	cc-pVDZ	74.10	−12	$9.932 \cdot 10^{-13}$	$2.842 \cdot 10^{-12}$
LiH	STO-3G	36.70	−10	$1.809 \cdot 10^{-10}$	$1.500 \cdot 10^{-10}$
LiH	cc-pVDZ	39.30	−10	$1.886 \cdot 10^{-10}$	$1.452 \cdot 10^{-10}$
CH^+	STO-3G	58.70	−10	$2.804 \cdot 10^{-10}$	$3.523 \cdot 10^{-11}$
CH^+	cc-pVDZ	62.20	−10	$3.063 \cdot 10^{-10}$	$3.265 \cdot 10^{-11}$

Table A.1: Showing results from imaginary time evolution calculated for different systems in different basis sets using CCD. The propagation was run until all norms of the amplitude equations reached a lower value than ϵ, corresponding to the imaginary time $\pi'_\pm$. $\delta\tau_1$ and $\delta\tau_1$ being the norm of the difference between the imaginary time evolved solution and fixed point solution converged to ϵ, both evaluated at $\pi'_\pm$. All energy differences were smaller than 10^{-12} and therefore not listed.

System	Basis	π'_+	$\log_{10}\epsilon$	$\delta\tau_1(\pi'_+)$	$\delta\lambda_1(\pi'_-)$	$\delta\tau_2(\pi'_+)$	$\delta\lambda_2(\pi'_-)$
He	cc-pVDZ	12.05	-12	$2.800 \cdot 10^{-13}$	$5.136 \cdot 10^{-13}$	$3.383 \cdot 10^{-14}$	$5.208 \cdot 10^{-14}$
Be	STO-3G	57.25	-12	0.0	0.0	$4.971 \cdot 10^{-13}$	$2.095 \cdot 10^{-12}$
Be	cc-pVDZ	74.30	-12	$6.952 \cdot 10^{-14}$	$2.342 \cdot 10^{-13}$	$9.444 \cdot 10^{-13}$	$2.849 \cdot 10^{-12}$
LiH	STO-3G	139.85	-10	$7.533 \cdot 10^{-10}$	$1.505 \cdot 10^{-10}$	$5.499 \cdot 10^{-10}$	$7.298 \cdot 10^{-11}$
LiH	cc-pVDZ	141.55	-10	$7.830 \cdot 10^{-10}$	$8.206 \cdot 10^{-11}$	$5.567 \cdot 10^{-10}$	$4.004 \cdot 10^{-11}$
CH^+	STO-3G	58.75	-10	$6.363 \cdot 10^{-12}$	$8.778 \cdot 10^{-13}$	$2.915 \cdot 10^{-10}$	$1.572 \cdot 10^{-11}$
CH^+	cc-pVDZ	62.45	-10	$8.752 \cdot 10^{-12}$	$8.942 \cdot 10^{-12}$	$3.195 \cdot 10^{-10}$	$3.596 \cdot 10^{-11}$

Table A.2: Showing results from imaginary time evolution calculated for different systems in different basis sets using CCSD. The propagation was run until all norms of the amplitude equations reached a lower value than ϵ, corresponding to the imaginary time $\pi'_\pm$. $\delta\tau_1, \delta\tau_2, \delta\lambda_1$ and $\delta\lambda_2$ being the norm of the difference between the imaginary time evolved solution and fixed point solution converged to ϵ, both evaluated at $\pi'_\pm$. All energy differences were smaller than 10^{-12} and therefore not listed.

A.3 Equilibrium Geometries

In Table A.3, we present the equilibrium geometries used through the entirety of Sec. 6.3, in addition to the molecules in Table 6.1. All coordinates are given with the nuclear charge center as the origin.

System	Element	x [a_0]	y [a_0]	z [a_0]
HF	H	0	0	-1.55925
	F	0	0	0.17325
LiH	Li	0	0	-0.75353
	H	0	0	2.26058
CH^+	C	0	0	-0.30530
	H	0	0	1.83183
BeO	Be	0	0	-1.68463
	O	0	0	0.84231
N_2	N	0	0	-1.05069
	N	0	0	1.05069
H_2O	O	0	0	0.22866
	H	0	1.41918	-0.91463
	H	0	1.41918	-0.91463
BeH_2	Be	0	0	0
	H	0	0	-2.52656
	H	0	0	2.52656

Table A.3: Equilibrium geometries in charge-center coordinates, calculated in the cc-pVDZ basis set.

Appendix B

Configurational Coefficients Algebraic Equations

This appendix shows the longer expressions for the configurational coefficients, including the additions to $\tilde{c}_\mu$ required for QCCD and QCCSD, in addition to the triples and quadruples coefficients. The following equations are calculated using a combination of `Drudge`, `SymPy`, and `quadratictheory`. Efforts have been made to make full use of the permutation operators from Eq. 3.91, however, this endeavor was only partially successful. Through the entirety of App. B, repeated indices in the same term imply a sum over those indices.

Firstly, the QCCSD addition to the references right-state coefficients is

$$\begin{aligned}
&\frac{1}{2}\langle\Phi_0|\hat{\Lambda}^2 e^{-\hat{T}}|\Phi_0\rangle = \\
&-\frac{1}{2}\lambda^i_a\lambda^j_b\tau^{ab}_{ij} + \frac{1}{2}\lambda^i_a\lambda^j_b\tau^a_i\tau^b_j - \frac{1}{2}\lambda^i_a\lambda^j_b\tau^a_j\tau^b_i \\
&+\lambda^i_a\tau^b_j\lambda^{jk}_{bc}\tau^{ac}_{ik} + \frac{1}{4}\lambda^i_a\tau^a_i\lambda^{jk}_{bc}\tau^{bc}_{jk} - \frac{1}{2}\lambda^i_a\tau^a_j\lambda^{jk}_{bc}\tau^{bc}_{ik} - \frac{1}{2}\lambda^i_a\tau^b_i\lambda^{jk}_{bc}\tau^{ac}_{jk} \\
&+\frac{1}{2}\lambda^i_a\tau^a_i\tau^b_j\tau^c_k\lambda^{jk}_{bc} - \lambda^i_a\tau^a_j\tau^b_i\tau^c_k\lambda^{jk}_{bc} + \frac{1}{32}\lambda^{jk}_{ab}\lambda^{il}_{cd}\tau^{ab}_{il}\tau^{cd}_{jk} + \frac{1}{32}\lambda^{jk}_{ab}\lambda^{il}_{cd}\tau^{ab}_{jk}\tau^{cd}_{il} \\
&+\frac{1}{4}\lambda^{jk}_{ab}\lambda^{il}_{cd}\tau^{ac}_{jl}\tau^{bd}_{ik} - \frac{1}{8}\lambda^{jk}_{ab}\lambda^{il}_{cd}\tau^{ab}_{jl}\tau^{cd}_{ik} - \frac{1}{8}\lambda^{jk}_{ab}\lambda^{il}_{cd}\tau^{ac}_{jk}\tau^{bd}_{il} + \frac{1}{2}\tau^a_i\tau^b_j\tau^c_k\tau^d_l\lambda^{jk}_{ab}\lambda^{il}_{cd} \\
&+\frac{1}{8}\tau^a_i\tau^b_l\tau^c_j\tau^d_k\lambda^{jk}_{ab}\lambda^{il}_{cd} + \frac{1}{8}\tau^a_j\tau^b_k\tau^c_i\tau^d_l\lambda^{jk}_{ab}\lambda^{il}_{cd}.
\end{aligned} \tag{B.1}$$

The QCCSD addition to the singles right-state coefficients is

$$\begin{aligned}
&\frac{1}{2}\langle\Phi_0|\hat{\Lambda}^2 e^{-\hat{T}}|\Phi^a_i\rangle = \\
&\lambda^j_a\lambda^i_b\tau^b_j - \lambda^i_a\lambda^j_b\tau^b_j + \frac{1}{2}\lambda^j_a\lambda^{ik}_{bc}\tau^{bc}_{jk} + \frac{1}{2}\lambda^i_b\lambda^{jk}_{ac}\tau^{bc}_{jk} \\
&-\lambda^j_b\lambda^{ik}_{ac}\tau^{bc}_{jk} + \lambda^j_b\tau^b_j\tau^c_k\lambda^{ik}_{ac} - \frac{1}{4}\lambda^i_a\lambda^{jk}_{bc}\tau^{bc}_{jk} + \frac{1}{2}\lambda^i_a\tau^b_j\tau^c_k\lambda^{jk}_{bc} \\
&-\lambda^j_a\tau^b_j\tau^c_k\lambda^{ik}_{bc} - \lambda^i_b\tau^b_j\tau^c_k\lambda^{jk}_{ac} - \lambda^j_b\tau^b_k\tau^c_j\lambda^{ik}_{ac} + \tau^b_j\lambda^{il}_{ad}\lambda^{jk}_{bc}\tau^{cd}_{kl} \\
&+\frac{1}{2}\tau^b_l\lambda^{il}_{ad}\lambda^{jk}_{bc}\tau^{cd}_{jk} + \frac{1}{2}\tau^d_j\lambda^{il}_{ad}\lambda^{jk}_{bc}\tau^{bc}_{kl} + \frac{1}{4}\tau^d_l\lambda^{il}_{ad}\lambda^{jk}_{bc}\tau^{bc}_{jk} + \frac{1}{2}\tau^b_j\lambda^{kl}_{ad}\lambda^{ij}_{bc}\tau^{cd}_{kl} \\
&-\tau^b_k\lambda^{kl}_{ad}\lambda^{ij}_{bc}\tau^{cd}_{jl} + \frac{1}{4}\tau^d_j\lambda^{kl}_{ad}\lambda^{ij}_{bc}\tau^{bc}_{kl} + \tau^b_j\tau^c_l\tau^d_k\lambda^{il}_{ad}\lambda^{jk}_{bc} - \frac{1}{2}\tau^d_k\lambda^{kl}_{ad}\lambda^{ij}_{bc}\tau^{bc}_{jl} \\
&-\tau^b_j\tau^c_k\tau^d_l\lambda^{kl}_{ad}\lambda^{ij}_{bc} - \frac{1}{2}\tau^b_j\tau^c_k\tau^d_l\lambda^{il}_{ad}\lambda^{jk}_{bc} - \frac{1}{2}\tau^b_k\tau^c_l\tau^d_j\lambda^{kl}_{ad}\lambda^{ij}_{bc}.
\end{aligned} \tag{B.2}$$

Lastly, the contribution to the QCCSD doubles right-state coefficients is

$$\begin{aligned}
&\frac{1}{2}\langle\Phi_0|\hat{\Lambda}^2 e^{-\hat{T}}|\Phi_{ij}^{ab}\rangle = \\
&\hat{P}(ij)\lambda_a^i\lambda_b^j - \lambda_c^k\tau_k^c\lambda_{ab}^{ij} - \hat{P}(ab)\lambda_a^k\tau_k^c\lambda_{bc}^{ij} - \hat{P}(ij)\lambda_c^i\tau_k^c\lambda_{ab}^{jk} \\
&- \hat{P}(ab)\hat{P}(ij)\lambda_a^i\tau_k^c\lambda_{bc}^{jk} - \frac{1}{4}\lambda_{ab}^{ij}\lambda_{cd}^{kl}\tau_{kl}^{cd} - \frac{1}{4}\lambda_{ab}^{kl}\lambda_{cd}^{ij}\tau_{kl}^{cd} + \frac{1}{2}\tau_k^c\tau_l^d\lambda_{ab}^{ij}\lambda_{cd}^{kl} \\
&+ \frac{1}{2}\tau_k^c\tau_l^d\lambda_{ab}^{kl}\lambda_{cd}^{ij} - \hat{P}(ij)\lambda_{ac}^{ik}\lambda_{bd}^{jl}\tau_{kl}^{cd} + \frac{\hat{P}(ab)}{2}\lambda_{ac}^{kl}\lambda_{bd}^{ij}\tau_{kl}^{cd} + \hat{P}(ij)\tau_k^c\tau_l^d\lambda_{ab}^{il}\lambda_{cd}^{jk} \\
&+ \hat{P}(ij)\tau_k^c\tau_l^d\lambda_{ac}^{ik}\lambda_{bd}^{jl} - \frac{\hat{P}(ij)}{2}\lambda_{ab}^{il}\lambda_{cd}^{jk}\tau_{kl}^{cd} - \hat{P}(ij)\tau_l^c\tau_k^d\lambda_{ac}^{ik}\lambda_{bd}^{jl} - \hat{P}(ab)\tau_k^c\tau_l^d\lambda_{ac}^{kl}\lambda_{bd}^{ij}.
\end{aligned} \tag{B.3}$$

The triple and quadrouple left-state coefficients are not present in CCD and CCSD. For QCCSD, the triples left-state coefficients is

$$\begin{aligned}
\tilde{c}_{ijk}^{abc} &= \lambda_c^k\lambda_{ab}^{ij} + \hat{P}(ab)\lambda_a^k\lambda_{bc}^{ij} + \hat{P}(ij)\lambda_c^i\lambda_{ab}^{jk} + \hat{P}(ab)\hat{P}(ij)\lambda_a^i\lambda_{bc}^{jk} - \tau_l^d\lambda_{ab}^{ij}\lambda_{cd}^{kl} - \tau_l^d\lambda_{ab}^{kl}\lambda_{cd}^{ij} \\
&+ \hat{P}(ab)\tau_l^d\lambda_{ac}^{ij}\lambda_{bd}^{kl} + \hat{P}(ij)\tau_l^d\lambda_{ad}^{ik}\lambda_{bc}^{jl} - \hat{P}(ab)\tau_l^d\lambda_{ad}^{ij}\lambda_{bc}^{kl} - \hat{P}(ij)\tau_l^d\lambda_{ad}^{il}\lambda_{bc}^{jk} \\
&+ \hat{P}(bc)\hat{P}(ij)\tau_l^d\lambda_{ab}^{ik}\lambda_{cd}^{jl} - \hat{P}(bc)\hat{P}(ij)\tau_l^d\lambda_{ab}^{il}\lambda_{cd}^{jk},
\end{aligned} \tag{B.4}$$

while the quadrouples left-state coefficients is

$$\tilde{c}_{ijkl}^{abcd} = \lambda_{ab}^{ij}\lambda_{cd}^{kl} + \lambda_{ab}^{kl}\lambda_{cd}^{ij} - \hat{P}(ab)\hat{P}(cd)\lambda_{ac}^{kl}\lambda_{bd}^{ij} - \hat{P}(ij)\hat{P}(kl)\lambda_{ad}^{ik}\lambda_{bc}^{jl} - \hat{P}(bc)\hat{P}(ij)\hat{P}(kl)\lambda_{ab}^{ik}\lambda_{cd}^{jl}. \tag{B.5}$$

Both the standard and quadratic CC theories have the same right-state coefficients, truncating only at the N-particle limit. The triples weight is expressed as

$$\begin{aligned}
c_{ijk}^{abc} &= \tau_k^c\tau_{ij}^{ab} + \hat{P}(ab)\tau_k^a\tau_{ij}^{bc} + \hat{P}(ij)\tau_i^c\tau_{jk}^{ab} + \hat{P}(ij)\tau_i^a\tau_j^b\tau_k^c \\
&+ \hat{P}(ab)\hat{P}(ij)\tau_i^a\tau_{jk}^{bc} - \hat{P}(ab)\hat{P}(ij)\tau_i^a\tau_k^b\tau_j^c,
\end{aligned} \tag{B.6}$$

while the quadratic weight

$$\begin{aligned}
c_{ijkl}^{abcd} &= \tau_{ij}^{ab}\tau_{kl}^{cd} + \tau_{kl}^{ab}\tau_{ij}^{cd} + \hat{P}(ij)\tau_i^a\tau_j^b\tau_{kl}^{cd} + \hat{P}(kl)\tau_k^a\tau_l^b\tau_{ij}^{cd} + \hat{P}(ij)\tau_i^c\tau_j^d\tau_{kl}^{ab} + \hat{P}(kl)\tau_k^c\tau_l^d\tau_{ij}^{ab} \\
&- \hat{P}(ab)\hat{P}(cd)\tau_{kl}^{ac}\tau_{ij}^{bd} - \hat{P}(ij)\hat{P}(kl)\tau_{ik}^{ad}\tau_{jl}^{bc} - \hat{P}(bc)\hat{P}(ij)\hat{P}(kl)\tau_{ik}^{ab}\tau_{jl}^{cd} + \hat{P}(ij)\hat{P}(kl)\tau_i^a\tau_j^b\tau_k^c\tau_l^d \\
&+ \hat{P}(ab)\hat{P}(ij)\hat{P}(kl)\tau_k^a\tau_i^b\tau_{jl}^{cd} + \hat{P}(ij)\hat{P}(kl)\tau_k^a\tau_l^b\tau_i^c\tau_j^d + \hat{P}(cd)\hat{P}(ij)\hat{P}(kl)\tau_k^c\tau_i^d\tau_{jl}^{ab} \\
&- \hat{P}(ab)\hat{P}(cd)\hat{P}(ij)\tau_i^a\tau_j^c\tau_{kl}^{bd} - \hat{P}(ab)\hat{P}(cd)\hat{P}(kl)\tau_k^a\tau_l^c\tau_{ij}^{bd} + \hat{P}(ab)\hat{P}(cd)\hat{P}(ij)\hat{P}(kl)\tau_i^a\tau_k^c\tau_{jl}^{bd} \\
&- \hat{P}(ab)\hat{P}(cd)\hat{P}(ij)\hat{P}(kl)\tau_k^a\tau_i^c\tau_{jl}^{bd} + \hat{P}(ab)\hat{P}(cd)\hat{P}(ij)\hat{P}(kl)\tau_k^a\tau_i^b\tau_j^c\tau_l^d.
\end{aligned} \tag{B.7}$$

Appendix C

CCSD Algebraic Equations

C.1 Energy and amplitudes

In this appendix, we will present the algebraic equations for CCSD. The CCD equations can be found by setting $\tau_i^a = \lambda_a^i = 0$ and disregarding the singles equation. In an HF basis, $f_{ai} = 0$, however, it is included in the following for completeness. Equations are calculated using a combination of `Drudge`, `SymPy`, and `quadratictheory`. Despite efforts to utilize the permutation operators from Eq. 3.91, this endeavor was only partially successful. The Einstein summation convention is applied for the totality of App. C.

We begin with the CCSD energy equation

$$\langle \Phi_0 | \overline{H} | \Phi_0 \rangle = f_{ia}\tau_i^a + \frac{1}{4}\tau_{ij}^{ab}u_{ab}^{ij} + \frac{1}{2}\tau_i^a\tau_j^b u_{ab}^{ij}. \tag{C.1}$$

Next the CCSD τ_1 equations is

$$\begin{aligned}
&\langle \Phi_i^a | \overline{H} | \Phi_0 \rangle = \\
&f_{ai} - f_{ji}\tau_j^a + f_{ab}\tau_i^b + f_{jb}\tau_{ij}^{ab} - \tau_j^b u_{bi}^{aj} - f_{jb}\tau_j^a\tau_i^b \\
&+ \frac{1}{2}\tau_{jk}^{ab}u_{bi}^{jk} + \tau_j^a\tau_k^b u_{bi}^{jk} + \frac{1}{2}\tau_{ij}^{bc}u_{bc}^{aj} + \tau_i^b\tau_j^c u_{bc}^{aj} + \tau_j^b\tau_{ik}^{ac}u_{bc}^{jk} - \frac{1}{2}\tau_j^a\tau_{ik}^{bc}u_{bc}^{jk} \\
&- \frac{1}{2}\tau_i^b\tau_{jk}^{ac}u_{bc}^{jk} - \tau_j^a\tau_i^b\tau_k^c u_{bc}^{jk},
\end{aligned} \tag{C.2}$$

while the CCSD τ_2 equations takes the form

$$\begin{aligned}
&\langle \Phi_{ij}^{ab} | \overline{H} | \Phi_0 \rangle = \\
&u_{ij}^{ab} + \hat{P}(ij)f_{ki}\tau_{jk}^{ab} + \hat{P}(ab)\tau_k^a u_{ij}^{bk} + \hat{P}(ij)\tau_i^c u_{cj}^{ab} \\
&- \hat{P}(ab)f_{ac}\tau_{ij}^{bc} + \frac{1}{2}\tau_{kl}^{ab}u_{ij}^{kl} + \tau_k^a\tau_l^b u_{ij}^{kl} + \hat{P}(ab)f_{kc}\tau_k^a\tau_{ij}^{bc} \\
&+ \hat{P}(ij)f_{kc}\tau_i^c\tau_{jk}^{ab} - \hat{P}(ab)\hat{P}(ij)\tau_{ik}^{ac}u_{cj}^{bk} + \hat{P}(ab)\hat{P}(ij)\tau_k^a\tau_i^c u_{cj}^{bk} + \frac{1}{2}\tau_{ij}^{cd}u_{cd}^{ab} \\
&+ \tau_i^c\tau_j^d u_{cd}^{ab} + \frac{\hat{P}(ij)}{2}\tau_i^c\tau_{kl}^{ab}u_{cj}^{kl} - \hat{P}(ij)\tau_k^c\tau_{il}^{ab}u_{cj}^{kl} + \hat{P}(ij)\tau_k^a\tau_l^b\tau_i^c u_{cj}^{kl} \\
&- \hat{P}(ab)\hat{P}(ij)\tau_k^a\tau_{il}^{bc}u_{cj}^{kl} + \frac{\hat{P}(ab)}{2}\tau_k^a\tau_{ij}^{cd}u_{cd}^{bk} - \hat{P}(ab)\tau_k^c\tau_{ij}^{ad}u_{cd}^{bk} + \hat{P}(ab)\tau_k^a\tau_i^c\tau_j^d u_{cd}^{bk} \\
&- \hat{P}(ab)\hat{P}(ij)\tau_i^c\tau_{jk}^{ad}u_{cd}^{bk} + \frac{1}{4}\tau_{kl}^{ab}\tau_{ij}^{cd}u_{cd}^{kl} + \hat{P}(ij)\tau_{ik}^{ac}\tau_{jl}^{bd}u_{cd}^{kl} + \frac{1}{2}\tau_k^a\tau_l^b\tau_{ij}^{cd}u_{cd}^{kl} \\
&+ \frac{1}{2}\tau_i^c\tau_j^d\tau_{kl}^{ab}u_{cd}^{kl} - \tau_i^c\tau_k^d\tau_{jl}^{ab}u_{cd}^{kl} - \tau_k^c\tau_j^d\tau_{il}^{ab}u_{cd}^{kl} + \frac{\hat{P}(ij)}{2}\tau_{il}^{ab}\tau_{jk}^{cd}u_{cd}^{kl} \\
&+ \frac{\hat{P}(ab)}{2}\tau_{ij}^{ad}\tau_{kl}^{bc}u_{cd}^{kl} + \tau_k^a\tau_l^b\tau_i^c\tau_j^d u_{cd}^{kl} - \hat{P}(ab)\tau_k^a\tau_l^c\tau_{ij}^{bd}u_{cd}^{kl} - \hat{P}(ab)\hat{P}(ij)\tau_k^a\tau_i^c\tau_{jl}^{bd}u_{cd}^{kl}.
\end{aligned} \tag{C.3}$$

Considering the left-state, the CCSD λ_1 equation takes the form

$$
\begin{aligned}
&\langle\Phi_0|(1+\hat{\Lambda})[\overline{H},\hat{X}_i^a]\,|\Phi_0\rangle = \\
&f_{ia} - \lambda_a^j f_{ij} + \lambda_b^i f_{ba} + \tau_j^b u_{ab}^{ij} - \lambda_b^j u_{aj}^{bi} - \lambda_a^j f_{ib}\tau_j^b \\
&- \lambda_b^i f_{ja}\tau_j^b + \frac{1}{2}\lambda_{ab}^{jk}u_{jk}^{bi} + \lambda_a^j\tau_k^b u_{bj}^{ik} - \lambda_b^j\tau_k^b u_{aj}^{ik} + \frac{1}{2}\lambda_{bc}^{ij}u_{aj}^{bc} + \lambda_b^i\tau_j^c u_{ac}^{bj} \\
&- \lambda_b^j\tau_j^c u_{ac}^{bi} + \frac{1}{2}\tau_l^b\lambda_{ab}^{jk}u_{jk}^{il} + \lambda_b^j\tau_{jk}^{bc}u_{ac}^{ik} + \tau_j^c\lambda_{ab}^{jk}u_{ck}^{bi} + \tau_k^b\lambda_{bc}^{ij}u_{aj}^{ck} + \frac{1}{2}f_{ic}\lambda_{ab}^{jk}\tau_{jk}^{bc} \\
&+ \frac{1}{2}f_{ka}\lambda_{bc}^{ij}\tau_{jk}^{bc} - \frac{1}{2}\lambda_a^j\tau_{jk}^{bc}u_{bc}^{ik} - \frac{1}{2}\lambda_b^i\tau_{jk}^{bc}u_{ac}^{jk} - \lambda_a^j\tau_j^b\tau_k^c u_{bc}^{ik} - \lambda_b^i\tau_j^b\tau_k^c u_{ac}^{jk} - \lambda_b^j\tau_k^b\tau_j^c u_{ac}^{ik} \\
&+ \frac{1}{2}\tau_j^d\lambda_{bc}^{ij}u_{ad}^{bc} - \lambda_{ab}^{jk}\tau_{jl}^{bc}u_{ck}^{il} + \frac{1}{4}\lambda_{bc}^{ij}\tau_{kl}^{bc}u_{aj}^{kl} + \tau_l^b\tau_j^c\lambda_{ab}^{jk}u_{ck}^{il} - \frac{1}{2}\lambda_{bc}^{jk}\tau_{jl}^{bc}u_{ak}^{il} + \frac{1}{2}\tau_k^b\tau_l^c\lambda_{bc}^{ij}u_{aj}^{kl} \\
&+ \frac{1}{4}\lambda_{ab}^{jk}\tau_{jk}^{cd}u_{cd}^{bi} - \lambda_{bc}^{ij}\tau_{jk}^{bd}u_{ad}^{ck} + \tau_k^b\tau_j^d\lambda_{bc}^{ij}u_{ad}^{ck} - \frac{1}{2}\lambda_{bc}^{jk}\tau_{jk}^{bd}u_{ad}^{ci} + \frac{1}{2}\tau_j^c\tau_k^d\lambda_{ab}^{jk}u_{cd}^{bi} + \frac{1}{4}\tau_l^b\lambda_{ab}^{jk}\tau_{jk}^{cd}u_{cd}^{il} \\
&- \tau_j^c\lambda_{ab}^{jk}\tau_{kl}^{bd}u_{cd}^{il} - \tau_k^b\lambda_{bc}^{ij}\tau_{jl}^{cd}u_{ad}^{kl} + \frac{1}{4}\tau_j^d\lambda_{bc}^{ij}\tau_{kl}^{bc}u_{ad}^{kl} + \frac{1}{2}\tau_l^b\lambda_{bc}^{jk}\tau_{jk}^{cd}u_{ad}^{il} + \frac{1}{2}\tau_j^d\lambda_{bc}^{jk}\tau_{kl}^{bc}u_{ad}^{il} - \frac{1}{2}\tau_l^c\lambda_{ab}^{jk}\tau_{jk}^{bd}u_{cd}^{il} \\
&- \frac{1}{2}\tau_k^d\lambda_{bc}^{ij}\tau_{jl}^{bc}u_{ad}^{kl} + \frac{1}{2}\tau_l^b\tau_j^c\tau_k^d\lambda_{ab}^{jk}u_{cd}^{il} + \frac{1}{2}\tau_k^b\tau_l^c\tau_j^d\lambda_{bc}^{ij}u_{ad}^{kl}.
\end{aligned}
\tag{C.4}
$$

Similarly, the CCSD λ_2 is expressed as

$$
\begin{aligned}
&\langle\Phi_0|(1+\hat{\Lambda})[\overline{H},\hat{X}_{ij}^{ab}]\,|\Phi_0\rangle = \\
&u_{ab}^{ij} + \hat{P}(ab)\hat{P}(ij)\lambda_a^i f_{jb} + \hat{P}(ab)\lambda_a^k u_{bk}^{ij} + \hat{P}(ij)f_{ik}\lambda_{ab}^{jk} \\
&+ \hat{P}(ij)\lambda_c^i u_{ab}^{cj} - \hat{P}(ab)f_{ca}\lambda_{bc}^{ij} + \frac{1}{2}\lambda_{ab}^{kl}u_{kl}^{ij} + \hat{P}(ab)\lambda_a^k\tau_k^c u_{bc}^{ij} \\
&+ \hat{P}(ij)\lambda_c^i\tau_k^c u_{ab}^{jk} + \hat{P}(ij)f_{ic}\tau_k^c\lambda_{ab}^{jk} + \hat{P}(ab)f_{ka}\tau_k^c\lambda_{bc}^{ij} - \hat{P}(ab)\hat{P}(ij)\lambda_{ac}^{ik}u_{bk}^{cj} \\
&+ \hat{P}(ab)\hat{P}(ij)\lambda_a^i\tau_k^c u_{bc}^{jk} + \frac{1}{2}\lambda_{cd}^{ij}u_{ab}^{cd} + \tau_k^c\lambda_{ab}^{kl}u_{cl}^{ij} + \hat{P}(ij)\tau_l^c\lambda_{ab}^{ik}u_{ck}^{jl} \\
&- \hat{P}(ab)\hat{P}(ij)\tau_l^c\lambda_{ac}^{ik}u_{bk}^{jl} + \tau_k^c\lambda_{cd}^{ij}u_{ab}^{dk} + \hat{P}(ab)\tau_k^d\lambda_{ac}^{ij}u_{bd}^{ck} - \hat{P}(ab)\hat{P}(ij)\tau_k^d\lambda_{ac}^{ik}u_{bd}^{cj} \\
&+ \frac{1}{4}\lambda_{ab}^{kl}\tau_{kl}^{cd}u_{cd}^{ij} + \frac{1}{4}\lambda_{cd}^{ij}\tau_{kl}^{cd}u_{ab}^{kl} + \frac{1}{2}\tau_k^c\tau_l^d\lambda_{ab}^{kl}u_{cd}^{ij} + \frac{1}{2}\tau_k^c\tau_l^d\lambda_{cd}^{ij}u_{ab}^{kl} \\
&+ \hat{P}(ab)\hat{P}(ij)\lambda_{ac}^{ik}\tau_{kl}^{cd}u_{bd}^{jl} - \frac{\hat{P}(ij)}{2}\lambda_{ab}^{ik}\tau_{kl}^{cd}u_{cd}^{jl} - \frac{\hat{P}(ab)}{2}\lambda_{ac}^{ij}\tau_{kl}^{cd}u_{bd}^{kl} - \frac{\hat{P}(ab)}{2}\lambda_{ac}^{kl}\tau_{kl}^{cd}u_{bd}^{ij} \\
&- \frac{\hat{P}(ij)}{2}\lambda_{cd}^{ik}\tau_{kl}^{cd}u_{ab}^{jl} - \hat{P}(ij)\tau_k^c\tau_l^d\lambda_{ab}^{ik}u_{cd}^{jl} - \hat{P}(ab)\tau_k^c\tau_l^d\lambda_{ac}^{ij}u_{bd}^{kl} - \hat{P}(ab)\hat{P}(ij)\tau_l^c\tau_k^d\lambda_{ac}^{ik}u_{bd}^{jl}.
\end{aligned}
\tag{C.5}
$$

C.2 Density matrices

Next, we present algebraic expressions for the CCSD reduced density matrices. The reduced one-body density matrix is calculated in four different blocks, explicitly

$$\gamma_{ji} = \delta_{ji} - \lambda_a^i\tau_i^a + \frac{1}{2}\lambda_{ab}^{kj}\tau_{ik}^{ab}, \tag{C.6}$$

$$\gamma_{ba} = \lambda_a^i\tau_i^b + \frac{1}{2}\lambda_{ac}^{ij}\tau_{ij}^{bc}, \tag{C.7}$$

$$\gamma_{ai} = \tau_i^a - \frac{1}{2}\tau_j^a\lambda_{bc}^{jk}\tau_{ik}^{bc} - \frac{1}{2}\tau_i^b\lambda_{bc}^{jk}\tau_{jk}^{ac} + \lambda_b^j\tau_{ij}^{ab} - \lambda_b^j\tau_j^a\tau_i^b, \tag{C.8}$$

$$\gamma_{ia} = \lambda_a^i. \tag{C.9}$$

Considering the reduced two-body density Γ_{rs}^{pq}, each of the four indices can be either a particle or a hole index. Thus, in principle, $2^4 = 16$ different contributions should be considered. However, since the CC two-body densities are antisymmetric in exchange of either the upper indices or the lower indices, we have

$$\Gamma_{ia}^{jb} = -\Gamma_{ia}^{bj} = -\Gamma_{ai}^{jb} = \Gamma_{ai}^{bj}$$

in addition to the four relations

$$\begin{aligned}\Gamma_{ij}^{ka} &= -\Gamma_{ij}^{ak},\\ \Gamma_{ia}^{jk} &= -\Gamma_{ai}^{jk},\\ \Gamma_{ab}^{ci} &= -\Gamma_{ab}^{ic},\\ \Gamma_{ai}^{bc} &= -\Gamma_{ia}^{bc}.\end{aligned}$$

Therefore, since seven different expressions are related, we have a total of nine unique expressions to consider. Beginning with the all occupied and all virtual blocks, the explicit expressions are

$$\begin{aligned}\Gamma_{ij}^{kl} =&\hat{P}(ij)\delta_{jl}\delta_{ik} + \hat{P}(ij)\delta_{jk}\lambda_a^l\tau_i^a - \hat{P}(ij)\delta_{jl}\lambda_a^k\tau_i^a + \frac{1}{2}\lambda_{ab}^{kl}\tau_{ij}^{ab},\\ &+ \tau_i^a\tau_j^b\lambda_{ab}^{kl} + \frac{1}{2}\hat{P}(ij)\hat{P}(kl)\delta_{jk}\lambda_{ab}^{lm}\tau_{im}^{ab} \qquad \text{(C.10)}\\ \Gamma_{ab}^{cd} =&\frac{1}{2}\lambda_{ab}^{ij}\tau_{ij}^{cd} + \tau_i^c\tau_j^d\lambda_{ab}^{ij}. \qquad \text{(C.11)}\end{aligned}$$

For the contributions where two indices are occupied and virtual, we have

$$\begin{aligned}\Gamma_{ij}^{ab} =&\tau_{ij}^{ab} + \hat{P}(ij)\tau_i^a\tau_j^b + \hat{P}(ab)\lambda_c^k\tau_k^a\tau_{ij}^{bc} + \hat{P}(ij)\lambda_c^k\tau_i^c\tau_{jk}^{ab} + \hat{P}(ab)\hat{P}(ij)\lambda_c^k\tau_i^a\tau_{jk}^{bc}\\ &+ \hat{P}(ab)\hat{P}(ij)\lambda_c^k\tau_k^a\tau_i^b\tau_j^c + \frac{1}{4}\lambda_{cd}^{kl}\tau_{kl}^{ab}\tau_{ij}^{cd} + \hat{P}(ij)\lambda_{cd}^{kl}\tau_{ik}^{ac}\tau_{jl}^{bd} + \frac{1}{2}\tau_k^a\tau_l^b\lambda_{cd}^{kl}\tau_{ij}^{cd} + \frac{1}{2}\tau_i^c\tau_j^d\lambda_{cd}^{kl}\tau_{kl}^{ab}\\ &+ \frac{\hat{P}(ij)}{2}\lambda_{cd}^{kl}\tau_{il}^{ab}\tau_{jk}^{cd} + \tau_k^a\tau_l^b\tau_i^c\tau_j^d\lambda_{cd}^{kl} - \frac{\hat{P}(ab)}{2}\lambda_{cd}^{kl}\tau_{kl}^{ac}\tau_{ij}^{bd} + \frac{\hat{P}(ab)\hat{P}(ij)}{2}\tau_k^a\tau_i^b\lambda_{cd}^{kl}\tau_{jl}^{cd}\\ &- \hat{P}(ab)\hat{P}(ij)\tau_k^a\tau_i^c\lambda_{cd}^{kl}\tau_{jl}^{bd} - \frac{\hat{P}(ab)\hat{P}(ij)}{2}\tau_i^a\tau_j^c\lambda_{cd}^{kl}\tau_{kl}^{bd}, \qquad \text{(C.12)}\\ \Gamma_{ab}^{ij} =&\lambda_{ab}^{ij}, \qquad \text{(C.13)}\\ \Gamma_{ia}^{jb} =&-\lambda_a^j\tau_i^b + \delta_{ij}\lambda_a^k\tau_k^b - \lambda_{ac}^{jk}\tau_{ik}^{bc} + \tau_k^b\tau_i^c\lambda_{ac}^{jk} + \frac{\delta_{ij}}{2}\lambda_{ac}^{kl}\tau_{kl}^{bc}. \qquad \text{(C.14)}\end{aligned}$$

Lastly, with either three indices as occupied and one virtual or three virtual and one occupied

$$\begin{aligned}\Gamma_{ij}^{ka} =&-\hat{P}(ij)\delta_{jk}\tau_i^a + \lambda_b^k\tau_{ij}^{ab} + \hat{P}(ij)\lambda_b^k\tau_i^a\tau_j^b - \hat{P}(ij)\delta_{jk}\lambda_b^l\tau_{il}^{ab}\\ &+ \hat{P}(ij)\delta_{jk}\lambda_b^l\tau_l^a\tau_i^b + \frac{1}{2}\tau_l^a\lambda_{bc}^{kl}\tau_{ij}^{bc} + \tau_l^a\tau_i^b\tau_j^c\lambda_{bc}^{kl} + \frac{\hat{P}(ij)}{2}\tau_i^a\lambda_{bc}^{kl}\tau_{jl}^{bc} - \hat{P}(ij)\tau_i^b\lambda_{bc}^{kl}\tau_{jl}^{ac}\\ &+ \frac{\hat{P}(ij)}{2}\delta_{jk}\tau_l^a\lambda_{bc}^{lm}\tau_{im}^{bc} + \frac{\hat{P}(ij)}{2}\delta_{jk}\tau_i^b\lambda_{bc}^{lm}\tau_{lm}^{ac}, \qquad \text{(C.15)}\\ \Gamma_{ia}^{jk} =&\delta_{ij}\lambda_a^k - \delta_{ik}\lambda_a^j + \tau_i^b\lambda_{ab}^{jk}, \qquad \text{(C.16)}\\ \Gamma_{ab}^{ci} =&-\tau_j^c\lambda_{ab}^{ij}, \qquad \text{(C.17)}\\ \Gamma_{ai}^{bc} =&-\lambda_a^j\tau_{ij}^{bc} + \lambda_a^j\tau_j^b\tau_i^c - \lambda_a^j\tau_i^b\tau_j^c + \tau_j^b\lambda_{ad}^{jk}\tau_{ik}^{cd} + \frac{1}{2}\tau_i^c\lambda_{ad}^{jk}\tau_{jk}^{bd},\\ &-\tau_j^c\lambda_{ad}^{jk}\tau_{ik}^{bd} - \frac{1}{2}\tau_i^b\lambda_{ad}^{jk}\tau_{jk}^{cd} - \frac{1}{2}\tau_i^d\lambda_{ad}^{jk}\tau_{jk}^{bc} - \tau_j^b\tau_k^c\tau_i^d\lambda_{ad}^{jk}. \qquad \text{(C.18)}\end{aligned}$$

Appendix D

QCCSD Algebraic Equations

D.1 Amplitude equations

In this appendix, we present the algebraic equations for QCCSD, where QCCD is recovered by setting $\lambda_a^i = 0$. These equations are very long, thus all following expressions assume a $\hat{T}_1$-transformed Hamiltonian, such that $\tau_i^a = 0$. In the amplitude equations we have included the off-diagonal contributions from the Fock matrix, however, these are zero when we use an HF basis. The equations are calculated using a combination of `Drudge`, `SymPy`, and `quadratictheory`, with attempts made to fully utilize the permutation operators from Eq. 3.91, albeit only partially successful. Einstein's summation convention is used throughout.

We begin with the quadratic additions to the τ equations. This is separated into contributions from $\hat{\Lambda}_1$ and $\hat{\Lambda}_2$ respectively

$$\langle \Phi_\mu | \hat{\Lambda} \overline{H} | \Phi_0 \rangle = \langle \Phi_\mu | \hat{\Lambda}_1 \overline{H} | \Phi_0 \rangle + \langle \Phi_\mu | \hat{\Lambda}_2 \overline{H} | \Phi_0 \rangle .$$

The τ_1-addition from the $\hat{\Lambda}_1$ term is

$$\begin{aligned}
&\langle \Phi_i^a | \hat{\Lambda}_1 \overline{H} | \Phi_0 \rangle = \\
&\lambda_b^j u_{ij}^{ab} + \lambda_b^j f_{ki} \tau_{jk}^{ab} - \lambda_b^j f_{kj} \tau_{ik}^{ab} + \lambda_b^j f_{bc} \tau_{ij}^{ac} - \lambda_b^j f_{ac} \tau_{ij}^{bc} \\
&+ \frac{1}{2} \lambda_b^j \tau_{kl}^{ab} u_{ij}^{kl} + \lambda_b^j \tau_{jk}^{ac} u_{ci}^{bk} + \lambda_b^j \tau_{ik}^{bc} u_{cj}^{ak} - \lambda_b^j \tau_{ik}^{ac} u_{cj}^{bk} - \lambda_b^j \tau_{jk}^{bc} u_{ci}^{ak} \\
&+ \frac{1}{2} \lambda_b^j \tau_{ij}^{cd} u_{cd}^{ab} + \lambda_b^j \tau_{il}^{ad} \tau_{jk}^{bc} u_{cd}^{kl} + \frac{1}{2} \lambda_b^j \tau_{il}^{ab} \tau_{jk}^{cd} u_{cd}^{kl} + \frac{1}{4} \lambda_b^j \tau_{kl}^{ab} \tau_{ij}^{cd} u_{cd}^{kl} + \frac{1}{2} \lambda_b^j \tau_{ij}^{ad} \tau_{kl}^{bc} u_{cd}^{kl} \\
&- \lambda_b^j \tau_{jl}^{ad} \tau_{ik}^{bc} u_{cd}^{kl} + \frac{1}{2} \lambda_b^j \tau_{kl}^{ad} \tau_{ij}^{bc} u_{cd}^{kl} - \frac{1}{2} \lambda_b^j \tau_{jl}^{ab} \tau_{ik}^{cd} u_{cd}^{kl},
\end{aligned} \tag{D.1}$$

while the $\hat{\Lambda}_2$ contribution is,

$$\begin{aligned}
&\langle \Phi_i^a | \hat{\Lambda}_2 \overline{H} | \Phi_0 \rangle = \\
&\frac{1}{2} \lambda_{bc}^{jk} \tau_{il}^{ab} u_{jk}^{cl} - \lambda_{bc}^{jk} \tau_{jl}^{ab} u_{ik}^{cl} + \frac{1}{4} \lambda_{bc}^{jk} \tau_{il}^{bc} u_{jk}^{al} - \frac{1}{2} \lambda_{bc}^{jk} \tau_{jl}^{bc} u_{ik}^{al} + \frac{1}{2} \lambda_{bc}^{jk} \tau_{ij}^{ad} u_{dk}^{bc} \\
&+ \frac{1}{4} \lambda_{bc}^{jk} \tau_{jk}^{ad} u_{di}^{bc} - \lambda_{bc}^{jk} \tau_{ij}^{bd} u_{dk}^{ac} - \frac{1}{2} \lambda_{bc}^{jk} \tau_{jk}^{bd} u_{di}^{ac} - f_{ld} \lambda_{bc}^{jk} \tau_{kl}^{ac} \tau_{ij}^{bd} + \frac{1}{4} f_{ld} \lambda_{bc}^{jk} \tau_{jk}^{ad} \tau_{il}^{bc} \\
&- \frac{1}{2} f_{ld} \lambda_{bc}^{jk} \tau_{il}^{ac} \tau_{jk}^{bd} - \frac{1}{2} f_{ld} \lambda_{bc}^{jk} \tau_{ik}^{ad} \tau_{jl}^{bc} + \lambda_{bc}^{jk} \tau_{jm}^{ac} \tau_{il}^{bd} u_{dk}^{lm} + \lambda_{bc}^{jk} \tau_{km}^{ac} \tau_{jl}^{bd} u_{di}^{lm} - \lambda_{bc}^{jk} \tau_{im}^{ac} \tau_{jl}^{bd} u_{dk}^{lm} \\
&+ \frac{1}{4} \lambda_{bc}^{jk} \tau_{ij}^{ad} \tau_{lm}^{bc} u_{dk}^{lm} + \frac{1}{2} \lambda_{bc}^{jk} \tau_{im}^{ad} \tau_{jl}^{bc} u_{dk}^{lm} + \frac{1}{8} \lambda_{bc}^{jk} \tau_{jk}^{ad} \tau_{lm}^{bc} u_{di}^{lm} - \frac{1}{2} \lambda_{bc}^{jk} \tau_{lm}^{ac} \tau_{ij}^{bd} u_{dk}^{lm} - \frac{1}{4} \lambda_{bc}^{jk} \tau_{lm}^{ac} \tau_{jk}^{bd} u_{di}^{lm} \\
&- \frac{1}{2} \lambda_{bc}^{jk} \tau_{jm}^{ad} \tau_{il}^{bc} u_{dk}^{lm} - \frac{1}{2} \lambda_{bc}^{jk} \tau_{km}^{ad} \tau_{jl}^{bc} u_{di}^{lm} + \lambda_{bc}^{jk} \tau_{kl}^{ae} \tau_{ij}^{bd} u_{de}^{cl} + \lambda_{bc}^{jk} \tau_{jl}^{bd} \tau_{ik}^{ce} u_{de}^{al} + \frac{1}{4} \lambda_{bc}^{jk} \tau_{il}^{ab} \tau_{jk}^{de} u_{de}^{cl} \\
&+ \frac{1}{2} \lambda_{bc}^{jk} \tau_{kl}^{ab} \tau_{ij}^{de} u_{de}^{cl} - \lambda_{bc}^{jk} \tau_{ik}^{ae} \tau_{jl}^{bd} u_{de}^{cl} + \frac{1}{2} \lambda_{bc}^{jk} \tau_{il}^{ae} \tau_{jk}^{bd} u_{de}^{cl} + \frac{1}{2} \lambda_{bc}^{jk} \tau_{jk}^{ae} \tau_{il}^{bd} u_{de}^{cl} + \frac{1}{8} \lambda_{bc}^{jk} \tau_{il}^{bc} \tau_{jk}^{de} u_{de}^{al} \\
&- \frac{1}{4} \lambda_{bc}^{jk} \tau_{jl}^{bc} \tau_{ik}^{de} u_{de}^{al} - \frac{1}{2} \lambda_{bc}^{jk} \tau_{jk}^{bd} \tau_{il}^{ce} u_{de}^{al}.
\end{aligned} \tag{D.2}$$

Similarly, the τ_2 equations are split into two contributions. The $\hat{\Lambda}_1$ part is expressed as

$$
\begin{aligned}
&\langle \Phi_{ij}^{ab} | \hat{\Lambda}_1 \overline{H} | \Phi_0 \rangle = \\
&\lambda_c^k \tau_{kl}^{ab} u_{ij}^{cl} + \hat{P}(ij) \lambda_c^k \tau_{il}^{ab} u_{jk}^{cl} - \hat{P}(ab) \lambda_c^k \tau_{kl}^{ac} u_{ij}^{bl} - \hat{P}(ab)\hat{P}(ij) \lambda_c^k \tau_{il}^{ac} u_{jk}^{bl} \\
&+ \lambda_c^k \tau_{ij}^{cd} u_{dk}^{ab} + \hat{P}(ab) \lambda_c^k \tau_{ij}^{ad} u_{dk}^{bc} - \hat{P}(ij) \lambda_c^k \tau_{ik}^{cd} u_{dj}^{ab} - \hat{P}(ab)\hat{P}(ij) \lambda_c^k \tau_{ik}^{ad} u_{dj}^{bc} \\
&+ \lambda_c^k f_{ld} \tau_{kl}^{ab} \tau_{ij}^{cd} + \hat{P}(ij) \lambda_c^k f_{ld} \tau_{il}^{ab} \tau_{jk}^{cd} - \hat{P}(ij) \lambda_c^k f_{ld} \tau_{il}^{ac} \tau_{jk}^{bd} - \hat{P}(ab) \lambda_c^k f_{ld} \tau_{kl}^{ac} \tau_{ij}^{bd} \\
&- \hat{P}(ij) \lambda_c^k f_{ld} \tau_{ik}^{ad} \tau_{jl}^{bc} + \frac{1}{2} \lambda_c^k \tau_{lm}^{ab} \tau_{ij}^{cd} u_{dk}^{lm} + \hat{P}(ij) \lambda_c^k \tau_{im}^{ab} \tau_{jl}^{cd} u_{dk}^{lm} + \hat{P}(ij) \lambda_c^k \tau_{km}^{ab} \tau_{il}^{cd} u_{dj}^{lm} \\
&+ \hat{P}(ij) \lambda_c^k \tau_{il}^{ac} \tau_{jm}^{bd} u_{dk}^{lm} - \hat{P}(ij) \lambda_c^k \tau_{im}^{ab} \tau_{kl}^{cd} u_{dj}^{lm} + \frac{\hat{P}(ab)}{2} \lambda_c^k \tau_{ij}^{ad} \tau_{lm}^{bc} u_{dk}^{lm} - \hat{P}(ij) \lambda_c^k \tau_{il}^{ad} \tau_{jm}^{bc} u_{dk}^{lm} \\
&+ \hat{P}(ab)\hat{P}(ij) \lambda_c^k \tau_{im}^{ac} \tau_{kl}^{bd} u_{dj}^{lm} + \hat{P}(ab)\hat{P}(ij) \lambda_c^k \tau_{kl}^{ac} \tau_{im}^{bd} u_{dj}^{lm} - \frac{\hat{P}(ij)}{2} \lambda_c^k \tau_{lm}^{ab} \tau_{ik}^{cd} u_{dj}^{lm} - \frac{\hat{P}(ab)\hat{P}(ij)}{2} \lambda_c^k \tau_{ik}^{ad} \tau_{lm}^{bc} u_{dj}^{lm} \\
&+ \frac{1}{2} \lambda_c^k \tau_{kl}^{ab} \tau_{ij}^{de} u_{de}^{cl} + \hat{P}(ij) \lambda_c^k \tau_{ik}^{ad} \tau_{jl}^{be} u_{de}^{cl} + \frac{\hat{P}(ij)}{2} \lambda_c^k \tau_{il}^{ab} \tau_{jk}^{de} u_{de}^{cl} - \hat{P}(ij) \lambda_c^k \tau_{il}^{ad} \tau_{jk}^{be} u_{de}^{cl} \\
&- \hat{P}(ab) \lambda_c^k \tau_{kl}^{ad} \tau_{ij}^{be} u_{de}^{cl} - \hat{P}(ab) \lambda_c^k \tau_{ij}^{ae} \tau_{kl}^{cd} u_{de}^{bl} - \hat{P}(ab) \lambda_c^k \tau_{kl}^{ae} \tau_{ij}^{cd} u_{de}^{bl} + \hat{P}(ab)\hat{P}(ij) \lambda_c^k \tau_{ik}^{ae} \tau_{jl}^{cd} u_{de}^{bl} \\
&- \frac{\hat{P}(ab)}{2} \lambda_c^k \tau_{kl}^{ac} \tau_{ij}^{de} u_{de}^{bl} - \hat{P}(ab)\hat{P}(ij) \lambda_c^k \tau_{il}^{ae} \tau_{jk}^{cd} u_{de}^{bl} - \frac{\hat{P}(ab)\hat{P}(ij)}{2} \lambda_c^k \tau_{il}^{ac} \tau_{jk}^{de} u_{de}^{bl},
\end{aligned}
\tag{D.3}
$$

with the $\hat{\Lambda}_2$ contribution as

$$
\begin{aligned}
&\langle \Phi_{ij}^{ab} | \hat{\Lambda}_2 \overline{H} | \Phi_0 \rangle = \\
&\lambda_{cd}^{kl} \tau_{km}^{ac} \tau_{ln}^{bd} u_{ij}^{mn} - \frac{1}{2} \lambda_{cd}^{kl} \tau_{ln}^{ab} \tau_{km}^{cd} u_{ij}^{mn} + \frac{\hat{P}(ij)}{4} \lambda_{cd}^{kl} \tau_{in}^{ab} \tau_{jm}^{cd} u_{kl}^{mn} + \frac{\hat{P}(ij)}{2} \lambda_{cd}^{kl} \tau_{kn}^{ab} \tau_{im}^{cd} u_{jl}^{mn} \\
&+ \frac{\hat{P}(ij)}{2} \lambda_{cd}^{kl} \tau_{im}^{ac} \tau_{jn}^{bd} u_{kl}^{mn} + \hat{P}(ab)\hat{P}(ij) \lambda_{cd}^{kl} \tau_{km}^{ac} \tau_{in}^{bd} u_{jl}^{mn} - \frac{\hat{P}(ij)}{2} \lambda_{cd}^{kl} \tau_{in}^{ab} \tau_{km}^{cd} u_{jl}^{mn} - \lambda_{cd}^{kl} \tau_{km}^{ab} \tau_{ij}^{ce} u_{el}^{dm} \\
&+ \hat{P}(ij) \lambda_{cd}^{kl} \tau_{im}^{ac} \tau_{jk}^{be} u_{el}^{dm} + \hat{P}(ab) \lambda_{cd}^{kl} \tau_{km}^{ad} \tau_{ij}^{ce} u_{el}^{bm} + \hat{P}(ij) \lambda_{cd}^{kl} \tau_{ik}^{ae} \tau_{jm}^{bc} u_{el}^{dm} - \hat{P}(ij) \lambda_{cd}^{kl} \tau_{im}^{ab} \tau_{jk}^{ce} u_{el}^{dm} \\
&- \hat{P}(ij) \lambda_{cd}^{kl} \tau_{lm}^{ab} \tau_{ik}^{ce} u_{ej}^{dm} - \hat{P}(ab) \lambda_{cd}^{kl} \tau_{ij}^{ae} \tau_{km}^{bc} u_{el}^{dm} + \hat{P}(ab)\hat{P}(ij) \lambda_{cd}^{kl} \tau_{im}^{ad} \tau_{jk}^{ce} u_{el}^{bm} + \hat{P}(ab)\hat{P}(ij) \lambda_{cd}^{kl} \tau_{lm}^{ad} \tau_{ik}^{ce} u_{ej}^{bm} \\
&+ \hat{P}(ab)\hat{P}(ij) \lambda_{cd}^{kl} \tau_{il}^{ae} \tau_{km}^{bc} u_{ej}^{dm} - \frac{\hat{P}(ij)}{2} \lambda_{cd}^{kl} \tau_{im}^{ab} \tau_{kl}^{ce} u_{ej}^{dm} - \frac{\hat{P}(ab)}{2} \lambda_{cd}^{kl} \tau_{ij}^{ae} \tau_{km}^{cd} u_{el}^{bm} + \frac{\hat{P}(ab)\hat{P}(ij)}{2} \lambda_{cd}^{kl} \tau_{im}^{ad} \tau_{kl}^{ce} u_{ej}^{bm} \\
&+ \frac{\hat{P}(ab)\hat{P}(ij)}{2} \lambda_{cd}^{kl} \tau_{ik}^{ae} \tau_{jm}^{cd} u_{el}^{bm} + \frac{\hat{P}(ab)\hat{P}(ij)}{2} \lambda_{cd}^{kl} \tau_{il}^{ae} \tau_{km}^{cd} u_{ej}^{bm} - \frac{\hat{P}(ab)\hat{P}(ij)}{2} \lambda_{cd}^{kl} \tau_{kl}^{ae} \tau_{im}^{bc} u_{ej}^{dm} - \frac{\hat{P}(ab)\hat{P}(ij)}{4} \lambda_{cd}^{kl} \tau_{kl}^{ae} \tau_{im}^{cd} u_{ej}^{bm} \\
&+ \lambda_{cd}^{kl} \tau_{ik}^{ce} \tau_{jl}^{dg} u_{eg}^{ab} - \frac{1}{2} \lambda_{cd}^{kl} \tau_{kl}^{ce} \tau_{ij}^{dg} u_{eg}^{ab} + \frac{\hat{P}(ij)}{2} \lambda_{cd}^{kl} \tau_{ik}^{ae} \tau_{jl}^{bg} u_{eg}^{cd} + \frac{\hat{P}(ab)}{4} \lambda_{cd}^{kl} \tau_{ij}^{ag} \tau_{kl}^{be} u_{eg}^{cd} \\
&- \frac{\hat{P}(ab)}{2} \lambda_{cd}^{kl} \tau_{ij}^{ag} \tau_{kl}^{ce} u_{eg}^{bd} - \frac{\hat{P}(ab)}{2} \lambda_{cd}^{kl} \tau_{kl}^{ag} \tau_{ij}^{ce} u_{eg}^{bd} - \hat{P}(ab)\hat{P}(ij) \lambda_{cd}^{kl} \tau_{il}^{ag} \tau_{jk}^{ce} u_{eg}^{bd} + \lambda_{cd}^{kl} \tau_{ln}^{ab} \tau_{im}^{ce} \tau_{jk}^{dg} u_{eg}^{mn} \\
&+ \lambda_{cd}^{kl} \tau_{ln}^{ab} \tau_{km}^{ce} \tau_{ij}^{dg} u_{eg}^{mn} + \lambda_{cd}^{kl} \tau_{km}^{ag} \tau_{ln}^{bd} \tau_{ij}^{ce} u_{eg}^{mn} - \lambda_{cd}^{kl} \tau_{ln}^{ab} \tau_{ik}^{ce} \tau_{jm}^{dg} u_{eg}^{mn} + \frac{1}{2} \lambda_{cd}^{kl} \tau_{mn}^{ab} \tau_{ik}^{ce} \tau_{jl}^{dg} u_{eg}^{mn} \\
&+ \frac{1}{2} \lambda_{cd}^{kl} \tau_{km}^{ac} \tau_{ln}^{bd} \tau_{ij}^{eg} u_{eg}^{mn} - \lambda_{cd}^{kl} \tau_{km}^{ad} \tau_{ln}^{bg} \tau_{ij}^{ce} u_{eg}^{mn} + \hat{P}(ij) \lambda_{cd}^{kl} \tau_{in}^{ab} \tau_{km}^{ce} \tau_{jl}^{dg} u_{eg}^{mn} + \hat{P}(ab) \lambda_{cd}^{kl} \tau_{ij}^{ag} \tau_{ln}^{bd} \tau_{km}^{ce} u_{eg}^{mn} \\
&- \frac{1}{4} \lambda_{cd}^{kl} \tau_{ln}^{ab} \tau_{km}^{cd} \tau_{ij}^{eg} u_{eg}^{mn} - \frac{1}{4} \lambda_{cd}^{kl} \tau_{mn}^{ab} \tau_{kl}^{ce} \tau_{ij}^{dg} u_{eg}^{mn} + \frac{\hat{P}(ij)}{8} \lambda_{cd}^{kl} \tau_{in}^{ab} \tau_{jm}^{cd} \tau_{kl}^{eg} u_{eg}^{mn} + \frac{\hat{P}(ij)}{4} \lambda_{cd}^{kl} \tau_{im}^{ac} \tau_{jn}^{bd} \tau_{kl}^{eg} u_{eg}^{mn} \\
&- \hat{P}(ij) \lambda_{cd}^{kl} \tau_{in}^{ad} \tau_{jl}^{bg} \tau_{km}^{ce} u_{eg}^{mn} + \frac{\hat{P}(ab)}{4} \lambda_{cd}^{kl} \tau_{mn}^{ad} \tau_{kl}^{bg} \tau_{ij}^{ce} u_{eg}^{mn} + \frac{\hat{P}(ij)}{4} \lambda_{cd}^{kl} \tau_{ik}^{ae} \tau_{jl}^{bg} \tau_{mn}^{cd} u_{eg}^{mn} + \frac{\hat{P}(ij)}{2} \lambda_{cd}^{kl} \tau_{in}^{ae} \tau_{jl}^{bg} \tau_{km}^{cd} u_{eg}^{mn} \\
&+ \frac{\hat{P}(ab)}{2} \lambda_{cd}^{kl} \tau_{ln}^{ae} \tau_{ij}^{bg} \tau_{km}^{cd} u_{eg}^{mn} - \hat{P}(ij) \lambda_{cd}^{kl} \tau_{il}^{ag} \tau_{jn}^{bd} \tau_{km}^{ce} u_{eg}^{mn} + \frac{\hat{P}(ij)}{2} \lambda_{cd}^{kl} \tau_{im}^{ag} \tau_{jn}^{bd} \tau_{kl}^{ce} u_{eg}^{mn} + \hat{P}(ab)\hat{P}(ij) \lambda_{cd}^{kl} \tau_{in}^{ad} \tau_{lm}^{bg} \tau_{jk}^{ce} u_{eg}^{mn} \\
&+ \hat{P}(ab)\hat{P}(ij) \lambda_{cd}^{kl} \tau_{il}^{ag} \tau_{kn}^{bd} \tau_{jm}^{ce} u_{eg}^{mn} - \frac{\hat{P}(ij)}{4} \lambda_{cd}^{kl} \tau_{in}^{ab} \tau_{km}^{cd} \tau_{jl}^{eg} u_{eg}^{mn} - \frac{\hat{P}(ij)}{2} \lambda_{cd}^{kl} \tau_{in}^{ab} \tau_{kl}^{ce} \tau_{jm}^{dg} u_{eg}^{mn} - \frac{\hat{P}(ij)}{4} \lambda_{cd}^{kl} \tau_{ln}^{ab} \tau_{im}^{cd} \tau_{jk}^{eg} u_{eg}^{mn} \\
&- \frac{\hat{P}(ij)}{2} \lambda_{cd}^{kl} \tau_{im}^{ad} \tau_{jn}^{bg} \tau_{kl}^{ce} u_{eg}^{mn} - \frac{\hat{P}(ij)}{2} \lambda_{cd}^{kl} \tau_{il}^{ae} \tau_{jn}^{bg} \tau_{km}^{cd} u_{eg}^{mn} - \frac{\hat{P}(ab)}{8} \lambda_{cd}^{kl} \tau_{kl}^{ae} \tau_{ij}^{bg} \tau_{mn}^{cd} u_{eg}^{mn} - \frac{\hat{P}(ab)}{4} \lambda_{cd}^{kl} \tau_{ij}^{ag} \tau_{mn}^{bd} \tau_{kl}^{ce} u_{eg}^{mn} \\
&+ \frac{\hat{P}(ab)\hat{P}(ij)}{2} \lambda_{cd}^{kl} \tau_{kn}^{ae} \tau_{il}^{bg} \tau_{jm}^{cd} u_{eg}^{mn} - \hat{P}(ab)\hat{P}(ij) \lambda_{cd}^{kl} \tau_{in}^{ag} \tau_{lm}^{bd} \tau_{jk}^{ce} u_{eg}^{mn} + \frac{\hat{P}(ab)\hat{P}(ij)}{4} \lambda_{cd}^{kl} \tau_{in}^{ag} \tau_{kl}^{be} \tau_{jm}^{cd} u_{eg}^{mn} - \frac{\hat{P}(ab)\hat{P}(ij)}{2} \lambda_{cd}^{kl} \tau_{lm}^{ac} \tau_{in}^{bd} \tau_{jk}^{eg} u_{eg}^{mn} \\
&- \frac{\hat{P}(ab)\hat{P}(ij)}{2} \lambda_{cd}^{kl} \tau_{il}^{ag} \tau_{mn}^{bd} \tau_{jk}^{ce} u_{eg}^{mn} - \frac{\hat{P}(ab)\hat{P}(ij)}{2} \lambda_{cd}^{kl} \tau_{kl}^{ag} \tau_{in}^{bd} \tau_{jm}^{ce} u_{eg}^{mn}.
\end{aligned}
\tag{D.4}
$$

Collecting the results, we can calculate the full QCCSD τ_1 equation using the CCSD contribution from Eq. C.2 (with $\tau_i^a = 0$, assuming a $\hat{T}_1$-transformation) and adding Eqs. D.1 and D.2. Similarly, the τ_2 equation follows from Eq. C.3 (with $\tau_i^a = 0$), with the added terms from Eq. D.3.

Next we consider the addition to the λ equations. This can be separated into three contributions for different $\hat{\Lambda}_n$ combinations

$$
\frac{1}{2} \langle \Phi_0 | \hat{\Lambda}^2 [\overline{H}, \hat{X}_\mu] | \Phi_0 \rangle = \langle \Phi_0 | (\hat{\Lambda}_1^2 + \hat{\Lambda}_1 \hat{\Lambda}_2 + \hat{\Lambda}_2^2) [\overline{H}, \hat{X}_\mu] | \Phi_0 \rangle .
$$

The $\hat{\Lambda}_1^2$ contribution to the λ_1 equations is

$$
\begin{aligned}
&\frac{1}{2}\langle\Phi|\hat{\Lambda}_1^2[\overline{H},\hat{X}_i^a]|\Phi_0\rangle = \\
&\lambda_a^j\lambda_b^k u_{jk}^{bi} + \lambda_b^i\lambda_c^j u_{aj}^{bc} + \lambda_a^j\lambda_b^k f_{ic}\tau_{jk}^{bc} + \lambda_b^i\lambda_c^j f_{ka}\tau_{jk}^{bc} + \lambda_a^j\lambda_b^k\tau_{kl}^{bc}u_{cj}^{il} \\
&- \lambda_a^j\lambda_b^k\tau_{jl}^{bc}u_{ck}^{il} + \frac{1}{2}\lambda_b^i\lambda_c^j\tau_{kl}^{bc}u_{aj}^{kl} - \lambda_b^j\lambda_c^k\tau_{jl}^{bc}u_{ak}^{il} + \lambda_b^i\lambda_c^j\tau_{jk}^{cd}u_{ad}^{bk} + \frac{1}{2}\lambda_a^j\lambda_b^k\tau_{jk}^{cd}u_{cd}^{bi} \\
&- \lambda_b^i\lambda_c^j\tau_{jk}^{bd}u_{ad}^{ck} - \lambda_b^j\lambda_c^k\tau_{jk}^{bd}u_{ad}^{ci} + \frac{1}{2}\lambda_a^j\lambda_{bc}^{kl}\tau_{km}^{bc}u_{jl}^{im} + \frac{1}{2}\lambda_b^j\lambda_{ac}^{kl}\tau_{jm}^{bc}u_{kl}^{im} - \lambda_b^j\lambda_{ac}^{kl}\tau_{km}^{bc}u_{jl}^{im} \\
&- \frac{1}{4}\lambda_a^j\lambda_{bc}^{kl}\tau_{jm}^{bc}u_{kl}^{im} + \lambda_b^j\lambda_{ac}^{kl}\tau_{jk}^{bd}u_{dl}^{ci} + \lambda_b^j\lambda_{cd}^{ik}\tau_{jl}^{bc}u_{ak}^{dl} - \lambda_a^j\lambda_{bc}^{kl}\tau_{jk}^{bd}u_{dl}^{ci} - \lambda_b^i\lambda_{cd}^{jk}\tau_{jl}^{bc}u_{ak}^{dl} \\
&+ \frac{1}{2}\lambda_b^j\lambda_{ac}^{kl}\tau_{kl}^{bd}u_{dj}^{ci} - \lambda_b^j\lambda_{ac}^{kl}\tau_{jk}^{cd}u_{dl}^{bi} - \lambda_b^j\lambda_{cd}^{ik}\tau_{kl}^{bc}u_{aj}^{dl} + \frac{1}{2}\lambda_b^j\lambda_{cd}^{ik}\tau_{jl}^{cd}u_{ak}^{bl} - \frac{1}{2}\lambda_a^j\lambda_{bc}^{kl}\tau_{kl}^{bd}u_{dj}^{ci} \\
&- \frac{1}{2}\lambda_b^i\lambda_{cd}^{jk}\tau_{jl}^{cd}u_{ak}^{bl} - \frac{1}{2}\lambda_b^j\lambda_{ac}^{kl}\tau_{kl}^{cd}u_{dj}^{bi} - \frac{1}{2}\lambda_b^j\lambda_{cd}^{ik}\tau_{kl}^{cd}u_{aj}^{bl} + \frac{1}{2}\lambda_b^i\lambda_{cd}^{jk}\tau_{jk}^{ce}u_{ae}^{bd} + \frac{1}{2}\lambda_b^j\lambda_{cd}^{ik}\tau_{jk}^{be}u_{ae}^{cd} \\
&- \lambda_b^j\lambda_{cd}^{ik}\tau_{jk}^{ce}u_{ae}^{bd} - \frac{1}{4}\lambda_b^i\lambda_{cd}^{jk}\tau_{jk}^{be}u_{ae}^{cd} + \lambda_a^j\lambda_{bc}^{kl}\tau_{jk}^{bd}\tau_{lm}^{ce}u_{de}^{im} + \lambda_b^i\lambda_{cd}^{jk}\tau_{jl}^{bc}\tau_{km}^{de}u_{ae}^{lm} + \lambda_b^j\lambda_{ac}^{kl}\tau_{lm}^{be}\tau_{jk}^{cd}u_{de}^{im} \\
&+ \lambda_b^j\lambda_{cd}^{ik}\tau_{km}^{bd}\tau_{jl}^{ce}u_{ae}^{lm} + \frac{1}{2}\lambda_a^j\lambda_{bc}^{kl}\tau_{kl}^{bd}\tau_{jm}^{ce}u_{de}^{im} + \frac{1}{4}\lambda_b^i\lambda_{cd}^{jk}\tau_{lm}^{bd}\tau_{jk}^{ce}u_{ae}^{lm} + \frac{1}{2}\lambda_b^i\lambda_{cd}^{jk}\tau_{jl}^{cd}\tau_{km}^{be}u_{ae}^{lm} + \frac{1}{4}\lambda_b^j\lambda_{ac}^{kl}\tau_{jm}^{bc}\tau_{kl}^{de}u_{de}^{im} \\
&+ \frac{1}{2}\lambda_b^j\lambda_{ac}^{kl}\tau_{lm}^{bc}\tau_{jk}^{de}u_{de}^{im} - \lambda_b^j\lambda_{ac}^{kl}\tau_{jk}^{bd}\tau_{lm}^{ce}u_{de}^{im} + \frac{1}{2}\lambda_b^j\lambda_{ac}^{kl}\tau_{jm}^{be}\tau_{kl}^{cd}u_{de}^{im} - \lambda_b^j\lambda_{cd}^{ik}\tau_{jl}^{bc}\tau_{km}^{de}u_{ae}^{lm} + \frac{1}{2}\lambda_b^j\lambda_{cd}^{ik}\tau_{lm}^{bc}\tau_{jk}^{de}u_{ae}^{lm} \\
&+ \frac{1}{4}\lambda_b^j\lambda_{cd}^{ik}\tau_{jk}^{be}\tau_{lm}^{cd}u_{ae}^{lm} + \frac{1}{2}\lambda_b^j\lambda_{cd}^{ik}\tau_{jm}^{be}\tau_{kl}^{cd}u_{ae}^{lm} - \frac{1}{8}\lambda_a^j\lambda_{bc}^{kl}\tau_{jm}^{bc}\tau_{kl}^{de}u_{de}^{im} - \frac{1}{4}\lambda_a^j\lambda_{bc}^{kl}\tau_{lm}^{bc}\tau_{jk}^{de}u_{de}^{im} - \frac{1}{8}\lambda_b^i\lambda_{cd}^{jk}\tau_{jk}^{be}\tau_{lm}^{cd}u_{ae}^{lm} \\
&- \frac{1}{2}\lambda_b^j\lambda_{ac}^{kl}\tau_{kl}^{bd}\tau_{jm}^{ce}u_{de}^{im} - \frac{1}{2}\lambda_b^j\lambda_{cd}^{ik}\tau_{km}^{be}\tau_{jl}^{cd}u_{ae}^{lm}.
\end{aligned}
\tag{D.5}
$$

Moving on to the $\hat{\Lambda}_1\hat{\Lambda}_2$ contribution, we have

$$
\begin{aligned}
&\langle\Phi|\hat{\Lambda}_1\hat{\Lambda}_2[\overline{H},\hat{X}_{ij}^{ab}]\,|\Phi_0\rangle = \\
&\lambda_b^i\lambda_{cd}^{jk}\tau_{jl}^{bc}u_{ak}^{ld} + \lambda_b^j\lambda_{ac}^{kl}\tau_{jk}^{bd}u_{ld}^{ic} + \lambda_b^j\lambda_{cd}^{ik}\tau_{kl}^{bc}u_{aj}^{ld} + \frac{1}{2}\lambda_b^i\lambda_{cd}^{jk}\tau_{jl}^{cd}u_{ak}^{lb} \\
&+ \frac{1}{2}\lambda_b^j\lambda_{ac}^{kl}\tau_{kl}^{bd}u_{jd}^{ic} + \frac{1}{2}\lambda_b^j\lambda_{cd}^{ik}\tau_{kl}^{cd}u_{aj}^{lb} - \lambda_a^j\lambda_{bc}^{kl}\tau_{jk}^{bd}u_{ld}^{ic} - \lambda_b^j\lambda_{ac}^{kl}\tau_{jk}^{cd}u_{ld}^{ib} \\
&- \lambda_b^j\lambda_{cd}^{ik}\tau_{jl}^{bc}u_{ak}^{ld} - \frac{1}{2}\lambda_a^j\lambda_{bc}^{kl}\tau_{kl}^{bd}u_{jd}^{ic} - \frac{1}{2}\lambda_b^j\lambda_{ac}^{kl}\tau_{kl}^{cd}u_{jd}^{ib} - \frac{1}{2}\lambda_b^j\lambda_{cd}^{ik}\tau_{jl}^{cd}u_{ak}^{lb} \\
&+ \frac{1}{2}\lambda_a^j\lambda_{bc}^{kl}\tau_{km}^{bc}u_{jl}^{im} + \frac{1}{2}\lambda_b^j\lambda_{ac}^{kl}\tau_{jm}^{bc}u_{kl}^{im} - \lambda_b^j\lambda_{ac}^{kl}\tau_{km}^{bc}u_{jl}^{im} - \frac{1}{4}\lambda_a^j\lambda_{bc}^{kl}\tau_{jm}^{bc}u_{kl}^{im} \\
&+ \lambda_a^j\lambda_{bc}^{kl}\tau_{jk}^{bd}\tau_{lm}^{ce}u_{de}^{im} + \lambda_b^i\lambda_{cd}^{jk}\tau_{jl}^{bc}\tau_{km}^{de}u_{ae}^{lm} + \lambda_b^j\lambda_{ac}^{kl}\tau_{lm}^{be}\tau_{jk}^{cd}u_{de}^{im} + \lambda_b^j\lambda_{cd}^{ik}\tau_{km}^{bd}\tau_{jl}^{ce}u_{ae}^{lm} \\
&+ \frac{1}{2}\lambda_a^j\lambda_{bc}^{kl}\tau_{kl}^{bd}\tau_{jm}^{ce}u_{de}^{im} + \frac{1}{2}\lambda_b^i\lambda_{cd}^{jk}\tau_{km}^{be}\tau_{jl}^{cd}u_{ae}^{lm} + \frac{1}{2}\lambda_b^j\lambda_{ac}^{kl}\tau_{lm}^{bc}\tau_{jk}^{de}u_{de}^{im} + \frac{1}{2}\lambda_b^j\lambda_{ac}^{kl}\tau_{jm}^{be}\tau_{kl}^{cd}u_{de}^{im} \\
&+ \frac{1}{2}\lambda_b^j\lambda_{cd}^{ik}\tau_{lm}^{bc}\tau_{jk}^{de}u_{ae}^{lm} + \frac{1}{2}\lambda_b^j\lambda_{cd}^{ik}\tau_{jm}^{be}\tau_{kl}^{cd}u_{ae}^{lm} - \lambda_b^j\lambda_{ac}^{kl}\tau_{jk}^{bd}\tau_{lm}^{ce}u_{de}^{im} - \lambda_b^j\lambda_{cd}^{ik}\tau_{jl}^{bc}\tau_{km}^{de}u_{ae}^{lm} \\
&- \lambda_b^j\lambda_{cd}^{kl}\tau_{lm}^{bd}\tau_{jk}^{ce}u_{ae}^{im} - \frac{1}{2}\lambda_b^j\lambda_{ac}^{kl}\tau_{kl}^{bd}\tau_{jm}^{ce}u_{de}^{im} - \frac{1}{2}\lambda_b^j\lambda_{cd}^{ik}\tau_{km}^{be}\tau_{jl}^{cd}u_{ae}^{lm} - \frac{1}{2}\lambda_b^j\lambda_{cd}^{kl}\tau_{jm}^{bd}\tau_{kl}^{ce}u_{ae}^{im} \\
&- \frac{1}{2}\lambda_b^j\lambda_{cd}^{kl}\tau_{jl}^{be}\tau_{km}^{cd}u_{ae}^{im} - \frac{1}{4}\lambda_a^j\lambda_{bc}^{kl}\tau_{lm}^{bc}\tau_{jk}^{de}u_{de}^{im} - \frac{1}{8}\lambda_a^j\lambda_{bc}^{kl}\tau_{jm}^{bc}\tau_{kl}^{de}u_{de}^{im} - \frac{1}{8}\lambda_b^i\lambda_{cd}^{jk}\tau_{jk}^{be}\tau_{lm}^{cd}u_{ae}^{lm} \\
&+ \frac{1}{4}\lambda_b^i\lambda_{cd}^{jk}\tau_{lm}^{bd}\tau_{jk}^{ce}u_{ae}^{lm} + \frac{1}{4}\lambda_b^j\lambda_{ac}^{kl}\tau_{jm}^{bc}\tau_{kl}^{de}u_{de}^{im} + \frac{1}{4}\lambda_b^j\lambda_{cd}^{ik}\tau_{jk}^{be}\tau_{lm}^{cd}u_{ae}^{lm} + \frac{1}{4}\lambda_b^j\lambda_{cd}^{kl}\tau_{kl}^{be}\tau_{jm}^{cd}u_{ae}^{im} \\
&+ \frac{1}{2}\lambda_b^i\lambda_{cd}^{jk}\tau_{jk}^{ce}u_{ae}^{bd} + \frac{1}{2}\lambda_b^j\lambda_{cd}^{ik}\tau_{jk}^{be}u_{ae}^{cd} - \lambda_b^j\lambda_{cd}^{ik}\tau_{jk}^{ce}u_{ae}^{bd} - \frac{1}{4}\lambda_b^i\lambda_{cd}^{jk}\tau_{jk}^{be}u_{ae}^{cd}.
\end{aligned}
\tag{D.6}
$$

Lastly, the $\hat{\Lambda}_2^2$ contribution is

$$
\begin{aligned}
&\frac{1}{2}\langle\Phi|\hat{\Lambda}_2^2[\overline{H},\hat{X}_i^a]|\Phi_0\rangle = \\
&\lambda_{ad}^{lm}\lambda_{bc}^{jk}\tau_{jl}^{be}\tau_{kn}^{cd}u_{em}^{in} + \frac{1}{2}\lambda_{ad}^{lm}\lambda_{bc}^{jk}\tau_{ln}^{bc}\tau_{jm}^{de}u_{ek}^{in} - \lambda_{ad}^{lm}\lambda_{bc}^{jk}\tau_{jl}^{be}\tau_{mn}^{cd}u_{ek}^{in} + \frac{1}{4}\lambda_{bc}^{jk}\lambda_{de}^{il}\tau_{jm}^{bc}\tau_{ln}^{de}u_{ak}^{mn} + \frac{1}{4}\lambda_{bc}^{jk}\lambda_{de}^{il}\tau_{ln}^{bc}\tau_{jm}^{de}u_{ak}^{mn} \\
&+ \frac{1}{2}\lambda_{bc}^{jk}\lambda_{de}^{il}\tau_{jm}^{bd}\tau_{kn}^{ce}u_{al}^{mn} - \lambda_{bc}^{jk}\lambda_{de}^{il}\tau_{jm}^{bd}\tau_{ln}^{ce}u_{ak}^{mn} - \frac{1}{2}\lambda_{ad}^{lm}\lambda_{bc}^{jk}\tau_{jn}^{bc}\tau_{kl}^{de}u_{em}^{in} - \frac{1}{4}\lambda_{ad}^{lm}\lambda_{bc}^{jk}\tau_{jn}^{bc}\tau_{lm}^{de}u_{ek}^{in} - \frac{1}{4}\lambda_{ad}^{lm}\lambda_{bc}^{jk}\tau_{ln}^{bc}\tau_{jk}^{de}u_{em}^{in} \\
&- \frac{1}{2}\lambda_{ad}^{lm}\lambda_{bc}^{jk}\tau_{jk}^{be}\tau_{ln}^{cd}u_{em}^{in} - \frac{1}{2}\lambda_{ad}^{lm}\lambda_{bc}^{jk}\tau_{lm}^{be}\tau_{jn}^{cd}u_{ek}^{in} - \frac{1}{4}\lambda_{bc}^{jk}\lambda_{de}^{il}\tau_{jm}^{bc}\tau_{kn}^{de}u_{al}^{mn} + \lambda_{bc}^{jk}\lambda_{de}^{il}\tau_{jl}^{bg}\tau_{km}^{cd}u_{ag}^{em} + \frac{1}{4}\lambda_{ad}^{lm}\lambda_{bc}^{jk}\tau_{jk}^{be}\tau_{lm}^{dg}u_{eg}^{ci} \\
&+ \frac{1}{2}\lambda_{ad}^{lm}\lambda_{bc}^{jk}\tau_{jl}^{be}\tau_{km}^{cg}u_{eg}^{di} - \lambda_{ad}^{lm}\lambda_{bc}^{jk}\tau_{jl}^{be}\tau_{km}^{dg}u_{eg}^{ci} - \lambda_{bc}^{jk}\lambda_{de}^{il}\tau_{km}^{be}\tau_{jl}^{dg}u_{ag}^{cm} + \frac{1}{2}\lambda_{bc}^{jk}\lambda_{de}^{il}\tau_{lm}^{be}\tau_{jk}^{dg}u_{ag}^{cm} - \frac{1}{4}\lambda_{ad}^{lm}\lambda_{bc}^{jk}\tau_{jk}^{be}\tau_{lm}^{cg}u_{eg}^{di} \\
&- \frac{1}{4}\lambda_{ad}^{lm}\lambda_{bc}^{jk}\tau_{lm}^{bg}\tau_{jk}^{de}u_{eg}^{ci} - \frac{1}{2}\lambda_{bc}^{jk}\lambda_{de}^{il}\tau_{jm}^{bc}\tau_{kl}^{dg}u_{ag}^{em} - \frac{1}{4}\lambda_{bc}^{jk}\lambda_{de}^{il}\tau_{lm}^{bc}\tau_{jk}^{dg}u_{ag}^{em} - \frac{1}{2}\lambda_{bc}^{jk}\lambda_{de}^{il}\tau_{jk}^{bg}\tau_{lm}^{cd}u_{ag}^{em} - \frac{1}{4}\lambda_{bc}^{jk}\lambda_{de}^{il}\tau_{jk}^{bg}\tau_{lm}^{de}u_{ag}^{cm} \\
&- \frac{1}{2}\lambda_{bc}^{jk}\lambda_{de}^{il}\tau_{kl}^{bg}\tau_{jm}^{de}u_{ag}^{cm}.
\end{aligned}
\tag{D.7}
$$

For the λ_2 equations, we have the $\hat{\Lambda}_1^2$ contribution

$$
\begin{aligned}
&\frac{1}{2}\langle\Phi|\hat{\Lambda}_1^2[\overline{H},\hat{X}_{ij}^{ab}]|\Phi_0\rangle = \\
&-\hat{P}(ab)\hat{P}(ij)\lambda_a^i\lambda_b^k f_{jk} + \hat{P}(ab)\hat{P}(ij)\lambda_a^i\lambda_c^j f_{cb} + \lambda_a^k\lambda_b^l u_{kl}^{ij} \\
&+\hat{P}(ab)\hat{P}(ij)\lambda_a^k\lambda_c^i u_{bk}^{cj} - \hat{P}(ab)\hat{P}(ij)\lambda_a^i\lambda_c^k u_{bk}^{cj} + \lambda_c^i\lambda_d^j u_{ab}^{cd} + \frac{\hat{P}(ij)}{2}\lambda_c^i\lambda_{ab}^{kl}u_{kl}^{cj} \\
&-\hat{P}(ij)\lambda_c^k\lambda_{ab}^{il}u_{kl}^{cj} + \frac{\hat{P}(ab)\hat{P}(ij)}{2}\lambda_a^i\lambda_{bc}^{kl}u_{kl}^{cj} - \hat{P}(ab)\hat{P}(ij)\lambda_a^k\lambda_{bc}^{il}u_{kl}^{cj} + \frac{\hat{P}(ab)}{2}\lambda_a^k\lambda_{cd}^{ij}u_{bk}^{cd} \\
&-\hat{P}(ab)\lambda_c^k\lambda_{ad}^{ij}u_{bk}^{cd} + \frac{\hat{P}(ab)\hat{P}(ij)}{2}\lambda_a^i\lambda_{cd}^{jk}u_{bk}^{cd} - \hat{P}(ab)\hat{P}(ij)\lambda_c^i\lambda_{ad}^{jk}u_{bk}^{cd} + \frac{1}{2}\lambda_a^k\lambda_b^l\tau_{kl}^{cd}u_{cd}^{ij} \\
&+\frac{1}{2}\lambda_c^i\lambda_d^j\tau_{kl}^{cd}u_{ab}^{kl} - \lambda_c^i\lambda_d^k\tau_{kl}^{cd}u_{ab}^{jl} - \lambda_c^k\lambda_d^j\tau_{kl}^{cd}u_{ab}^{il} + \hat{P}(ij)\lambda_c^k f_{id}\lambda_{ab}^{jl}\tau_{kl}^{cd} \\
&+\hat{P}(ab)\lambda_c^k f_{la}\lambda_{bd}^{ij}\tau_{kl}^{cd} - \hat{P}(ab)\lambda_a^k\lambda_c^l\tau_{kl}^{cd}u_{bd}^{ij} + \frac{\hat{P}(ab)}{2}\lambda_a^k f_{lb}\lambda_{cd}^{ij}\tau_{kl}^{cd} + \frac{\hat{P}(ij)}{2}\lambda_c^i f_{jd}\lambda_{ab}^{kl}\tau_{kl}^{cd} \\
&+\hat{P}(ab)\hat{P}(ij)\lambda_a^i\lambda_c^k\tau_{kl}^{cd}u_{bd}^{jl} + \hat{P}(ab)\hat{P}(ij)\lambda_a^k f_{id}\lambda_{bc}^{jl}\tau_{kl}^{cd} + \hat{P}(ab)\hat{P}(ij)\lambda_c^i f_{la}\lambda_{bd}^{jk}\tau_{kl}^{cd} + \frac{\hat{P}(ab)\hat{P}(ij)}{2}\lambda_a^i f_{jd}\lambda_{bc}^{kl}\tau_{kl}^{cd} \\
&+\frac{\hat{P}(ab)\hat{P}(ij)}{2}\lambda_a^i f_{lb}\lambda_{cd}^{jk}\tau_{kl}^{cd} - \hat{P}(ab)\hat{P}(ij)\lambda_a^k\lambda_c^i\tau_{kl}^{cd}u_{bd}^{jl} - \frac{\hat{P}(ab)\hat{P}(ij)}{2}\lambda_a^i\lambda_b^k\tau_{kl}^{cd}u_{cd}^{jl} - \frac{\hat{P}(ab)\hat{P}(ij)}{2}\lambda_a^i\lambda_c^j\tau_{kl}^{cd}u_{bd}^{kl} \\
&+\lambda_c^k\lambda_{ab}^{lm}\tau_{kl}^{cd}u_{dm}^{ij} + \frac{1}{2}\lambda_c^k\lambda_{ab}^{lm}\tau_{lm}^{cd}u_{dk}^{ij} + \hat{P}(ab)\lambda_a^k\lambda_{bc}^{lm}\tau_{kl}^{cd}u_{dm}^{ij} + \hat{P}(ij)\lambda_c^k\lambda_{ab}^{il}\tau_{km}^{cd}u_{dl}^{jm} \\
&+\frac{\hat{P}(ab)}{2}\lambda_a^k\lambda_{bc}^{lm}\tau_{lm}^{cd}u_{dk}^{ij} + \frac{\hat{P}(ab)}{4}\lambda_a^k\lambda_{cd}^{ij}\tau_{lm}^{cd}u_{bk}^{lm} - \hat{P}(ij)\lambda_c^i\lambda_{ab}^{kl}\tau_{km}^{cd}u_{dl}^{jm} - \hat{P}(ij)\lambda_c^k\lambda_{ab}^{il}\tau_{lm}^{cd}u_{dk}^{jm} \\
&+\hat{P}(ab)\hat{P}(ij)\lambda_a^k\lambda_{bc}^{il}\tau_{km}^{cd}u_{dl}^{jm} + \hat{P}(ab)\hat{P}(ij)\lambda_c^i\lambda_{ad}^{kl}\tau_{km}^{cd}u_{bl}^{jm} - \frac{\hat{P}(ab)}{2}\lambda_c^k\lambda_{ad}^{ij}\tau_{lm}^{cd}u_{bk}^{lm} - \hat{P}(ab)\hat{P}(ij)\lambda_a^i\lambda_{bc}^{kl}\tau_{km}^{cd}u_{dl}^{jm} \\
&+\frac{\hat{P}(ab)\hat{P}(ij)}{4}\lambda_a^i\lambda_{cd}^{jk}\tau_{lm}^{cd}u_{bk}^{lm} - \hat{P}(ab)\hat{P}(ij)\lambda_a^k\lambda_{bc}^{il}\tau_{lm}^{cd}u_{dk}^{jm} + \frac{\hat{P}(ab)\hat{P}(ij)}{2}\lambda_a^k\lambda_{cd}^{il}\tau_{km}^{cd}u_{bl}^{jm} - \frac{\hat{P}(ab)\hat{P}(ij)}{2}\lambda_a^k\lambda_{cd}^{il}\tau_{lm}^{cd}u_{bk}^{jm} \\
&-\frac{\hat{P}(ab)\hat{P}(ij)}{2}\lambda_c^i\lambda_{ad}^{jk}\tau_{lm}^{cd}u_{bk}^{lm} + \lambda_c^k\lambda_{de}^{ij}\tau_{kl}^{cd}u_{ab}^{el} + \frac{1}{2}\lambda_c^k\lambda_{de}^{ij}\tau_{kl}^{de}u_{ab}^{cl} + \hat{P}(ij)\lambda_c^i\lambda_{de}^{jk}\tau_{kl}^{cd}u_{ab}^{el} \\
&+\hat{P}(ab)\lambda_c^k\lambda_{ad}^{ij}\tau_{kl}^{ce}u_{be}^{dl} - \hat{P}(ab)\lambda_a^k\lambda_{cd}^{ij}\tau_{kl}^{ce}u_{be}^{dl} + \frac{\hat{P}(ij)}{4}\lambda_c^i\lambda_{ab}^{kl}\tau_{kl}^{de}u_{de}^{cj} + \frac{\hat{P}(ij)}{2}\lambda_c^i\lambda_{de}^{jk}\tau_{kl}^{de}u_{ab}^{cl} \\
&-\hat{P}(ab)\lambda_c^k\lambda_{ad}^{ij}\tau_{kl}^{de}u_{be}^{cl} + \hat{P}(ab)\hat{P}(ij)\lambda_a^k\lambda_{cd}^{il}\tau_{kl}^{ce}u_{be}^{dj} + \hat{P}(ab)\hat{P}(ij)\lambda_c^i\lambda_{ad}^{jk}\tau_{kl}^{ce}u_{be}^{dl} - \frac{\hat{P}(ij)}{2}\lambda_c^k\lambda_{ab}^{il}\tau_{kl}^{de}u_{de}^{cj} \\
&+\frac{\hat{P}(ab)\hat{P}(ij)}{4}\lambda_a^i\lambda_{bc}^{kl}\tau_{kl}^{de}u_{de}^{cj} - \hat{P}(ab)\hat{P}(ij)\lambda_a^i\lambda_{cd}^{jk}\tau_{kl}^{ce}u_{be}^{dl} - \hat{P}(ab)\hat{P}(ij)\lambda_c^i\lambda_{ad}^{jk}\tau_{kl}^{de}u_{be}^{cl} + \frac{\hat{P}(ab)\hat{P}(ij)}{2}\lambda_c^i\lambda_{ad}^{kl}\tau_{kl}^{ce}u_{be}^{dj} \\
&-\frac{\hat{P}(ab)\hat{P}(ij)}{2}\lambda_a^k\lambda_{bc}^{il}\tau_{kl}^{de}u_{de}^{cj} - \frac{\hat{P}(ab)\hat{P}(ij)}{2}\lambda_c^i\lambda_{ad}^{kl}\tau_{kl}^{de}u_{be}^{cj} + \frac{\hat{P}(ij)}{2}\lambda_{ab}^{lm}\lambda_{cd}^{ik}\tau_{ln}^{cd}u_{km}^{jn} - \frac{\hat{P}(ij)}{4}\lambda_{ab}^{lm}\lambda_{cd}^{ik}\tau_{kn}^{cd}u_{lm}^{jn} \\
&+\frac{\hat{P}(ab)\hat{P}(ij)}{2}\lambda_{ac}^{kl}\lambda_{bd}^{im}\tau_{mn}^{cd}u_{kl}^{jn} - \hat{P}(ab)\hat{P}(ij)\lambda_{ad}^{im}\lambda_{bc}^{kl}\tau_{kn}^{cd}u_{lm}^{jn} + \hat{P}(ab)\lambda_{ae}^{kl}\lambda_{cd}^{ij}\tau_{km}^{ce}u_{bl}^{dm} - \hat{P}(ij)\lambda_{ab}^{lm}\lambda_{cd}^{ik}\tau_{kl}^{ce}u_{em}^{dj} \\
&+\hat{P}(ab)\hat{P}(ij)\lambda_{ac}^{kl}\lambda_{bd}^{im}\tau_{km}^{de}u_{el}^{cj} + \hat{P}(ab)\hat{P}(ij)\lambda_{ad}^{im}\lambda_{bc}^{kl}\tau_{km}^{ce}u_{el}^{dj} + \hat{P}(ab)\hat{P}(ij)\lambda_{ae}^{il}\lambda_{cd}^{jk}\tau_{km}^{ce}u_{bl}^{dm} - \frac{\hat{P}(ij)}{2}\lambda_{ab}^{lm}\lambda_{cd}^{ik}\tau_{lm}^{ce}u_{ek}^{dj} \\
&-\frac{\hat{P}(ab)}{2}\lambda_{ae}^{kl}\lambda_{cd}^{ij}\tau_{km}^{cd}u_{bl}^{em} + \frac{\hat{P}(ab)\hat{P}(ij)}{2}\lambda_{ac}^{kl}\lambda_{bd}^{im}\tau_{kl}^{ce}u_{em}^{dj} + \frac{\hat{P}(ab)\hat{P}(ij)}{2}\lambda_{ae}^{il}\lambda_{cd}^{jk}\tau_{lm}^{cd}u_{bk}^{em} - \hat{P}(ab)\hat{P}(ij)\lambda_{ae}^{il}\lambda_{cd}^{jk}\tau_{lm}^{ce}u_{bk}^{dm} \\
&-\frac{\hat{P}(ab)\hat{P}(ij)}{2}\lambda_{ac}^{kl}\lambda_{bd}^{im}\tau_{kl}^{de}u_{em}^{cj} - \frac{\hat{P}(ab)\hat{P}(ij)}{2}\lambda_{ae}^{il}\lambda_{cd}^{jk}\tau_{km}^{cd}u_{bl}^{em} - \frac{\hat{P}(ab)}{2}\lambda_{ae}^{kl}\lambda_{cd}^{ij}\tau_{kl}^{cg}u_{bg}^{de} - \frac{\hat{P}(ab)}{4}\lambda_{ae}^{kl}\lambda_{cd}^{ij}\tau_{kl}^{eg}u_{bg}^{cd} \\
&-\hat{P}(ab)\hat{P}(ij)\lambda_{ae}^{il}\lambda_{cd}^{jk}\tau_{kl}^{cg}u_{bg}^{de} - \frac{\hat{P}(ab)\hat{P}(ij)}{2}\lambda_{ae}^{il}\lambda_{cd}^{jk}\tau_{kl}^{eg}u_{bg}^{cd} + \frac{1}{4}\lambda_{ac}^{kl}\lambda_{bd}^{mn}\tau_{kl}^{ce}\tau_{mn}^{dg}u_{eg}^{ij} - \lambda_{ac}^{kl}\lambda_{bd}^{mn}\tau_{km}^{ce}\tau_{ln}^{dg}u_{eg}^{ij} \\
&+\frac{1}{4}\lambda_{cd}^{ik}\lambda_{eg}^{jl}\tau_{km}^{cd}\tau_{ln}^{eg}u_{ab}^{mn} + \frac{1}{4}\lambda_{cd}^{ik}\lambda_{eg}^{jl}\tau_{ln}^{cd}\tau_{km}^{eg}u_{ab}^{mn} - \lambda_{cd}^{ik}\lambda_{eg}^{jl}\tau_{km}^{ce}\tau_{ln}^{dg}u_{ab}^{mn} + \hat{P}(ij)\lambda_{ab}^{lm}\lambda_{cd}^{ik}\tau_{kl}^{ce}\tau_{mn}^{dg}u_{eg}^{jn} \\
&-\frac{1}{4}\lambda_{ac}^{kl}\lambda_{bd}^{mn}\tau_{mn}^{cg}\tau_{kl}^{de}u_{eg}^{ij} + \frac{\hat{P}(ij)}{2}\lambda_{ab}^{lm}\lambda_{cd}^{ik}\tau_{lm}^{ce}\tau_{kn}^{dg}u_{eg}^{jn} + \frac{\hat{P}(ab)}{2}\lambda_{ae}^{kl}\lambda_{cd}^{ij}\tau_{km}^{cd}\tau_{ln}^{eg}u_{bg}^{mn} - \hat{P}(ab)\lambda_{ae}^{kl}\lambda_{cd}^{ij}\tau_{km}^{ce}\tau_{ln}^{dg}u_{bg}^{mn} \\
&+\hat{P}(ab)\hat{P}(ij)\lambda_{ad}^{im}\lambda_{bc}^{kl}\tau_{ln}^{cg}\tau_{km}^{de}u_{eg}^{jn} + \hat{P}(ab)\hat{P}(ij)\lambda_{ae}^{il}\lambda_{cd}^{jk}\tau_{km}^{cg}\tau_{ln}^{de}u_{bg}^{mn} + \hat{P}(ab)\hat{P}(ij)\lambda_{ae}^{lm}\lambda_{cd}^{ik}\tau_{kl}^{cg}\tau_{mn}^{de}u_{bg}^{jn} - \frac{\hat{P}(ij)}{8}\lambda_{ab}^{lm}\lambda_{cd}^{ik}\tau_{kn}^{cd}\tau_{lm}^{eg}u_{eg}^{jn} \\
&-\frac{\hat{P}(ij)}{4}\lambda_{ab}^{lm}\lambda_{cd}^{ik}\tau_{mn}^{cd}\tau_{kl}^{eg}u_{eg}^{jn} - \frac{\hat{P}(ab)}{8}\lambda_{ae}^{kl}\lambda_{cd}^{ij}\tau_{mn}^{cd}\tau_{kl}^{eg}u_{bg}^{mn} - \frac{\hat{P}(ab)}{4}\lambda_{ae}^{kl}\lambda_{cd}^{ij}\tau_{kl}^{cg}\tau_{mn}^{de}u_{bg}^{mn} - \hat{P}(ab)\hat{P}(ij)\lambda_{ad}^{im}\lambda_{bc}^{kl}\tau_{km}^{ce}\tau_{ln}^{dg}u_{eg}^{jn} \\
&+\frac{\hat{P}(ab)\hat{P}(ij)}{2}\lambda_{ae}^{il}\lambda_{cd}^{jk}\tau_{km}^{cd}\tau_{ln}^{eg}u_{bg}^{mn} - \hat{P}(ab)\hat{P}(ij)\lambda_{ae}^{il}\lambda_{cd}^{jk}\tau_{km}^{ce}\tau_{ln}^{dg}u_{bg}^{mn} + \frac{\hat{P}(ab)\hat{P}(ij)}{2}\lambda_{ae}^{il}\lambda_{cd}^{jk}\tau_{mn}^{ce}\tau_{kl}^{dg}u_{bg}^{mn} + \frac{\hat{P}(ab)\hat{P}(ij)}{4}\lambda_{ae}^{lm}\lambda_{cd}^{ik}\tau_{kn}^{cd}\tau_{lm}^{eg}u_{bg}^{jn} \\
&+\frac{\hat{P}(ab)\hat{P}(ij)}{2}\lambda_{ae}^{lm}\lambda_{cd}^{ik}\tau_{lm}^{cg}\tau_{kn}^{de}u_{bg}^{jn} - \frac{\hat{P}(ab)\hat{P}(ij)}{2}\lambda_{ac}^{kl}\lambda_{bd}^{im}\tau_{ln}^{cd}\tau_{km}^{eg}u_{eg}^{jn} - \frac{\hat{P}(ab)\hat{P}(ij)}{2}\lambda_{ac}^{kl}\lambda_{bd}^{im}\tau_{kl}^{ce}\tau_{mn}^{dg}u_{eg}^{jn} - \frac{\hat{P}(ab)\hat{P}(ij)}{4}\lambda_{ad}^{im}\lambda_{bc}^{kl}\tau_{mn}^{cd}\tau_{kl}^{eg}u_{eg}^{jn} \\
&-\frac{\hat{P}(ab)\hat{P}(ij)}{2}\lambda_{ad}^{im}\lambda_{bc}^{kl}\tau_{mn}^{cg}\tau_{kl}^{de}u_{eg}^{jn} - \frac{\hat{P}(ab)\hat{P}(ij)}{2}\lambda_{ae}^{il}\lambda_{cd}^{jk}\tau_{lm}^{cd}\tau_{kn}^{eg}u_{bg}^{mn} - \frac{\hat{P}(ab)\hat{P}(ij)}{4}\lambda_{ae}^{il}\lambda_{cd}^{jk}\tau_{mn}^{cd}\tau_{kl}^{eg}u_{bg}^{mn} - \frac{\hat{P}(ab)\hat{P}(ij)}{2}\lambda_{ae}^{lm}\lambda_{cd}^{ik}\tau_{ln}^{cd}\tau_{km}^{eg}u_{bg}^{jn}.
\end{aligned}
\tag{D.8}
$$

The $\hat{\Lambda}_1\hat{\Lambda}_2$ contribution is

$$
\begin{aligned}
&\langle\Phi|\hat{\Lambda}_1\hat{\Lambda}_2[\overline{H},\hat{X}^{ab}_{ij}]\,|\Phi_0\rangle = \\
&\lambda^k_a\lambda^{il}_{bc}\tau^{cd}_{km}u^{mj}_{ld} + \lambda^k_a\lambda^{lj}_{bc}\tau^{cd}_{lm}u^{im}_{kd} + \lambda^i_b\lambda^{kl}_{ac}\tau^{cd}_{km}u^{mj}_{ld} + \lambda^j_b\lambda^{kl}_{ac}\tau^{cd}_{km}u^{im}_{ld} + \lambda^k_b\lambda^{il}_{ac}\tau^{cd}_{lm}u^{mj}_{kd} + \lambda^k_b\lambda^{lj}_{ac}\tau^{cd}_{km}u^{im}_{ld} \\
&+ \lambda^k_b\lambda^{lm}_{ac}\tau^{cd}_{kl}u^{ij}_{md} + \lambda^i_c\lambda^{kl}_{bd}\tau^{cd}_{km}u^{mj}_{al} + \lambda^j_c\lambda^{kl}_{bd}\tau^{cd}_{km}u^{im}_{al} + \lambda^k_c\lambda^{il}_{ab}\tau^{cd}_{km}u^{mj}_{ld} + \lambda^k_c\lambda^{lj}_{ab}\tau^{cd}_{lm}u^{im}_{kd} + \lambda^k_c\lambda^{il}_{ad}\tau^{cd}_{km}u^{mj}_{bl} \\
&+ \lambda^k_c\lambda^{lj}_{ad}\tau^{cd}_{lm}u^{im}_{bk} + \lambda^k_c\lambda^{il}_{bd}\tau^{cd}_{lm}u^{mj}_{ak} + \lambda^k_c\lambda^{lj}_{bd}\tau^{cd}_{km}u^{im}_{al} + \frac{1}{2}\lambda^i_a\lambda^{kl}_{cd}\tau^{cd}_{km}u^{mj}_{bl} + \frac{1}{2}\lambda^j_a\lambda^{kl}_{cd}\tau^{cd}_{km}u^{im}_{bl} + \frac{1}{2}\lambda^k_a\lambda^{il}_{cd}\tau^{cd}_{lm}u^{mj}_{bk} \\
&+ \frac{1}{2}\lambda^k_a\lambda^{lj}_{cd}\tau^{cd}_{km}u^{im}_{bl} + \frac{1}{2}\lambda^k_b\lambda^{lm}_{ac}\tau^{cd}_{lm}u^{ij}_{kd} + \frac{1}{2}\lambda^k_b\lambda^{il}_{cd}\tau^{cd}_{km}u^{mj}_{al} + \frac{1}{2}\lambda^k_b\lambda^{lj}_{cd}\tau^{cd}_{lm}u^{im}_{ak} + \frac{1}{2}\lambda^i_c\lambda^{kj}_{ad}\tau^{cd}_{lm}u^{lm}_{bk} + \frac{1}{2}\lambda^j_c\lambda^{ik}_{ad}\tau^{cd}_{lm}u^{lm}_{bk} \\
&+ \frac{1}{2}\lambda^k_c\lambda^{ij}_{bd}\tau^{cd}_{lm}u^{lm}_{ak} - \lambda^i_a\lambda^{kl}_{bc}\tau^{cd}_{km}u^{mj}_{ld} - \lambda^j_a\lambda^{kl}_{bc}\tau^{cd}_{km}u^{im}_{ld} - \lambda^k_a\lambda^{il}_{bc}\tau^{cd}_{lm}u^{mj}_{kd} - \lambda^k_a\lambda^{lj}_{bc}\tau^{cd}_{km}u^{im}_{ld} - \lambda^k_a\lambda^{lm}_{bc}\tau^{cd}_{kl}u^{ij}_{md} \\
&- \lambda^k_b\lambda^{il}_{ac}\tau^{cd}_{km}u^{mj}_{ld} - \lambda^k_b\lambda^{lj}_{ac}\tau^{cd}_{lm}u^{im}_{kd} - \lambda^i_c\lambda^{kl}_{ab}\tau^{cd}_{km}u^{mj}_{ld} - \lambda^i_c\lambda^{kl}_{ad}\tau^{cd}_{km}u^{mj}_{bl} - \lambda^j_c\lambda^{kl}_{ab}\tau^{cd}_{km}u^{im}_{ld} - \lambda^j_c\lambda^{kl}_{ad}\tau^{cd}_{km}u^{im}_{bl} \\
&- \lambda^k_c\lambda^{il}_{ab}\tau^{cd}_{lm}u^{mj}_{kd} - \lambda^k_c\lambda^{lj}_{ab}\tau^{cd}_{km}u^{im}_{ld} - \lambda^k_c\lambda^{lm}_{ab}\tau^{cd}_{kl}u^{ij}_{md} - \lambda^k_c\lambda^{il}_{ad}\tau^{cd}_{lm}u^{mj}_{bk} - \lambda^k_c\lambda^{lj}_{ad}\tau^{cd}_{km}u^{im}_{bl} - \lambda^k_c\lambda^{il}_{bd}\tau^{cd}_{km}u^{mj}_{al} \\
&- \lambda^k_c\lambda^{lj}_{bd}\tau^{cd}_{lm}u^{im}_{ak} - \frac{1}{2}\lambda^k_a\lambda^{lm}_{bc}\tau^{cd}_{lm}u^{ij}_{kd} - \frac{1}{2}\lambda^k_a\lambda^{il}_{cd}\tau^{cd}_{km}u^{mj}_{bl} - \frac{1}{2}\lambda^k_a\lambda^{lj}_{cd}\tau^{cd}_{lm}u^{im}_{bk} - \frac{1}{2}\lambda^i_b\lambda^{kl}_{cd}\tau^{cd}_{km}u^{mj}_{al} - \frac{1}{2}\lambda^j_b\lambda^{kl}_{cd}\tau^{cd}_{km}u^{im}_{al} \\
&- \frac{1}{2}\lambda^k_b\lambda^{il}_{cd}\tau^{cd}_{lm}u^{mj}_{ak} - \frac{1}{2}\lambda^k_b\lambda^{lj}_{cd}\tau^{cd}_{km}u^{im}_{al} - \frac{1}{2}\lambda^i_c\lambda^{kj}_{bd}\tau^{cd}_{lm}u^{lm}_{ak} - \frac{1}{2}\lambda^j_c\lambda^{ik}_{bd}\tau^{cd}_{lm}u^{lm}_{ak} - \frac{1}{2}\lambda^k_c\lambda^{lm}_{ab}\tau^{cd}_{lm}u^{ij}_{kd} - \frac{1}{2}\lambda^k_c\lambda^{ij}_{ad}\tau^{cd}_{lm}u^{lm}_{bk} \\
&- \frac{1}{4}\lambda^i_a\lambda^{kj}_{cd}\tau^{cd}_{lm}u^{lm}_{bk} - \frac{1}{4}\lambda^j_a\lambda^{ik}_{cd}\tau^{cd}_{lm}u^{lm}_{bk} - \frac{1}{4}\lambda^k_b\lambda^{ij}_{cd}\tau^{cd}_{lm}u^{lm}_{ak} + \frac{1}{4}\lambda^k_a\lambda^{ij}_{cd}\tau^{cd}_{lm}u^{lm}_{bk} + \frac{1}{4}\lambda^i_b\lambda^{kj}_{cd}\tau^{cd}_{lm}u^{lm}_{ak} + \frac{1}{4}\lambda^j_b\lambda^{ik}_{cd}\tau^{cd}_{lm}u^{lm}_{ak} \\
&+ \lambda^k_a\lambda^{lj}_{bc}u^{ic}_{kl} + \lambda^k_b\lambda^{il}_{ac}u^{cj}_{kl} + \lambda^k_c\lambda^{lj}_{ab}u^{ic}_{kl} + \frac{1}{2}\lambda^i_a\lambda^{kl}_{bc}u^{cj}_{kl} + \frac{1}{2}\lambda^j_a\lambda^{kl}_{bc}u^{ic}_{kl} + \frac{1}{2}\lambda^i_c\lambda^{kl}_{ab}u^{cj}_{kl} \\
&+ \frac{1}{2}\lambda^j_c\lambda^{kl}_{ab}u^{ic}_{kl} - \lambda^k_a\lambda^{il}_{bc}u^{cj}_{kl} - \lambda^k_b\lambda^{lj}_{ac}u^{ic}_{kl} - \lambda^k_c\lambda^{il}_{ab}u^{cj}_{kl} - \frac{1}{2}\lambda^i_b\lambda^{kl}_{ac}u^{cj}_{kl} - \frac{1}{2}\lambda^j_b\lambda^{kl}_{ac}u^{ic}_{kl} \\
&+ \lambda^k_b f_{id}\lambda^{lj}_{ac}\tau^{cd}_{kl} + \lambda^k_b f_{jd}\lambda^{il}_{ac}\tau^{cd}_{kl} + \lambda^i_c f_{lb}\lambda^{kj}_{ad}\tau^{cd}_{kl} + \lambda^j_c f_{lb}\lambda^{ik}_{ad}\tau^{cd}_{kl} + \lambda^k_c f_{la}\lambda^{ij}_{bd}\tau^{cd}_{kl} + \frac{1}{2}\lambda^i_a f_{jd}\lambda^{kl}_{bc}\tau^{cd}_{kl} \\
&+ \frac{1}{2}\lambda^k_a f_{lb}\lambda^{ij}_{cd}\tau^{cd}_{kl} + \frac{1}{2}\lambda^i_b f_{la}\lambda^{kj}_{cd}\tau^{cd}_{kl} + \frac{1}{2}\lambda^j_b f_{id}\lambda^{kl}_{ac}\tau^{cd}_{kl} + \frac{1}{2}\lambda^j_b f_{la}\lambda^{ik}_{cd}\tau^{cd}_{kl} + \frac{1}{2}\lambda^i_c f_{jd}\lambda^{kl}_{ab}\tau^{cd}_{kl} - \lambda^k_a f_{id}\lambda^{lj}_{bc}\tau^{cd}_{kl} \\
&- \lambda^k_a f_{jd}\lambda^{il}_{bc}\tau^{cd}_{kl} - \lambda^i_c f_{la}\lambda^{kj}_{bd}\tau^{cd}_{kl} - \lambda^j_c f_{la}\lambda^{ik}_{bd}\tau^{cd}_{kl} - \lambda^k_c f_{id}\lambda^{lj}_{ab}\tau^{cd}_{kl} - \lambda^k_c f_{jd}\lambda^{il}_{ab}\tau^{cd}_{kl} - \lambda^k_c f_{lb}\lambda^{ij}_{ad}\tau^{cd}_{kl} \\
&- \frac{1}{2}\lambda^i_a f_{lb}\lambda^{kj}_{cd}\tau^{cd}_{kl} - \frac{1}{2}\lambda^j_a f_{id}\lambda^{kl}_{bc}\tau^{cd}_{kl} - \frac{1}{2}\lambda^j_a f_{lb}\lambda^{ik}_{cd}\tau^{cd}_{kl} - \frac{1}{2}\lambda^i_b f_{jd}\lambda^{kl}_{ac}\tau^{cd}_{kl} - \frac{1}{2}\lambda^k_b f_{la}\lambda^{ij}_{cd}\tau^{cd}_{kl} - \frac{1}{2}\lambda^j_c f_{id}\lambda^{kl}_{ab}\tau^{cd}_{kl} \\
&+ \lambda^k_a\lambda^{ij}_{cd}\tau^{ce}_{kl}u^{ld}_{be} + \lambda^k_a\lambda^{il}_{cd}\tau^{ce}_{kl}u^{dj}_{be} + \lambda^i_b\lambda^{kj}_{cd}\tau^{ce}_{kl}u^{ld}_{ae} + \lambda^j_b\lambda^{ik}_{cd}\tau^{ce}_{kl}u^{ld}_{ae} + \lambda^k_b\lambda^{lj}_{cd}\tau^{ce}_{kl}u^{id}_{ae} + \lambda^i_c\lambda^{kj}_{ad}\tau^{ce}_{kl}u^{ld}_{be} \\
&+ \lambda^i_c\lambda^{kj}_{bd}\tau^{de}_{kl}u^{lc}_{ae} + \lambda^i_c\lambda^{kj}_{de}\tau^{cd}_{kl}u^{le}_{ab} + \lambda^j_c\lambda^{ik}_{ad}\tau^{ce}_{kl}u^{ld}_{be} + \lambda^j_c\lambda^{ik}_{bd}\tau^{de}_{kl}u^{lc}_{ae} + \lambda^j_c\lambda^{ik}_{de}\tau^{cd}_{kl}u^{le}_{ab} + \lambda^k_c\lambda^{ij}_{ad}\tau^{de}_{kl}u^{lc}_{be} \\
&+ \lambda^k_c\lambda^{il}_{ad}\tau^{de}_{kl}u^{cj}_{be} + \lambda^k_c\lambda^{lj}_{ad}\tau^{ce}_{kl}u^{id}_{be} + \lambda^k_c\lambda^{ij}_{bd}\tau^{ce}_{kl}u^{ld}_{ae} + \lambda^k_c\lambda^{il}_{bd}\tau^{ce}_{kl}u^{dj}_{ae} + \lambda^k_c\lambda^{lj}_{bd}\tau^{de}_{kl}u^{ic}_{ae} + \frac{1}{2}\lambda^k_a\lambda^{lj}_{bc}\tau^{de}_{kl}u^{ic}_{de} \\
&+ \frac{1}{2}\lambda^i_b\lambda^{kl}_{cd}\tau^{ce}_{kl}u^{dj}_{ae} + \frac{1}{2}\lambda^j_b\lambda^{kl}_{cd}\tau^{ce}_{kl}u^{id}_{ae} + \frac{1}{2}\lambda^k_b\lambda^{il}_{ac}\tau^{de}_{kl}u^{cj}_{de} + \frac{1}{2}\lambda^i_c\lambda^{kl}_{ad}\tau^{ce}_{kl}u^{dj}_{be} + \frac{1}{2}\lambda^i_c\lambda^{kl}_{bd}\tau^{de}_{kl}u^{cj}_{ae} + \frac{1}{2}\lambda^i_c\lambda^{kj}_{de}\tau^{de}_{kl}u^{lc}_{ab} \\
&+ \frac{1}{2}\lambda^j_c\lambda^{kl}_{ad}\tau^{ce}_{kl}u^{id}_{be} + \frac{1}{2}\lambda^j_c\lambda^{kl}_{bd}\tau^{de}_{kl}u^{ic}_{ae} + \frac{1}{2}\lambda^j_c\lambda^{ik}_{de}\tau^{de}_{kl}u^{lc}_{ab} + \frac{1}{2}\lambda^k_c\lambda^{lj}_{ab}\tau^{de}_{kl}u^{ic}_{de} - \lambda^i_a\lambda^{kj}_{cd}\tau^{ce}_{kl}u^{ld}_{be} - \lambda^j_a\lambda^{ik}_{cd}\tau^{ce}_{kl}u^{ld}_{be} \\
&- \lambda^k_a\lambda^{lj}_{cd}\tau^{ce}_{kl}u^{id}_{be} - \lambda^k_b\lambda^{ij}_{cd}\tau^{ce}_{kl}u^{ld}_{ae} - \lambda^k_b\lambda^{il}_{cd}\tau^{ce}_{kl}u^{dj}_{ae} - \lambda^i_c\lambda^{kj}_{ad}\tau^{de}_{kl}u^{lc}_{be} - \lambda^i_c\lambda^{kj}_{bd}\tau^{ce}_{kl}u^{ld}_{ae} - \lambda^j_c\lambda^{ik}_{ad}\tau^{de}_{kl}u^{lc}_{be} \\
&- \lambda^j_c\lambda^{ik}_{bd}\tau^{ce}_{kl}u^{ld}_{ae} - \lambda^k_c\lambda^{ij}_{ad}\tau^{ce}_{kl}u^{ld}_{be} - \lambda^k_c\lambda^{il}_{ad}\tau^{ce}_{kl}u^{dj}_{be} - \lambda^k_c\lambda^{lj}_{ad}\tau^{de}_{kl}u^{ic}_{be} - \lambda^k_c\lambda^{ij}_{bd}\tau^{de}_{kl}u^{lc}_{ae} - \lambda^k_c\lambda^{il}_{bd}\tau^{de}_{kl}u^{cj}_{ae} \\
&- \lambda^k_c\lambda^{lj}_{bd}\tau^{ce}_{kl}u^{id}_{ae} - \lambda^k_c\lambda^{ij}_{de}\tau^{cd}_{kl}u^{le}_{ab} - \frac{1}{2}\lambda^i_a\lambda^{kl}_{cd}\tau^{ce}_{kl}u^{dj}_{be} - \frac{1}{2}\lambda^j_a\lambda^{kl}_{cd}\tau^{ce}_{kl}u^{id}_{be} - \frac{1}{2}\lambda^k_a\lambda^{il}_{bc}\tau^{de}_{kl}u^{cj}_{de} - \frac{1}{2}\lambda^k_b\lambda^{lj}_{ac}\tau^{de}_{kl}u^{ic}_{de} \\
&- \frac{1}{2}\lambda^i_c\lambda^{kl}_{ad}\tau^{de}_{kl}u^{cj}_{be} - \frac{1}{2}\lambda^i_c\lambda^{kl}_{bd}\tau^{ce}_{kl}u^{dj}_{ae} - \frac{1}{2}\lambda^j_c\lambda^{kl}_{ad}\tau^{de}_{kl}u^{ic}_{be} - \frac{1}{2}\lambda^j_c\lambda^{kl}_{bd}\tau^{ce}_{kl}u^{id}_{ae} - \frac{1}{2}\lambda^k_c\lambda^{il}_{ab}\tau^{de}_{kl}u^{cj}_{de} - \frac{1}{2}\lambda^k_c\lambda^{ij}_{de}\tau^{de}_{kl}u^{lc}_{ab} \\
&- \frac{1}{4}\lambda^i_b\lambda^{kl}_{ac}\tau^{de}_{kl}u^{cj}_{de} - \frac{1}{4}\lambda^j_b\lambda^{kl}_{ac}\tau^{de}_{kl}u^{ic}_{de} + \frac{1}{4}\lambda^i_a\lambda^{kl}_{bc}\tau^{de}_{kl}u^{cj}_{de} + \frac{1}{4}\lambda^j_a\lambda^{kl}_{bc}\tau^{de}_{kl}u^{ic}_{de} + \frac{1}{4}\lambda^i_c\lambda^{kl}_{ab}\tau^{de}_{kl}u^{cj}_{de} + \frac{1}{4}\lambda^j_c\lambda^{kl}_{ab}\tau^{de}_{kl}u^{ic}_{de} \\
&+ \lambda^i_c\lambda^{kj}_{ad}u^{cd}_{bk} + \lambda^j_c\lambda^{ik}_{ad}u^{cd}_{bk} + \lambda^k_c\lambda^{ij}_{bd}u^{cd}_{ak} + \frac{1}{2}\lambda^k_a\lambda^{ij}_{cd}u^{cd}_{bk} + \frac{1}{2}\lambda^i_b\lambda^{kj}_{cd}u^{cd}_{ak} + \frac{1}{2}\lambda^j_b\lambda^{ik}_{cd}u^{cd}_{ak} \\
&- \lambda^i_c\lambda^{kj}_{bd}u^{cd}_{ak} - \lambda^j_c\lambda^{ik}_{bd}u^{cd}_{ak} - \lambda^k_c\lambda^{ij}_{ad}u^{cd}_{bk} - \frac{1}{2}\lambda^i_a\lambda^{kj}_{cd}u^{cd}_{bk} - \frac{1}{2}\lambda^j_a\lambda^{ik}_{cd}u^{cd}_{bk} - \frac{1}{2}\lambda^k_b\lambda^{ij}_{cd}u^{cd}_{ak}
\end{aligned}
\tag{D.9}
$$

Finally, the $\hat{\Lambda}_2^2$ contribution to the λ_2 equations is

$$
\begin{aligned}
&\frac{1}{2}\langle\Phi|\hat{\Lambda}_2^2[\overline{H},\hat{X}_{ij}^{ab}]\,|\Phi_0\rangle = \\
&\frac{\hat{P}(ij)}{2}\lambda_{ab}^{lm}\lambda_{cd}^{ik}\tau_{ln}^{cd}u_{km}^{jn} - \frac{\hat{P}(ij)}{2}\lambda_{ab}^{im}\lambda_{cd}^{kl}\tau_{kn}^{cd}u_{lm}^{jn} - \frac{\hat{P}(ij)}{4}\lambda_{ab}^{im}\lambda_{cd}^{kl}\tau_{mn}^{cd}u_{kl}^{jn} - \frac{\hat{P}(ij)}{4}\lambda_{ab}^{lm}\lambda_{cd}^{ik}\tau_{kn}^{cd}u_{lm}^{jn} \\
&+ \frac{\hat{P}(ab)\hat{P}(ij)}{2}\lambda_{ac}^{kl}\lambda_{bd}^{im}\tau_{mn}^{cd}u_{kl}^{jn} - \hat{P}(ab)\hat{P}(ij)\lambda_{ad}^{im}\lambda_{bc}^{kl}\tau_{kn}^{cd}u_{lm}^{jn} + \hat{P}(ij)\lambda_{ab}^{im}\lambda_{cd}^{kl}\tau_{km}^{ce}u_{el}^{dj} + \hat{P}(ab)\lambda_{ae}^{ij}\lambda_{cd}^{kl}\tau_{km}^{ce}u_{bl}^{dm} \\
&+ \hat{P}(ab)\lambda_{ae}^{kl}\lambda_{cd}^{ij}\tau_{km}^{ce}u_{bl}^{dm} - \hat{P}(ij)\lambda_{ab}^{lm}\lambda_{cd}^{ik}\tau_{kl}^{ce}u_{em}^{dj} + \hat{P}(ab)\hat{P}(ij)\lambda_{ac}^{kl}\lambda_{bd}^{im}\tau_{km}^{de}u_{el}^{cj} + \hat{P}(ab)\hat{P}(ij)\lambda_{ad}^{im}\lambda_{bc}^{kl}\tau_{km}^{ce}u_{el}^{dj} \\
&+ \hat{P}(ab)\hat{P}(ij)\lambda_{ae}^{il}\lambda_{cd}^{jk}\tau_{km}^{ce}u_{bl}^{dm} - \frac{\hat{P}(ij)}{2}\lambda_{ab}^{im}\lambda_{cd}^{kl}\tau_{kl}^{ce}u_{em}^{dj} - \frac{\hat{P}(ij)}{2}\lambda_{ab}^{lm}\lambda_{cd}^{ik}\tau_{lm}^{ce}u_{ek}^{dj} - \frac{\hat{P}(ab)}{2}\lambda_{ae}^{ij}\lambda_{cd}^{kl}\tau_{km}^{cd}u_{bl}^{em} \\
&- \frac{\hat{P}(ab)}{2}\lambda_{ae}^{kl}\lambda_{cd}^{ij}\tau_{km}^{cd}u_{bl}^{em} + \frac{\hat{P}(ab)\hat{P}(ij)}{2}\lambda_{ac}^{kl}\lambda_{bd}^{im}\tau_{kl}^{ce}u_{em}^{dj} + \frac{\hat{P}(ab)\hat{P}(ij)}{2}\lambda_{ae}^{il}\lambda_{cd}^{jk}\tau_{lm}^{cd}u_{bk}^{em} - \hat{P}(ab)\hat{P}(ij)\lambda_{ae}^{il}\lambda_{cd}^{jk}\tau_{lm}^{ce}u_{bk}^{dm} \\
&- \frac{\hat{P}(ab)\hat{P}(ij)}{2}\lambda_{ac}^{kl}\lambda_{bd}^{im}\tau_{kl}^{de}u_{em}^{cj} - \frac{\hat{P}(ab)\hat{P}(ij)}{2}\lambda_{ae}^{il}\lambda_{cd}^{jk}\tau_{km}^{cd}u_{bl}^{em} - \frac{\hat{P}(ab)}{2}\lambda_{ae}^{ij}\lambda_{cd}^{kl}\tau_{kl}^{cg}u_{bg}^{de} - \frac{\hat{P}(ab)}{4}\lambda_{ae}^{ij}\lambda_{cd}^{kl}\tau_{kl}^{eg}u_{bg}^{cd} \\
&- \frac{\hat{P}(ab)}{2}\lambda_{ae}^{kl}\lambda_{cd}^{ij}\tau_{kl}^{cg}u_{bg}^{de} - \frac{\hat{P}(ab)}{4}\lambda_{ae}^{kl}\lambda_{cd}^{ij}\tau_{kl}^{eg}u_{bg}^{cd} - \hat{P}(ab)\hat{P}(ij)\lambda_{ae}^{il}\lambda_{cd}^{jk}\tau_{kl}^{cg}u_{bg}^{de} - \frac{\hat{P}(ab)\hat{P}(ij)}{2}\lambda_{ae}^{il}\lambda_{cd}^{jk}\tau_{kl}^{eg}u_{bg}^{cd} \\
&+ \frac{1}{2}\lambda_{ab}^{mn}\lambda_{cd}^{kl}\tau_{km}^{ce}\tau_{ln}^{dg}u_{eg}^{ij} + \frac{1}{4}\lambda_{ac}^{kl}\lambda_{bd}^{mn}\tau_{kl}^{ce}\tau_{mn}^{dg}u_{eg}^{ij} - \lambda_{ac}^{kl}\lambda_{bd}^{mn}\tau_{km}^{ce}\tau_{ln}^{dg}u_{eg}^{ij} + \frac{1}{4}\lambda_{cd}^{ik}\lambda_{eg}^{jl}\tau_{km}^{cd}\tau_{ln}^{eg}u_{ab}^{mn} \\
&+ \frac{1}{4}\lambda_{cd}^{ik}\lambda_{eg}^{jl}\tau_{ln}^{cd}\tau_{km}^{eg}u_{ab}^{mn} - \lambda_{cd}^{ik}\lambda_{eg}^{jl}\tau_{km}^{ce}\tau_{ln}^{dg}u_{ab}^{mn} + \frac{1}{2}\lambda_{cd}^{kl}\lambda_{eg}^{ij}\tau_{km}^{ce}\tau_{ln}^{dg}u_{ab}^{mn} + \hat{P}(ij)\lambda_{ab}^{lm}\lambda_{cd}^{ik}\tau_{kl}^{ce}\tau_{mn}^{dg}u_{eg}^{jn} \\
&- \frac{1}{4}\lambda_{ab}^{mn}\lambda_{cd}^{kl}\tau_{kl}^{ce}\tau_{mn}^{dg}u_{eg}^{ij} - \frac{1}{4}\lambda_{ac}^{kl}\lambda_{bd}^{mn}\tau_{mn}^{cg}\tau_{kl}^{de}u_{eg}^{ij} - \frac{1}{4}\lambda_{cd}^{kl}\lambda_{eg}^{ij}\tau_{km}^{cd}\tau_{ln}^{eg}u_{ab}^{mn} + \frac{\hat{P}(ij)}{4}\lambda_{ab}^{im}\lambda_{cd}^{kl}\tau_{ln}^{cd}\tau_{km}^{eg}u_{eg}^{jn} \\
&+ \frac{\hat{P}(ij)}{2}\lambda_{ab}^{im}\lambda_{cd}^{kl}\tau_{kl}^{ce}\tau_{mn}^{dg}u_{eg}^{jn} - \hat{P}(ij)\lambda_{ab}^{im}\lambda_{cd}^{kl}\tau_{km}^{ce}\tau_{ln}^{dg}u_{eg}^{jn} + \frac{\hat{P}(ij)}{2}\lambda_{ab}^{lm}\lambda_{cd}^{ik}\tau_{lm}^{ce}\tau_{kn}^{dg}u_{eg}^{jn} + \frac{\hat{P}(ab)}{2}\lambda_{ae}^{ij}\lambda_{cd}^{kl}\tau_{km}^{cd}\tau_{ln}^{eg}u_{bg}^{mn} \\
&- \hat{P}(ab)\lambda_{ae}^{ij}\lambda_{cd}^{kl}\tau_{km}^{ce}\tau_{ln}^{dg}u_{bg}^{mn} + \frac{\hat{P}(ab)}{2}\lambda_{ae}^{kl}\lambda_{cd}^{ij}\tau_{km}^{cd}\tau_{ln}^{eg}u_{bg}^{mn} - \hat{P}(ab)\lambda_{ae}^{kl}\lambda_{cd}^{ij}\tau_{km}^{ce}\tau_{ln}^{dg}u_{bg}^{mn} + \hat{P}(ab)\hat{P}(ij)\lambda_{ad}^{im}\lambda_{bc}^{kl}\tau_{ln}^{cg}\tau_{km}^{de}u_{eg}^{jn} \\
&+ \hat{P}(ab)\hat{P}(ij)\lambda_{ae}^{il}\lambda_{cd}^{jk}\tau_{km}^{cg}\tau_{ln}^{de}u_{bg}^{mn} + \hat{P}(ab)\hat{P}(ij)\lambda_{ae}^{lm}\lambda_{cd}^{ik}\tau_{kl}^{cg}\tau_{mn}^{de}u_{bg}^{jn} - \frac{\hat{P}(ij)}{8}\lambda_{ab}^{im}\lambda_{cd}^{kl}\tau_{mn}^{cd}\tau_{kl}^{eg}u_{eg}^{jn} - \frac{\hat{P}(ij)}{8}\lambda_{ab}^{lm}\lambda_{cd}^{ik}\tau_{kn}^{cd}\tau_{lm}^{eg}u_{eg}^{jn} \\
&- \frac{\hat{P}(ij)}{4}\lambda_{ab}^{lm}\lambda_{cd}^{ik}\tau_{mn}^{cd}\tau_{kl}^{eg}u_{eg}^{jn} - \frac{\hat{P}(ab)}{8}\lambda_{ae}^{ij}\lambda_{cd}^{kl}\tau_{mn}^{cd}\tau_{kl}^{eg}u_{bg}^{mn} - \frac{\hat{P}(ab)}{4}\lambda_{ae}^{ij}\lambda_{cd}^{kl}\tau_{kl}^{cg}\tau_{mn}^{de}u_{bg}^{mn} - \frac{\hat{P}(ab)}{8}\lambda_{ae}^{kl}\lambda_{cd}^{ij}\tau_{mn}^{cd}\tau_{kl}^{eg}u_{bg}^{mn} \\
&- \frac{\hat{P}(ab)}{4}\lambda_{ae}^{kl}\lambda_{cd}^{ij}\tau_{kl}^{cg}\tau_{mn}^{de}u_{bg}^{mn} - \hat{P}(ab)\hat{P}(ij)\lambda_{ad}^{im}\lambda_{bc}^{kl}\tau_{km}^{ce}\tau_{ln}^{dg}u_{eg}^{jn} + \frac{\hat{P}(ab)\hat{P}(ij)}{2}\lambda_{ae}^{il}\lambda_{cd}^{jk}\tau_{km}^{cd}\tau_{ln}^{eg}u_{bg}^{mn} - \hat{P}(ab)\hat{P}(ij)\lambda_{ae}^{il}\lambda_{cd}^{jk}\tau_{km}^{ce}\tau_{ln}^{dg}u_{bg}^{mn} \\
&+ \frac{\hat{P}(ab)\hat{P}(ij)}{2}\lambda_{ae}^{il}\lambda_{cd}^{jk}\tau_{mn}^{ce}\tau_{kl}^{dg}u_{bg}^{mn} + \frac{\hat{P}(ab)\hat{P}(ij)}{2}\lambda_{ae}^{im}\lambda_{cd}^{kl}\tau_{kn}^{cd}\tau_{lm}^{eg}u_{bg}^{jn} + \frac{\hat{P}(ab)\hat{P}(ij)}{4}\lambda_{ae}^{im}\lambda_{cd}^{kl}\tau_{mn}^{cd}\tau_{kl}^{eg}u_{bg}^{jn} + \frac{\hat{P}(ab)\hat{P}(ij)}{2}\lambda_{ae}^{im}\lambda_{cd}^{kl}\tau_{kl}^{cg}\tau_{mn}^{de}u_{bg}^{jn} \\
&- \hat{P}(ab)\hat{P}(ij)\lambda_{ae}^{im}\lambda_{cd}^{kl}\tau_{km}^{cg}\tau_{ln}^{de}u_{bg}^{jn} + \frac{\hat{P}(ab)\hat{P}(ij)}{4}\lambda_{ae}^{lm}\lambda_{cd}^{ik}\tau_{kn}^{cd}\tau_{lm}^{eg}u_{bg}^{jn} + \frac{\hat{P}(ab)\hat{P}(ij)}{2}\lambda_{ae}^{lm}\lambda_{cd}^{ik}\tau_{lm}^{cg}\tau_{kn}^{de}u_{bg}^{jn} - \frac{\hat{P}(ab)\hat{P}(ij)}{2}\lambda_{ac}^{kl}\lambda_{bd}^{im}\tau_{ln}^{cd}\tau_{km}^{eg}u_{eg}^{jn} \\
&- \frac{\hat{P}(ab)\hat{P}(ij)}{2}\lambda_{ac}^{kl}\lambda_{bd}^{im}\tau_{kl}^{ce}\tau_{mn}^{dg}u_{eg}^{jn} - \frac{\hat{P}(ab)\hat{P}(ij)}{4}\lambda_{ad}^{im}\lambda_{bc}^{kl}\tau_{mn}^{cd}\tau_{kl}^{eg}u_{eg}^{jn} - \frac{\hat{P}(ab)\hat{P}(ij)}{2}\lambda_{ad}^{im}\lambda_{bc}^{kl}\tau_{mn}^{cg}\tau_{kl}^{de}u_{eg}^{jn} - \frac{\hat{P}(ab)\hat{P}(ij)}{2}\lambda_{ae}^{il}\lambda_{cd}^{jk}\tau_{lm}^{cd}\tau_{kn}^{eg}u_{bg}^{mn} \\
&- \frac{\hat{P}(ab)\hat{P}(ij)}{4}\lambda_{ae}^{il}\lambda_{cd}^{jk}\tau_{mn}^{cd}\tau_{kl}^{eg}u_{bg}^{mn} - \frac{\hat{P}(ab)\hat{P}(ij)}{2}\lambda_{ae}^{lm}\lambda_{cd}^{ik}\tau_{ln}^{cd}\tau_{km}^{eg}u_{bg}^{jn}.
\end{aligned}
\tag{D.10}
$$

Summarizing the expressions, we calculate the QCCSD λ_1 equations by using the CCSD amplitude equation from Eq. C.4 with $\tau_i^a = 0$ and adding the three expressions from Eqs. D.5 to D.7. For the QCCSD λ_2 equations, we have the CCSD contribution from Eq. C.5 ($\tau_i^a = 0$), with the added QCCSD terms of Eqs. D.8 to D.10.

D.2 Density matrices

The addition of the quadratic de-excitation operator in the left-state adds contribution to the reduced one- and two-body density matrices, expanding upon the CCSD density matrices presented in App. C.

Therefore, we separate the QCCSD reduced one-body density as

$$
\gamma_{pq} = \langle\Phi_0|(1+\hat{\Lambda}+\frac{1}{2}\hat{\Lambda}^2)e^{-\hat{T}}a_q^\dagger a_p e^{\hat{T}}|\Phi_0\rangle = \widetilde{\gamma}_{pq} + \Delta\gamma_{pq}, \tag{D.11}
$$

where $\widetilde{\gamma}_{pq}$ is the CCSD reduced one-body density expressed in App. C, and we have defined

$$
\Delta\gamma_{pq} \equiv \frac{1}{2}\langle\Phi_0|\hat{\Lambda}^2 e^{-\hat{T}}a_q^\dagger a_p e^{\hat{T}}|\Phi_0\rangle\,, \tag{D.12}
$$

as the additional QCCSD contribution we have to calculate.

Using the block calculations as in App. C, the additional terms we need to add are

$$\Delta\gamma_{ji} = \lambda_a^k \lambda_b^j \tau_{ik}^{ab}, \tag{D.13}$$

$$\Delta\gamma_{ba} = \lambda_a^i \lambda_k^c \tau_{ij}^{bc}, \tag{D.14}$$

$$\begin{aligned}\Delta\gamma_{ai} =& \hat{P}(ij)\lambda_b^j \lambda_c^k \tau_j^a \tau_{ki}^{bc} + \frac{1}{2}\lambda_b^j \lambda_{cd}^{kl} \tau_{kl}^{ad} \tau_{ij}^{bc} - \lambda_b^j \lambda_{cd}^{kl} \tau_{jl}^{ad} \tau_{ik}^{bc}, \\ & - \frac{1}{2}\lambda_b^j \lambda_{cd}^{kl} \tau_{jl}^{ab} \tau_{ik}^{cd} + \frac{1}{4}\lambda_b^j \lambda_{cd}^{kl} \tau_{kl}^{ab} \tau_{ij}^{cd},\end{aligned} \tag{D.15}$$

$$\Delta\gamma_{ia} = 0. \tag{D.16}$$

The reduced two-body density separates in the same way, thus we need the contribution

$$\Delta\Gamma_{rs}^{pq} \equiv \frac{1}{2}\left\langle \Phi_0 | \hat{\Lambda}^2 e^{-\hat{T}} a_r^\dagger a_s^\dagger a_q a_p e^{\hat{T}} | \Phi_0 \right\rangle,$$

in addition to the CCSD reduced two-body density expressions. The all occupied and all virtual blocks are

$$\begin{aligned}\Delta\Gamma_{ij}^{kl} =& \lambda_a^k \lambda_b^l \tau_{ij}^{ab} + \hat{P}(ij)\delta_{jl}\lambda_a^m \lambda_b^k \tau_{im}^{ab} - \hat{P}(ij)\delta_{jk}\lambda_a^m \lambda_b^l \tau_{im}^{ab} + \lambda_{ab}^{km} \lambda_{cd}^{ln} \tau_{in}^{ac} \tau_{jm}^{bd} \\ & + \lambda_{ab}^{mn} \lambda_{cd}^{kl} \tau_{im}^{ac} \tau_{jn}^{bd} - \lambda_{ab}^{km} \lambda_{cd}^{ln} \tau_{im}^{ac} \tau_{jn}^{bd} - \frac{1}{4}\lambda_{ab}^{mn} \lambda_{cd}^{kl} \tau_{im}^{ab} \tau_{jn}^{cd} - \frac{1}{4}\lambda_{ab}^{mn} \lambda_{cd}^{kl} \tau_{jn}^{ab} \tau_{im}^{cd} \\ & + \frac{\hat{P}(ij)}{4}\lambda_{ab}^{km} \lambda_{cd}^{ln} \tau_{im}^{ab} \tau_{jn}^{cd} - \frac{\hat{P}(ij)}{4}\lambda_{ab}^{km} \lambda_{cd}^{ln} \tau_{in}^{ab} \tau_{jm}^{cd},\end{aligned} \tag{D.17}$$

$$\begin{aligned}\Delta\Gamma_{ab}^{cd} =& \lambda_a^i \lambda_b^j \tau_{ij}^{cd} + \lambda_{ab}^{kl} \lambda_{ef}^{ij} \tau_{ik}^{ce} \tau_{jl}^{df} + \lambda_{ae}^{ij} \lambda_{bf}^{kl} \tau_{ik}^{cf} \tau_{jl}^{de} + \frac{1}{4}\lambda_{ae}^{ij} \lambda_{bf}^{kl} \tau_{ij}^{ce} \tau_{kl}^{df} \\ & - \lambda_{ae}^{ij} \lambda_{bf}^{kl} \tau_{ik}^{ce} \tau_{jl}^{df} + \frac{1}{4}\lambda_{ae}^{ij} \lambda_{bf}^{kl} \tau_{kl}^{ce} \tau_{ij}^{df} - \frac{1}{4}\lambda_{ab}^{kl} \lambda_{ef}^{ij} \tau_{ij}^{ce} \tau_{kl}^{df} - \frac{1}{4}\lambda_{ab}^{kl} \lambda_{ef}^{ij} \tau_{kl}^{ce} \tau_{ij}^{df} \\ & - \frac{1}{4}\lambda_{ae}^{ij} \lambda_{bf}^{kl} \tau_{ij}^{cf} \tau_{kl}^{de} - \frac{1}{4}\lambda_{ae}^{ij} \lambda_{bf}^{kl} \tau_{kl}^{cf} \tau_{ij}^{de}.\end{aligned} \tag{D.18}$$

For the blocks with two occupied indices and two virtual indices, we have

$$\begin{aligned}\Delta\Gamma_{ij}^{ab} =& \frac{1}{2}\lambda_c^k \lambda_d^l \tau_{kl}^{ab} \tau_{ij}^{cd} + \hat{P}(ij)\lambda_c^k \lambda_d^l \tau_{il}^{ab} \tau_{jk}^{cd} + \hat{P}(ij)\lambda_c^k \lambda_d^l \tau_{ik}^{ac} \tau_{jl}^{bd} - \hat{P}(ab)\lambda_c^k \lambda_d^l \tau_{kl}^{ac} \tau_{ij}^{bd} \\ & - \hat{P}(ij)\lambda_c^l \lambda_d^k \tau_{ik}^{ac} \tau_{jl}^{bd} + \frac{1}{4}\lambda_{cd}^{km} \lambda_{ef}^{ln} \tau_{mn}^{ab} \tau_{ik}^{cd} \tau_{jl}^{ef} + \frac{1}{2}\lambda_{cd}^{km} \lambda_{ef}^{ln} \tau_{kl}^{ae} \tau_{mn}^{bf} \tau_{ij}^{cd} + \frac{1}{4}\lambda_{cd}^{ln} \lambda_{ef}^{km} \tau_{mn}^{ab} \tau_{ik}^{cd} \tau_{jl}^{ef} \\ & + \frac{1}{4}\lambda_{ce}^{kl} \lambda_{df}^{mn} \tau_{kl}^{ae} \tau_{mn}^{bf} \tau_{ij}^{cd} - \lambda_{ce}^{km} \lambda_{df}^{ln} \tau_{mn}^{ab} \tau_{ik}^{cd} \tau_{jl}^{ef} - \lambda_{ce}^{km} \lambda_{df}^{ln} \tau_{kl}^{ae} \tau_{mn}^{bf} \tau_{ij}^{cd} + \frac{1}{2}\lambda_{ce}^{mn} \lambda_{df}^{kl} \tau_{mn}^{ab} \tau_{ik}^{cd} \tau_{jl}^{ef} \\ & - \frac{1}{8}\lambda_{cd}^{kl} \lambda_{ef}^{mn} \tau_{mn}^{ab} \tau_{ik}^{cd} \tau_{jl}^{ef} - \frac{1}{8}\lambda_{cd}^{kl} \lambda_{ef}^{mn} \tau_{kl}^{ae} \tau_{mn}^{bf} \tau_{ij}^{cd} - \frac{1}{8}\lambda_{cd}^{mn} \lambda_{ef}^{kl} \tau_{mn}^{ab} \tau_{ik}^{cd} \tau_{jl}^{ef} - \frac{1}{8}\lambda_{cd}^{mn} \lambda_{ef}^{kl} \tau_{kl}^{ae} \tau_{mn}^{bf} \tau_{ij}^{cd} \\ & - \frac{1}{4}\lambda_{cf}^{kl} \lambda_{de}^{mn} \tau_{kl}^{ae} \tau_{mn}^{bf} \tau_{ij}^{cd} + \hat{P}(ab)\hat{P}(ij)\lambda_{cf}^{kl} \lambda_{de}^{mn} \tau_{in}^{af} \tau_{lm}^{be} \tau_{jk}^{cd} + \frac{\hat{P}(ab)\hat{P}(ij)}{4}\lambda_{cd}^{kn} \lambda_{ef}^{lm} \tau_{in}^{af} \tau_{lm}^{be} \tau_{jk}^{cd} \\ & + \frac{\hat{P}(ab)\hat{P}(ij)}{4}\lambda_{cd}^{lm} \lambda_{ef}^{kn} \tau_{in}^{af} \tau_{lm}^{be} \tau_{jk}^{cd} - \hat{P}(ab)\hat{P}(ij)\lambda_{ce}^{kl} \lambda_{df}^{mn} \tau_{in}^{af} \tau_{lm}^{be} \tau_{jk}^{cd} + \frac{\hat{P}(ab)\hat{P}(ij)}{2}\lambda_{cf}^{lm} \lambda_{de}^{kn} \tau_{in}^{af} \tau_{lm}^{be} \tau_{jk}^{cd} \\ & - \frac{\hat{P}(ab)\hat{P}(ij)}{2}\lambda_{cd}^{kl} \lambda_{ef}^{mn} \tau_{lm}^{ae} \tau_{in}^{bf} \tau_{jk}^{cd} - \frac{\hat{P}(ab)\hat{P}(ij)}{2}\lambda_{cd}^{ln} \lambda_{ef}^{km} \tau_{in}^{af} \tau_{lm}^{be} \tau_{jk}^{cd} \\ & - \frac{\hat{P}(ab)\hat{P}(ij)}{2}\lambda_{ce}^{lm} \lambda_{df}^{kn} \tau_{in}^{af} \tau_{lm}^{be} \tau_{jk}^{cd},\end{aligned} \tag{D.19}$$

$$\Delta\Gamma_{ab}^{ij} = \hat{P}(ij)\lambda_a^i \lambda_b^j, \tag{D.20}$$

$$\begin{aligned}\Delta\Gamma_{ia}^{jb} =& \lambda_a^k \lambda_c^j \tau_{ik}^{bc} - \lambda_a^j \lambda_c^k \tau_{ik}^{bc} + \delta_{ij}\lambda_a^k \lambda_c^l \tau_{kl}^{bc} + \lambda_{ae}^{jm} \lambda_{cd}^{kl} \tau_{lm}^{bd} \tau_{ik}^{ce} \\ & + \frac{1}{2}\lambda_{ae}^{jm} \lambda_{cd}^{kl} \tau_{kl}^{bd} \tau_{im}^{ce} - \lambda_{ae}^{lm} \lambda_{cd}^{jk} \tau_{km}^{bd} \tau_{il}^{ce} + \frac{1}{2}\lambda_{ae}^{lm} \lambda_{cd}^{jk} \tau_{lm}^{bd} \tau_{ik}^{ce} + \frac{1}{2}\lambda_{ae}^{lm} \lambda_{cd}^{jk} \tau_{km}^{be} \tau_{il}^{cd} \\ & - \frac{1}{4}\lambda_{ae}^{jm} \lambda_{cd}^{kl} \tau_{kl}^{be} \tau_{im}^{cd} - \frac{1}{2}\lambda_{ae}^{jm} \lambda_{cd}^{kl} \tau_{lm}^{be} \tau_{ik}^{cd} - \frac{1}{4}\lambda_{ae}^{lm} \lambda_{cd}^{jk} \tau_{lm}^{be} \tau_{ik}^{cd}.\end{aligned} \tag{D.21}$$

Lastly, with either one virtual and three occupied indices, or one occupied and three virtual in-

dices, we have

$$\begin{aligned}
\Delta\Gamma_{ij}^{ka} =& \frac{1}{4}\lambda_b^k\lambda_{cd}^{lm}\tau_{lm}^{ab}\tau_{ij}^{cd} + \frac{1}{2}\lambda_b^k\lambda_{cd}^{lm}\tau_{lm}^{ad}\tau_{ij}^{bc} - \lambda_b^l\lambda_{cd}^{km}\tau_{lm}^{ad}\tau_{ij}^{bc} + \hat{P}(ij)\lambda_b^k\lambda_{cd}^{lm}\tau_{im}^{ad}\tau_{jl}^{bc} \\
&+ \hat{P}(ij)\lambda_b^l\lambda_{cd}^{km}\tau_{il}^{ad}\tau_{jm}^{bc} - \frac{1}{2}\lambda_b^l\lambda_{cd}^{km}\tau_{lm}^{ab}\tau_{ij}^{cd} + \frac{\hat{P}(ij)}{2}\lambda_b^k\lambda_{cd}^{lm}\tau_{im}^{ab}\tau_{jl}^{cd} + \frac{\hat{P}(ij)}{2}\lambda_b^l\lambda_{cd}^{km}\tau_{il}^{ab}\tau_{jm}^{cd} \\
&- \hat{P}(ij)\lambda_b^l\lambda_{cd}^{km}\tau_{im}^{ad}\tau_{jl}^{bc} - \frac{\hat{P}(ij)}{2}\lambda_b^l\lambda_{cd}^{km}\tau_{im}^{ab}\tau_{jl}^{cd} + \hat{P}(ij)\delta_{jk}\lambda_b^l\lambda_{cd}^{mn}\tau_{ln}^{ad}\tau_{im}^{bc} + \frac{\hat{P}(ij)}{2}\delta_{jk}\lambda_b^l\lambda_{cd}^{mn}\tau_{ln}^{ab}\tau_{im}^{cd} \\
&- \frac{\hat{P}(ij)}{4}\delta_{jk}\lambda_b^l\lambda_{cd}^{mn}\tau_{mn}^{ab}\tau_{il}^{cd} - \frac{\hat{P}(ij)}{2}\delta_{jk}\lambda_b^l\lambda_{cd}^{mn}\tau_{mn}^{ad}\tau_{il}^{bc} + \tau_n^a\lambda_{bc}^{lm}\lambda_{de}^{kn}\tau_{il}^{bd}\tau_{jm}^{ce} - \frac{1}{4}\tau_n^a\lambda_{bc}^{lm}\lambda_{de}^{kn}\tau_{il}^{bc}\tau_{jm}^{de} \\
&- \frac{1}{4}\tau_n^a\lambda_{bc}^{lm}\lambda_{de}^{kn}\tau_{jm}^{bc}\tau_{il}^{de}, \qquad \text{(D.22)} \\
\Delta\Gamma_{ia}^{jk} =& \lambda_b^k\lambda_{ac}^{jl}\tau_{il}^{bc} + \frac{1}{2}\lambda_a^j\lambda_{bc}^{kl}\tau_{il}^{bc} + \frac{1}{2}\lambda_a^l\lambda_{bc}^{jk}\tau_{il}^{bc} - \lambda_b^j\lambda_{ac}^{kl}\tau_{il}^{bc} \\
&- \lambda_b^l\lambda_{ac}^{jk}\tau_{il}^{bc} - \frac{1}{2}\lambda_a^k\lambda_{bc}^{jl}\tau_{il}^{bc}, \qquad \text{(D.23)} \\
\Delta\Gamma_{ab}^{ci} =& \lambda_d^j\lambda_{ab}^{ik}\tau_{jk}^{cd} + \hat{P}(ab)\lambda_a^j\lambda_{bd}^{ik}\tau_{jk}^{cd} - \frac{1}{2}\lambda_d^i\lambda_{ab}^{jk}\tau_{jk}^{cd} - \frac{\hat{P}(ab)}{2}\lambda_a^i\lambda_{bd}^{jk}\tau_{jk}^{cd}, \qquad \text{(D.24)} \\
\Delta\Gamma_{ai}^{bc} =& \lambda_a^j\lambda_{de}^{kl}\tau_{jk}^{bd}\tau_{il}^{ce} + \lambda_d^j\lambda_{ae}^{kl}\tau_{il}^{be}\tau_{jk}^{cd} + \lambda_d^j\lambda_{ae}^{kl}\tau_{jk}^{be}\tau_{il}^{cd} + \frac{1}{2}\lambda_a^j\lambda_{de}^{kl}\tau_{jl}^{bc}\tau_{ik}^{de} \\
&+ \frac{1}{2}\lambda_a^j\lambda_{de}^{kl}\tau_{kl}^{bd}\tau_{ij}^{ce} - \lambda_a^j\lambda_{de}^{kl}\tau_{il}^{be}\tau_{jk}^{cd} - \lambda_d^j\lambda_{ae}^{kl}\tau_{jl}^{bc}\tau_{ik}^{de} + \frac{1}{2}\lambda_d^j\lambda_{ae}^{kl}\tau_{kl}^{bc}\tau_{ij}^{de} \\
&- \lambda_d^j\lambda_{ae}^{kl}\tau_{il}^{bd}\tau_{jk}^{ce} - \lambda_d^j\lambda_{ae}^{kl}\tau_{jk}^{bd}\tau_{il}^{ce} + \frac{1}{2}\lambda_d^j\lambda_{ae}^{kl}\tau_{ij}^{be}\tau_{kl}^{cd} + \frac{1}{2}\lambda_d^j\lambda_{ae}^{kl}\tau_{kl}^{be}\tau_{ij}^{cd} \\
&- \frac{1}{4}\lambda_a^j\lambda_{de}^{kl}\tau_{kl}^{bc}\tau_{ij}^{de} - \frac{1}{2}\lambda_a^j\lambda_{de}^{kl}\tau_{ij}^{be}\tau_{kl}^{cd} - \frac{1}{2}\lambda_d^j\lambda_{ae}^{kl}\tau_{ij}^{bd}\tau_{kl}^{ce} - \frac{1}{2}\lambda_d^j\lambda_{ae}^{kl}\tau_{kl}^{bd}\tau_{ij}^{ce} \\
&+ \frac{1}{4}\tau_i^f\lambda_{af}^{lm}\lambda_{de}^{jk}\tau_{jk}^{bd}\tau_{lm}^{ce} - \tau_i^f\lambda_{af}^{lm}\lambda_{de}^{jk}\tau_{jl}^{bd}\tau_{km}^{ce} + \frac{1}{4}\tau_i^f\lambda_{af}^{lm}\lambda_{de}^{jk}\tau_{lm}^{bd}\tau_{jk}^{ce}. \qquad \text{(D.25)}
\end{aligned}$$

Bibliography

[1] S. Flügge, *Practical quantum mechanics*. Springer Science & Business Media, 2012.

[2] S. Albeverio, F. Gesztesy, R. Hoegh-Krohn, and H. Holden, *Solvable models in quantum mechanics*. Springer Science & Business Media, 2012.

[3] F. Marsiglio, "The harmonic oscillator in quantum mechanics: A third way ," *American Journal of Physics*, vol. 77, pp. 253–258, 2009.

[4] E. Barnes and S. D. Sarma, "Analytically solvable driven time-dependent two-level quantum systems," *Physical review letters*, vol. 109, p. 060401, 2012.

[5] H. J. Lipkin, N. Meshkov, and A. Glick, "Validity of many-body approximation methods for a solvable model: (I). Exact solutions and perturbation theory," *Nuclear Physics*, vol. 62, pp. 188–198, 1965.

[6] R. Broglia, "The pairing model," *Annals of Physics*, vol. 80, pp. 60–85, 1973.

[7] D. R. Hartree, "The Wave Mechanics of an Atom with a Non-Coulomb Central Field. Part II. Some Results and Discussion," *Mathematical Proceedings of the Cambridge Philosophical Society*, vol. 24, pp. 111–132, 1928.

[8] V. Fock, "Näherungsmethode zur Lösung des quantenmechanischen Mehrkörperproblems," *Zeitschrift für Physik*, vol. 61, pp. 126–148, Jan 1930.

[9] J. C. Slater, "Note on Hartree's Method," *Physical Review*, vol. 35, pp. 210–211, 1930.

[10] P. Hohenberg and W. Kohn, "Inhomogeneous Electron Gas," *Physical Review*, vol. 136, pp. 864–871, 1964.

[11] S. Andermatt, J. Cha, F. Schiffmann, and J. VandeVondele, "Combining Linear-Scaling DFT with Subsystem DFT in Born–Oppenheimer and Ehrenfest Molecular Dynamics Simulations: From Molecules to a Virus in Solution," *Journal of Chemical Theory and Computation*, vol. 12, pp. 3214–3227, 2016.

[12] L. Hung and E. A. Carter, "Accurate simulations of metals at the mesoscale: Explicit treatment of 1 million atoms with quantum mechanics," *Chemical Physics Letters*, vol. 475, pp. 163–170, 2009.

[13] D. R. Bowler and T. Miyazaki, "Calculations for millions of atoms with density functional theory: linear scaling shows its potential," *Journal of Physics: Condensed Matter*, vol. 22, p. 074207, 2010.

[14] C. D. Sherrill and I. Schaefer, Henry F., "The Configuration Interaction Method: Advances in Highly Correlated Approaches," *Advances in Quantum Chemistry*, vol. 34, pp. 143–269, 1999.

[15] W. Tobocman, "Many-Body Perturbation Theory," *Physical Review*, vol. 107, pp. 203–208, 1957.

[16] F. Coester, "Bound states of a many-particle system," *Nuclear Physics*, vol. 7, pp. 421–424, 1958.

[17] F. Coester and H. Kümmel, "Short-range correlations in nuclear wave functions," *Nuclear Physics*, vol. 17, pp. 477–485, 1960.

[18] J. A. Pople, J. S. Binkley, and R. Seeger, "Theoretical models incorporating electron correlation," *International Journal of Quantum Chemistry*, vol. 10, pp. 1–19, 1976.

[19] P. G. Szalay, M. Nooijen, and R. J. Bartlett, "Alternative ansätze in single reference coupled-cluster theory. III. A critical analysis of different methods," *The Journal of chemical physics*, vol. 103, pp. 281–298, 1995.

[20] R. J. Bartlett and M. Musiał, "Coupled-cluster theory in quantum chemistry," *Reviews of Modern Physics*, vol. 79, p. 291, 2007.

[21] I. Shavitt and R. J. Bartlett, *Many-Body Methods in Chemistry and Physics: MBPT and Coupled-Cluster Theory*, ser. Cambridge Molecular Science. Cambridge: Cambridge University Press, 2009.

[22] I. W. Bulik, T. M. Henderson, and G. E. Scuseria, "Can Single-Reference Coupled Cluster Theory Describe Static Correlation?" *Journal of Chemical Theory and Computation*, vol. 11, pp. 3171–3179, 2015.

[23] A. Chakraborty and R. Maitra, "Fixing the catastrophic breakdown of single reference coupled cluster theory for strongly correlated systems: Two paradigms toward the implicit inclusion of high-rank correlation with low-spin channels," *The Journal of Chemical Physics*, vol. 159, p. 024106, 2023.

[24] T. Van Voorhis and M. Head-Gordon, "The quadratic coupled cluster doubles model," *Chemical Physics Letters*, vol. 330, pp. 585–594, 2000.

[25] J. S. Arponen, R. F. Bishop, and E. Pajanne, "Extended coupled-cluster method. I. Generalized coherent bosonization as a mapping of quantum theory into classical Hamiltonian mechanics," *Physical Review A*, vol. 36, pp. 2519–2538, 1987.

[26] E. F. C. Byrd, T. Van Voorhis, and M. Head-Gordon, "Quadratic coupled-cluster doubles: Implementation and assessment of perfect pairing optimized geometries," *The Journal of Physical Chemistry B*, vol. 106, pp. 8070–8077, 2002.

[27] P.-D. Fan, K. Kowalski, and P. Piecuch*, "Non-iterative corrections to extended coupled-cluster energies employing the generalized method of moments of coupled-cluster equations," *Molecular Physics*, vol. 103, pp. 2191–2213, 2005.

[28] X. Li, N. Govind, C. Isborn, A. E. DePrince III, and K. Lopata, "Real-time time-dependent electronic structure theory," *Chemical Reviews*, vol. 120, pp. 9951–9993, 2020.

[29] D. R. Nascimento and A. E. DePrince III, "Simulation of near-edge X-ray absorption fine structure with time-dependent equation-of-motion coupled-cluster theory," *The journal of physical chemistry letters*, vol. 8, pp. 2951–2957, 2017.

[30] A. I. Krylov, "Equation-of-Motion Coupled-Cluster Methods for Open-Shell and Electronically Excited Species: The Hitchhiker's Guide to Fock Space," *Annual Review of Physical Chemistry*, vol. 59, pp. 433–462, 2008.

[31] H. Koch *et al.*, "Coupled cluster response functions," *The Journal of chemical physics*, vol. 93, pp. 3333–3344, 1990.

[32] T. Helgaker, P. Jørgensen, and J. Olsen, *Molecular electronic-structure theory*. Wiley, 2014.

[33] R. McWeeny, "Natural units in atomic and molecular physics," *Nature*, vol. 243, pp. 196–198, 1973.

[34] A. Szabo and N. Ostlund, *Modern Quantum Chemistry: Introduction to Advanced Electronic Structure Theory*, ser. Dover Books on Chemistry. Dover Publications, 1996.

[35] T. D. Crawford and H. F. Schaefer III, "An Introduction to Coupled Cluster Theory for Computational Chemists," in *Reviews in Computational Chemistry*. John Wiley & Sons, Ltd, 2000, pp. 33–136.

[36] D. Griffiths, *Introduction to quantum mechanics*, ser. Pearson international edition. Pearson Prentice Hall, 2005.

[37] G. C. Wick, "The Evaluation of the Collision Matrix," *Physical Review*, vol. 80, pp. 268–272, 1950.

[38] Y. W. H. March, N. H. and S. Sampanthar, *The Many-Body Problem in Quantum Mechanics*. Cambridge University Press, London, 1967.

[39] E. A. Salter, G. W. Trucks, and R. J. Bartlett, "Analytic energy derivatives in many-body methods. i. first derivatives," *The Journal of Chemical Physics*, vol. 90, pp. 1752–1766, 1989.

[40] S. Höfinger and M. Wendland, "Method/basis set dependence of the traceless quadrupole moment calculation for N_2, CO_2, SO_2, HCl, CO, NH_3, PH_3, HF, and H_2O," *International Journal of Quantum Chemistry*, vol. 86, pp. 199–217, 2002.

[41] H. B. Schlegel, "Geometry optimization," *Wiley Interdisciplinary Reviews: Computational Molecular Science*, vol. 1, pp. 790–809, 2011.

[42] C. Hättig, "Geometry optimizations with the coupled-cluster model cc2 using the resolution-of-the-identity approximation," *The Journal of chemical physics*, vol. 118, pp. 7751–7761, 2003.

[43] M. Heckert, M. Kállay, and J. Gauss, "Molecular equilibrium geometries based on coupled-cluster calculations including quadruple excitations," *Molecular Physics*, vol. 103, pp. 2109–2115, 2005.

[44] C. J. Joachain, N. J. Kylstra, and R. M. Potvliege, *Atoms in intense laser fields*. Cambridge University Press, 2012.

[45] H. E. Kristiansen, B. S. Ofstad, E. Hauge, E. Aurbakken, Ø. S. Schøyen, S. Kvaal, and T. B. Pedersen, "Linear and nonlinear optical properties from tdomp2 theory," *Journal of chemical theory and computation*, vol. 18, pp. 3687–3702, 2022.

[46] M. Repisky, L. Konecny, M. Kadek, S. Komorovsky, O. L. Malkin, V. G. Malkin, and K. Ruud, "Excitation Energies from Real-Time Propagation of the Four-Component Dirac-Kohn-Sham Equation," *Journal of Chemical Theory and Computation*, vol. 11, pp. 980–991, 2015.

[47] B. Sverdrup Ofstad, E. Aurbakken, Ø. Sigmundson Schøyen, H. E. Kristiansen, S. Kvaal, and T. B. Pedersen, "Time-dependent coupled-cluster theory," *Wiley Interdisciplinary Reviews: Computational Molecular Science*, vol. 13, p. e1666, 2023.

[48] H. E. Kristiansen, Ø. S. Schøyen, S. Kvaal, and T. B. Pedersen, "Numerical stability of time-dependent coupled-cluster methods for many-electron dynamics in intense laser pulses," *The Journal of chemical physics*, vol. 152, 2020.

[49] B. Ghojogh, F. Karray, and M. Crowley, "Eigenvalue and Generalized Eigenvalue Problems: Tutorial," 2023.

[50] P. R. Surján, *Second quantized approach to quantum chemistry: an elementary introduction*. Springer Science & Business Media, 2012.

[51] R. Harrison and N. Handy, "Full CI calculations on BH, H_2O, NH_3, and HF," *Chemical Physics Letters*, vol. 95, pp. 386–391, 1983.

[52] C. D. Sherrill and H. F. Schaefer III, "The configuration interaction method: Advances in highly correlated approaches," in *Advances in quantum chemistry*. Elsevier, 1999, vol. 34, pp. 143–269.

[53] E. A. Hylleraas and B. Undheim, "Numerische berechnung der 2 s-terme von ortho-und par-helium," *Zeitschrift für Physik*, vol. 65, pp. 759–772, 1930.

[54] J. K. L. MacDonald, "Successive Approximations by the Rayleigh-Ritz Variation Method," *Physical Review*, vol. 43, pp. 830–833, 1933.

[55] J. Čížek, "On the Correlation Problem in Atomic and Molecular Systems. Calculation of Wavefunction Components in Ursell-Type Expansion Using Quantum-Field Theoretical Methods," *The Journal of Chemical Physics*, vol. 45, pp. 4256–4266, 1966.

[56] H. J. Monkhorst, "Calculation of properties with the coupled-cluster method," *International Journal of Quantum Chemistry*, vol. 12, pp. 421–432, 1977.

[57] R. J. Bartlett, "Many-body perturbation theory and coupled cluster theory for electron correlation in molecules," *Annual review of physical chemistry*, vol. 32, pp. 359–401, 1981.

[58] M. Nooijen, K. Shamasundar, and D. Mukherjee, "Reflections on size-extensivity, size-consistency and generalized extensivity in many-body theory," *Molecular Physics*, vol. 103, pp. 2277–2298, 2005.

[59] B. Cooper and P. J. Knowles, "Benchmark studies of variational, unitary and extended coupled cluster methods," *The Journal of Chemical Physics*, vol. 133, p. 234102, 2010.

[60] R. J. Bartlett, S. A. Kucharski, and J. Noga, "Alternative coupled-cluster ansätze ii. the unitary coupled-cluster method," *Chemical physics letters*, vol. 155, pp. 133–140, 1989.

[61] J. Liu, A. Asthana, L. Cheng, and D. Mukherjee, "Unitary coupled-cluster based self-consistent polarization propagator theory: A third-order formulation and pilot applications," *The Journal of Chemical Physics*, vol. 148, p. 244110, 2018.

[62] M. Fink, "A new method for evaluating the density matrix and its application to the ground state form factors of ^{4}He and ^{16}O," *Nuclear Physics A*, vol. 221, pp. 163–172, 1974.

[63] R. P. Feynman, "Forces in Molecules," *Physical Review*, vol. 56, pp. 340–343, 1939.

[64] S. Kvaal, "Variational formulations of the coupled-cluster method in quantum chemistry," *Molecular Physics*, vol. 111, pp. 1100–1108, 2013.

[65] J. Arponen, "Variational principles and linked-cluster exp S expansions for static and dynamic many-body problems," *Annals of Physics*, vol. 151, pp. 311–382, 1983.

[66] T. Helgaker and P. Jørgensen, "Analytical calculation of geometrical derivatives in molecular electronic structure theory," *Advances in quantum chemistry*, vol. 19, pp. 183–245, 1988.

[67] T. Helgaker and P. Jørgensen, "Configuration-interaction energy derivatives in a fully variational formulation," *Theoretica chimica acta*, vol. 75, pp. 111–127, 1989.

[68] P.-O. Löwdin, P. Froelich, and M. Mishra, "Some properties of the bivariational Hartree–Fock scheme for complex symmetric many-particle operators," *International journal of quantum chemistry*, vol. 36, pp. 93–103, 1989.

[69] S. Kvaal, "Ab initio quantum dynamics using coupled-cluster," *The Journal of Chemical Physics*, vol. 136, p. 194109, 2012.

[70] A. Laestadius and S. Kvaal, "Analysis of the Extended Coupled-Cluster Method in Quantum Chemistry," *SIAM Journal on Numerical Analysis*, vol. 56, pp. 660–683, 2018.

[71] P. a. M. Dirac, "Note on Exchange Phenomena in the Thomas Atom," *Mathematical Proceedings of the Cambridge Philosophical Society*, vol. 26, pp. 376–385, 1930.

[72] T. B. Pedersen and H. Koch, "On the time-dependent Lagrangian approach in quantum chemistry ," *The Journal of Chemical Physics*, vol. 108, pp. 5194–5204, 1998.

[73] T. B. Pedersen, H. E. Kristiansen, T. Bodenstein, S. Kvaal, and Ø. S. Schøyen, "Interpretation of Coupled-Cluster Many-Electron Dynamics in Terms of Stationary States," *Journal of Chemical Theory and Computation*, vol. 17, pp. 388–404, 2021.

[74] T. B. Pedersen and S. Kvaal, "Symplectic integration and physical interpretation of time-dependent coupled-cluster theory," *The Journal of Chemical Physics*, vol. 150, p. 144106, 2019.

[75] P. Bader, S. Blanes, and F. Casas, "Solving the schrödinger eigenvalue problem by the imaginary time propagation technique using splitting methods with complex coefficients," *The Journal of chemical physics*, vol. 139, 2013.

[76] C. R. Harris, K. J. Millman, S. J. van der Walt, R. Gommers, P. Virtanen, D. Cournapeau, E. Wieser, J. Taylor, S. Berg, N. J. Smith, R. Kern, M. Picus, S. Hoyer, M. H. van Kerkwijk, M. Brett, A. Haldane, J. F. del Río, M. Wiebe, P. Peterson, P. Gérard-Marchant, K. Sheppard, T. Reddy, W. Weckesser, H. Abbasi, C. Gohlke, and T. E. Oliphant, "Array programming with NumPy," *Nature*, vol. 585, pp. 357–362, 2020.

[77] P. Echenique and J. L. Alonso, "A mathematical and computational review of hartree–fock scf methods in quantum chemistry," *Molecular Physics*, vol. 105, pp. 3057–3098, 2007.

[78] S. Lehtola, "Assessment of Initial Guesses for Self-Consistent Field Calculations. Superposition of Atomic Potentials: Simple yet Efficient," *Journal of Chemical Theory and Computation*, vol. 15, pp. 1593–1604, 2019.

[79] P. L. Lions, "Solutions of hartree-fock equations for coulomb systems," *Communications in Mathematical Physics*, vol. 109, pp. 33–97, 1987.

[80] Q. Sun, X. Zhang, S. Banerjee, P. Bao, M. Barbry, N. S. Blunt, N. A. Bogdanov, G. H. Booth, J. Chen, Z.-H. Cui, J. J. Eriksen, Y. Gao, S. Guo, J. Hermann, M. R. Hermes, K. Koh, P. Koval, S. Lehtola, Z. Li, J. Liu, N. Mardirossian, J. D. McClain, M. Motta, B. Mussard, H. Q. Pham, A. Pulkin, W. Purwanto, P. J. Robinson, E. Ronca, E. R. Sayfutyarova, M. Scheurer, H. F. Schurkus, J. E. T. Smith, C. Sun, S.-N. Sun, S. Upadhyay, L. K. Wagner, X. Wang, A. White, J. D. Whitfield, M. J. Williamson, S. Wouters, J. Yang, J. M. Yu, T. Zhu, T. C. Berkelbach, S. Sharma, A. Y. Sokolov, and G. K.-L. Chan, "Recent developments in the PySCF program package ," *The Journal of Chemical Physics*, vol. 153, p. 024109, 2020.

[81] Q. Sun, T. C. Berkelbach, N. S. Blunt, G. H. Booth, S. Guo, Z. Li, J. Liu, J. D. McClain, E. R. Sayfutyarova, S. Sharma, S. Wouters, and G. K.-L. Chan, "PySCF: the Python-based simulations of chemistry framework," *WIREs Computational Molecular Science*, vol. 8, p. e1340, 2018.

[82] M. Hjorth-Jensen, M. P. Lombardo, and U. Van Kolck, "An advanced course in computational nuclear physics," *Springer Lecture Notes in Physics*, vol. 936, 2017.

[83] P. Pulay, "Convergence acceleration of iterative sequences. The case of SCF iteration," *Chemical Physics Letters*, vol. 73, pp. 393–398, 1980.

[84] P. Pulay, "Improved SCF convergence acceleration," *Journal of Computational Chemistry*, vol. 3, pp. 556–560, 1982.

[85] E. A. Hylleraas, "Über den grundzustand des heliumatoms," *Zeitschrift für Physik*, vol. 48, pp. 469–494, 1928.

[86] H. Shull and P.-O. Löwdin, "Role of the continuum in superposition of configurations," *The Journal of Chemical Physics*, vol. 23, pp. 1362–1362, 1955.

[87] H. Hettema, *Quantum chemistry: classic scientific papers*. World Scientific, 2000, vol. 8.

[88] J. C. Slater, "Atomic shielding constants," *Physical review*, vol. 36, p. 57, 1930.

[89] F. Jensen, *Introduction to Computational Chemistry*. Wiley, 2007.

[90] J. G. Hill, "Gaussian basis sets for molecular applications," *International Journal of Quantum Chemistry*, vol. 113, pp. 21–34, 2013.

[91] S. Lehtola, "A review on non-relativistic, fully numerical electronic structure calculations on atoms and diatomic molecules," *International Journal of Quantum Chemistry*, vol. 119, p. e25968, 2019.

[92] J. T. Fermann and E. F. Valeev, "Fundamentals of Molecular Integrals Evaluation," 2020.

[93] B. P. Pritchard, D. Altarawy, B. Didier, T. D. Gibson, and T. L. Windus, "New Basis Set Exchange: An Open, Up-to-Date Resource for the Molecular Sciences Community," *J. Chem. Inf. Model.*, 2019.

[94] Q. Sun, "Libcint: An efficient general integral library for Gaussian basis functions," *Journal of Computational Chemistry*, vol. 36, pp. 1664–1671, 2015.

[95] R. A. Kendall, J. Dunning, Thom H., and R. J. Harrison, "Electron affinities of the first-row atoms revisited. Systematic basis sets and wave functions," *The Journal of Chemical Physics*, vol. 96, pp. 6796–6806, 1992.

[96] W. J. Hehre, R. F. Stewart, and J. A. Pople, "Self-Consistent Molecular-Orbital Methods. I. Use of Gaussian Expansions of Slater-Type Atomic Orbitals ," *The Journal of Chemical Physics*, vol. 51, pp. 2657–2664, 1969.

[97] T. H. Dunning, "Gaussian basis functions for use in molecular calculations. i. contraction of (9s5p) atomic basis sets for the first-row atoms," *J. Chem. Phys.*, vol. 53, pp. 2823–2833, 1970.

[98] T. H. Dunning and P. J. Hay, "Gaussian basis sets for molecular calculations," in *Methods of Electronic Structure Theory*, ser. Modern Theoretical Chemistry, H. F. Schaefer, Ed. Springer, 1977, vol. 3.

[99] R. Ditchfield, W. J. Hehre, and J. A. Pople, "Self-consistent molecular-orbital methods. ix. an extended gaussian-type basis for molecular-orbital studies of organic molecules," *The Journal of Chemical Physics*, vol. 54, pp. 724–728, 1971.

[100] T. Clark, J. Chandrasekhar, G. W. Spitznagel, and P. V. R. Schleyer, "Efficient diffuse function-augmented basis sets for anion calculations. III. The 3-21+G basis set for first-row elements, Li-F," *J. Comput. Chem.*, vol. 4, pp. 294–301, 1983.

[101] R. Krishnan, J. S. Binkley, R. Seeger, and J. A. Pople, "Self-consistent molecular orbital methods. XX. A basis set for correlated wave functions," *J. Chem. Phys.*, vol. 72, pp. 650–654, 1980.

[102] T. H. Dunning Jr, "Gaussian basis sets for use in correlated molecular calculations. i. the atoms boron through neon and hydrogen," *The Journal of chemical physics*, vol. 90, pp. 1007–1023, 1989.

[103] B. P. Prascher, D. E. Woon, K. A. Peterson, T. H. Dunning, and A. K. Wilson, "Gaussian basis sets for use in correlated molecular calculations. VII. Valence, core-valence, and scalar relativistic basis sets for Li, Be, Na, and Mg," *Theor. Chem. Acc.*, vol. 128, pp. 69–82, 2011.

[104] E. Papajak, H. R. Leverentz, J. Zheng, and D. G. Truhlar, "Efficient Diffuse Basis Sets: cc-pVxZ+ and maug-cc-pVxZ," *Journal of Chemical Theory and Computation*, vol. 5, pp. 1197–1202, 2009.

[105] J. Gauss and J. F. Stanton, "Coupled-cluster calculations of nuclear magnetic resonance chemical shifts," *The Journal of chemical physics*, vol. 103, pp. 3561–3577, 1995.

[106] "Drudge symbolic algebra system," 2017, https://github.com/tschijnmo/drudge, accessed 2024-05-04.

[107] "Gristmill symbolic algebra system for automatic optimization and code generation of tensor computations," 2017, https://github.com/tschijnmo/gristmill, accessed 2024-05-04.

[108] A. Meurer, C. P. Smith, M. Paprocki, O. Čertík, S. B. Kirpichev, M. Rocklin, A. Kumar, S. Ivanov, J. K. Moore, S. Singh, T. Rathnayake, S. Vig, B. E. Granger, R. P. Muller, F. Bonazzi, H. Gupta, S. Vats, F. Johansson, F. Pedregosa, M. J. Curry, A. R. Terrel, v. Roučka, A. Saboo, I. Fernando, S. Kulal, R. Cimrman, and A. Scopatz, "SymPy: symbolic computing in Python," *PeerJ Computer Science*, vol. 3, p. e103, 2017.

[109] H. Koch, O. Christiansen, R. Kobayashi, P. Jørgensen, and T. Helgaker, "A direct atomic orbital driven implementation of the coupled cluster singles and doubles (CCSD) model," *Chemical physics letters*, vol. 228, pp. 233–238, 1994.

[110] M. B. Hansen, N. K. Madsen, A. Zoccante, and O. Christiansen, "Time-dependent vibrational coupled cluster theory: Theory and implementation at the two-mode coupling level," *The Journal of Chemical Physics*, vol. 151, 2019.

[111] S. P. N. Ernst Hairer, Gerhard Wanner, *Solving Ordinary Differential Equations I: Nonstiff Problems*. Springer, 1993, vol. 8.

[112] E. Hairer, M. Hochbruck, A. Iserles, and C. Lubich, "Geometric numerical integration," *Oberwolfach Reports*, vol. 3, pp. 805–882, 2006.

[113] Z. Wang, B. G. Peyton, and T. D. Crawford, "Accelerating Real-Time Coupled Cluster Methods with Single-Precision Arithmetic and Adaptive Numerical Integration," *Journal of Chemical Theory and Computation*, vol. 18, pp. 5479–5491, 2022.

[114] T. Sato, H. Pathak, Y. Orimo, and K. L. Ishikawa, "Communication: Time-dependent optimized coupled-cluster method for multielectron dynamics," *The Journal of Chemical Physics*, vol. 148, p. 051101, 2018.

[115] M. Hochbruck and A. Ostermann, "Exponential integrators," *Acta Numerica*, vol. 19, pp. 209–286, 2010.

[116] P. Virtanen, R. Gommers, T. E. Oliphant, M. Haberland, T. Reddy, D. Cournapeau, E. Burovski, P. Peterson, W. Weckesser, J. Bright, S. J. van der Walt, M. Brett, J. Wilson, K. J. Millman, N. Mayorov, A. R. J. Nelson, E. Jones, R. Kern, E. Larson, C. J. Carey, İ. Polat, Y. Feng, E. W. Moore, J. VanderPlas, D. Laxalde, J. Perktold, R. Cimrman, I. Henriksen, E. A. Quintero, C. R. Harris, A. M. Archibald, A. H. Ribeiro, F. Pedregosa, P. van Mulbregt, and SciPy 1.0 Contributors, "SciPy 1.0: Fundamental Algorithms for Scientific Computing in Python," *Nature Methods*, vol. 17, pp. 261–272, 2020.

[117] R. D. E. Johnson III, "NIST Computational Chemistry Comparison and Benchmark Database, NIST Standard Reference Database Number 101, Release 22," 2022.

[118] D. J. Thouless, "Stability conditions and nuclear rotations in the Hartree-Fock theory," *Nuclear Physics*, vol. 21, pp. 225–232, 1960.

[119] X. Li, S. M. Smith, A. N. Markevitch, D. A. Romanov, R. J. Levis, and H. B. Schlegel, "A time-dependent hartree–fock approach for studying the electronic optical response of molecules in intense fields," *Physical Chemistry Chemical Physics*, vol. 7, pp. 233–239, 2005.

[120] M. Rubinstein and I. Shavitt, "Theoretical study of the potential surface for the h4 system by double-zeta configuration-interaction calculations," *The Journal of Chemical Physics*, vol. 51, pp. 2014–2024, 1969.

[121] J. Olsen, A. M. S. De Meŕas, H. J. A. Jensen, and P. Jørgensen, "Excitation energies, transition moments and dynamic polarizabilities for ch+. a comparison of multiconfigurational linear response and full configuration interaction calculations," *Chemical physics letters*, vol. 154, pp. 380–386, 1989.

[122] H. Koch, H. J. Jensen, T. Helgaker *et al.*, "Excitation energies from the coupled cluster singles and doubles linear response function (ccsdlr). applications to Be, CH^+, CO, and H_2O," *The Journal of chemical physics*, vol. 93, pp. 3345–3350, 1990.

[123] A. I. Vistnes, "Physics of oscillations and waves," *Physics of Oscillations and Waves*, 2018.

[124] R. J. Bartlett, Y. C. Park, N. P. Bauman, A. Melnichuk, D. Ranasinghe, M. Ravi, and A. Perera, "Index of multi-determinantal and multi-reference character in coupled-cluster theory," *The Journal of Chemical Physics*, vol. 153, 2020.

[125] G. E. Scuseria and H. F. Schaefer, "The optimization of molecular orbitals for coupled cluster wavefunctions," *Chemical Physics Letters*, vol. 142, pp. 354–358, 1987.

[126] T. B. Pedersen, B. Fernández, and H. Koch, "Gauge invariant coupled cluster response theory using optimized nonorthogonal orbitals," *The Journal of chemical physics*, vol. 114, pp. 6983–6993, 2001.

[127] T. B. Pedersen, H. Koch, and C. Hättig, "Gauge invariant coupled cluster response theory," *The Journal of chemical physics*, vol. 110, pp. 8318–8327, 1999.

[128] J. L. Whitten, "Coulombic potential energy integrals and approximations," *The Journal of Chemical Physics*, vol. 58, pp. 4496–4501, 1973.

[129] M. Schütz and F. R. Manby, "Linear scaling local coupled cluster theory with density fitting. part i: 4-external integrals," *Physical Chemistry Chemical Physics*, vol. 5, pp. 3349–3358, 2003.

[130] U. Bozkaya and C. D. Sherrill, "Analytic energy gradients for the coupled-cluster singles and doubles with perturbative triples method with the density-fitting approximation," *The Journal of Chemical Physics*, vol. 147, 2017.

[131] T. B. Pedersen, S. Lehtola, I. Fdez. Galván, and R. Lindh, "The versatility of the cholesky decomposition in electronic structure theory," *Wiley Interdisciplinary Reviews: Computational Molecular Science*, vol. 14, p. e1692, 2024.

[132] R. Shepard and M. Minkoff, "Some comments on the DIIS method," *Molecular Physics*, vol. 105, pp. 2839–2848, 2007.